KU LEUVEN

ARENBERG DOCTORAL SCHOOL
Faculty of Engineering Science

Demand response for residential heat pumps in interaction with the electricity generation system

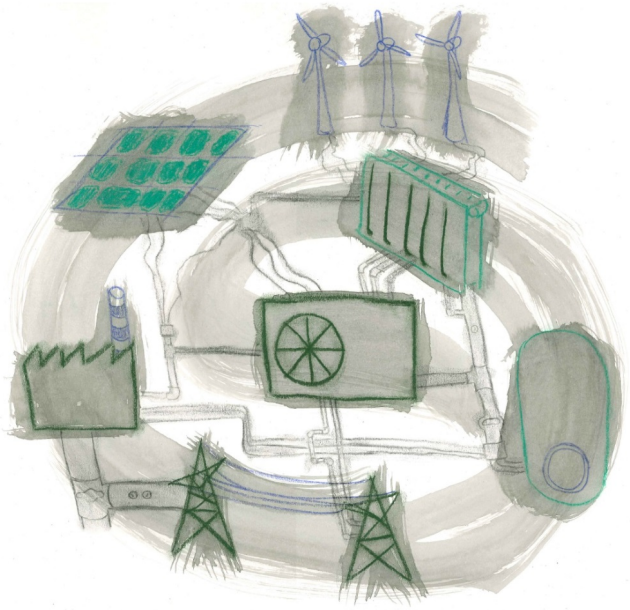

Dieter Patteeuw

Supervisor:
Prof. dr. ir. L. Helsen

Dissertation presented in partial fulfillment of the requirements for the degree of Doctor of Engineering Science (PhD): Mechanical Engineering

September 2016

Demand response for residential heat pumps in interaction with the electricity generation system

Dieter PATTEEUW

Examination committee:
Prof. dr. ir. O. Van der Biest, chair
Prof. dr. ir. L. Helsen, supervisor
Prof. dr. ir. W. D'haeseleer
Prof. dr. ir.-arch. D. Saelens
Prof. dr. ir. G. Deconinck
Prof. dr. G.P. Henze
(University of Colorado Boulder)
Prof. dr. C. Jones
(Ecole Polytechnique Fédérale de Lausanne)

Dissertation presented in partial fulfillment of the requirements for the degree of Doctor of Engineering Science (PhD): Mechanical Engineering

September 2016

Preface - Dankwoord

Het dankwoord is zowat het meest gelezen deel van een doctoraat, vandaar dat er dan ook het minste tijd in gestopt wordt. Indien u als lezer toch ietwat geïnteresseerd bent, raad ik u aan om toch het abstract te lezen en misschien zelfs de conclusie. Naast deze noot wil ik natuurlijk heel wat mensen bedanken die me in de laatste 4,96 jaar (klinkt beter dan 5) gesteund hebben.

Allereerst, Lieve. Al 6 jaar mijn promotor. Zes jaar waarin je me heel wat vrijheid liet, met af en toe een subtiele suggestie in de een of andere richting, zodat mijn focus zeker zou leiden tot dit boekje. Ik heb me steeds door jou gesteund en ondersteund gevoeld. Je geloofde soms meer in mijn werk dan ikzelf, maar nu dit resultaat er is, kan ik dat geloof ook delen. Je toewijding, correctheid en spontaniteit werken enorm inspirerend voor mij. En ook al zullen we later misschien meer collega's dan promotor en (doctoraats)student zijn, voor mij zal je altijd een deel promotor blijven. Bedankt voor de kansen die je mij bood en biedt. Ik kijk al uit naar onze verdere samenwerking.

I would like to thank the members of the jury for the thorough review of the text and the interesting discussion during the preliminary defense. Dirk en William, bedankt voor het mede begeleiden gedurende de afgelopen jaren en het reviewen van onze papers. Jullie inbreng kwam de waarde van het werk zeker ten goede. Geert, bedankt voor de suggesties om mijn tekst te verbeteren. Gregor, thank you for the interesting cooperation on our paper and for the help in applying for travel funds. I'm looking forward to an exciting stay at your research group. Colin, thank you for the interesting debate during the preliminary defense. Omer, bedankt voor de organisatie van de verdediging en het geduld bij de videoconferentie met twee buitenlandse juryleden.

Dit werk was nooit in zijn huidige vorm tot stand gekomen zonder de substantiële bijdrage van een aantal mensen. Kenneth B., bedankt voor onze boeiende samenwerking. Ik heb heel veel van je geleerd, niet alleen over unit commitment modellen, maar ook over deadlines stellen, lay-out, werkorganisatie, motivatie

en zoveel meer. Daarnaast was je ook een zeer aangename collega zowel binnen als buiten de werkuren. Alessia, embassador of Italy, I enjoyed our cooperation and your general advice on life very much. Glenn and Christina, thank you both for the nice cooperation. With your help, I could include the building stock in my models, knowing it was based on decent work. I always enjoyed coming over to building physics for our meetings. Erik, bedankt voor je kritische inbreng en discussies, de ene keer over investeringsmodellen, de andere keer over het al dan niet meegaan naar de alma.

Furthermore, I would like to thank the other members and former members of the GOA project: Ritu, Juan, Hakan, Yves, Arne, Felix, Ronnie and Johan for the meetings and discussions, which opened my eyes to other aspects of the energy system.

Volgende op de lijst zijn mijn (ex-)bureaugenoten, die dag in dag uit mijn vele lawaai moesten verduren. Damien, met vier jaar op de teller heb je veruit het meeste tijd met mij doorgebracht. Vier jaar, wat vliegt de tijd. In die tijd heb ik je zien trouwen (prachtig huwelijk) en vader worden. Bedankt voor de vele pauzes samen. Verder ken ik je als een gedreven en correcte onderzoeker, en ben ik er zeker van dat je een degelijk doctoraat zal afleggen. Clara, je hebt me enorm geïnspireerd met je enthousiasme voor de goede zaak en ik vond het fijn om je thesisstudent en bureaugenoot te zijn. Je hebt een heel stevige basis gelegd voor dit werk en ik hoop dat ik er een even volwaardig deel aan heb kunnen toevoegen. Brecht, ook al was je een parttime bureaugenoot, ik vond het altijd aangenaam om je erbij te hebben. Onze discussies, over opslagvaten, over je indrukwekkende verbouwingen en domotica en zoveel meer, vond ik heel boeiend.

Verder had ik het geluk om deel uit te mogen maken van een zeer gedreven en dynamische onderzoeksgroep, the sysi's (thermal system simulators), ook al ben ik nog steeds geen volledige voorstander van die afkorting. Stefan, van thesisbegeleider naar collega, altijd even positief, opgewekt en sociaal. Je observerende blik op alles wat er rond je gebeurde, gaf steeds aanleiding tot leuke gesprekken. Jan, we zijn niet lang collega's geweest, maar ik vond onze praatjes zeer aangenaam. Maarten, je staat zo stevig in het leven en weet altijd hoe of wat. Maar dat maakt je grapjes er zeker niet minder op. Roel, je bent een zeer inspirerende collega en persoon met je rotsvaste overtuiging in duurzaamheid. Ik heb enorm veel van je geleerd, zelfs Modelica (dat zegt al veel), op heel veel vlakken. Ercan, I still remember our nice day in Copenhagen and I hope you're doing well. Mats, ik vond onze uitstapjes tot in de late uren op conferenties en TME weekends altijd plezant, zelfs als dat zingen met zatte Ieren inhield. Filip, je kennis en kunde vind ik echt indrukwekkend en ik ben er zeker van dat je doctoraat en je huis in Mechelen zeer degelijk zullen zijn. Arnout, ik vond je een zeer fijne collega en ik zie je zeker nog vaak in

de toekomst. Bram, ik heb in jou een zeer betrouwbaar persoon leren kennen met gevatte humor op onverwachte momenten. Verder wil ik ook nog Nicholas, Anouk, Joachim, Igor, Muhannad en Edorta bedanken om zulke fijne collega's en mensen te zijn.

Naast een toffe onderzoeksgroep, maakte ik ook deel uit van een zeer leuke divisie: TME. Tijdens ieder weekend, barbecue, fietstocht, happy hour, alma dag, middageten en nachtelijke uitstap, blijkt er steeds een verborgen levensgenieter in iedere TME-er te schuilen. Ik heb me dan ook als een vis in het water gevoeld in deze groep. Ik zal altijd tevreden op deze periode terugkijken. Geert, je hebt een groot hart en ik heb daar steeds mogen van genieten in onze vele gesprekken en uitstappen. Joris, je hebt me geleerd dat er nog zoveel andere zaken zijn naast het werk en ik bewonder je enthousiasme in alles wat je doet. Tijs, je uitdagende pseudo-wetenschappelijke stellingen zorgden steeds voor boeiende middaggesprekken, hetgeen nooit meer hetzelfde is geweest nadat je vertrok. Kenneth Vdb, onze contactstop is niet ver geraakt, maar ik ben er zeker van dat je je andere projecten en doelen tot een indrukwekkend einde zult brengen. Je bent daarin zeker een voorbeeld voor mij. Ruben, je religieuze overtuiging zal me blijven inspireren. Jeroen, ik vind je vele verhalen altijd boeiend en ben steeds benieuwd naar je volgende bestemming. Juliana, so much fun you have in everything, even in supporting for that team that's beneath Belgium in the FIFA ranking. Dries, je kan steeds scherp en grappig uit de hoek komen. Kris, na het taakje voor ECMS, onverwacht collega geworden, ik apprecieer je humor enorm. Pieter, nog nooit zo'n goede gesprekspartner gehad over sciencefiction tot wielrennen. I won't go into a full list of all people at TME. I enjoyed every conversation with all of you, even if that was limited to a short 'hello' in the hallway sometimes. I hope that the nice atmosphere in TME continues to exist just like I had the privilege of experiencing the last 5 years.

Verder wil ik ook Valérie en Kathleen bedanken voor de goede ondersteuning, maar ook om zulke toffe vrouwen te zijn. Zo werd papierwerk een goed excuus voor een leuke babbel op het secretariaat. Valérie, je uitgebreide kennis van sciencefiction en fantasy blijft me verbazen. Kathleen, ik vond je humor steeds fijn en ik hoop dat mijn kabouter Wesley cartoon je ook goed heeft kunnen doen lachen.

Bij deze wil ik ook mijn ouders bedanken. Mama, papa, jullie hebben me steeds alle kansen geboden, me beschermd en losgelaten waar nodig. Jullie liefde voor elkaar en jullie entourage zijn steeds een voorbeeld voor mij. Thijs, ik weet dat wij niet veel woorden nodig hebben, om onze appreciatie voor elkaar duidelijk te maken. Jens, het doet me altijd zo'n plezier om je creativiteit en enthousiasme te zien. Ellen en Yana, bedankt om zo goed voor m'n broers te zorgen. Emmy, ik zal de kerstvakantie steeds met onze Donkey Kong avonturen associëren.

Meme, je hebt maar weinig van deze periode in m'n leven kunnen meemaken, maar ik waardeer je als enorm rijke persoonlijkheid. Ik ben blij dat je toch Véronique hebt leren kennen. Pepe, je hebt steeds gezegd dat je je eigen pad moet kiezen, en ik probeer dat ook te doen. Meme, je bent zo'n intelligente vrouw en ik ben trots je petekind te zijn. Alle nonkels en tantes, neven en nichten, jullie zijn stuk voor stuk fantastische mensen en een inspiratie voor hoe ik wil dat m'n familie eruit ziet. Tine, je hebt me zoveel geleerd en gesteund.

Tim en Kenneth, onze reizen en avonturen samen hebben me echt veranderd en ik geniet nog steeds met volle teugen van onze momenten samen. Simon, je bent er al heel m'n leven soms wat meer of minder, maar elke keer als we samen zitten, lijkt het alsof het gisteren was. Maxime, Tuur en Valentine, ik ben blij dat we met ons P&O groepje nog steeds samen komen. Maxime en Tine, bedankt voor de vele uitnodigingen, ik kom steeds met plezier langs. Tuur en Lien, wat een leuk koppel zijn jullie toch. Hopelijk spreken we in enkele jaren toch via Trigger af. Valentine, we hebben al veel momenten gedeeld en ik vind het steeds fijn als je er bij kan zijn.

Nathalie, Stefanie, Kristof, Hubert, Monique, Alice en Charles, bij jullie heb ik een tweede familie gevonden en ik kom steeds met plezier af naar Moere.

Véronique, ik verwonder me nog steeds over hoe we elkaar zijn hebben leren kennen en hoe dat het begin was van al vier fantastische jaren samen. Ik ben zo blij dat we samen gaan afronden en zo samen die sprong naar Amerika kunnen maken. Je steunt me enorm en ieder vrij moment samen, is altijd genieten. Ik had nooit gedacht dat ik met zo'n fantastische vrouw zou samen zijn. Met jou aan m'n zij, kan ik alles aan.

Dieter Patteeuw

Juli 2016

Abstract

Renewable energy sources (RES) will play a vital role in reducing the impact of climate change. Solar and wind energy, captured by PV-panels and wind turbines respectively, are two major RES that pose enormous potential but have two important disadvantages: a limited predictability and variability. Demand response (DR) is often put forward as part of the solution for variability, by shifting electricity demand away or towards times of shortages or abundances of RES respectively. One of the major technologies that pose significant potential for DR are electrical heating and cooling systems. Within these systems, this work focuses on the heating of residential buildings by means of a heat pump. Residential buildings with heat pumps show potential for DR as the building structure and domestic hot water tank can be used as thermal energy storage. This allows a decoupling in time of the delivery of thermal comfort and the heat pump electricity demand.

One of the factors hampering a widespread implementation of DR for heat pumps is a thorough understanding of the potential benefits. To this aim, this work presents an integrated modeling approach that captures both the incentives for DR by explicitly modeling the electricity generation system as well as the flexibility potential of residential buildings with heat pumps. In contrast to the literature, a bottom-up representation of this flexibility potential is developed, resulting in a linear optimal control problem (OCP). This linear OCP of buildings with heat pumps is combined with a state of the art unit commitment and economic dispatch model of the electricity generation system. The added value of this integrated modeling approach is shown with respect to typical other approaches in the literature. It correctly captures the maximal potential for DR, weighs the thermal losses against the supply side incentives and includes the feedback with the electricity generation system.

This integrated model is employed in a number of case studies to explore the potential benefits of DR for residential heat pumps. In a first case study for a Belgian context, it is shown that DR with residential heat pumps can shift

electricity demand towards moments of curtailment in order to avoid electricity demand later on when fuel fired power plants are running. In this case study, half of the shifted electricity demand was directly lost due to thermal losses in the residential buildings. In this manner, applying DR to residential heat pumps allows reducing the CO_2 emission further by an extra 15 % on top of the CO_2 emission reduction of installing a heat pump. Furthermore, the contribution of the electricity demand of residential heat pumps to the peak electricity demand is almost one on one in case no DR is applied. With DR, well insulated buildings can significantly shift their electricity demand away from the peak. Buildings which are not well insulated are shown to be unattractive for installing heat pumps, even with a DR implementation.

In a second case study, the monetary benefits of applying DR for residential heat pumps are identified to go up to 150 EUR per participant per year from operational savings and up to 300 EUR per participant per year by avoiding peak electricity demand. These cost savings are shown to diminish as the participation in DR rises. This discourages extreme configurations in the residential buildings: high spreads on temperature set points or high domestic hot water tank sizes pose little added value in case of higher DR participation.

The integrated model has potential for a practical implementation of DR with residential heat pumps. It can be employed to anticipate, in a day ahead setting, the reaction of residential heat pumps to incentives from the electricity generation system. Residential heat pumps controlled by MPC are shown to be very greedy to these incentives. In this manner, sending an electricity price profile leads to poor performance when a high number of buildings, 100,000 in this work, join in on DR. Sending an electricity demand profile for the residential heat pumps to follow attains superior performance in this context.

Finally, this work combines the integrated model with a heating system design optimization in order to investigate whether heating systems should be designed differently in the light of high RES shares in the electricity generation system. Two modeling additions towards this aim, temperature level and electricity generation side modeling, show limited added value to the heating system optimization but does allow a correct quantification of the CO_2 emissions. From the results it follows that a residential building is best equipped with a single main heat production system. A storage tank for space heating and solar thermal panels appear to be unattractive technologies. A large scale combined heat and power unit is attractive but the CO_2 emission strongly depends on the CO_2 emission calculation method. The combination of heat pump and PV panel reduces the CO_2 emission of the building with up to 2 ton per building per year compared to typical fuel fired options for a limited extra cost.

Beknopte samenvatting

Hernieuwbare energie zal een grote rol spelen in het beperken van de klimaatopwarming. Zonnepanelen en windturbines, twee belangrijke hernieuwbare energietechnologieën, vertonen een enorm potentieel maar hebben twee nadelen: een beperkte voorspelbaarheid en variabiliteit. Vraagsturing wordt vaak voorgesteld als een deel van de oplossing voor variabiliteit, door het deels verschuiven van de elektriciteitsvraag om een betere overeenstemming te bekomen met de elektriciteitsopwekking door zonnepanelen en windturbines. De sector van verwarming en koeling met behulp van elektriciteit vertoont een groot potentieel voor vraagsturing. Dit werk focust zich op residentiële gebouwen die verwarmd worden met behulp van een warmtepomp. Deze gebouwen voorzien vraagsturing door het benutten als thermische energieopslag van de gebouwmassa en het warmwatervat. Dit laat toe om de vraag naar thermisch comfort los te koppelen in de tijd van het elektriciteitsgebruik van de warmtepomp.

Een van de factoren die een wijdverspreide toepassing van vraagsturing voor warmtepompen in de weg staat, is een grondige kennis van de mogelijke voordelen. Om dit tegen te gaan, presenteert dit werk een geïntegreerde modellering die een expliciete modellering combineert van zowel het elektriciteitsopwekkingssysteem als de flexibiliteit in residentiële gebouwen met warmtepompen. In tegenstelling tot de literatuur wordt er een bottom-up voorstelling van deze flexibiliteit ontwikkeld dat voor te stellen is in een lineair optimaal controle probleem. Dit lineair model wordt gecombineerd met een geavanceerd operationeel model van het elektriciteitsopwekkingssysteem. De toegevoegde waarde van deze geïntegreerde modelleringsaanpak wordt aangetoond tegenover andere klassieke modelleringsmethodes in de literatuur.

Dit geïntegreerd model wordt toegepast in een aantal gevalstudies om de mogelijke voordelen van vraagsturing voor residentiële warmtepompen te verkennen. Een eerste gevalstudie in een Belgische context toont aan dat de elektriciteitsvraag van de warmtepompen verschoven kan worden naar momenten wanneer hernieuwbare energie te veel produceert en waarbij een deel

zou ingeperkt worden. Deze aansturing zorgt ervoor dat op een later tijdstip, een gasgestookte centrale minder elektriciteit dient op te wekken. Op deze manier slaagt vraagsturing erin om de CO_2-uitstoot van verwarming van residentiële gebouwen met een extra 15 % te verminderen bovenop de vermindering in CO_2-uitstoot door het installeren van een warmtepomp. Bovendien kan vraagsturing, vooral bij goed geïsoleerde gebouwen, de bijdrage significant beperken van de elektriciteitsvraag van residentiële warmtepompen aan de piekvraag in de winter. Minder goed geïsoleerde gebouwen zijn onaantrekkelijk voor het installeren van warmtepompen, zelfs na implementatie van vraagsturing.

Een tweede gevalstudie onderzoekt de financiële voordelen van het toepassen van vraagsturing voor residentiële warmtepompen. Er wordt aangetoond dat de operationele besparingen kunnen oplopen tot 150 euro per deelnemer per jaar en dat het vermijden van bijdragen aan de piekvraag een besparing kan opleveren tot 300 euro per deelnemer per jaar. Verder toont deze gevalstudie aan dat deze kostenbesparingen per deelnemer afnemen naarmate meer huishoudens deelnemen aan vraagsturing. Dit fenomeen ontmoedigt een extreme configuratie van het verwarmingssysteem in residentiële gebouwen, zoals een hogere spreiding op de instellingen voor de binnenhuistemperatuur of een groter vat voor warm water.

Het geïntegreerd model vertoont potentieel voor een praktische implementatie van vraagsturing met residentiële warmtepompen. Dit model kan gebruikt worden om een dag op voorhand te anticiperen op de reactie van deze vraagsturing op financiële prikkels. Bij een groter aantal deelnemende huishoudens aan vraagsturing, zwakt de performantie van een elektriciteitsprijsprofiel af. Het sturen van een elektriciteitsvraagprofiel, dat gevolgd dient te worden door de warmtepompen, leidt tot betere resultaten.

Uiteindelijk wordt het geïntegreerd model ook gecombineerd met een ontwerpoptimalisatie van het verwarmingssysteem, om te onderzoeken of dit ontwerp anders dient te gebeuren in de context van een hoog aandeel van hernieuwbare energie in het elektriciteitsopwekkingssysteem. Twee methodologische uitbreidingen hiertoe, het toevoegen van temperatuursniveaus en het modelleren van het elektriciteitsopwekkingssysteem, vertonen een beperkte toegevoegde waarde maar laten wel een nauwkeurige bepaling van de CO_2-uitstoot toe. Een opslagtank voor ruimteverwarming en een zonneboiler blijken onaantrekkelijke technologieën te zijn. De combinatie van een warmtepomp met vloerverwarming en zonnepanelen kunnen de jaarlijkse CO_2-uitstoot van een woning tot 2 ton per gebouw per jaar verminderen in vergelijking met een gasboiler, aan een beperkte meerkost.

Abbreviations

ACH	Air changes per hour
ACHP	Air coupled heat pump
CCGT	Combined cycle gas turbine
CHP	Combined heat and power
CGB	Condensing gas boiler
COP	Coefficient of performance
DHW	Domestic hot water
DR	Demand response
DRR	Demand recovery ratio
DSM	Demand side management
EAC	Equivalent annual cost
ED	Economic dispatch
ERH	Electric resistance heater
Fh	Floor heating
GCHP	Ground coupled heat pump
GHG	Greenhouse gas
HOB	Heating oil boiler
HP	Heat pump
HS	Heating system
ICT	Information and communication technology
IM	Integrated model
LP	Linear programming
MILP	Mixed integer linear programming
MO	Merit order
MPC	Model predictive control
NZEB	Nearly zero energy building
OCGT	Open cycle gas turbine
OCP	Optimal control problem
OPEX	Operational expenditure
PEF	Primary energy factor
PP	Power plant
PV	Photovoltaic
Rad	Radiator
RES	Renewable energy sources

RMSE	Root mean square error
ROM	Reduced order model
SH	Space heating
SPF	Seasonal performance factor
SR	Spinning reserve
STC	Solar thermal collector
TES	Thermal energy storage
TOU	Time of use
TSO	Transmission system operator
UC	Unit commitment
UK	United Kingdom
US	United States of America
VGM	Virtual generator model

Nomenclature

Indices

b	Building index
i	Power plant index
j	Time step
l	Temperature level
t	Time period

Symbols

For clarity reasons in the nomenclature, the indices of the symbols are omitted. The proper index of each symbol follows from the context throughout the text.

$\mathbf{A}, \mathbf{B}, \mathbf{C}, \mathbf{D}$	General state space matrices
$\mathbf{A}^{sh}, \mathbf{B}^{sh}$	State space matrices of building structure thermal behavior
a	Investment annuity
A^{stc}	Area of the STC providing heat [m^2]
AC^{CO_2}	CO_2 abatement cost [EUR/ton]
bd	General boolean decision variable
$bdem$	DHW demand boolean
C	Thermal capacitance [J/K]
C^{rad}	Thermal capacitance of a radiator [J/K]
c_p	Specific heat capacity [J/kgK]
cf	Fuel cost running PP at minimum power level [EUR]
CO_2	Annual CO_2 emission [ton/year]
co_2t	Cost stemming from CO_2 price [EUR]
co_2p	CO_2 price [EUR/ton]
COP^{dhw}	Coefficient of performance while delivering DHW
COP^{sh}	Coefficient of performance while delivering space heating
ct	CO_2 emission running PP at minimum power level [ton]
cur	Curtailment factor

$cost$	General cost function
$cost^{fix}$	Fixed investment cost component [EUR]
$cost^{var}$	Variable investment cost component [EUR/x]
$\Delta^{max,down}$	Maximum ramping down of a power plant [MW/h]
$\Delta^{max,up}$	Maximum ramping up of a power plant [MW/h]
Δt	Time step duration [s]
ΔT^{layer}	Layer temperature range [$^{\circ}C$]
d^{hp}	Heat pump electricity demand [MW]
$d^{hp,fix}$	HP electricity demand not participating in DR [MW]
$d^{hp,var}$	HP electricity demand participating in DR [MW]
d^{trad}	Traditional electricity demand [MW]
dc^{ccgt}	Dynamic cost of operating a CCGT [EUR]
dT^{aux}	Auxiliary heater influenced DHW tank temperature [$^{\circ}C$]
ϵ	Price elasticity
EAC	Equivalent annual cost [EUR/year]
eq	General equality constraints
η^0,k_1,k_2	Technical parameters STC
η^{cgb}	Condensing gas boiler efficiency
$\eta^{chp,el}$	Electrical efficiency CHP
$\eta^{chp,th}$	Thermal efficiency CHP
$\bar{\eta}^{egs}$	Mean electricity generation system efficiency
$\eta^{network}$	Efficiency district heating
f^{dem}	Demand side model
f^{gen}	Electricity generation system model
$\dot{F}^{cgb}$	Rate of fuel input to the CGB [W]
$\dot{F}^{chp}$	Rate of fuel input to the CHP [W]
fc	Fuel cost from power plant [EUR]
g^{ccgt}	Electricity generation by CCGT [MW]
g^{chp}	Electricity generation by CHP [MW]
g^{max}	Maximum generation level of a power plant [MW]
g^{min}	Minimum generation level of a power plant [MW]
g^{nuc}	Electricity generation by nuclear power plants [MW]
g^{ocgt}	Electricity generation by OCGT [MW]
g^{pp}	Electricity generation by a power plant [MW]
g^{res}	Electricity generation by renewable energy sources [MW]
$g^{rPV,b}$	Electricity by residential PV to the building [MW]
$g^{rPV,g}$	Electricity by residential PV to the grid [MW]
i	Discount rate for annuity calculation
iz	Component investment decision (binary decision variable)
$ineq$	General inequality constraints
Inv	Investment cost [EUR]
mdt	Minimum down time of a power plant [h]
mf	Marginal fuel cost above minimum power level [EUR/MW]
mt	Marginal CO_2 emission above minimum power [ton/MW]
M^{tes}	Size of TES [kg]

mut	Minimum up time of a power plant [h]
n	Number of years for annuity calculation
nb	Number of buildings
O	Heating system component operational aspect
$OPEX$	Operational expenditures [EUR/year]
p	Electricity price [EUR/MWh]
P^{aux}	Auxiliary heater electricity consumption [W]
$P^{aux,max}$	Auxiliary heater maximum electricity consumption [W]
p^{dr}	Share of heat pumps participating in DR
P^{hp}	Heat pump electricity consumption [W]
$P^{hp,dhw}$	HP electricity consumption dedicated to DHW [W]
$P^{hp,sh}$	HP electricity consumption dedicated to SH [W]
$P^{int,hp,sh}$	Integer HP electricity consumption for SH [W]
$P^{max,hp}$	Maximum HP electricity consumption [W]
$P^{min,hp,sh}$	Minimum HP modulation for SH [W]
$P^{pump,emi}$	Electricity consumption of circulation pump [W]
PEF	Primary energy factor
$price^{G}$	Price profile from electricity generation system [EUR]
$price^{I}$	Price profile from integrated model [EUR]
$\dot{q}^{sol}$	Solar irradiation per square meter [W/m^2]
$\dot{q}^{stc}$	Useful heat flux STC [W/m^2]
$\dot{Q}^{aux,dhw}$	DHW provided by the auxiliary heater [W]
$\dot{Q}^{cgb}$	Heat provided by the condensing gas boiler [W]
$\dot{Q}^{dem}$	Heat loss through DHW demand [W]
$\dot{Q}^{emi}$	Heat provided through emission system [W]
$\dot{Q}^{hp,dhw}$	DHW provided by heat pump [W]
$\dot{Q}^{hp,sh}$	Space heating provided by heat pump [W]
$\dot{Q}^{int}$	Internal heat gain [W]
$\dot{Q}^{sol}$	Heat gain by solar irradiation [W]
Q^{TES}	Energy content of TES [kWh]
$\dot{Q}^{stc}$	Heat by solar thermal collector [W]
$\dot{Q}^{toDem}$	Heat to demand (SH or DHW) [W]
$\dot{Q}^{toTes}$	Heat to TES [W]
$Q^{dem,year}$	Heat demand of a building for a full year [kWh]
ρ	Density [kg/m^3]
R	Thermal resistance [K/W]
rc	Expenditure on power plant ramping [EUR]
$raco$	Ramping cost of a power plant [EUR]
S	Heating system component size
sc	Expenditure on power plant start-ups [EUR]
SPF	Seasonal performance factor
$stco$	Start-up cost of a power plant [EUR]
T^{cold}	Cold tap water temperature [$^\circ C$]
T^{dem}	Desired DHW tap water temperature [$^\circ C$]
T^{e}	Ambient (outside) temperature [$^\circ C$]

T^f	Floor temperature $[°C]$
T^{fi}	Internal floor temperature $[°C]$
T^g	Ground temperature $[°C]$
T^{hp}	Heat pump influenced DHW tank temperature $[°C]$
$T^{hp,max}$	Heat pump maximum supply temperature $[°C]$
T^i	Indoor air temperature $[°C]$
T^{level}	Temperature of a level $[°C]$
T^{rad}	Radiator temperature $[°C]$
T^{roof}	Roof temperature $[°C]$
T^{sh}	Space heating state vector $[°C]$
$T^{sh,max}$	Maximum indoor air temperature $[°C]$
$T^{sh,min}$	Minimum indoor air temperature $[°C]$
$\bar{T}^{source}$	Mean heat pump source temperature $[°C]$
T^{surr}	DHW tank surroundings temperature $[°C]$
T^{tank}	Average DHW tank temperature $[°C]$
$T^{tank,max}$	Maximum allowed DHW tank temperature $[°C]$
T^{we}	Exterior wall temperature $[°C]$
T^{wi}	Internal wall temperature $[°C]$
u	General input vector
UA^{rad}	Thermal conductance from radiator to zone [W/K]
UA^{tank}	Thermal conductance of the tank exterior [W/K]
v	Start-up of a power plant (binary decision variable)
V^{tank}	Volume of a DHW tank $[m^3]$
w	Shut-down of a power plant (binary decision variable)
w_{ls}	Weighing factor load shaping
w_t	Rescaling factor of a time period to a year
x	General state vector
y	General output vector
z^{dhw}	Heat pump able to supply DHW (binary decision variable)
$z^{hp,dhw}$	Heat pump commitment to DHW (binary decision variable)
$z^{hp,sh}$	Heat pump commitment to space heating (binary decision variable)
z^{pp}	Commitment status of a power plant (binary decision variable)

Contents

Abstract v

Abbreviations ix

Nomenclature xiii

Contents xvii

1 Introduction 1

1.1 Context and motivation 1

1.2 Goal and research questions 2

1.3 Outline 3

1.4 Main assumptions 5

1.5 Focus 6

2 Concepts and boundary conditions 7

2.1 Concepts and definitions 7

2.1.1 Optimal control 7

2.1.2 Demand side management 9

2.2 General boundary conditions 11

2.3 Electric power system operational research 13

2.3.1 Unit Commitment and Economic Dispatch model [169] 14
2.3.2 Merit Order model 15
2.4 Building performance simulation 16
2.4.1 Building structure 17
2.4.2 Occupant behavior 18
2.4.3 Weather 21
2.5 Conclusion 22

3 Integrated model development 23
3.1 Introduction 23
3.2 Review of demand response with heat pumps: integrated models 27
3.2.1 Models with focus on the supply side 27
3.2.2 Models with focus on the demand side 28
3.2.3 Integrated operational models 28
3.3 Emulator building level model 30
3.4 Reduced order building level model 32
3.4.1 Heat pump model 33
3.4.2 Domestic hot water tank 36
3.4.3 Heat emission system 39
3.5 Verification with respect to the emulator model 39
3.6 Aggregation with respect to user behavior 46
3.7 Integrated model set up 49
3.8 Typical output integrated model 53
3.9 Conclusion 55

4 Comparison integrated model to other modeling approaches in the literature 57
4.1 Introduction 57

4.2 Methodological case study 59
4.3 Comparison of different modeling approaches 60
4.3.1 Integrated model results 61
4.3.2 Unit commitment and economic dispatch models with a price elasticity model on the demand side 65
4.3.3 Unit commitment and economic dispatch models with virtual generator models on the demand side 66
4.3.4 State-space models with a price profile-model on the supply side 68
4.3.5 State-space models with a merit order model on the supply side 71
4.3.6 Model comparison 73
4.4 Conclusion 74

5 Case study I: Greenhouse gas abatement cost of heat pumps in a Belgian residential context 77

5.1 Introduction 77
5.2 Methodology 79
5.2.1 CO_2 abatement cost 80
5.2.2 Integrated model description 82
5.3 Results 88
5.3.1 CO_2 abatement cost 89
5.3.2 CO_2 emissions 90
5.3.3 Operational aspects 93
5.3.4 Peak capacity 96
5.4 Discussion 98
5.5 Conclusion 101

6 Case study II: Impact of market penetration 103

6.1 Introduction . . . 103
6.2 Methodology . . . 104
6.3 Results: reference case . . . 107
6.3.1 Operational cost savings . . . 108
6.3.2 Peak shaving . . . 112
6.4 Results: influence of the DR technology . . . 113
6.4.1 Flexibility in building thermal mass . . . 113
6.4.2 Flexibility in DHW tank . . . 116
6.4.3 DR technology and peak shaving . . . 118
6.5 Results: influence of the RES share . . . 119
6.6 Discussion . . . 123
6.7 Conclusion . . . 124

7 Comparison of DR incentives in attaining integrated model performance 127

7.1 Introduction . . . 127
7.2 Methodology . . . 129
7.2.1 Models and parameters . . . 130
7.2.2 Incentive scenarios . . . 132
7.3 Results . . . 135
7.3.1 Illustration of model output . . . 135
7.3.2 Best case DR potential . . . 137
7.3.3 Comparison of incentives scenarios . . . 138
7.3.4 Comparison on metrics . . . 141
7.3.5 Hybrid incentive scenarios . . . 142
7.4 Discussion . . . 143
7.5 Conclusion . . . 146

8 Demand response: implications for residential heating system design 147

8.1 Introduction 147

8.2 Combined design and control optimization framework 151

8.2.1 Optimization problem set-up 151

8.2.2 Objective function 153

8.2.3 Heat demand 153

8.2.4 Heating system 154

8.2.5 Electricity generation 160

8.3 Case study 163

8.3.1 General 163

8.3.2 Buildings 164

8.3.3 Heating system 164

8.3.4 Electricity system 164

8.3.5 Disturbance profiles 166

8.3.6 Scenarios 167

8.4 Results 169

8.4.1 Example result of integrated design and control 169

8.4.2 Results with fixed design (selection and sizing) 171

8.4.3 Results with fixed selection 172

8.4.4 MILP results 176

8.4.5 Sensitivity analysis 179

8.5 Discussion 183

8.6 Conclusion 187

9 Conclusion 189

9.1 Main conclusions 189

9.2 Critical reflections 193

9.3 Recommendations for future research 194

Bibliography **197**

Curriculum **215**

List of publications **217**

Chapter 1

Introduction

1.1 Context and motivation

On 22 April 2016, 175 countries signed the Paris agreement, stating as one of the main goals to keep the increase in global average temperature below $2\,^{\circ}C$ above pre-industrial levels [168]. To attain the $2\,^{\circ}C$ limit, the energy related greenhouse gas (GHG) emissions in 2040 should be less than the GHG emissions in 1990, while the global economy is expected to grow more than twofold [21, 128], a major challenge. Residential and commercial buildings make up a quarter of these energy related GHG emissions [103] and hence represent an important sector in this context.

In the European Union, the European Commission has set out a roadmap for the building sector to reduce its GHG emissions by about 90 % in 2050 compared to the year 1990 [59]. First, this goal is being pursued by setting rigorous efficiency standards, as the obligation that all new buildings from 2020 onward should be "nearly zero energy buildings" (NZEB) and by stimulating major renovations in existing buildings [63]. Second, the remaining energy demand should to a large extent be covered by local renewable energy [63] or by shifting energy demand towards low carbon electricity by means of heat pumps [59].

The present work focusses on the second step: the use of low carbon electricity by means of heat pumps in the building sector, and more precisely, in the residential building sector. As outlined in multiple future energy scenarios [21, 46], electricity stemming from PV-panels and wind turbines will play a vital role in achieving this low carbon electricity. These two renewable energy sources (RES) show numerous advantages, such as a vast potential, decreasing

investment cost [29] and zero marginal operational cost and GHG emissions. The two main drawbacks of these RES are its limited predictability and variability, which can cause curtailment and hence can lower the value of these RES. In an electricity system where demand and supply must be balanced at all times, these two drawbacks pose great challenges. The current work focuses on the issue of variability and hence does not consider limited predictability.

In order to gain a better match between electricity demand and electricity generation by variable RES, demand response (DR) will play an important role [164]. Demand response is defined by the U.S. Federal Energy Regulatory Commission as "*changes in electric use by demand-side resources from their normal consumption patterns in response to changes in the price of electricity, or to incentive payments designed to induce lower electricity use at times of high wholesale market prices or when system reliability is jeopardized*". Technically, demand response will be attained as an application of the so-called smart grid: the integration of information and communication technology (ICT) with the electric system [65]. In a residential context, the typical electricity-driven applications that can participate in demand response are electric vehicles, white good appliances and thermostatically controlled loads such as heat pumps [52]. These applications can shift their electricity demand in time without compromising the delivery of their service.

The presented work investigates the application of demand response on heat pumps in a residential context and its potential in tackling the challenges of variable electricity generation by PV-panels and wind turbines. Heat pumps in residential buildings show potential for demand response since they translate a heat demand into an electricity demand, and thermal energy storage (TES) can be exploited in the building structure [153, 81], domestic hot water tank [174] or by installing a dedicated tank for TES [6]. This TES allows decoupling in time of the electricity demand from the thermal demand, in order to tackle the aforementioned challenges without compromising thermal comfort. As stated by Strbac [164], one of the main factors hampering the application of demand response, is a thorough quantification of the benefits associated with DR.

1.2 Goal and research questions

The main goal of this work is *to investigate the potential of residential heat pumps in demand response and the potential benefits for the electricity generation system.* The Belgian context typically serves here as a case study for the potential studies. The goal of this work can be translated in following research questions:

- How should the interaction between residential heat pumps and the electricity generation system be modeled?
- What are the maximum attainable benefits from applying DR to residential heat pumps?
- How could DR with residential heat pumps be realized in practice?
- Will the residential heating system be designed differently in order to benefit from the DR potential?

In order to answer these research questions (see Figure 1.1), this work features the development of a bottom up representation of the flexibility potential of residential buildings with heat pumps. The resulting linear model is combined with an electricity generation model into an integrated model. Furthermore, this integrated model is applied to a number of case studies in order to answer the above mentioned research questions. Finally, the integrated model is combined with a heating system design optimization to answer the last research question.

1.3 Outline

Figure 1.1 illustrates how the research questions formulated above are addressed in the following chapters.

Chapter 2 provides the major concepts and definitions used throughout this work. Furthermore, this chapter describes in depth the most important boundary conditions in this work: the residential buildings and the central electricity generation system. Both boundary conditions are explicitly modeled throughout this work.

Chapter 3 provides a literature review on modeling approaches towards demand response with heat pumps. Furthermore, this chapter develops the integrated model which combines the operational aspects of the residential buildings, heat pumps and electricity generation system. In order to allow this system integration, a bottom-up model of the residential buildings with heat pumps is developed.

Chapter 4 shows the added value of the integrated modeling approach with respect to typical other approaches in the literature, which typically study the perspective of either the building owner or the electricity generation system.

Chapters 5 and 6 apply the integrated model to case studies. In chapter 5, a wide range of different building types and heating system types are compared

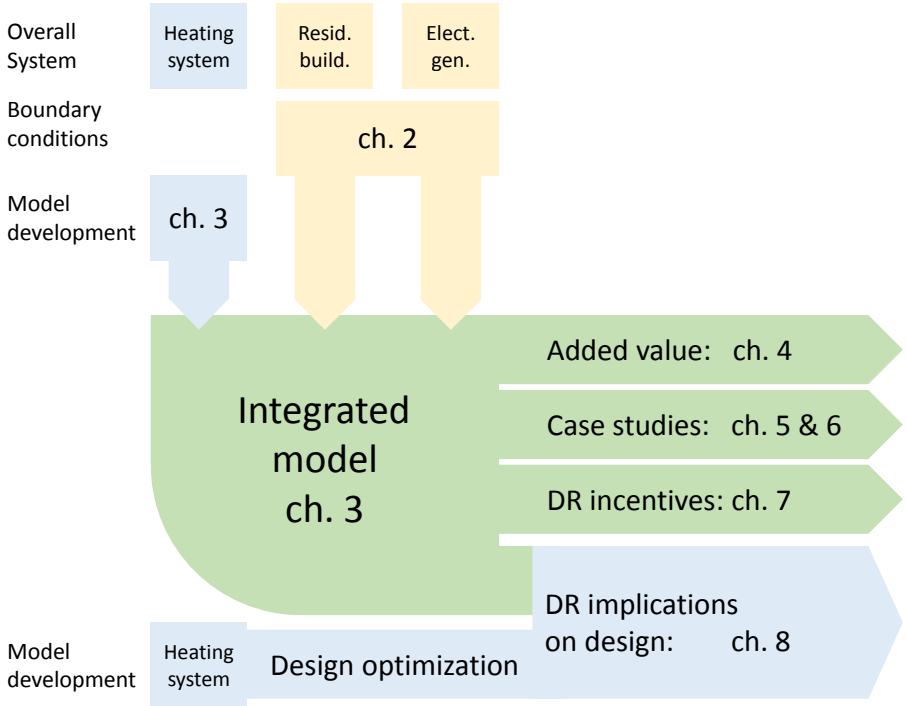

Figure 1.1: This thesis studies the interaction between heating systems in residential buildings (resid. build.) and the electricity generation system (elect. gen.). Chapters 2 and 3 develop the integrated model, which is used for a number of studies in chapters 4 to 8. In Chapter 8, this integrated model is combined with design optimization of the heating system.

based on their CO_2 emissions, investment cost and potential for peak shaving, which is summarized in a CO_2 abatement cost. In chapter 6, the sensitivity of the DR potential is investigated towards market penetration, temperature setpoints and size of the domestic hot water tank.

Chapter 7 explores how the benefits of applying DR to residential buildings with heat pumps, can be realized in practice. Two typical approaches based on either price information or load profile information are compared as well as hybrid approaches. Here, the integrated model serves as an upper bound to which savings are attainable.

Chapter 8 combines heating system design optimization with the integrated model. Hence, it investigates whether the residential heating system design will

reap financial benefits from the DR context. Does complementing a heat pump with other heating system components, such as a back-up gas boiler, a thermal energy storage tank for space heating, solar thermal panels or rooftop PV, present added value in terms of equivalent annual cost and/or CO_2 emissions?

Finally, chapter 9 summarizes the conclusions of the different chapters and provides an outlook on future research.

1.4 Main assumptions

As with all research, assumptions were made in order to keep the problem size feasible. What follows are the main assumptions used throughout this work.

First, the electricity transmission and distribution grid are assumed to be a copper plate: they do not pose any congestion problems and do not show losses. This work only considers the interaction with the electricity generation system, which entails that supply and demand of electricity must be balanced at all times. The inclusion of electricity grids, with all their characteristics, is recommended as a research topic within the electrical engineering field. Also, considering the grid as a copper plate nullifies the difference between rooftop and large-scale PV systems. Only Chapter 8 considers the difference between both.

Second, there is no competition from other technologies in performing demand response. Hence, electric vehicles, flexible industrial processes and white good appliances all operate as if there were no incentives to modify their electricity demand. Also competition with import and export of electricity is neglected. From this, it follows that at a moment where electricity generation by RES exceeds the electricity demand, this overproduction is either used by the heating systems or it is curtailed. However, the methodological framework allows extension to these competitive technologies.

Third, the DR potential is regarded from a systems perspective: there is perfect competition between all involved parties and their total cost is minimized. The influence of imperfect market operation could be a topic for further research.

Finally, the presented operational models employ perfect predictions of all disturbances involved. Hence, on an electricity generation level, the capacity and imbalance markets are not studied and the uncertainty related to imperfect predictions of the demand side is neglected.

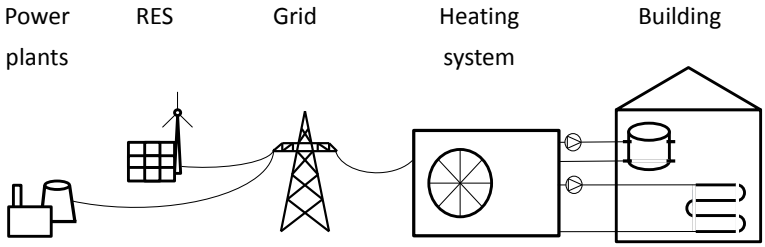

	Power plants	RES	Grid	Heating system	Building
Modeled	v	v	x	v	v
Control	v	(v)	x	v	(v)
Design	(v)	x	x	v	x

Figure 1.2: Summary of the focus of this thesis.

1.5 Focus

Figure 1.2 summarizes the focus of this thesis. The electricity generation side, consisting of dispatchable power plants and RES, is explicitly modeled to set the correct monetary incentives in dealing with the variability of RES. This variability is tackled by altering the control of heat pumps in residential buildings.

In terms of control, the studied control actions are: the commitment and dispatch of power plants, the curtailment of RES and the control of the heat pump in supplying space heating and domestic hot water. Low-level building controllers are not considered.

Considering design in the electricity generation system, only the investment in peak power plant capacity is studied. On the residential building level, the heating system design in this context is studied extensively in Chapter 8.

The added value of this thesis lies in five points. First, a bottom-up heating system model is developed that fits in an integrated model. This integrated model studies the interaction with the electricity generation system and the flexibility in residential buildings. Second, this work shows the added value of this integrated model with respect to other approaches in the literature. Third, the potential of demand response for residential heat pumps is studied. Fourth, ways of practically employing this integrated model to attain DR are studied. Finally, the impact of RES variability on residential heating system design is illustrated.

Chapter 2

Concepts and boundary conditions

The aim of this chapter is twofold. First, Section 2.1 presents the main concepts and definitions employed in this dissertation, in order to avoid repetition throughout the text. Second, Section 2.2 illustrates how this work is at the crossroad of two different research fields: electric power system operational research (Section 2.3) and building performance simulation (Section 2.4). Finally, Section 2.5 concludes this chapter.

2.1 Concepts and definitions

This section describes a number of concepts and definitions which are used throughout the thesis, in the fields of optimal control (Section 2.1.1) and demand side management (Section 2.1.2)

2.1.1 Optimal control

Consider a physical system for which the state at a discrete time step[1] j can be fully described by a state vector x_j containing a set of physical properties of that system. When controlling this system, some inputs u_j can be manipulated

[1] In this work, the words 'time step' and 'time instant' generally mean the same, except in the context of modeling of thermal energy storage.

in order to get a desired set of outputs y_j. Given that the dependencies between these states, inputs and outputs are first order differential equations, this system can be represented by a linear state space model:

$$\forall j : x_{j+1} = \mathbf{A} \cdot x_j + \mathbf{B} \cdot u_j \tag{2.1}$$

$$\forall j : y_j = \mathbf{C} \cdot x_j + \mathbf{D} \cdot u_j \tag{2.2}$$

with $\mathbf{A}$, $\mathbf{B}$, $\mathbf{C}$ and $\mathbf{D}$ the time-invariant real matrices depending on the parameters of the system. Disturbances are assumed to be perfectly known throughout this work and can thus be included in the inputs vector u_j.

Given that there is a cost $cost(x_j, u_j)$ associated with operating this linear system over a number of j_{max} time steps, this cost can be minimized by solving the optimal control problem (OCP):

$$\min \sum_{j=0}^{j_{max}} cost(x_j, u_j) \tag{2.3}$$

subject to

$$\forall j : x_{j+1} = \mathbf{A} \cdot x_j + \mathbf{B} \cdot u_j \tag{2.4}$$

$$\forall j : ineq(x_j, u_j) \geq 0 \tag{2.5}$$

$$\forall j : eq(x_j, u_j) = 0. \tag{2.6}$$

The aforementioned state space model hence becomes a set of equality constraints in the optimization, assuring that the dynamics of the system are respected. Note that the system output and the associated output equation (Eq. 2.2) are typically omitted in an OCP, since all states are explicitly known. Additional operational inequality $ineq(x_j, u_j)$ and equality $eq(x_j, u_j)$ constraints can be added to make sure that the system behaves properly. If these constraints and the cost functions are linear operations of x_j and u_j, the optimization problem (Eq. 2.3 - Eq. 2.6) is a linear programming (LP) problem. Throughout this work, the optimization software package CPLEX is generally used to solve this LP problem, solving a problem with 10^5 variables in the order of seconds.

The other type of OCP in this study is an extension of Eq. 2.3 - Eq. 2.6 with boolean decision variables bd_j which are either 0 or 1 in time step j. This variable denotes whether a certain component in the system is on or off. The OCP is hence:

$$\min \sum_{j=0}^{j_{max}} cost(x_j, bd_j, u_j) \tag{2.7}$$

subject to

$$\forall j : ineq(x_j, bd_j, u_j) \geq 0 \tag{2.8}$$

$$\forall j : eq(x_j, bd_j, u_j) = 0. \tag{2.9}$$

In this type of OCP, the state space notation is less common. The dynamical constraints are incorporated in the equality constraints. Including boolean decision variables makes the optimization problem (Eq. 2.7 - Eq. 2.9) a mixed integer linear programming (MILP) problem. Again, CPLEX is used to solve the optimization problem throughout this work. The MILP problem is much harder to solve than the LP problem: an optimization could take hours up to days without reaching a desirable solution. Typically, the optimization problem is terminated when a certain user-determined optimality gap is reached or when a certain maximum calculation time is reached. When solving the MILP problem, the solver first determines the best attainable linear solution by relaxing all boolean decision variables to real variables between 0 and 1. The difference between this relaxed linear solution and the best attained solution with a certain combination of boolean decision variables, is defined as the optimality gap.

2.1.2 Demand side management

According to Strbac [164], demand side management (DSM) groups a range of measures aimed at a more efficient use of existing electricity generation, transmission and distribution infrastructure as well as improving the balance with variable RES. In the case of an existing infrastructure, the aim is generally to reduce electricity demand at times of high peak demand and grid congestion, which would otherwise need expensive infrastructure investments. In the case of improving the balance with variable RES, this entails the temporary increase or decrease in demand when RES generation is very high or low respectively. Additionally, Gellings [71] also includes in the concept of DSM the strategic conservation of energy, stimulated by utilities. This is performed in order to address shortages in generation capacity, fuels or strained hydro resources. Finally, Warren [184] notes that DSM in the form of energy efficiency is also pursued by policy makers, driven by environmental and economical concerns.

Palenski and Dietrich [129] identified the range of DSM measures as: energy efficiency, time of use tariffs (TOU), spinning reserve (SR) and demand response (DR) (Figure 2.1). Energy efficiency implies the permanent reduction in electricity demand, which could coincide with times of peak electricity demand. The other measures are aimed towards shifting the electricity demand in time, instead of an overall reduction. Time of use tariffs aim at reducing the demand at typical peak periods throughout the day (17h-19h) or shift a large fraction

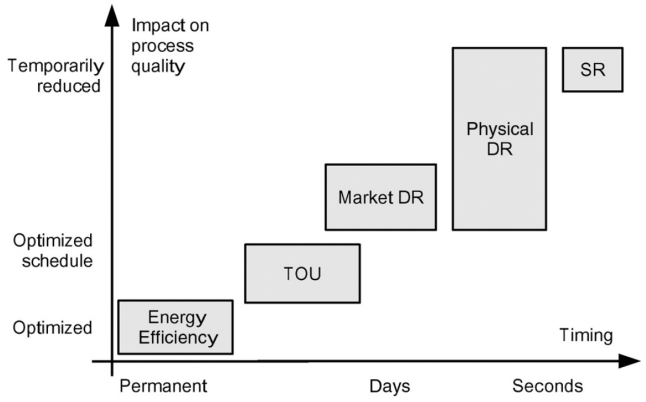

Figure 2.1: Overview of the different measures that fall under demand side management. Figure from Palensky and Dietrich [129].

of the demand to the night to increase the share of base load power plants. An electrical load could also be employed to provide spinning reserves, where it aids in maintaining the correct frequency of the electrical grid. This is typically performed in time scales within one hour.

In this thesis, the focus is on demand response. Here, demand response entails the preheating of the building structure or domestic hot water tank, in order to avoid electricity demand later on. This is done to avoid costs for the electricity generation system, while maintaining thermal comfort. This work does not consider the cost savings for the consumer. In practice, part of the cost savings for the electricity generation system will trickle down to the consumer through certain compensation schemes. The typical time scale of preheating in this work is one hour (the smallest time step considered) to one week (the longest OCP horizon considered). The term DR is used to describe this, while a large variety of terms are used throughout the literature, which in some cases mean the same thing:

- Market and physical DR [129] where market DR is stimulated by economical incentives while physical DR refers to automated grid support.
- Automated demand response (e.g. www.openadr.org) which is an open communication standard to realize DR in a practical setting.
- Active and passive DR where active DR is basically the same as the definition used for DR in this thesis while passive DR attains a demand reduction without consumer interaction, for example through rolling blackouts.

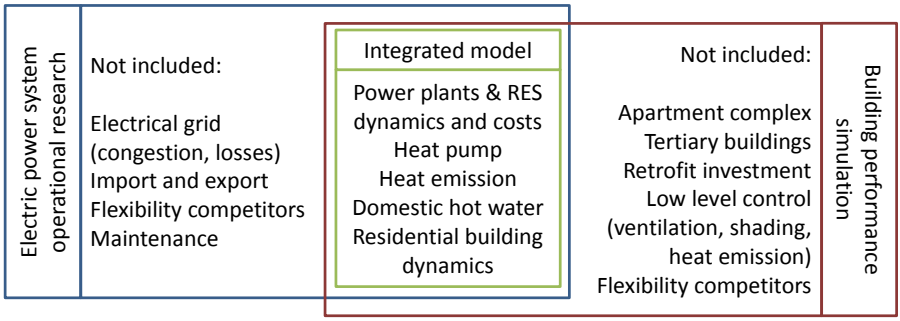

Figure 2.2: An integrated model is developed which combines elements from power system operational research and building performance simulation.

- Load shaping [88] involves the change of electricity demand in time in order to obtain a desirable load profile throughout time.
- Load shifting [71] entails the shifting of electricity demand from peak periods to non-peak periods. In the buildings context, the demand is shifted to before the peak periods in order to maintain thermal comfort.

2.2 General boundary conditions

In order to study the potential of performing demand response with residential heat pumps in tackling the variability of RES, two different systems need to be considered. On the one hand, there is the electric power system, which consists of electricity generation, transmission and distribution. This scale creates the incentives for demand response: operational cost savings for electric power plants (see Section 2.3). On the other hand, there is the building scale which defines the load shifting potential of buildings equipped with heat pumps (see Section 2.4). In this work, both scales are merged in an integrated model (Figure 2.2).

Electric power system Regarding the electric power system, the main interest of this work is to investigate the potential of DR in decreasing costs associated with the variability of RES. Towards this aim, the dynamic aspects and costs of electricity generation from RES and central power plants are explicitly modeled. This is described more in detail in Section 2.3. DR could also contribute to providing reserves as shown by Bruninx [25]. In a case study, Bruninx illustrated that providing reserves with residential heat pumps increases the

total operational cost savings for the electricity generation by 1 % on top of the 6 % cost savings attained by load shifting.

DR can also decrease costs associated with grid congestion, but this is not considered in this thesis. As such, the transmission and distribution grid are assumed to be a copper plate and pose no congestion problems or losses. The distribution grid can be a significant bottleneck for local PV [13], electric vehicles [33] and heat pumps [146]. This poses opportunities for local DR, for example by preheating DHW storage tanks [40] or altering load schedules for electric vehicles [32]. Congestion on the transmission grid can also present opportunities for DR, where it can aid in avoiding high local electricity prices [23]. Congestion might limit the DR potential of residential heat pumps studied in this work. For example, a coordinated electricity demand due to DR in response to curtailment of RES, could not be attainable for the electric grid. Furthermore, Belgium is electrically regarded as an island: no import or export of electricity is considered[2]. As identified by Tröster et al. [167], investing in the order of tens of billions EUR in the European transmission grid capacity can roughly half the curtailment of RES, but this potential is not studied in this work.

Throughout this work, no competition in providing flexibility from industry, electric vehicles, pumped hydro storage and energy storage is considered. In practice, these flexibility providers can be complementary to residential heat pumps, as shown in a case study with pumped hydro storage [25]. However, the combination of having both flexibility in the electricity demand of residential heat pumps and in one of the competing flexible demands, can also lead to cost savings which are lower than the sum of both separately, as shown for the combination of heat pumps and electric vehicles in [130].

Given these assumptions, when electricity generation from RES exceeds the electrical demand there are only two choices: either to increase the electricity demand of the heat pumps or to curtail this generation. *Hence, in this study, curtailment of RES is driven by the electricity generation system and not by grid congestion.* The main occurrence of curtailment stems from electricity generation from RES overshooting electricity demand. Finally, power plant outages and costs associated with maintenance of the electricity generation system are not taken into account.

Building and heating system On the building scale, the dynamics of the building and heating system are explicitly modeled in order to accurately represent their flexibility. The dynamics of the building structure are modeled

[2]This is in sharp contrast with the current reality for Belgium, where about a quarter of the electricity was imported during 2015 [54].

in order to represent its load shifting potential offered by its thermal capacity. A detailed description of these dynamics is given in Section 2.4. Furthermore, the heating system is included, which consists of a heat pump, heat emission and domestic hot water tank. A model is developed for the heating system which is fully described in Chapter 3.

This work focuses on single family residential buildings, hence no apartment complexes or tertiary buildings are included in this study. The vast size of some tertiary buildings make these buildings interesting for DR as altering the control of a few appliances can already unlock the flexibility in the order of megawatts. The DR potential of these building types has already been thoroughly studied in the literature [73, 83, 105] and will not be considered in this work.

Moreover, the low level controls of ventilation, solar shading and heat emission are not included. These controllers are typically more focused on increasing energy efficiency, such as in [53, 144], than in performing DR. Another assumption in this work is that the building is regarded as one or two thermal zones. Furthermore, it is assumed that there is no feedback from the occupants on the control actions taken.

The resulting model equations of the integrated models are presented in Section 3.7. Section 3.8 provides examples of the output of this model.

2.3 Electric power system operational research

There are numerous modeling approaches for the electricity generation system, depending on the goal and scope. As this thesis focuses on CO_2 emissions and operational cost savings, the electricity generation system is modeled as a unit commitment (UC) and economic dispatch (ED) problem. A UC model aims to schedule the most cost-effective combination of power plants to meet the demand for electric power. The ED model determines the production levels of each unit on the basis of the least cost usage of the committed assets. Using the classification of Delarue [43], this approach assumes perfect competition and a single node electrical network. The model focuses on short term operational aspects which are translated in a single objective: total system operational cost. There is no elasticity of demand considered, except for the heat pump demand which is discussed in Section 3.7.

The resulting equations used throughout this study are based on Van den Bergh et al. [169]. The resulting model is a MILP problem implemented in GAMS 24.4 and MATLAB 2015b, using the MATLAB–GAMS coupling as described by Ferris [68] with CPLEX 12.6 as solver. This Unit Commitment and Economic

Dispatch model is presented in Section 2.3.1. A simplified version of this model is the Merit Order model, presented in Section 2.3.2.

In this work, the typical power plant types considered for electricity generation are nuclear power plants, coal-fired power plants and to a minor extent oil-fired power plants. Furthermore, gas-fired power plants are considered which are split up between combined cycle gas turbines (CCGT) and the less efficient open cycle gas turbine (OCGT).

2.3.1 Unit Commitment and Economic Dispatch model [169]

The optimization criterion is to minimize total operational cost of the electricity generation system composed of electric power plants with index i and over all time steps with index j:

$$min \quad \sum_i \sum_j fc_{i,j} + co_2t_{i,j} + sc_{i,j} + rc_{i,j}. \tag{2.10}$$

Towards this aim, the main optimization variables are the generation level ($g_{i,j}^{pp}$) and commitment status (binary variable $z_{i,j}^{pp}$) of each power plant with index i. These determine the fuel cost ($fc_{i,j}$), CO_2 cost ($co_2t_{i,j}$), start-up cost ($sc_{i,j}$) and ramping cost ($rc_{i,j}$):

$$\forall i, \forall j : fc_{i,j} = cf_i \cdot z_{i,j}^{pp} + mf_i \cdot (g_{i,j}^{pp} - g_i^{min} \cdot z_{i,j}^{pp}) \tag{2.11}$$

$$\forall i, \forall j : co_2t_{i,j} = co_2p \cdot [ct_i \cdot z_{i,j}^{pp} + mt_i \cdot (g_{i,j}^{pp} - g_i^{min} \cdot z_{i,j}^{pp})] \tag{2.12}$$

$$\forall i, \forall j : sc_{i,j} = stco_i \cdot v_{i,j} \tag{2.13}$$

$$\forall i, \forall j : rc_{i,j} \geq raco_i \cdot (g_{i,j}^{pp} - g_{i,j-1}^{pp} - v_{i,j} \cdot g_i^{max}) \tag{2.14}$$

$$\forall i, \forall j : rc_{i,j} \geq raco_i \cdot (g_{i,j-1}^{pp} - g_{i,j}^{pp} - w_{i,j} \cdot g_i^{max}) \tag{2.15}$$

in which the binary variables $v_{i,j}$ and $w_{i,j}$ respectively denote a start-up or shut-down of power plant i in time step j. The parameter cf_i is the fuel cost for running the plant at its minimum power level (g_i^{min}) and mf_i is the marginal cost for the generation level on top of the minimum power level. The CO_2 emissions also consist of an emission ct_i at minimum power level and a term accounting for the marginal emissions (mt_i). The CO_2 cost is then determined via a CO_2 price co_2p. Furthermore, $stco_i$ and $raco_i$ respectively denote the start-up cost and ramping cost of power plant i. In determining the ramping cost, the maximum power level (g_i^{max}) is conditionally subtracted in order not to allocate ramping costs to a start-up or shut-down of a power plant.

In each time step, the sum of the generation levels of the power plants and the electricity generation from RES (g_j^{res}) must equal the traditional electricity demand (d_j^{trad}), which is expressed in the market clearing condition:

$$\forall j : d_j^{trad} = cur_j \cdot g_j^{res} + \sum_i g_{i,j}^{pp} \tag{2.16}$$

$$\forall j : \quad 0 \leq cur_j \leq 1 \tag{2.17}$$

with cur_j determining the curtailment of electricity generation from RES. Curtailment costs are assumed to be internal transfers within the model as this study employs a system perspective. Hence, curtailment costs are not explicitly modeled. The only net cost perceived by the system is the opportunity cost of not using the zero-cost RES power available. Finally, each power plant is submitted to a series of technical constraints:

$$\forall i, \forall j : g_{i,j}^{pp} \leq g_i^{max} \cdot z_{i,j}^{pp} \tag{2.18}$$

$$\forall i, \forall j : g_{i,j}^{pp} \geq g_i^{min} \cdot z_{i,j}^{pp} \tag{2.19}$$

$$\forall i, \forall j : g_{i,j}^{pp} \leq g_{i,j-1}^{pp} + \Delta_i^{max,up} \tag{2.20}$$

$$\forall i, \forall j : g_{i,j}^{pp} \geq g_{i,j-1}^{pp} - \Delta_i^{max,down} \tag{2.21}$$

$$\forall i, \forall j : 1 - z_{i,j}^{pp} \geq \sum_{j'=j+1-mdt_i}^{j} w_{i,j'} \tag{2.22}$$

$$\forall i, \forall j : z_{i,j}^{pp} \geq \sum_{j'=j+1-mut_i}^{j} v_{i,j'} \tag{2.23}$$

$$\forall i, \forall j : z_{i,j-1}^{pp} - z_{i,j}^{pp} + v_{i,j} - w_{i,j} = 0. \tag{2.24}$$

The maximum ramping-up ($\Delta_i^{max,up}$) and maximum ramping-down ($\Delta_i^{max,down}$) values are derived from the maximum ramping rates of the power plants. The minimum up-time and down-time of power plant i is denoted by mut_i and mdt_i respectively.

2.3.2 Merit Order model

In this thesis, the simulations with the UC and ED model usually take hours to solve. To avoid these long computation times, a simplification is in some cases

employed, namely a Merit Order (MO) approach. A full comparison between both approaches is performed in Section 4.3.5. In this approach, all dynamic constraints and associated start-up costs and ramping costs are neglected. The equations of the Merit Order model are:

$$min \quad \sum_i \sum_j fc_{i,j} + co_2t_{i,j} \tag{2.25}$$

subject to:

$$\forall j : d_j^{trad} = cur_j \cdot g_j^{res} + \sum_i g_{i,j}^{pp} \tag{2.26}$$

$$\forall j : \quad 0 \leq cur_j \leq 1 \tag{2.27}$$

$$\forall i, \forall j : fc_{i,j} = cf_i \cdot z_{i,j}^{pp} + mf_i \cdot (g_{i,j}^{pp} - g_i^{min} \cdot z_{i,j}^{pp}) \tag{2.28}$$

$$\forall i, \forall j : co_2t_{i,j} = co_2p \cdot [ct_i \cdot z_{i,j}^{pp} + mt_i \cdot (g_{i,j}^{pp} - g_i^{min} \cdot z_{i,j}^{pp})] \tag{2.29}$$

$$\forall i, \forall j : g_{i,j}^{pp} \leq g_i^{max} \cdot z_{i,j}^{pp} \tag{2.30}$$

$$\forall i, \forall j : g_{i,j}^{pp} \geq g_i^{min} \cdot z_{i,j}^{pp}. \tag{2.31}$$

Hence, in each time step the generation level and commitment status are determined in order to meet the market clearing condition. This is determined regardless of what happens in other time steps. The minimum operating points of the power plants are still respected, which necessitates the integer decision variable of the commitment status. The MO model is hence still a MILP problem, but only takes of the order of minutes to solve.

2.4 Building performance simulation

Regarding building performance simulation, Spitler [162] states that:

> *Simulation of building thermal performance using digital computers has been an active area of investigation since the 1960s, with much of the early work focusing on load calculations and energy analysis. Over time, the simulation domain has grown richer and more integrated, with available tools integrating simulation of heat and mass transfer in the building fabric, airflow in and through the building, daylighting, and a vast array of system types and components.*

In this work, only the elements that appear relevant for studying the flexibility of heat pump operation were taken from building performance simulation. As such, the thermal dynamics of the building structure (Section 2.4.1) are considered along with the most relevant boundary conditions: the occupant behavior (Section 2.4.2) and weather conditions (Section 2.4.3). The dynamics of the heating system are described in Chapter 3.

2.4.1 Building structure

The heating demand of a building depends on the heat transfer in the building structure by transmission and ventilation losses. Given the heat capacity of the indoor air, furniture and building materials, this heating demand will be a dynamic phenomenon. This dynamic behavior can be modeled using different levels of detail.

In this work, the highest level of detail in the dynamics of the building structure is based on models available in the IDEAS library in Modelica, described by Baetens et al. [13]. The building structure is modeled using a finite volume method of all components and this is complemented by a detailed radiative heat transfer model. This modeling environment has been verified and validated using the BESTEST methodology [91]. In the remainder of this text, a building model developed according to this approach will be referred to as “emulator building model". However, this modeling approach features highly non-linear equations, which are impractical for the envisioned integrated model.

By applying system identification using the emulator building models, Reynders et al. [152] deduced linear models of the building structure. Figure 2.3a shows an example of such a linear model with five states. These five states are the indoor air temperature T^i and the temperature of inner walls T^{wi}, roof T^{roof}, floor T^f and exterior walls T^{we}. These states are lumped in the vector T_j^{sh} where index j represents the time step. The thermal capacities and heat transfer coefficients associated with these states have the same indices. Inputs to the model are the ambient air temperature T_j^e, ground temperature T^g and the heat gains due to solar irradiation $\dot{Q}_j^{sol}$, internal gains $\dot{Q}_j^{int}$ and heat emission $\dot{Q}_{s,j}^{emi}$. This model shows a root mean square error (RMSE) error of only $0.3\,°C$ on a two day ahead prediction of the indoor air temperature of the detailed physical model. Figure 2.3b shows the comparison between both models. The linear model can be translated in the following state space equations:

$$\forall s, j : T_{j+1}^{sh} = \mathbf{A}^{sh} \cdot T_j^{sh} + \mathbf{B}^{sh} \cdot [\dot{Q}_j^{emi}, T_j^e, T_j^g, \dot{Q}_j^{sol}, \dot{Q}_j^{int}] \tag{2.32}$$

with state space matrices $\mathbf{A}^{sh}$ and $\mathbf{B}^{sh}$ based on the thermal capacities and resistances shown in Figure 2.3a.

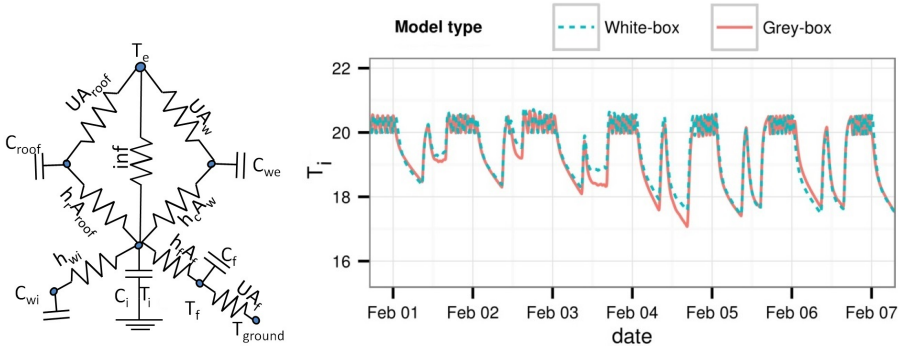

(a) Linear building model (b) Comparison of indoor temperature for linear (Grey-box) and detailed physical (White-box) model

Figure 2.3: The linear model (left) comprises of five thermal capacities and hence five states is able to approximate the behavior of the detailed physical model (right). Figure from Reynders et al. [152]. Heat transfer coefficients are denoted by h and U, while A represents surface area and C thermal capacitance.

In a later stage, Reynders et al. [151] also developed a more detailed linear model of the building (Figure 2.4). In contrast to the model of Figure 2.3a which considers the building as one thermal zone, the building is now split up in two thermal zones. The first zone is the “day zone" which contains all rooms in which the occupants are active by day. The second zone, “night zone", consists of the bedrooms and all other rooms. Both zones typically have different comfort requirements regarding temperature setpoints.

Both linear models are used throughout this text. The one zone model (Figure 2.3) is employed in the two following chapters (Chapter 3 and 4). The two zone model (Figure 2.4) is used in the remaining chapters (Chapters 5 to 8).

2.4.2 Occupant behavior

Another factor that influences a buildings heating demand is the occupancy behavior, which determines the setpoints for the indoor air temperature and the demand for domestic hot water (DHW). Since the heat demand is calculated dynamically, also the time schedules of these setpoints and DHW demand are important. In this work, these setpoints and DHW demand profiles are fixed, predetermined profiles. These profiles were based on the work of Richardson et al. [154] and Baetens and Saelens [14] and are shown in Figure 2.5.

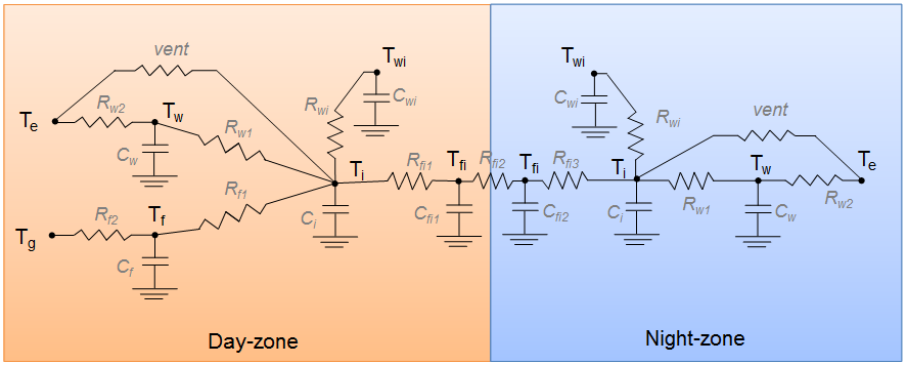

Figure 2.4: The structure of the reduced order building model as developed by Reynders et al. [151]. The day zone consists of 5 states: the temperatures of the indoor air (T^i), internal walls (T^{wi}), external walls (T^w), ground floor (T^f) and floor connecting the day zone and night zone (T^{fi}). The night zone also has a state for this connection, along with a temperature for indoor air, internal walls and a lumped state for external walls and roof (T^w). The parameters for the different R and C values can be derived based on Protopapadaki et al. [147]. The ambient air temperature (T^e) and ground temperature (T^g) are boundary conditions to the model. Figure from Reynders et al. [151]

Richardson et al. [154] provide profiles for occupancy through a Microsoft Excel workbook. These profiles are generated by the Markov-Chain technique, based on time-use survey data from the UK in 2000. These survey data only provide information on when the occupants are present and awake. Hence, this data can only be used when the building is regarded as one thermal zone. Based on Peeters et al. [140], the lower temperature setpoint is 20 °C when the occupants are present and awake and 16 °C when they are not. The upper bound for thermal comfort is taken to be 24 °C. The domestic hot water demand is based on Peuser et al. [143].

The “StROBe" model of Baetens and Saelens [12, 14] provides a more complete data set for determining the heat demand of a residence. This includes the temperature set points for aforementioned day and night zones along with domestic hot water demand and internal heat gains. The profiles are generated using survival models and are based on a Belgian time-use survey from 2005. In previous work of the author [7, 137, 138], the profiles Baetens1 (see Figure 2.5) were employed. For the sake of uniformity, this work employs the profiles Baetens2. This causes a difference in the results of the previous work and Chapters 5 to 7. However, the trends in these results are identical, while the change in the numerical values is less than 5 %.

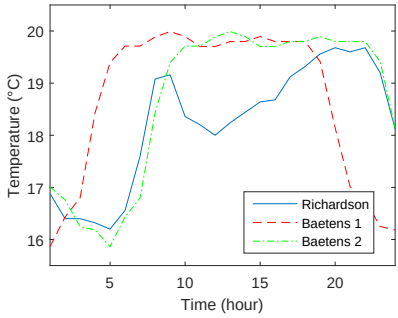

(a) Average lower temperature bound during a weekday

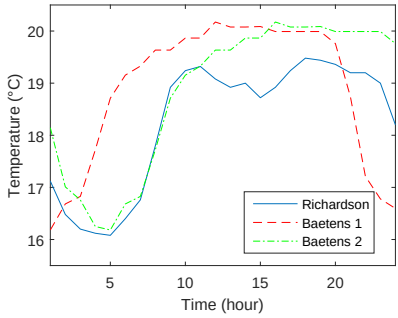

(b) Average lower temperature bound during a weekend day

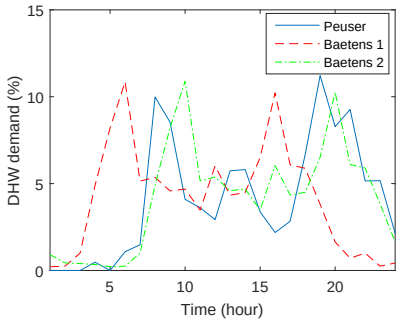

(c) Average DHW demand during a weekday

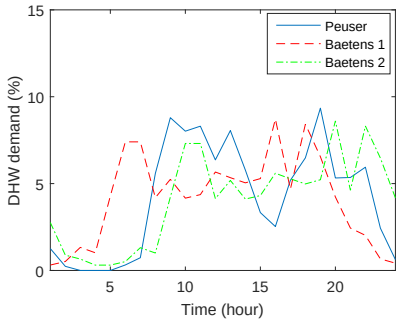

(d) Average DHW demand during a weekend day

Figure 2.5: Average profiles derived for the lower temperature set point from Richardson et al. [154] (Richardson) and DHW demand from Peuser et al. [143] (Peuser). The same data is shown from Baetens and Saelens [154] (Baetens1 and Baetens2).

The temperature set points determine the minimum ($T_j^{sh,min}$) and maximum ($T_j^{sh,max}$) temperature bounds for the appropriate state of the state vector T_j^{sh}:

$$\forall j : T_j^{sh,min} \leq T_j^{sh} \leq T_j^{sh,max}. \tag{2.33}$$

This equation is a hard constraint on the indoor air temperature, which means thermal comfort is always met in terms of minimum and maximum allowed temperatures. Given the assumption of perfect predictions of all disturbances and temperature setpoints, it is always possible to attain this thermal comfort throughout this work. Hence, it is not necessary to make a trade-off between

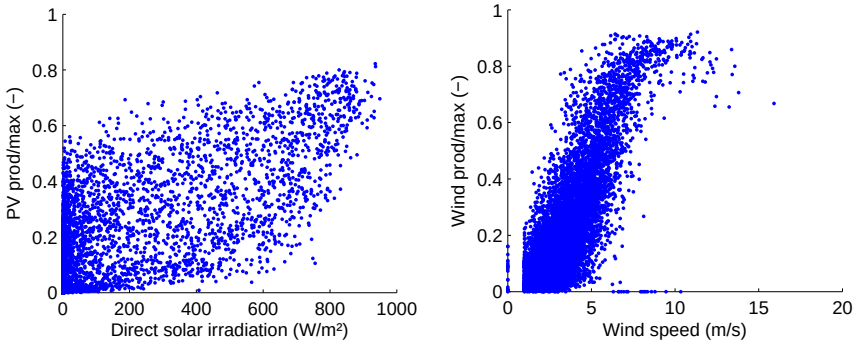

(a) PV production (b) Wind power production

Figure 2.6: Comparison between meteo data and RES production data, respectively on the x and y axis. The meteo data on direct solar irradiation and the wind speed can be correlated to Belgium's PV production (Figure 2.6a) and wind power production (Figure 2.6b) respectively.

thermal comfort and energy cost in this work, as is typically done in studies on model predictive control such as [123, 178].

2.4.3 Weather

The last crucial factor determining the heat demand is the weather, primarily the solar heat gains and ambient air temperature. It is important that these weather profiles are taken from the exact same period as the disturbances to the electricity generation model, being fixed electricity demand and electricity generation from RES. As a consequence, it is not possible to take a standard year for the weather, as is often done in building simulation. The year 2013 in Belgium is chosen, as it is the first year for which the Belgian transmission system operator (TSO) Elia [54] provides full year data on electricity generation from RES.

For the building model, weather measurements in the Belgian city Uccle are taken. In this data set, the average temperature is $10.2\,°C$, the minimal temperature $-9.3\,°C$ and with respect to a reference indoor temperature of $16\,°C$, the number of heating degree days is 2474. The consistency between the weather data and the RES generation is shown in figure 2.6. The PV and wind production are not fully correlated to respectively the direct solar irradiation and the wind speed in the weather measurements as these do not have the same

spatial diversification. For PV, the coefficient of determination (R^2) is 0.614 for a linear fit. For wind, R^2 is 0.678 for a third order polynomial fit. The data of RES production is based on thousands different sites throughout Belgium, while the data from the Belgian meteorological institute is based on measurements on one particular location (Uccle).

2.5 Conclusion

This chapter sets the scene for this thesis by defining the main concepts and boundary conditions. These boundary conditions are explicitly modeled in this study, for which the author acknowledges the work of colleagues listed in the bibliography. The main methodological contributions of this thesis to these boundary conditions are presented in the following chapter that describes the development of the integrated model.

Chapter 3

Integrated model development

Parts of this chapter are based on:
PATTEEUW, D., and HELSEN, L. Residential buildings with heat pumps, a verified bottom-up model for demand side management studies. In International Conference on System Simulation in Buildings Edition 9 (Liège, Belgium, December 2014), pp. 498–516.

3.1 Introduction

This chapter presents an integrated modeling approach to investigate the DR potential of residential buildings with heat pumps. As noted by Strbac [164], this potential assessment is one of the factors hampering a large scale roll-out of flexible demand side technologies. In order to quantify the effects of introducing DR programs, the interaction between the electricity supply (the electricity generation system) and demand side (the residential buildings with heat pumps) is of paramount importance. Many models however still fail to incorporate the interactions between demand and supply in DR programs. Figure 3.1 shows a conceptual schematic of the interdependence of the demand side and the supply side. The electricity price profile, typically the result of a supply side model, is a necessary input to the demand side model. Similarly, the demand for electricity, an output of the demand side model, is a necessary input of the supply side model. In short: the electricity prices change with the demand for electricity

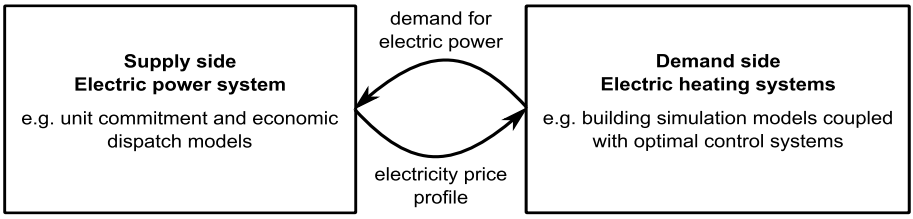

Figure 3.1: Conceptual schematic of the interaction between the supply side, the electricity generation system typically represented via unit commitment and economic dispatch models, and the demand side, heat pumps in this thesis typically studied via building simulation models with optimal control systems.

and vice-versa. In light of this challenge, an integrated model is presented in this chapter.

In the literature on DR, often the supply side or the demand side are represented simplistically, as discussed in Section 3.2. When the focus is on electricity generation, most researchers employ typical unit commitment models and economic dispatch models, extended with an aggregated representation of the flexibility in demand. Two typical representations of the flexible demand side are considered in this work: price-elasticity models [23, 41, 42, 98, 158] and so-called virtual generator models [47, 93, 165, 166]. In contrast, in studies which are focused on the energy demand of buildings, researchers often take the supply side of electricity into account by considering a (fluctuating) electricity price [2, 83, 113, 120, 149, 179]. Although all of these modeling techniques have proven their merits, they are inadequate to study the true interaction between the demand side and the supply side under DR, especially when storage-type customers are involved. Recently, some authors [28, 80, 132, 133, 134, 181, 182, 185] proposed integrated models of both the supply and demand.

The integrated model developed in this chapter falls in this last category. This approach merges two optimization problems (Figure 3.2). The first is the optimal control problem of a residential building with a heat pump f^{dem}. The objective function is typically to minimize the heat pumps' electricity consumption. The second is a unit commitment and economic dispatch model of the electricity generation system f^{gen}, which optimizes the operation of power plants in order to minimize overall system cost. Combining both optimization problems leads to the following optimization problem, called "integrated model" (IM) in this work. A simplified form of this integrated model is given by the following

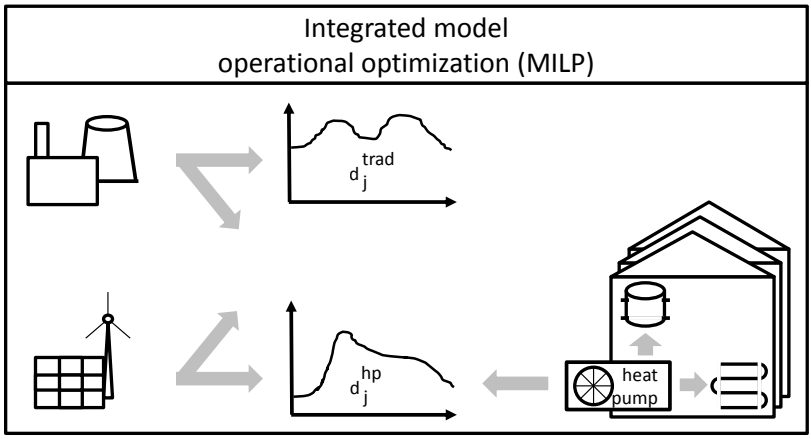

Figure 3.2: Overview of the integrated model, which combines the operational optimization of an electricity generation system and a set of residential buildings with heat pump.

equations:

$$\min \sum_{i,j} cost(g_{i,j}^{pp}) \tag{3.1}$$

subject to

$$\forall j : d_j^{trad} + nb \cdot d_j^{hp} = cur_j \cdot g_j^{res} + \sum_i g_{i,j}^{pp} \tag{3.2}$$

$$\forall i, j : f^{gen}(g_{i,j}^{pp}) = 0 \tag{3.3}$$

$$\forall j : d_j^{hp} = f^{dem}(T_{b,j}). \tag{3.4}$$

Combining both optimal control problems allows for the explicit modeling of the flexibility in the electricity demand of the heat pumps. This explicit modeling allows for a correct representation of the potential of DR for buildings with heat pumps, as shown in Chapter 4.

In this integrated model, electricity can be delivered by power plants $g_{i,j}^{pp}$ or by curtailable (by factor cur_j) renewable energy sources g_j^{res}. The total cost of this electricity generation $cost(g_{i,j}^{pp})$ is minimized, given that the electricity demand is met at all times. This electricity demand consists of two parts, the first of which is the traditional electricity demand d_j^{trad} encompassing all electricity demand except that of the heat pumps. As no competition in providing flexibility is

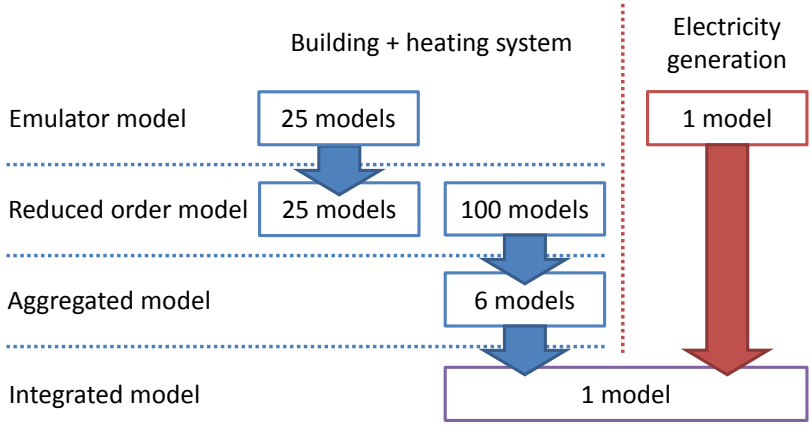

Figure 3.3: This chapter deduces a reduced order model for a set of residential buildings with heat pump by starting from an emulator model. Furthermore, an aggregation methodology is proposed towards user behavior. Finally, this bottom up model is combined with the unit commitment and economic dispatch model to form the "integrated model".

assumed (Section 2.2), this traditional demand is a fixed profile. The second part of the electricity demand stems from heat pumps d_j^{hp} and can be chosen freely as long as the thermal comfort within the residential buildings is guaranteed. A limited number of buildings, with index b, are explicitly modeled ($f^{dem}(T_{b,j})$) in order to represent the building flexibility. The demand is scaled up by a factor nb in order to represent a higher number of buildings equipped with heat pumps and to have a significant impact on the electricity generation system.

The purpose of this chapter is to build up and illustrate the integrated model of the electricity generation system and residential buildings with heat pumps. Section 3.2 presents the other typical modeling approaches taken in the literature. The added value of the integrated model with respect to these other approaches is thoroughly assessed in Chapter 4. What follows is a gradual build up of the integrated model, starting from a detailed emulator model (Figure 3.3). Section 3.3 presents the emulator model for the demand side for which a reduced order model f^{dem} is proposed in Section 3.4 and verified in Section 3.5. In Section 3.6, an aggregation methodology is proposed and assessed which aggregates a large number of similar buildings with different user behavior. This bottom up aggregated model is then combined with the electricity generation model from Section 2.3 in the integrated model. Section 3.7 provides a full overview of this integrated model. Finally, some examples of typical output of this model is provided in Section 3.8.

3.2 Review of demand response with heat pumps: integrated models

Demand response with heat pumps is typically studied from the supply side or demand side perspective of the electricity market. In this section, a review of the state-of-the-art models is presented showing models with a focus on the supply side (Section 3.2.1), models with a focus on the demand side (Section 3.2.2) and models with an integrated approach, taking into account the physical behavior of demand side technologies together with the techno-economic characteristics of the electric power system (Section 3.2.3). The focus is on the literature in which thermostatically controlled loads are subjected to demand response.

3.2.1 Models with focus on the supply side

To study electric power system-wide effects of flexible consumers, most researchers employ typical unit commitment and economic dispatch models, extended with an aggregated representation of the flexibility in demand. Two main representations of the flexible demand side can be identified: price-elasticities and so-called virtual generator models (VGM).

The price-elasticity is a measure of the change in demand in response to a change in the price of electricity. The assumed range of elasticities used in these models typically stem from analyses of historical data [41, 69], sometimes combined with a simulation model [17]. Among others, De Jonghe et al. [41, 42] developed an elasticity-based operational and investment model to determine the optimal generation mix. Sioshansi and Short [158] employed an elasticity-based model, comparable to that proposed in [41], to study the effect of real-time pricing on the usage of wind power. Kirschen and Strbac [98] proposed a general scheme to incorporate the short-term elasticity in generation scheduling and price setting. Bompard et al. [23] studied the effect of demand elasticity on congestion and market clearing prices via a linear price-elasticity model combined with an optimal power flow formulation.

Virtual generator models are typically used when a modeler wants to include the technical limitations of the demand side technology. The demand is modeled as an electricity generating or storage unit with a negative output. Demand reductions and shifts can be constrained in e.g. amount, time and ramping rate. Energy storage and possible losses can be incorporated (e.g. via a demand recovery ratio; see Section 4.3.3). The constraints can be based on observations or detailed physical models. The VGM is dispatched similarly as a conventional power plant and therefore often used in the setting of direct load control [41].

These VGM have been used in various studies, e.g. to investigate the impact of DR on the marginal benefit for consumers [165], the effect of DR on reserve markets [166], the impact of DR in electric power systems with large wind power penetrations [47] and the benefits of demand side participation in the provision of ancillary services [93].

However, in both cases a modeler cannot assess the benefit of the studied DR scheme for the consumer based on these aggregated representations. Moreover, the feasibility of the resulting demand can be questioned, as one has no guarantee that the resulting electric power demand profile will be sufficient to ensure the required thermal comfort for the end-consumer.

3.2.2 Models with focus on the demand side

Kosek et al. [102] give an overview of the possibilities of implementing DR. The approach taken in that paper is that of predictive and direct load control. Assuming perfect predictions and no model mismatch, this is the best case scenario for DR, and hence ideal for impact studies. Thermal energy storage is often investigated in the literature as a demand side technology. E.g., Hewitt [84] studied the use of the thermal inertia of the built environment as a TES, in the case of a heat pump delivering space heating and domestic hot water. Hewitt found that both the building and the hot water tank are possible candidates for DR and, in order to assess the benefits for the consumers and generators under DR, he highlighted the necessity of taking into account the dynamics of both the demand and supply side. However, when assessing the potential of a thermal system for DR, most authors start from a fixed electricity price profile [2, 83, 113, 120, 149, 179] to determine the electrical load pattern modification. The authors typically conclude how much the electricity cost can be reduced for the owner of the system, but do not consider a feedback of the shifted electrical load pattern on the electricity price.

Based on such models, one can only draw conclusions for a single, small consumer. As of a certain number of consumers participating in the studied DR program, their modified behavior would start affecting the price. This feedback of user behavior on the price of electricity is not taken into account in these models.

3.2.3 Integrated operational models

Recently, a number of authors have developed integrated models. Both the demand side and the supply side are represented by physical models and jointly optimized. A group of researchers at the university of Victoria (Canada) have

recently published a number of papers [132, 133, 134, 181, 182, 185], inspired by the model of Callaway [28], closely related to the objective of this work. They studied comfort-constrained distributed heat pump management and intelligent charging of electric vehicles as balancing services, with a particular focus on balancing wind power, as a spinning reserve resource and as a voltage stabilizing measure. The physical models of the heat pumps and electric vehicles are integrated in a linear programming representation of the electric power system. Hedegaard et al. [80, 81] developed an integrated model, including different types of TES and emission systems, to assess the potential of DR to balance wind power. However, some aspects of the thermal system were represented too simplistically in the model. E.g., the heat pump COP (coefficient of performance) is not temperature dependent and the solar transmission through the windows is not taken into account. Dallinger and Wietschel [39] assessed the electric vehicles potential for balancing the fluctuations of renewable energy sources, while representing the generation side by a MO model.

Typically, these integrated models start from a supply side perspective and tend to oversimplify the building: a heat pump is often considered to have a constant coefficient of performance (COP) while solar heat gains and thermal energy storage in the building structure are often neglected. Regarding the COP, only two studies could be found that have a more realistic representation of the COP, namely by considering the COP either linearly [76] or non-linearly [181] dependent on ambient air temperature. Solar heat gains are sometimes indirectly included by considering these as part of the model's white noise [28, 92]. In order to shift a heat pump's electricity demand in time without compromising the users' comfort, some thermal energy storage must be present in the system. This can be either in storage tanks (active thermal storage) or in the building structure itself (passive thermal storage). Some authors focusing on active thermal energy storage in domestic hot water tanks [15, 101] or high capacity space heating systems [106, 118] consider buildings as providers of a fixed thermal energy demand profile, hereby neglecting the energy storage potential of the building structure.

In order to determine the DR potential of passive energy storage, the building structure is in some cases represented by two [139, 181] or three thermal capacities [80]. In general though, only one thermal capacity is considered [76, 81, 121]. Modeling the building structure as one thermal capacity allows the use of statistical aggregation techniques in order to study the DR potential of large sets of buildings [112, 92, 28]. Another advantage is that the model becomes similar to that of other thermostatically controlled loads, such as fridges and freezers, allowing similar modeling techniques [110, 115]. One could argue that a higher level of detail is needed to describe the transient behavior of a building. This is discussed in Section 3.5.

These integrated models incorporate in some way both the dynamic behavior of the supply side of the electric power system and the flexible electricity demand. Such an approach offers a number of advantages when a sufficiently detailed representation of the overall energy system is used. First, the electricity demand from the thermal systems is closer to reality, since the occupants behavior is taken into account, as well as the weather conditions and the thermal behavior of the considered heating systems and dwellings. Second, all feedback effects of the redistribution of the electrical load — on demand and supply side — are represented correctly. For example, the thermal losses associated with load shifting can be precisely determined. Third, it allows identifying the technology that was used to perform the electric load shifting, thus comparing the impact of multiple flexible demand side technologies. Last, it ensures the end-use functionality of the demand side technology, while simultaneously guaranteeing the availability of the balancing services provided by DR on the supply side. However, those models are not devoid of disadvantages. First, the representation of e.g. a realistic building stock and the stochastic behavior of the occupants requires a detailed demand side model, which is difficult to set up and calibrate. Second, these models are typically difficult to solve numerically, with a high computational cost as a consequence.

3.3 Emulator building level model

In contrast to the aforementioned literature, this work features the development of a bottom-up representation of residential buildings with heat pumps starting from a detailed emulator model. This emulator model of the building is developed using the IDEAS library in Modelica, described by Baetens et al. [13]. This building model has been verified and validated using the BESTEST methodology [91]. The parameters for the single zone building are taken from Reynders et al. [152], who interpreted the parameters of a typical post 2005 built Belgian dwelling as described in the TABULA project [38]. The building has a floor surface of 270 m^2 and a protected volume of 741 m^3. The combination of infiltration and ventilation cause 1.5 air changes per hour. The exterior walls, roof and windows have a U-value of 0.4 $\frac{W}{m^2K}$, 0.5 $\frac{W}{m^2K}$ and 1.4 $\frac{W}{m^2K}$ respectively. In each cardinal direction, the building has an average of about 10 m^2 window surface, resulting in a percentage glazing of 22%. The Belgian climate is considered, based on the measurements in Uccle and distributed by Meteonorm [119].

The heating system is also modeled using the IDEAS library. It consists of a modulating air coupled heat pump supplying both warm water to a radiator for space heating (SH) and a domestic hot water tank (Figure 3.4). All components

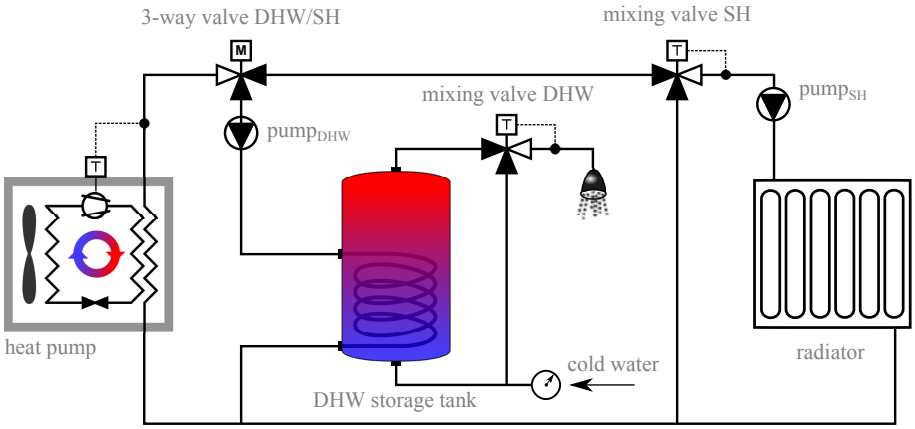

Figure 3.4: Hydraulic scheme of the heating system [40]. A modulating air coupled heat pump supplies heat for domestic hot water via a storage tank and space heating via a radiator. Figure from De Coninck et al. [40]

are modeled by physical equations, while the parameters for these components are determined from either manufacturer data or empirical correlations. A full description of the heat pump model, along with a validation of the domestic hot water tank model is presented by De Coninck et al. [40]. The model for the radiator is described by Baetens et al. [13]. The heat pump and radiator are sized to meet 80% of the design heat demand of 8900 $W_{thermal}$, in accordance with the code of good practice in Belgium [127]. The heat pump has a rated thermal capacity of 7200 W at a supply temperature of 45 $°C$ and an outdoor temperature of $-10\,°C$. The back-up heater is an electrical resistance heater.

Table 3.1: Multiple buildings are considered having a different number of occupants with each their own DHW tank for supplying domestic hot water. The distribution of the household size is based on Belgium [70].

Household size [Persons]	1	2	3	4	5	6
# households (25 case)	8	8	4	3	1	1
# households (100 case)	32	32	16	12	4	4
DHW at 50 $°C$ [liter/day]	62.5	125	162	200	237	300
DHW tank size [liter]	120	160	160	200	300	300
DHW tank UA [W/K]	0.117	0.098	0.098	0.085	0.085	0.077

Since the model is aimed to be scaled up in order to represent thousands of buildings, also various numbers of occupants per house are considered. To this aim, 25 buildings are considered, each having the same building structure, but

with different number of occupants and different occupant behavior (Table 3.1). For the aggregation method in Section 3.6, the aggregated model was compared to 100 reduced order models, each having again the same building model but different occupant behavior. The household size determines the daily DHW demand, which is based on Peuser et al. [143]. This daily demand determines the size of the DHW tank. The parameters of the tanks are based on the Vitocell 100-W gamma of Viessmann.

3.4 Reduced order building level model

The reduced order model (ROM) describes the dynamic behavior of both building and heating system with fewer equations and details than the emulator model. This ROM is the set of linear equations (such as in Eq. 3.4) that still has enough detail to describe the flexibility in electricity use provided by the presented system. In order to evaluate how the ROM performs with respect to the emulator model (Figure 3.6), the optimization problem (Eq. (3.1)-(3.4)) is reduced to:

$$\text{minimize} \qquad \sum_j cost_j \cdot d_j^{hp} \tag{3.5}$$

$$\text{subject to} \qquad \forall j : d_j^{hp} = f^{dem}(T_{b,j}) \tag{3.6}$$

in which $cost_j$ is the electricity price at time step j (Figure 3.9a). Thus given a specific electricity price profile, the optimization gives the resulting electricity consumption and temperatures, which can be compared to the ones obtained by the emulator model.

A linear model of the building was already developed by Reynders et al. [152] and is described in Section 2.4.1 and Figure 2.3. This linear model reduces the building structure to five temperature states, which describe the transient behavior of the building. This model shows an RMSE error of only $0.3\,°C$ on a two day ahead prediction of the indoor air temperature of the emulator building model.

This section mainly focuses on the reduced order model of the heating system. Table 3.2 summarizes various aspects of the heating systems that can be modeled in different ways. Section 3.4.1 describes in detail the multiple representations for the heat pump. Section 3.4.2 focuses on the DHW tank and finally Section 3.4.3 describes the radiator model.

Table 3.2: Component model description for the emulator model. Per component two options for the reduced order model are considered. T_{amb} is the ambient air temperature. P^{hp} is the electric power used by the heat pump.

Component	Emulator model	ROM option 1	ROM option 2
Heat pump COP	interpolation of manufacturer data	constant COP, average from correlation	COP from correlation, function of T_{amb}
Heat pump modulation	interpolation of manufacturer data	mixed integer formulation (Eq.3.7-3.10)	linear in P^{hp} (Eq.3.11-3.14) + post processing
DHW tank	multiple layers with energy balance equation	fully mixed, mixed integer constraint (Eq.3.17-3.18)	fully mixed with linear constraint (Eq.3.19-3.24)
Radiator	radiator formula and one thermal capacity	no radiator model	linearized heat transfer, 1 thermal capacity (Eq.3.25)

3.4.1 Heat pump model

In this thesis, the focus is on modulating heat pumps for which the performance strongly depends on modulation, supply and source temperature. Verhelst et al. [179] studied multiple representations of the heat pump COP based on these variables, among which non-linear representations. In the case study by Verhelst et al., the linear COP formulation lead to a cost increase of up to 16 %. However, since the ROMs discussed in this section are intended to be combined with electricity generation system models, a non-linear representation is out of the question. Hence only linear and mixed integer representations of heat pump performance are allowed. The two remaining options for this framework are thus a constant COP or a COP that is a function of the ambient air temperature only. Note that, throughout this study, in the cases where a constant COP is used, this COP is calculated based on the average supply and source temperature during the considered optimization horizon. The adequacy of this COP formulation will be tested in Section 3.5.

The heat pump integrated in the emulator model can supply warm water to both space heating and domestic hot water, hence the decision variables are the electric power of the heat pump to supply space heating $P_j^{hp,sh}$ or domestic hot water $P_j^{hp,dhw}$ at time step j. The most detailed mixed integer representation of the heat pumps performance is the set of equations (3.7)-(3.10). The equations

for the domestic hot water supply are analogous to (3.7)-(3.9).

$$\forall j : P_j^{hp,sh} = P_j^{min,hp,sh} \cdot z_j^{hp,sh} + P_j^{int,hp,sh} \tag{3.7}$$

$$\forall j : 0 \leq P_j^{int,hp,sh} \leq (P_j^{max,hp,sh} - P_j^{min,hp,sh}) \cdot z_j^{hp,sh} \tag{3.8}$$

$$\forall j : \dot{Q}_j^{hp,sh} = COP_j^{i,sh} \cdot P_j^{min,hp,sh} \cdot z_j^{hp,sh} + P_j^{int,hp,sh} \cdot (COP_j^{a,sh} - COP_j^{i,sh}) \tag{3.9}$$

$$\forall j : z_j^{hp,sh} + z_j^{hp,dhw} \leq 1 \tag{3.10}$$

This representation has the advantage of being directly convertible to control signals for the heat pump and the pumps connecting the heat pump to the DHW tank and space heating by means of the integer variables $z_j^{hp,dhw}$ and $z_j^{hp,sh}$ which can only be zero or one. It is also possible to take into account a different COP at full load $COP_j^{a,sh}$ and at minimal modulation $COP_j^{i,sh}$. The power that the heat pump consumes does not violate the working constraints, it is either off or between the maximal $P_j^{max,hp,sh}$ and minimal $P_j^{min,hp,sh}$ modulating power. The integer power level $P_j^{int,hp,sh}$ is a dummy variable to cope with these constraints. The disadvantage is the number of integers used, since these are known to cause the calculation time to explode. Solvers for mixed integer linear problems can typically handle problems with up to 10^5 integers, however when exceeding this order of magnitude, this becomes a lot harder [100]. Considering a time horizon of 48 hours with two integers each hour per house, this would limit the number of buildings in one optimization problem to 104 buildings.

Another option to represent the heat pump is a linear model (3.11)-(3.14), in which the electric power of the heat pump towards space heating or domestic hot water can vary between 0 and $P_j^{max,hp}$, as long as the sum of the two remains below $P_j^{max,hp}$. Linear optimization models are computationally very efficient to solve, the optimization takes only some seconds on a regular laptop while the mixed integer representation (3.7)-(3.10) can easily take minutes to hours to solve. This linear model consists of the following equations:

$$\forall j : P_j^{hp,sh} + P_j^{hp,dhw} \leq P_j^{max,hp} \tag{3.11}$$

$$\forall j : P_j^{hp,sh}, P_j^{hp,dhw} \geq 0 \tag{3.12}$$

$$\forall j : \dot{Q}_j^{hp,sh} = COP_j^{sh} \cdot P_j^{hp,sh} \tag{3.13}$$

$$\forall j : \dot{Q}_j^{hp,dhw} = COP_j^{dhw} \cdot P_j^{hp,dhw} \tag{3.14}$$

The disadvantage of the linear optimization model is the extra effort needed to derive control signals for the individual heat pump and circulation pumps, respecting the lower modulation level of the heat pump. To this aim, a post processing is applied in order to obtain feasible profiles for 'scheduled operation' as explained by Kosek et al. [102]. Since multiple buildings are controlled simultaneously, the electricity demand per building can be redivided among the buildings, as long as the sum of these electricity demands remains the same. In this way, some buildings that require less than the minimal modulation of the heat pump, are switched off and this difference is compensated for in other buildings. The buildings from which the heat pumps were switched off, are compensated for this fact in a later time step. In this chapter, this post processing consists of two steps.

A first step is needed to decide whether the heat pump will supply SH or DHW during a time step, since the linear formulation allows the provision of both at the same time. The approach taken here depends on the time step of the optimization. In case of a quarter of an hour time step, priority is given to DHW supply. The heat pump power to supply SH is then put to zero and will be accounted for later in the post-processing. In case the optimization time step is an hour, the first step is taken according to Table 3.3. The heat pump then first provides SH for 40 minutes after which the DHW tank is heated for 20 minutes. If there is more DHW demand than SH demand in that hour, the order is reversed. The division is performed in such a way that the same amount of electrical energy is demanded in that hour.

Table 3.3: Rescheduling of heat pump power to SH and DHW when the optimization time step is one hour or twenty minutes. The suffix 'hp' was omitted for clarity.

ROM output	Minute 0 to 20	Minute 20 to 40	Minute 40-60
$P_j^{sh} > P_j^{dhw} > 0$	$P_{j1}^{sh} = \frac{3}{2}P_j^{sh}$ $P_{j1}^{dhw} = 0$	$P_{j2}^{sh} = \frac{3}{2}P_j^{sh}$ $P_{j2}^{dhw} = 0$	$P_{j3}^{sh} = 0$ $P_{j3}^{dhw} = 3P_j^{dhw}$
$P_j^{dhw} > P_j^{sh} > 0$	$P_{j1}^{sh} = 0$ $P_{j1}^{dhw} = \frac{3}{2}P_j^{dhw}$	$P_{j2}^{sh} = 0$ $P_{j2}^{dhw} = \frac{3}{2}P_j^{dhw}$	$P_{j3}^{sh} = 3P_j^{sh}$ $P_{j3}^{dhw} = 0$
$P_j^{sh} = 0$	$P_{j1}^{dhw} = P_j^{dhw}$	$P_{j2}^{dhw} = P_j^{dhw}$	$P_{j3}^{dhw} = P_j^{dhw}$
$P_j^{dhw} = 0$	$P_{j1}^{sh} = P_j^{sh}$	$P_{j2}^{sh} = P_j^{sh}$	$P_{j3}^{sh} = P_j^{sh}$

The second step of the post-processing deals with power demands lower or greater than the minimum and maximum modulation respectively. The latter case can arise after rescaling the powers according to table 3.3. Since 25 buildings are considered simultaneously, the power demand during a specific time step can be redivided among all these buildings. The procedure is illustrated in Figure 3.5. The power demand for DHW supply for instance can be lower or higher

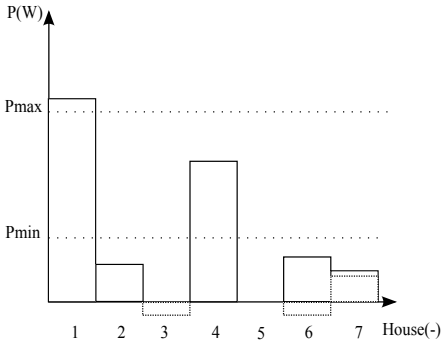

(a) Power demand for 7 buildings before redividing.

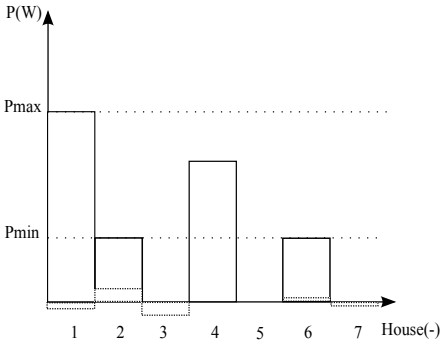

(b) Power demand for 7 buildings after redividing.

Figure 3.5: The power demand of a few houses before and after redividing the loads. The full lines represent the actual power demand while the dotted line represent an excess or deficit of power. An excess inherited from the previous time step means a particular house received too much power up to that point in time and a deficit vice versa. The redivision takes these quantities into account and updates these afterwards.

than the minimal and maximal modulation level (Figure 3.5a). The redividing of power then trims down the power demand which is too high and scales up the power where it is too low. In order to get the exact electricity demand that hour as predicted, some buildings are denied in scaling the power demand. This procedure can cause a certain building to have received an excess or a deficit of energy up to that point in time, which is taken into account by keeping track of this quantity when redividing the power in the next time step. In Figure 3.5b, the power is redivided: the heat pumps in all buildings receive a control signal which they are able to follow.

3.4.2 Domestic hot water tank

The central component in the DHW model is the DHW tank. This tank can either be modeled as perfectly stirred or perfectly stratified. In this work, the tank is assumed to be a perfectly stirred water tank, meaning that all water in the tank is at the same temperature T_j^{tank} at time instant j. The water in the DHW tank can either be heated up by the heat pump during time step j, $\dot{Q}_j^{hp,dhw}$ or by a back up electrical heater $\dot{Q}_j^{aux1,dhw}$. Heat is extracted from the DHW tank through demand for hot water $\dot{Q}_j^{dem}$ and heat loss to the

surroundings. The discretized version of the energy balance for the DHW tank leads to the following equation:

$$\forall j: \quad \rho c_p V^{tank} \frac{T_{j+1}^{tank} - T_j^{tank}}{\Delta t} = \dot{Q}_j^{hp,dhw} + \dot{Q}_j^{aux,dhw} - \dot{Q}_j^{dem} - UA^{tank} \cdot (T_j^{tank} - T_j^{surr}) \tag{3.15}$$

with ρ and c_p the density and heat capacity of water and V^{tank} the volume of the tank. With Δt the length of the optimization time step, the time derivative of T_j^{tank} is approximated as $\frac{T_{j+1}^{tank} - T_j^{tank}}{\Delta t}$. The term $UA \cdot (T_j^{tank} - T_j^{surr})$ determines the heat loss to the surroundings, which is at temperature T_j^{surr}. The thermal conductance UA^{tank} is that of the insulation around the DHW tank, which is the dominant resistance to heat transfer.

The temperature of the cold tap water T^{cold} and the temperature of the supplied DHW T^{dem} are both assumed to be constant. A lower boundary for the temperature of the water in the DHW tank stems from the demand for a comfortable temperature of DHW. Since the tank is perfectly stirred, the whole tank must be heated up to at least T^{dem} when the occupants desire hot water. In other time periods, the temperature of the water in the tank can get as low as T^{cold}:

$$\forall j: \quad T_j^{tank} \geq T^{dem} \cdot bdem_j + T^{cold} \cdot (1 - bdem_j) \tag{3.16}$$

with $bdem_{\mathrm{j}}$ a binary parameter which is 1 when hot water is demanded during time step j and 0 when this is not the case. The water in the DHW tank can be at a higher temperature than what is demanded, in which case a three way valve is used to mix it with the cold water to the desired temperature. Given the constant T^{cold} and T^{dem} and the fact that the whole tank is above T^{dem} in case of DHW demand, $\dot{Q}_j^{dem}$ is independent of the tank temperature [136].

The heat pump can deliver heat up to a maximum temperature $T^{hp,max}$, typically $60\,°C$, which is lower than the maximum allowed temperature of the DHW tank $T^{tank,max}$, typically $90\,°C$. This difference introduces the need for a boolean variable z_j^{dhw} and the following constraints

$$\forall j: \quad T_j^{tank} + \frac{\Delta t}{\rho \cdot V_{tank} \cdot c_p} \cdot \dot{Q}_j^{hp,dhw} \leq (1 - z_j^{dhw}) \cdot T^{hp,max} + z_j^{dhw} \cdot T^{tank,max} \tag{3.17}$$

$$\forall j: \quad \frac{\dot{Q}_j^{hp,dhw}}{COP_j^{dhw}} \leq (1 - z_j^{dhw}) \cdot P^{max,hp} \tag{3.18}$$

When z_j^{dhw} is zero, the temperature of the DHW tank is lower than $T^{hp,max}$ and the heat pump's output is limited by either the temperature up to which it can heat, Eq. (3.17), or by its maximal electric power, Eq. (3.18). In case z_j^{dhw} is one, the temperature of the DHW tank is higher than $T^{hp,max}$ and the heat pump's output is zero through Eq. (3.18). In that case, Eq. (3.17) becomes an upper constraint on the temperature of the DHW tank.

The boolean variable z_j^{dhw} makes the problem a mixed integer linear problem, with the above mentioned problems. In this work, a linear alternative for the model is developed. It defines the tank temperature T_j^{tank} as the sum of a temperature which is influenced by the heat pump T_j^{hp} and a temperature difference influenced by the auxiliary heater dT_j^{aux} (the latter for the temperature range above $60\,°C$). The model hence becomes:

$$\forall j: \quad \rho c_p V_{tank} \frac{T_{j+1}^{hp} - T_j^{hp}}{\Delta t} = \dot{Q}_j^{hp,dhw} + \dot{Q}_j^{aux1,dhw} - \dot{Q}_j^{hp,dem} - UA^{tank} \cdot (T_j^{hp} - T_j^{surr}) \tag{3.19}$$

$$\forall j: \quad \rho c_p V_{tank} \frac{dT_{j+1}^{aux} - dT_j^{aux}}{\Delta t} = \dot{Q}_j^{aux2,dhw} - \dot{Q}_j^{aux,dem} - UA^{tank} \cdot (dT_j^{aux}) \tag{3.20}$$

$$\forall j: \quad \dot{Q}_j^{hp,dem} + \dot{Q}_j^{aux,dem} = \dot{Q}_j^{dem} \tag{3.21}$$

$$\forall j: \quad \dot{Q}_j^{aux1,dhw} + \dot{Q}_j^{aux2,dhw} = \dot{Q}_j^{aux,dhw} \tag{3.22}$$

$$\forall j: \quad T^{hp,max} \geq T_j^{hp} \geq T^{dem} \cdot bdem_j + T^{cold} \cdot (1 - hdw_j) \tag{3.23}$$

$$\forall j: \quad (T^{tank,max} - T^{hp,max}) \geq dT_j^{aux} \geq 0 \tag{3.24}$$

The heat demand $\dot{Q}_j^{dem}$ for supplying DHW has to be extracted either from the heat pump influenced temperature $\dot{Q}_j^{hp,dem}$ or from the auxiliary influenced temperature $\dot{Q}_j^{aux,dem}$. The heat pump can only heat up T_j^{hp} to $T^{hp,max}$. The auxiliary heater can supply heat to both the heat pump influenced temperature ($\dot{Q}_j^{aux1,dhw}$) and the auxiliary heater influenced temperature ($\dot{Q}_j^{aux2,dhw}$).

For example when the water in the tank is at $70\,°C$, T_j^{hp} is $60\,°C$ and dT_j^{aux} is $10\,°C$. In this situation, the heat pump cannot heat up the tank any further. When hot water is tapped, this can be supplied by both temperature levels, but typically dT_j^{aux} will be depleted first. On the other hand, when the water

in the tank is at $55\,°C$[1], T_j^{hp} and dT_j^{aux} are $55\,°C$ and $0\,°C$ respectively. Now, the heat pump can still heat up the tank further. Also, the hot water can only be tapped from this temperature level. Note that summing Eq. 3.19 and Eq. 3.20 leads to obtaining Eq. 3.15 again.

In order for this linear representation to work properly, it was observed that the lower temperature bound (Eq. (3.23) should only be set on the heat pump influenced temperature. If this constraint was put on the sum of the two temperatures, dT_j^{aux} always equals its upper bound.

3.4.3 Heat emission system

The heat emission system is a radiator, which is modeled as a thermal capacity C^{rad} at a temperature T_j^{rad}:

$$\forall j: \quad C^{rad}\frac{T_{j+1}^{rad} - T_j^{rad}}{\Delta t} = \dot{Q}_j^{hp,sh} + \dot{Q}_j^{aux,sh} - UA^{rad} \cdot (T_j^{rad} - T_j^i). \quad (3.25)$$

The thermal capacity of the radiator C^{rad} is the sum of the thermal capacities of the radiator's dry mass and water content. The constant overall heat transfer coefficient UA^{rad} is attained by linearising the radiator formula around the design supply temperature.

3.5 Verification with respect to the emulator model

The reduced order model is verified with respect to the emulator model as shown in Figure 3.6. For multiple electricity price profiles, the ROM is used in the optimization (Eq. (3.5)-(3.6)) determining optimal system operation for a time period of 48 hours. From this optimization, profiles for the electricity consumption, indoor air temperature, COP, etc can be obtained. The verification is done by imposing the emulator model to track this electricity consumption profile with an intermediate post-processing in some cases. The resulting profiles for indoor air temperature and hot water storage tanks are then compared, as shown in Figure 3.7. In the ROM, the thermal comfort constraints are always met, since these are hard constraints in the optimization. Thermal comfort is not always met for the emulator model. As shown in Table 3.2, there are multiple ROM options for all components. All these model options were

[1] The DHW demand is typically tapped at $55\,°C$ while the COP of the heat pump supplying DHW is typically calculated for a supply water temperature of $60\,°C$. The difference between both denotes the temperature difference due to the heat exchanger in the DHW tank.

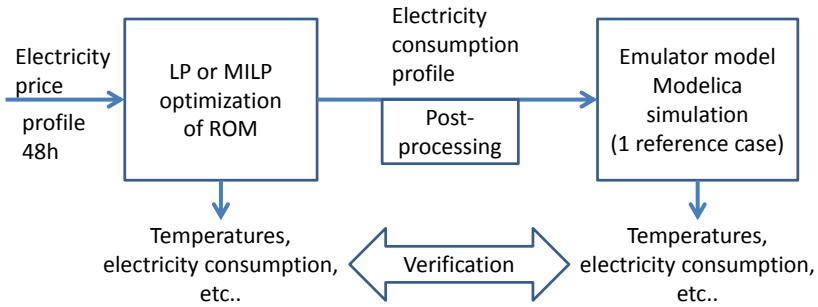

Figure 3.6: The verification of the ROM is performed as follows: the outcome of multiple ROMs is compared to the reference emulator model. The reference emulator model tries to track the electricity consumption profile from the ROM as closely as possible.

compared for three electricity price profiles, namely in the shape of a sine wave with a mean value of $0.10\frac{EUR}{kWh}$ and an amplitude of 0.01, 0.02 and $0.05\frac{EUR}{kWh}$. The results for the three electricity price profiles did not show much difference though, therefore the results of this section are only discussed for the electricity price profile with a mean value of $0.10\frac{EUR}{kWh}$ and with an amplitude of $0.02\frac{EUR}{kWh}$, as shown in Figure 3.9a.

Results reference case. As reference case, all model options 2 of Table 3.2 are chosen. So the reference ROM consists of a heat pump with a COP that is a function of the ambient air temperature and has no modulation constraints. The lack of modulation constraints is corrected by performing a post-processing on the electricity demand profile as explained in Section 3.4.1. In the reference model, the radiator is also included with a constant UA value and a thermal capacity. Finally, this reference ROM has the linear, fully mixed model for the domestic hot water tank. Figure 3.7 shows the indoor air temperature and DHW tank temperature averaged over the 25 buildings with an identical building structure and different user behavior as defined in Table 3.1. As can be seen from the figure, these buildings react upon the price profile (Figure 3.9a), preheating the zone and DHW tank when the price is low.

The indoor air temperature of the ROM shows an almost constant deviation from the emulator model. This is due to two factors, namely a deviation in tracking the electricity consumption profile and losses in the distribution pipes. First, the emulator model consumes 5% less electricity than the ROM, as shown in Figure 3.9b. Second, the lack of a distribution pipe model in the ROM causes an additional 5% difference in thermal energy supplied. Regarding the thermal

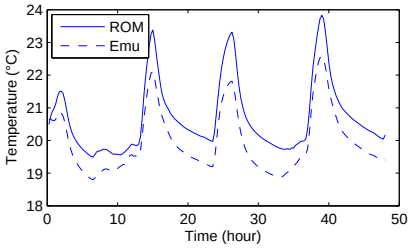

(a) Average indoor air temperature.

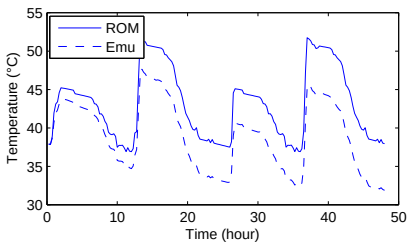

(b) Average DHW tank temperature.

Figure 3.7: Comparison of the average indoor air and DHW tank temperatures over all 25 buildings in case of the ROM and the emulator (Emu) model. The reduced order model approximates the detailed simulation model well, but there is still a (steady-state) deviation between both models.

comfort in the reference ROM, only the temperatures in periods when thermal comfort is demanded, are important. The distribution of indoor air temperature in the emulator model when occupants are present is shown in Figure 3.8a. The indoor air temperature drops regularly below the demanded temperature of $20\,°C$ but rarely below $19\,°C$[2]. This deviation is clearly noticeable in Figure 3.7: the indoor air temperature in the emulator model is between $0.5\,°C$ and $1\,°C$ lower than in the ROM. This causes a substantial thermal discomfort in the emulator model of $3.96Kh$ per building per day with respect to $20\,°C$. When taking a reference temperature of $19.5\,°C$ for thermal discomfort, this value is $1.04Kh$.

For the DHW tank model, the error of the ROM tends to become larger in time. This is mainly due to a small underestimation of the heat pump's COP, which tends to build up as the simulation time is longer. Figure 3.8b shows the distribution of temperatures when the occupants tap DHW from the tank. As can be seen from Figure 3.8b, the temperature at which the DHW is tapped is never below $45\,°C$. For the emulator model, the total discomfort for DHW with regard to the reference of $50\,°C$ is $0.87Kh$ per building per day.

Another important aspect of the comparison between ROM and emulator model is how good the emulator model is able to track the electricity consumption profile as determined by the ROM. This tracking performs well (Figure 3.9b), except when the electricity demand peaks significantly. The emulator model is

[2]Note that the aim of this figure is to illustrate the extent to which the emulator model can attain $20\,°C$ when this is attained by the ROM. These temperatures are fairly low in terms of thermal comfort, but the lower bound in the ROM can easily be adapted to a higher temperature.

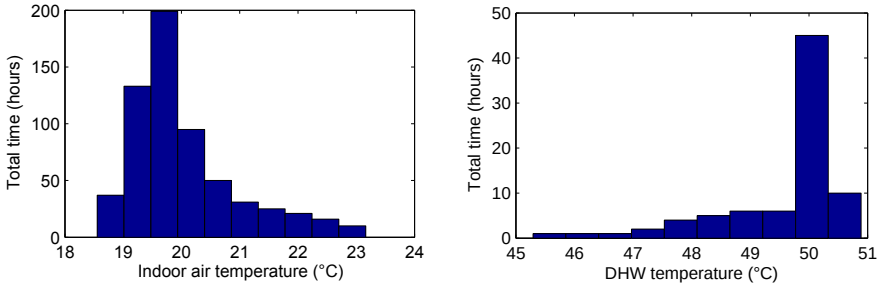

(a) Histogram indoor temperature. (b) Histogram DHW tap temperature.

Figure 3.8: Histogram of indoor air and DHW tank temperature during comfort periods summed over the 25 buildings in the emulator model. The indoor air temperature should be above $20\,°C$ (left). The temperature of the tapped domestic hot water should be above $50\,°C$ (right).

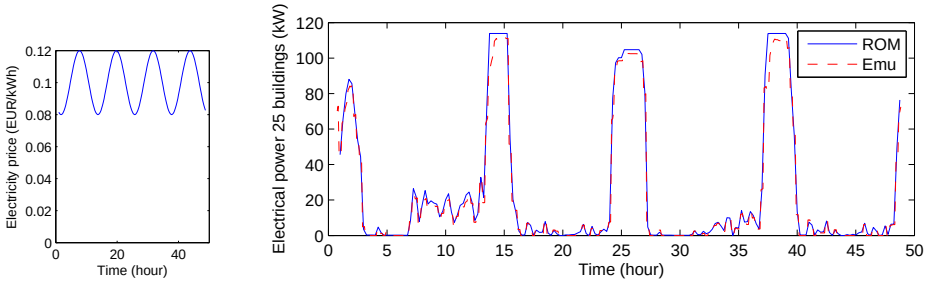

(a) Electricity price. (b) Electricity consumption.

Figure 3.9: The variation in electricity price (left) induces a reaction of the reduced order model (right). The emulator model (Emu) is not always able to attain the electricity consumption that the reduced order model (ROM) determined.

not able to attain this electric power, especially when starting up. This causes the total electricity consumption of the emulator model to be 4.8% lower than that of the ROM.

Discussion reference case. Table 3.4 shows the deviation of various ROMs compared to the emulator model with the first row representing the reference case. The RMSE on the electric power is about $200W$ per building, which is acceptable given the average power usage of $3500W$ per building when a heat

pump is switched on. In the reference case, the deviation of the indoor air temperature is about $0.8\,°C$. Do note that the deviation of the building linear model with respect to the emulator model is already $0.3\,°C$ [152] (Figure 2.3b). The addition of a ROM for the heating system seems to increase the error on the indoor air temperature. The DHW tank temperature in the emulator model was usually about $2.7\,°C$ lower than in the ROM, but this did not have a large effect on DWH comfort.

Table 3.4: Four results of the verification, the first three being the RMSE on electric power [W/building] -indoor air temperature [$°C$] -DHW tank temperature [$°C$] and the last being the calculation time of the ROM optimization [sec]. These quantities are shown for two selected time steps (15 and 60 minutes).

	RMSE			
	Electric power	Indoor temp.	DHW temp.	Calc. time
Time step (min)	15/60	15/60	15/60	15/60
Reference	208/375	0.80/0.71	2.75/3.50	8/1
No radiator	170/320	0.90/1.05	2.70/3.36	5/1
Constant COP	195/380	0.73/0.60	2.54/2.55	6/1
DHW tank integer	217/425	0.81/0.70	2.62/3.16	7200/7200
Switch SH/DHW	185/290	0.77/0.70	3.01/1.96	7200/7200
Modulation	210/(150)	0.71/(0.74)	2.80/(1.35)	7200/(20)

Results and discussion of comparison with other ROM options. Table 3.4 shows the deviation of various ROM options compared to the emulator model. The cases presented are variations of some aspects of the ROM compared to the reference. There are two other linear models, namely the 'No radiator' case, which eliminates the radiator model, and the 'Constant COP' case, which takes a constant COP instead of a COP as a function of the ambient air temperature. The other cases include integer variables, leading to longer calculation times for the ROM optimization. In the 'DHW tank integer' case, the higher limit for the DHW tank temperature is given by equations (3.17)-(3.18). The 'Switch SH/DHW' case introduces one integer variable to force the heat pump to supply either SH or DHW during a time step. In the final 'Modulation' model, the heat pump model includes boundaries for minimal modulation as given by equations (3.7)-(3.10). Table 3.4 shows that using a smaller time-step lowers the RMSE on the electric power, but does not always lower the RMSE on the temperatures.

As radiators have a relatively small time constant compared to that of the building structure, one could suggest to neglect it's thermal capacity. Leaving

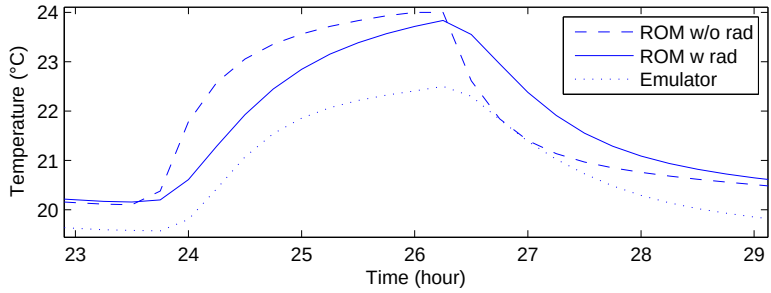

Figure 3.10: The indoor air temperature in the case of the reduced order model with (w) and without (w/o) a radiator model included. The ROM without radiator overestimates the rate at which the indoor temperature can rise and drop.

out the radiator lowers the error on the electric power but increases the error on the indoor temperature significantly. As Figure 3.10 shows, this increase is mainly due to a different dynamic behavior, which can be explained by the absence of the thermal capacitance associated to the emission system. Hence the radiator model is not negligible for the dynamic aspects of the model.

Figure 3.11 shows the COP of the emulator model as compared to that of the ROM with variable or constant COP. Note the large peaks in COP of the emulator model when the heat pump is switched on. This is because the distribution pipes are still cold at this point in time, allowing a high thermal power at condenser side. Part of this gain in COP is thus directly lost due to intermittent heating of these distribution pipes. As can be seen in Table 3.4, using a constant COP (3.8 for space heating and 2.4 for DHW) has an overall positive impact compared to the reference case on the performance of the ROM in terms of RMSE on the electric power and temperatures. This is because the constant COP model approximates the COP of the emulator heat pump model 4% better than the reference case. Note that this constant COP is the average of the COP in the reference case, which changes as a function of the ambient air temperature. The results of the influence of the COP calculation are in line with Verhelst et al. [179], who studied multiple COP formulations, from which there were two linear representations: a constant COP and a COP that is a function of the ambient air temperature only. When no electricity price profile was considered, a constant COP formulation performed better, since this formulation did not cause peaks in the electric power of the heat pump. When an optimization towards minimal cost was considered, both COP formulations performed equally.

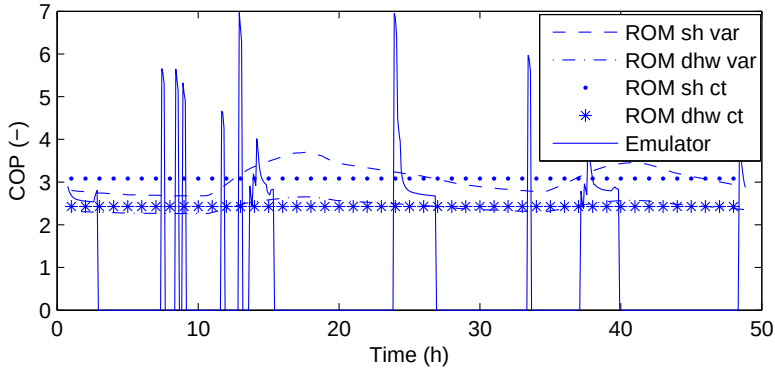

Figure 3.11: In the reference ROM, the COP is a function of the ambient temperature (var). In the "Constant COP" ROM, this COP is constant (ct). As the optimization sometimes chooses to operate the heat pump for only fifteen minutes, the COP in the emulator model can become very high. However, a part of this extra produced heat is lost when the heat distribution system cools down again.

The cases with integer variables 'DHW tank integer', 'Switch SH/DHW' and 'Modulation' do not show a significant improvement to the performance of the reference ROM (Table 3.4). The far longer calculation time (in most cases the maximum calculation time of 7200 seconds) is not worth the minor extra detail these integer variables add. Another possible advantage of the 'Modulation' case, namely the abolishment of a post-processing phase as the electricity usage is conform with the real heat pump constraints, is questionable. The linear reference model (8 seconds) with post processing as discussed in Section 3.4.1 (5 seconds) takes up 13 seconds in total, which is a lot faster than the 'Modulation' model.

The results for the case 'Modulation' with a time-step of 60 minutes are put between brackets because it is a special case. When the heat pump would operate at its lower modulation limit (30% of maximal power) for an hour to supply hot water to the DHW tank, the temperature would exceed the upper limit. So the solution attained is one in which the back-up electrical resistance heater covers all DHW demand. As one can note from the table, the model for this alternative heating performs well for the DHW tank temperature.

Throughout the rest of this thesis, the fully linear model with radiator model, constant COP and linear formulation of heat pump modulation and DHW tank constraint is employed (third row in Table 3.4) as it performs the best. Good performance is proven by its favorable computation time and smallest deviation

with respect to the detailed physical emulator model.

3.6 Aggregation with respect to user behavior

Aggregated model set up In order for a building model to represent thousands of buildings, the same building model is considered multiple times, each time with a different user behavior. The motivation to model multiple buildings with different user behavior, is to attain a reasonable load diversity in order to avoid an unrealistically high peak load. In the field of electricity distribution systems, Kersting [95] concluded that considering the electricity demand of 70 residential buildings is enough to represent the load diversity of a much larger cluster of buildings. In this section, some margin was taken and 100 buildings were considered. The number of inhabitants in each building was chosen in such a way that it represents the population structure in Belgium [70], see Table 3.1. The presented aggregation methodology can be applied to any set of occupancy schedule. For this chapter in particular, time profiles of how many occupants are present and awake in the building were extracted from the model of Richardson [154] and Peuser et al. [143] as described in Section 2.4.2.

A cluster of hundred building models, even if all these models are linear, is still a large problem to solve. A method is thus needed to reduce the number of buildings, namely by aggregation. In this section, a new methodology is presented to aggregate building models which have the same physical parameters but different user behavior. The distribution of the household size is given in Table 3.1. This methodology is illustrated in Figure 3.12. Assume that the 32 households consisting of one person have the same building structure and the same hot water storage tank. The models for these 32 households will be similar, except for the fact that these will have different temperature setpoints for the indoor air temperature and domestic hot water, along with different internal heat gains in the building and different heat demand for domestic hot water.

The aggregation principle is explained for the case of space heating in Figure 3.12, focusing on the lower thermal comfort bound. For each of the 32 buildings with one occupant, the actual lower bound for the indoor air temperature is determined. Thus not the setpoint is taken as a lower bound, but the lowest temperature possible if thermal comfort is to be attained. This actual lower bound is determined by taking into account the warm-up and cool-down behavior of the building. This bound is thus dependent on occupant behavior, ambient air temperature, building parameters and heating system parameters. The aggregated model then consists of one building model for which the lower

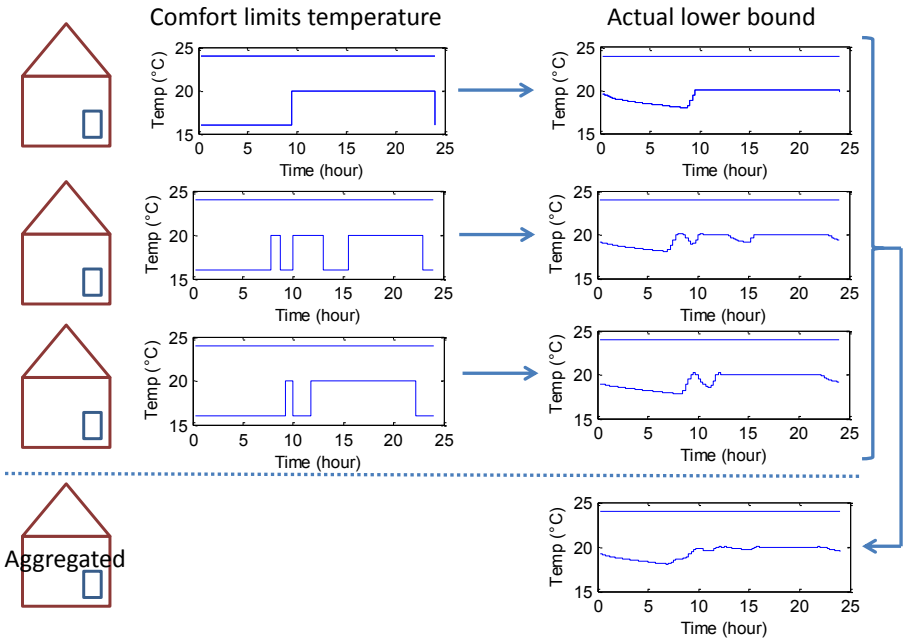

Figure 3.12: Concept of the aggregation. For multiple buildings with identical building structure but different user behavior, the actual lower temperature limits are determined from the occupant's temperature setpoints. The aggregated model then has the same building structure, but a lower bound for the indoor air temperature which is the mean of the actual lower temperature limits of the larger cluster of buildings.

temperature bound is the average of the 32 actual lower temperature bounds. The internal heat gains are averaged over the 32 internal heat gain profiles. A similar procedure is followed for domestic hot water: the actual lower bounds for the storage tank temperatures are determined along with the average hot water demand. As there are 6 cases of number of inhabitants, and hence 6 different hot water storage tanks, the aggregated model consists of 6 building models that represent the 100 building models. But these 6 building models could easily represent a thousand or more buildings, since the procedure is the same.

Performance of aggregation The way to determine the accuracy of this aggregated model in a DR context, is to examine whether it attains the same total electricity cost with respect to an identical electricity price profile. Figure

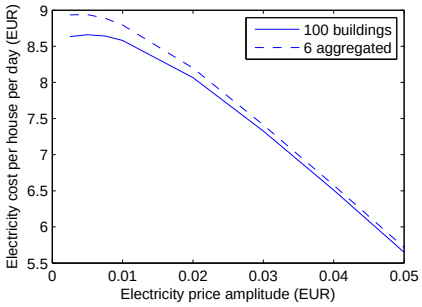

(a) Total electricity cost.

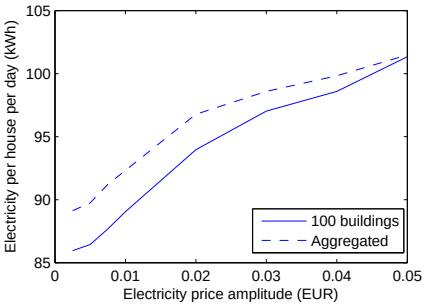

(b) Total electricity use.

Figure 3.13: The total electricity cost and electricity use per dwelling in case of the original model consisting of 100 buildings and the aggregated model consisting of 6 buildings. The aggregation shows an increase in cost between 1% to 3.5% and an increase in energy use between 0.5 % and 4 % compared to the larger cluster of buildings.

3.13a shows how the total electricity cost per dwelling changes with respect to a higher amplitude of a sine wave electricity price profile around a mean price of $0.10 \frac{EUR}{kWh}$. As this amplitude increases, the building structure and DHW tank are increasingly used as energy storage, lowering total electricity cost by shifting electricity demand to time periods of low price. The aggregated building model shows the same trend, and predicts this cost with an error between 1% and 3.5%. This decrease in total electricity cost has the downside of increasing the energy use, as Figure 3.13b shows since employing thermal energy storage generally leads to higher thermal losses. The electricity consumption of the aggregated model also shows the same trend, being between 0.5% and 4% higher than in the original model.

The comparison between the 100 buildings model and the aggregated 6 buildings model was also performed for random and wholesale market profiles. Figure 3.14 plots the relative difference in total electricity cost and mean indoor air and DHW tank temperature between the aggregated and the original model. The aggregated model overestimates the total electricity cost with about 1% to 3.5%, the indoor temperature with -2% to 2% and the DHW tank temperature with 4% to 8%.

A check was also performed, whether the 100 buildings model would be able to track the electricity use of the aggregated model. This was performed for all price profiles, by minimizing the deviation given the constraints of the 100 buildings model. This check proved to be successful: the deviation on the profile

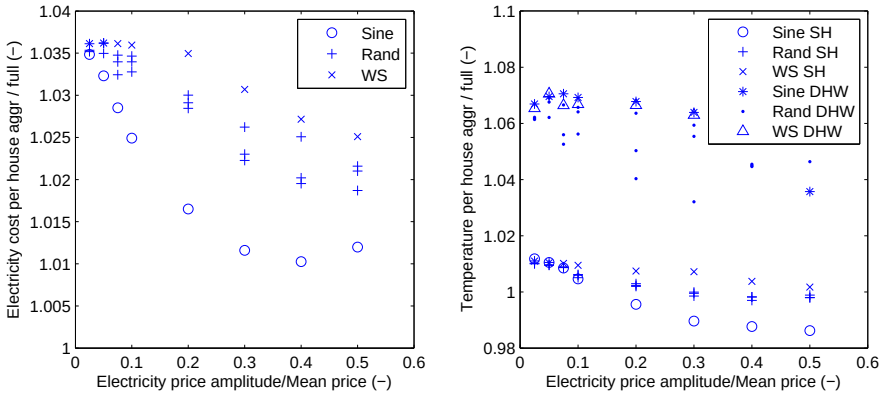

(a) Total electricity cost.

(b) Indoor and DHW temperature.

Figure 3.14: Difference in total cost, indoor air temperature (SH) and DHW tank temperature (DHW) in the aggregated case of 6 buildings compared to that of the original model with 100 buildings. This comparison was done for multiple price profiles with a certain amplitude and a shape based on a sine wave (sine), random (rand) or wholesale market prices (WS).

is lower than 0.1%.

Discussion The model with 100 buildings has a slightly higher potential for DR than the aggregated model: it can lower the electricity cost per building and attains lower energy use in doing so. This is because the model with 100 buildings has more options to shift some energy demand, as there will always be more opportunities to make a small change in very specific cases. Nevertheless the aggregated model comes very close to the larger model. Since the aggregated model always overestimates electricity cost and use, the aggregated model can act as a lower boundary for the performance of the larger model. In other words, the aggregated model always gives a small underestimation of the flexibility potential and is hence on the conservative side.

3.7 Integrated model set up

The integrated model combines the unit commitment and economic dispatch model of the electricity generation system model described in Section 2.3.1,

based on Van den Bergh et al. [169], with the optimal control formulation of the buildings with heat pumps developed in Section 3.4 to 3.6. The optimization criterion is to minimize total operational cost over all time steps with index j:

$$min \quad \sum_i \sum_j fc_{i,j} + co_2t_{i,j} + sc_{i,j} + rc_{i,j}. \tag{3.26}$$

For each power plant with index i, the generation level ($g_{i,j}^{pp}$) and commitment status (binary variable $z_{i,j}^{pp}$) determine the fuel cost ($fc_{i,j}$), CO_2 cost ($co_2t_{i,j}$), start-up cost ($sc_{i,j}$) and ramping cost ($rc_{i,j}$):

$$\forall i, \forall j : fc_{i,j} = cf_i \cdot z_{i,j}^{pp} + mf_i \cdot (g_{i,j}^{pp} - g_i^{min} \cdot z_{i,j}^{pp}) \tag{3.27}$$

$$\forall i, \forall j : co_2t_{i,j} = co_2p \cdot [ct_i \cdot z_{i,j}^{pp} + mt_i \cdot (g_{i,j}^{pp} - g_i^{min} \cdot z_{i,j}^{pp})] \tag{3.28}$$

$$\forall i, \forall j : sc_{i,j} = stco_i \cdot v_{i,j} \tag{3.29}$$

$$\forall i, \forall j : rc_{i,j} \geq raco_i \cdot (g_{i,j}^{pp} - g_{i,j-1}^{pp} - v_{i,j} \cdot g_i^{max}) \tag{3.30}$$

$$\forall i, \forall j : rc_{i,j} \geq raco_i \cdot (g_{i,j-1}^{pp} - g_{i,j}^{pp} - w_{i,j} \cdot g_i^{max}) \tag{3.31}$$

in which the binary variables $v_{i,j}$ and $w_{i,j}$ respectively denote a start-up or shut-down event of power plant i in time step j. The parameter cf_i is the fuel cost for running the plant at its minimum power level (g_i^{min}) and mf_i is the marginal cost for the generation level on top of the minimum power level. The CO_2 emissions also consist of an emission ct_i at minimum power level and a term accounting for the marginal emissions (mt_i). The CO_2 cost is then determined via a CO_2 price co_2p. Furthermore, $stco_i$ and $raco_i$ respectively denote the start-up cost and ramping cost of power plant i. Each power plant is submitted to a series of technical constraints:

$$\forall i, \forall j : g_{i,j}^{pp} \leq g_i^{max} \cdot z_{i,j}^{pp} \tag{3.32}$$

$$\forall i, \forall j : g_{i,j}^{pp} \geq g_i^{min} \cdot z_{i,j}^{pp} \tag{3.33}$$

$$\forall i, \forall j : g_{i,j}^{pp} \leq g_{i,j-1}^{pp} + \Delta_i^{max,up} \tag{3.34}$$

$$\forall i, \forall j : g_{i,j}^{pp} \geq g_{i,j-1}^{pp} - \Delta_i^{max,down} \tag{3.35}$$

$$\forall i, \forall j : 1 - z_{i,j}^{pp} \geq \sum_{j'=j+1-mdt_i}^{j} w_{i,j'} \tag{3.36}$$

$$\forall i, \forall j : z_{i,j}^{pp} \geq \sum_{j'=j+1-mut_i}^{j} v_{i,j'} \tag{3.37}$$

$$\forall i, \forall j : z_{i,j-1}^{pp} - z_{i,j}^{pp} + v_{i,j} - w_{i,j} = 0 \tag{3.38}$$

with g_i^{max} the maximum power level. The maximum ramping-up ($\Delta_i^{max,up}$) and maximum ramping-down ($\Delta_i^{max,down}$) values are derived from the maximum ramping rates of the power plants. The minimum up-time and down-time of power plant i are denoted by mut_i and mdt_i respectively.

The market clearing condition couples the electricity generation system model and the optimal control formulation of the buildings with heat pumps:

$$\forall j : d_j^{trad} + nb \cdot d_j^{hp} = cur_j \cdot g_j^{res} + \sum_i g_{i,j}^{pp} \tag{3.39}$$

$$\forall j : \quad 0 \leq cur_j \leq 1 \tag{3.40}$$

with cur_j determining the amount of curtailment of the electricity generation (g_j^{res}). As explained in Section 3.1, the traditional electricity demand d_j^{trad} entails all electricity demand except that of the heat pumps. As no competition in providing flexibility is assumed (Section 2.2), this traditional demand is a fixed profile. To this traditional demand, the scaled up (with the number of buildings factor nb) demand of the heat pumps (d_j^{hp}) is added.

The demand from the heat pumps can be adherent to a DR-scheme ($d_{\mathrm{j}}^{\mathrm{hp,var}}$) or can be fixed to a predefined profile ($d_{\mathrm{j}}^{\mathrm{hp,fix}}$):

$$\forall j : d_j^{hp} = (1 - p^{\mathrm{dr}}) \cdot d_{\mathrm{j}}^{\mathrm{hp,fix}} + p^{\mathrm{dr}} \cdot d_{\mathrm{j}}^{\mathrm{hp,var}}. \tag{3.41}$$

The share of flexible and inflexible demand is controlled by the DR participation parameter p^{dr}. The demand from heat pumps adherent to a DR-scheme is determined via the demand side model (Eq. (3.42)-(3.53)) explained below. The same demand side model is used to determine the electricity demand of heating systems not participating in a DR scheme ($d_{\mathrm{j}}^{\mathrm{hp,fix}}$) by minimizing the energy needed to meet the required thermal comfort, not considering the interaction with the supply side model.

The following equations present the optimal control formulation of the buildings with heat pumps, as described in Section 3.4. The demand $d_j^{hp,var}$ is the sum

of the electricity demand of multiple buildings with index b:

$$\sum_j d_j^{hp,var} = \sum_b \left(p_{b,j}^{hp} + p_{b,j}^{aux} \right) \tag{3.42}$$

and consists of the positive electricity demand of the heat pump $p_{b,j}^{hp,var}$ and an auxiliary electrical resistance heater $p_{b,j}^{aux}$. These positive demands are split up over delivering space heating (suffix sh) and DHW (suffix dhw) and are limited as follows

$$\forall j : p_{b,j}^{hp,sh} + p_{b,j}^{hp,dhw} \leq p^{hp,max} \tag{3.43}$$

$$\forall j : p_{b,j}^{aux,sh} + p_{b,j}^{aux,dhw} \leq p^{aux,max} \tag{3.44}$$

with $p^{hp,max}$ the maximum electric power of the heat pump which is predetermined and fixed each optimization horizon. Based on the results of Section 3.5, the heat pumps can modulate perfectly. The maximum power of the auxiliary heater ($p^{aux,max}$) is independent of the ambient temperature and is hence always the same value. The state space model of the building, with temperature states $T_{b,j+1}^{sh}$ and state space matrices $\mathbf{A}^{sh}$ and $\mathbf{B}^{sh}$ is:

$$\forall b, j : T_{b,j+1}^{sh} = \mathbf{A}^{sh} \cdot T_{b,j}^{sh} + \mathbf{B}^{sh} \cdot [P_{b,j}^{hp,sh}, P_{b,j}^{aux,sh}, T_j^e, T_j^g, \dot{Q}_j^{sol}, \dot{Q}_{b,j}^{int}] \tag{3.45}$$

and is submitted to the disturbances of ambient temperature (T_j^e), solar heat gain $\dot{Q}_j^{sol}$ and internal heat gains $\dot{Q}_{b,j}^{int}$. Some of the temperature states are constrained by minimum ($T_{b,j}^{sh,min}$) and maximum ($T_{b,j}^{sh,max}$) temperatures in order to maintain thermal comfort

$$\forall b, j : T_{b,j}^{sh,min} \leq T_{b,j} \leq T_{b,j}^{sh,max}. \tag{3.46}$$

The DHW tank is assumed to be a perfectly mixed storage tank. This tank can be heated above the maximum temperature that the heat pump can attain ($T^{hp,max}$) by the auxiliary heater. In order to avoid the need for an integer variable, Section 3.4.2 showed a linear alternative. This defines the tank temperature $T_{b,j}^{tank}$ as the sum of a temperature which is influenced by the heat pump $T_{b,j}^{hp}$ and a temperature difference influenced by the auxiliary heater $dT_{b,j}^{aux}$ (the latter for the temperature range above $T^{hp,max}$, typically $60\,°C$). The model equations are:

$$\begin{aligned} \forall b, j : \rho c_p V_b^{tank} \frac{1}{\Delta t} (T_{b,j+1}^{hp} - T_{b,j}^{hp}) = & P_{b,j}^{aux1,dhw} + cop^{dhw} \cdot P_{b,j}^{hp,dhw} \\ & - \dot{Q}_{b,j}^{hp,dem} - UA_b^{tank} \cdot (t_{b,j}^{hp} - t^{surr}) \end{aligned} \tag{3.47}$$

$$\forall b,j : \rho c_p V_b^{tank} \frac{1}{\Delta t}(dT_{b,j+1}^{aux} - dT_{b,j}^{aux}) = P_{b,j}^{aux2,dhw} - \dot{Q}_{b,j}^{aux,dem} - UA_b^{tank} \cdot (dT_{b,j}^{aux}) \tag{3.48}$$

with ρ and c_p respectively the density and heat capacity of water. The time step is denoted as Δt. The COP for delivering DHW (cop^{dhw}) is predetermined and assumed constant throughout the optimization horizon. The DHW tank in each building with index b has a certain volume V_b^{tank} and thermal conductance UA_b^{tank}. Further constraints are

$$\forall b,j : \dot{Q}_{b,j}^{hp,dem} + \dot{Q}_{b,j}^{aux,dem} = \dot{Q}_{b,j}^{dem} \tag{3.49}$$

$$\forall b,j : P_{b,j}^{aux1,dhw} + P_{b,j}^{aux2,dhw} = P_{b,j}^{aux,dhw} \tag{3.50}$$

$$\forall b,j : T_{b,j}^{hp} \leq T^{hp,max} \tag{3.51}$$

$$\forall b,j : T_{b,j}^{hp} \geq T^{dem} \cdot bdem_{b,j} + T^{cold} \cdot (1 - bdem_{b,j}) \tag{3.52}$$

$$\forall b,j : (T^{tank,max} - T^{hp,max}) \geq dT_{b,j}^{aux} \geq 0. \tag{3.53}$$

The heat demand $\dot{Q}_j^{dem}$ for supplying DHW has to be extracted either from the tank temperature influenced by the heat pump ($\dot{Q}_j^{hp,dem}$) or from the temperature difference influenced by the auxiliary heater ($\dot{Q}_j^{aux,dem}$). The heat pump can only heat $T_{b,j}^{hp}$ to $T^{hp,max}$. The auxiliary heater can supply heat to both the tank temperature influenced by the heat pump ($P_{b,j}^{aux1,dhw}$) and the temperature difference influenced by the auxiliary heater ($P_{b,j}^{aux2,dhw}$). Finally, $T^{tank,max}$ denotes the maximum allowable DHW tank temperature, T^{cold} the temperature of cold tap water and T^{dem} the minimum tank temperature needed when occupants demand hot water (denoted by the boolean $bdem_{b,j}$).

3.8 Typical output integrated model

Figure 3.15 illustrates a typical output of the integrated model in the case of 250,000 nearly zero energy, detached residential buildings and with the Belgian electricity generation mix where RES is scaled up to provide 30 % of the energy demand on a yearly basis. In case of no demand response, the average temperatures in the day zone and domestic hot water tank remain close to the lower temperature bound, in order to minimize the individual buildings

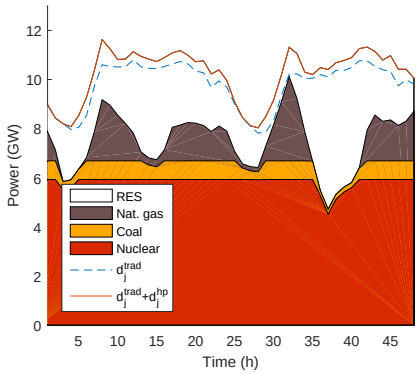

(a) Electricity generation, no DR

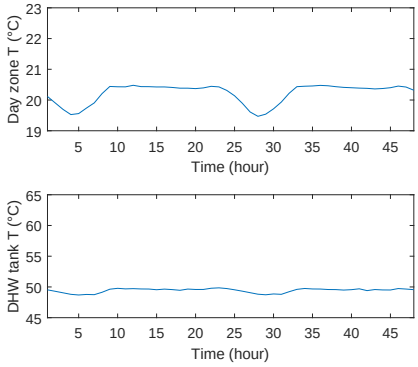

(b) Mean temperatures, no DR

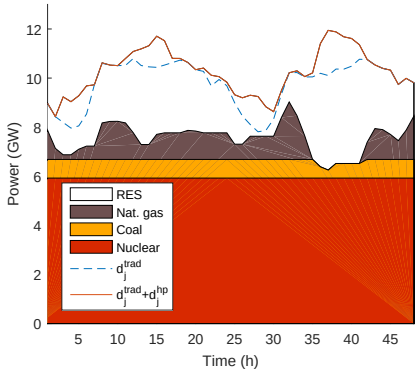

(c) Electricity generation, with DR

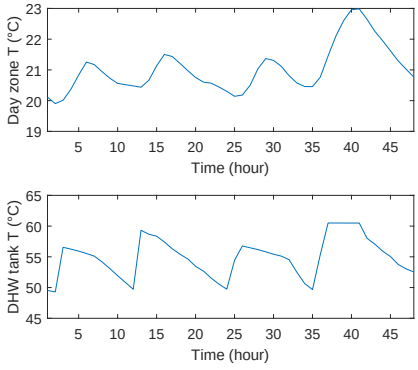

(d) Mean temperatures, with DR

Figure 3.15: Illustration of the integrated model output for two days in case of no demand response (Fig. 3.15a and Fig. 3.15b) and in case with demand response (Fig. 3.15c and Fig. 3.15d) in an optimization towards minimal operational costs.

electricity use (Fig. 3.15b). This heat pump control strategy causes the morning peak, around 8h, of the electricity demand to rise (Fig. 3.15a). Moreover, the electricity generation from RES is of that magnitude that some of the nuclear power plants need to go in part load operation, around 3h the first day and 13h the next day.

When demand response is allowed in the integrated model, the day zone of the building and the DHW tank are preheated during the early morning and

afternoon (Fig. 3.15d). For the electricity generation system (Fig. 3.15c), this clearly leads to a lower operating cost. First, the more expensive peak power plants generate less electricity in favor of the base load power plants. In this example, this enables the nuclear power plants to operate at full load the entire period. Next, the ramping of all power plants is clearly reduced as the demand follows more the electricity generation from RES. Finally, the thermal losses in the residential buildings are higher, as the average temperatures in the building structure and DHW tank are higher.

3.9 Conclusion

This chapter presents and illustrates the integrated model for studying DR for residential buildings with heat pumps. Starting from an emulator model available in a building performance simulation tool, a verified, aggregated building stock model is determined for a verification period of 48 hours. The mathematical formulation of the model is chosen such that it can be combined with electricity generation system models. Multiple reduced order models were studied, where the fully linear model with radiator model, constant COP and linear formulation of heat pump modulation and DHW tank constraint performed the best. This good performance is characterized by its favorable computation time and smallest deviation with respect to the detailed physical emulator model: $0.8\,°C$ on the indoor air temperature and $2.7\,°C$ on the DHW tank temperature. Hence, this reduced order model is employed in the remainder of this thesis. The output of this fully linear model is convertible to control signals to be applied to the physical emulator model or a real-life implementation by a post-processing method. Note that the analysis in this chapter was performed for one specific building type with radiators and represented by one thermal zone. The rest of this thesis employs similar models, but it is assumed that the presented heating system model is also applicable to other building and heating system types. The verification of all these various types is outside the scope of this work.

Additionally, an aggregation method is developed and presented, which is able to reduce the number of buildings needed in order to represent multiple user behaviors. This aggregated model can act as a conservative case for the performance of a large cluster of buildings, as it overestimates the costs with 1% to 4%.

The developed ROM and aggregation method are employed in the integrated model, for which the full model equations are provided. The integrated model output is illustrated by showing typical results.

As opposed to the integrated models in the literature as discussed in Section 3.2, the models for the residential buildings with heat pumps are determined based on detailed emulator models. This emulator model works as a reference from which a linear reduced order model of the heating system is deducted. Furthermore, the aggregation methodology allows for a slim representation of a large set of buildings with diversity in the user behavior. Hence, a bottom up representation of the flexibility of residential buildings with heat pumps is deducted in this chapter. This representation is suitable for a direct integration with a unit commitment and economic dispatch model. As Chapter 4 will show, this is the correct way of assessing the flexibility potential in residential buildings with heat pumps.

Chapter 4

Comparison integrated model to other modeling approaches in the literature

This chapter is based on a paper that was previously published as:
Patteeuw, D., Bruninx, K., Arteconi, A., Delarue, E., D'haeseleer, W., and Helsen, L. Integrated modeling of active demand response with electric heating systems coupled to thermal energy storage systems. Applied Energy 151 (2015), 306–319.

4.1 Introduction

The purpose of this chapter is to illustrate the relevance of using an integrated model to study DR, involving the interaction between the supply side and the demand side, building further on the work presented in [27]. To this end, a methodological case study of the integrated model is presented which will act as a reference. Using this methodological case study, the results from the proposed integrated model are compared to those from models with focus on either the supply side or the demand side. A comparison among several modeling approaches with a different level of complexity is presented in this chapter. Figure 4.1 shows schematically how the model detail and computational cost depend on the complexity of the supply side model and the demand side model. The analysis is performed starting from the integrated model representing in

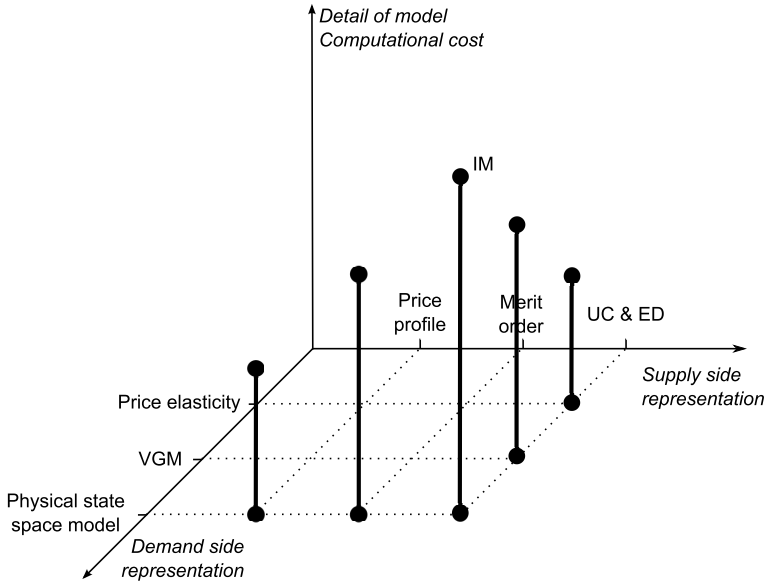

Figure 4.1: Schematic representation of the various modeling options, in order of ascending complexity and detail, in demand and supply side representations, and the combinations discussed in this chapter.

detail both the supply side and the demand side (Chapter 3), and then reducing step by step the complexity of the supply and the demand side representations respectively. The integrated model represents the supply side by means of a unit commitment and economic dispatch model and the demand side by means of a physical state space model of the building and its heating system. Moving along the reduced complexity of the demand side, the latter can be represented by a VGM or by a price elasticity based model, while the supply side is still represented via the unit commitment and economic dispatch model. Vice versa going toward a simplification of the supply side model, a MO model or an electricity price profile can simulate the supply side of the electricity generation system, keeping the physical state space model for the flexible demand. In every case the selected model is used in an optimization problem, with the purpose of minimizing the overall operational costs. The models mentioned above were selected because they are widely used in the literature. Note however that other models and combinations of models may exist.

This chapter is organized as follows. Section 4.2 presents the methodological case study on which the different approaches are tested. Results are first presented for the integrated model (Section 4.3.1) in order to facilitate the

interpretation of the shortcomings of other models. Subsequently, the challenges in modeling DR via price-elasticity models (Section 4.3.2) and virtual generator models (Section 4.3.3) for the demand side or price profile (Section 4.3.4) and merit order models (Section 4.3.5) for the supply side are illustrated. Based on these results, general conclusions for the use of these modeling approaches are formulated in Section 4.3.6. Throughout this investigation, the integrated model remains the reference model, used to validate other approaches.

4.2 Methodological case study

In this chapter, the integrated model as presented in Section 3.7 is employed. In order to provide numerical results for the comparison of different DR modeling approaches, a methodological case study is presented.

Table 4.1: Assumed electricity generation system mix and parameters. The fuel prices (per MWh of primary energy, MWh_{pr}) or (per MWh electrical energy, MWh_{el}) are based on [136] and references therein).

Power plant type	# units	Max. generation	Cost
Nuclear	1	1200 MW	7 EUR/MWh_{el}
Coal	5	4000 MW	12 EUR/MWh_{pr}
CCGT	10	4000 MW	25 EUR/MWh_{pr}
OCGT	5	500 MW	25 EUR/MWh_{pr}
Oil-fired	5	500 MW	35 EUR/MWh_{pr}

Table 4.1 gives an overview of the assumed power plants on the supply side of the electricity generation system in this chapter. It is assumed that RES-based electrical energy accounts for 20% of the generated electrical energy over the simulated period. A carbon price of 30 $\frac{EUR}{ton\ CO_2}$ is assumed, in line with the projected carbon price by 2030 according to IEA [171]. Note that this high carbon price increases the variable cost of coal-based generation above that of gas-based generation with CCGTs (see Figure 4.5). The fixed demand profile d_j^{fix} is scaled to represent a certain fraction of the total demand for electrical energy on the considered optimization horizon and to ensure that the peak demand does not exceed 90% of the installed conventional capacity. The fixed demand and RES-based electricity production profiles used are based on hourly data for Belgium[1] for 2010 [54].

[1]Note that the electricity generation system assumed in this case study is in no case representative for Belgium, in contrast to the fixed demand and RES profiles.

Twenty five identical buildings, with a different user behavior and number of users based on the demographic structure of Belgium [70], are considered (see Table 3.1). The degree to which the heating systems participate in DR (p^{DR}) is varied throughout the chapter, while the number of buildings nb is chosen in such a way that the heat pumps electricity demand represents 25% of the total electricity demand. For the building structure, the state space model with 5 states as presented by Reynders et al. [151] in Figure 2.3 is used. The building considered has a floor surface of 270 m^2 and a protected volume of 741 m^3. Infiltration and ventilation combined cause 1.5 air changes per hour. The exterior walls, roof and windows respectively have a U-value of $0.4\frac{W}{m^2K}$, $0.5\frac{W}{m^2K}$ and $1.4\frac{W}{m^2K}$. The building has an average of about 10 m^2 of window surface in each cardinal direction. Each building is equipped with an air coupled heat pump, with an electric capacity of 4 kW_{el} during the considered time period. Flexibility is available via thermal energy storage in the building shell [151] and the hot water storage tank (120 to 300 liters, depending on the number of occupants, see Table 3.1). The constraints on the thermal comfort required by the occupants is based on Richardson et al. [154] and Peuser et al. [143], as described in Section 2.4.2. This results in constraints on the electricity demand and on the flexibility offered to the supply side. For comparative purposes in this chapter, only 48 hours of a typical winter period are retained in the evaluation. Thorough testing with longer time horizons revealed that this period is sufficient to capture the thermal behavior of the chosen thermal systems and to illustrate the advantages and disadvantages of the various models. Cyclic boundary conditions are enforced during optimization.

All alternative models, as discussed in Section 3.2.1 and 3.2.2, are simplifications of the presented integrated model. For example, the use of a virtual generator model to represent the demand side flexibility would abolish the need for the linear state-space model, while leaving the supply side model unaffected. The linear state-space model could be replaced by a simpler generic model of a storage unit, with some constraints that ensure that sufficient electricity is 'consumed' to guarantee thermal comfort. Likewise, reducing the supply side model to a merit order model would strongly simplify the unit commitment model, while leaving the linear state-space model at the demand side unchanged.

4.3 Comparison of different modeling approaches

This section will show that the price-elasticity of storage-type consumers is difficult to estimate ex-ante, limiting the usability of price-elasticity-based models (Section 4.3.2). Furthermore, thermal energy storage losses, which are typically non-linearly dependent on e.g. the state of charge, are shown to be

difficult to capture in VGM-like models (Section 4.3.3). Section 4.3.4 illustrates that price profile representations of the electricity supply neglect the possible effect a changed demand profile may have on the electricity price. Finally, merit order models, in combination with a physical model of the demand side, are shown to allow approximating the operational performance of the integrated model at a reasonable computational cost (Section 4.3.5). To facilitate the interpretation of these results, the starting point of the presented analysis will be the results obtained with the integrated model (Section 4.3.1), which will act as a reference. To conclude this section, the most important results and differences between the various models are discussed in Section 4.3.6.

4.3.1 Integrated model results

Figure 4.2a shows the residual electricity demand obtained from the integrated model, calculated as the total electricity demand minus the RES-based generation. The controllable demand from the electric heating systems was assumed to participate to the DR program fully ($p^{\mathrm{DR}} = 100\%$ DR), partly ($p^{\mathrm{DR}} = 50\%$ DR) or not at all ($p^{\mathrm{DR}} = 0\%$ DR). In the last two cases, (part of) the consumers (is) are not exposed to the hour-to-hour variations of the electricity price. The demand of these consumers is given by the predefined electric heating demand profile $d_{\mathrm{j}}^{\mathrm{hp,fix}}$. When the customers adhere to the DR program, the demand is shifted to the hours of lower use, hence lower electricity costs, and so-called 'valley filling' occurs. Load shifting however leads to additional thermal losses, hence an increased overall energy use. From a system perspective, the total operational cost however decreases as a result of DR.

Figure 4.2b shows the electricity price profile obtained from the IM. For the minimum energy demand scenario ($p^{\mathrm{DR}} = 0\%$ DR), the price shows some peaks, corresponding to the peaks in demand, which leads to the activation of expensive peaking units (OCGT in Figure 4.2). Increasing the participation of the electric heating systems to the DR program flattens the price profile. The difference between the case with no participation to DR ($p^{\mathrm{DR}} = 0\%$ DR) and the case with a partial participation to the program ($p^{\mathrm{DR}} = 50\%$ DR) is evident, while the difference is less pronounced between the latter and the case with total participation to DR ($p^{\mathrm{DR}} = 100\%$ DR). This illustrates that after a certain threshold the marginal effect of DR on the production side is reduced. These observations are confirmed by the corresponding dispatch, shown in Figure 4.2, and the residual electricity demand profile, Figure 4.2a. Moving from a 0% DR participation to a 50% DR participation, the need for expensive peaking units disappears completely due to the flattened demand. The same units, being the CCGTs, set the price throughout the optimization period. As such, large price

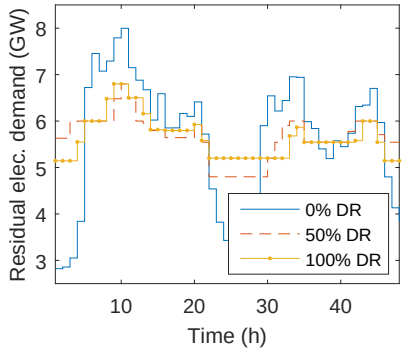

(a) Residual demand in three cases of DR participation ($p^{\mathrm{DR}} = 0\%, 50\%, 100\%$)

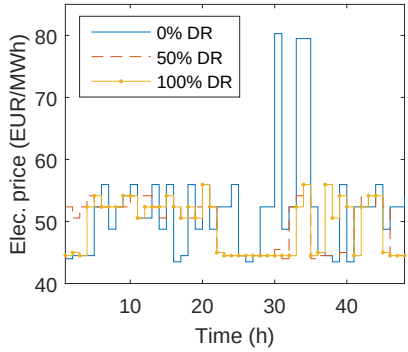

(b) Electricity price in three cases of DR participation ($p^{\mathrm{DR}} = 0\%, 50\%, 100\%$)

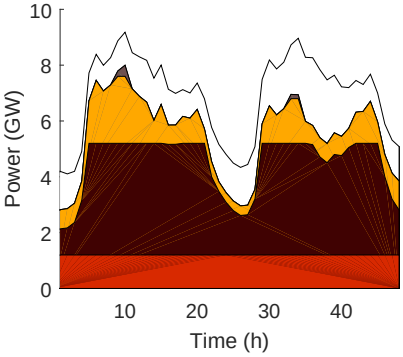

(c) Output of the committed power plants in case of no DR participation

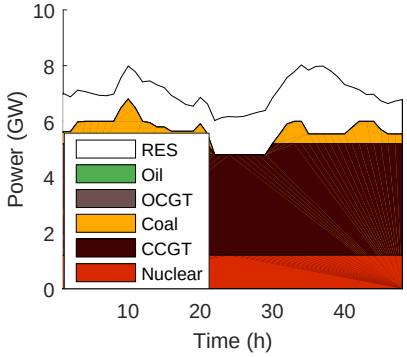

(d) Output of the committed power plants in case of 50 % DR participation

Figure 4.2: Illustration of results of the integrated model concerning the electricity generation system.

differences between hours – the driving force behind the demand redistribution under DR programs – disappear. Therefore, additional controllable heating systems will not result in significant changes in demand, nor electricity prices, on the level of the power system. Note however that, to obtain the same flexibility on a system level, each individual consumer needs to shift his demand less and the resulting thermal losses, thus additional energy use, per consumer will be lower.

With respect to the demand side, Figure 4.3a shows the trend of the demand

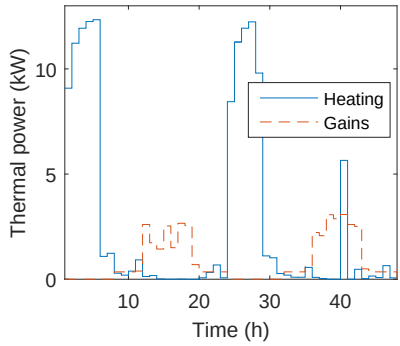

(a) Thermal power supplied to a building by heating system and (internal and solar) gains in the case of a 50% DR participation.

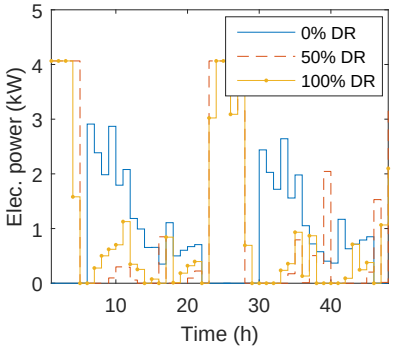

(b) Heating system electricity demand of a single building in three different cases of DR participation ($p^{\mathrm{DR}} = 0\%, 50\%, 100\%$).

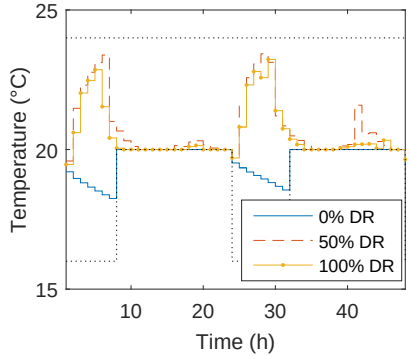

(c) Indoor air temperature over the two simulated days under different DR participation scenarios ($p^{\mathrm{DR}} = 0\%, 50\%, 100\%$)

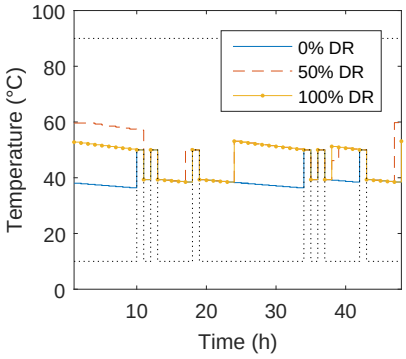

(d) Domestic hot water tank temperature over the two simulated days under different DR participation scenarios ($p^{\mathrm{DR}} = 0\%, 50\%, 100\%$)

Figure 4.3: Illustration of results of the integrated model concerning the building heating systems.

for space heating and domestic hot water of a building and its breakdown in the principal contributions, being the thermal power provided by the electric heating system ('heating' in Figure 4.3a) and the internal and solar gains due to the interaction of the building with users and surrounding ('gains' in Figure 4.3a). Figure 4.3a shows that the contribution of the internal and solar gains, especially in the afternoon hours of the day, represents an important share of the thermal energy demand, reducing the thermal energy to be provided by

the heating system. It is therefore crucial to take these gains into account and neglecting them would lead to a considerable error in assessing the thermal load of the heating system. Moreover, these gains are dependent on the outside temperature and solar irradiation, as well as on the user behavior.

Figure 4.3b instead shows the electricity consumption pattern of the heating system of a single building in different DR cases. With DR, the overall operational system costs are minimized by exploiting the flexibility of the electricity demand of the heating systems, offered by the storage capability of the thermal loads, both in the building envelope and in the DHW storage tank. Due to the availability of cheap generation capacity during the night, the building is preheated compared to the case without DR participation (0% DR) (Figure 4.3b). In fact, the electricity consumption is shifted to low price periods and the energy is stored in the thermal mass of the building (Figure 4.3c) or in the storage tank (Figure 4.3d). This causes more thermal losses and hence a higher energy use, though the overall operational system cost is lower. As a consequence, the inside temperature of whatever DR case, even if thermal comfort is maintained, can be higher than the minimum energy case, in which the temperature is as low as possible while maintaining thermal comfort (Figure 4.3).

The importance of a correct representation of the thermal losses at the demand side technology is illustrated by the demand recovery ratio (DRR). The DRR is defined as the ratio between the observed electrical energy used by the flexible electric heating systems and the minimum electrical energy use of those heating systems [41, 27]. DRR is therefore always greater than or equal to 100%. Results obtained with the integrated model indicate that the DRR varies widely depending on the share of variable demand and renewable energy in the system. At a 50% DR participation, the DRR varies between 105% and 109%, while this range reduces to 102 to 105% at a 100% DR participation rate. The DRR is lower for a 100% DR participation, since less load shifting per house is necessary when more customers are involved. Thus, the behavior of the flexible electric heating systems is not only dependent on the consumers themselves, but also on the boundary conditions under which they operate: the amount of renewable energy in the system and the behavior of other consumers.

Although the presented results highlight many advantages of the integrated modeling approach, it is not devoid of disadvantages. The most serious concern is the computational cost of solving such an integrated model. In this particular setting, solving the integrated model for 48 hours takes about 30 minutes on a 2.8 GHz quad-core machine with 4 GB of RAM. Therefore, modelers often resort to simplified models on the supply or demand side. This will be discussed in the next sections.

4.3.2 Unit commitment and economic dispatch models with a price elasticity model on the demand side

As outlined in Section 3.2.1, many studies on demand side flexibility use a price elasticity model to describe the price responsiveness of flexible customers. This elasticity is defined as

$$\epsilon_{\mathrm{u,j}} = \frac{\partial d_{\mathrm{u}}}{\partial p_{\mathrm{j}}} \cdot \frac{p_{0,\mathrm{j}}}{d_{0,\mathrm{u}}} \tag{4.1}$$

with p_{j} the price of electrical energy in hour j, and d_{u} the demand for electrical energy in hour u. The index 0 refers to the initial or anchor electricity demand and price levels, i.e. the reference demand and price levels to which the elasticity will be related. If j equals u, the elasticity is referred to as the own-elasticity of the demand. Cross-elasticities ($j \neq u$) indicate the change in demand for electricity in hour u in response to a change in the price of electricity in hour j. Cross-elasticities are needed as consumers are generally not willing to reduce their demand, but are more likely to redistribute some of their demand, shifting it away from peak price to low price periods. For example, as shown above, the redistribution of demand may yield a higher overall electricity consumption, which cannot be captured by own-elasticities alone. Price elasticities are a powerful tool to capture the price responsiveness of many customers. However, as shown below, these elasticities may not be suited to describe the responsiveness of storage type customers when storage is accompanied by losses not linearly dependent on the energy stored or on the power supplied, such as thermal systems.

When a modeler intends to use price-elasticities to model the behavior of price-responsive consumers, he needs to estimate these elasticities ex-ante. I.e., the modeler needs to assume a certain (range of) price-elasticity values before observing the reaction of the price-responsive customers. However, this is not a trivial task for electric heating systems. Moreover, one might observe behavior that cannot be captured via a linear relationship between price and demand. To illustrate this, the integrated model is used to assess the mutual change of price and demand induced by the modification of the RES profile. This is equivalent to shifting the supply curve along the demand axis (Figure 4.4 and 4.5). 180 RES profiles were considered (wind power profiles, obtained from the Belgian TSO, Elia, for the year 2013). Each of these profiles covers 20% of the demand. Due to a change in the RES profile, the consumers will see different electricity price levels as the supply curve changes. The thermal heating demand (i.e. thermal comfort) remains unchanged in these simulations. The electricity reference price as seen by the electric heating systems is here calculated as the marginal value of the market clearing condition (Eq. (3.39)) in the integrated model (Figure 4.4).

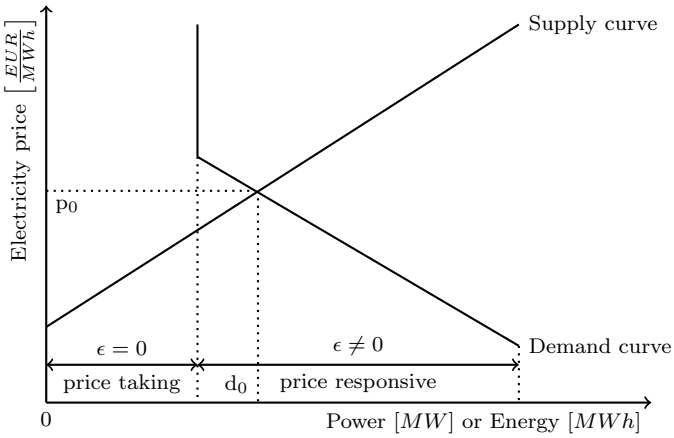

Figure 4.4: Schematic representation of the partly elastic, partly inelastic demand, simulated in this chapter. The intersection of the demand and supply curves yields the anchor points (p_0, d_0) for the elasticity calculation [165].

From these simulations, one can obtain the price-demand couples for each of the respective hours. Figure 4.5 shows the resulting price-demand couples for hour 30, in which the demand for thermal services is significant (Figure 4.3b). Similar effects are observed at other time steps. If a price-elasticity could describe the change in demand in response to changes in the cost or price of electricity, the price-demand couples would form a straight, downward sloping line, as schematically illustrated in Figure 4.4. However, as shown in Figure 4.5, this is not the case. First, one can observe some atypical increases in demand in response to an increase in the marginal cost of electricity generation. This would correspond to a positive own-elasticity, which is uncommon in the electricity sector [41]. Second, different demand levels appear optimal for the same price level. A(n) (own) price-elasticity does not allow capturing these effects. These results show the difficulty of correctly predicting the elasticity ex-ante, needed to study DR via an elasticity-based model, when storage-type customers are involved.

4.3.3 Unit commitment and economic dispatch models with virtual generator models on the demand side

A flexible demand can be modeled through a virtual generator model (see Section 3.2.1). In essence, the demand is described as a generating or storage unit with a negative output and a set of constraints on this output. A generic

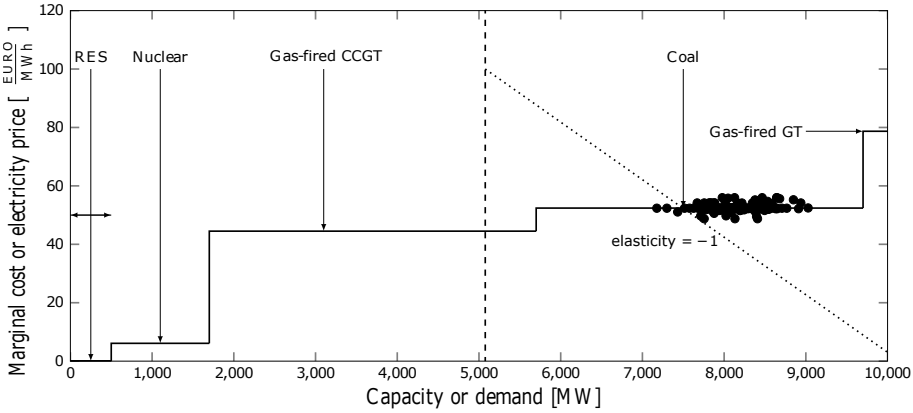

Figure 4.5: The resulting price-demand couples in hour 30, indicated by the black dots in the figure above, indicate that the price-responsiveness of thermal systems cannot be captured via an own-price elasticity. The solid line illustrates the supply curve, the dashed line indicates the inelastic part of the demand. The supply curve shown above is a simplified merit order-representation of the supply side of the electricity generation system. For illustrative purposes, the dotted line shows a demand curve characterized by an own elasticity of -1. The RES-based generation in hour 30 varies between 346 and 4,099 MW. The difference in the price-demand couples stems from different part-load and start-up behavior of the marginal power plant.

description of any storage unit can be formulated as follows:

$$\frac{E_{j+1} - E_j}{\Delta t} = -\dot{L}_j - \dot{D}_j + \dot{I}_j + \dot{G}_j \tag{4.2}$$

The state of charge of any storage system at a certain time j (E_j), is typically modeled based on the energy content at the next time j+1 (E_{j+1}), and the withdrawal and the addition of energy during that time step Δt. In this equation, E_j stands for the energy content of the virtual storage unit, $\dot{L}_j$ for the (thermal) losses of this unit, $\dot{D}_j$ for the energy demand (i.e. the amount of energy one extracts from the storage, the output), $\dot{I}_j$ for the power supplied to the storage and $\dot{G}_j$ for any other gains. Constraints on each term in Eq. (4.2) can be imposed to ensure that the technical constraints of the demand side technology and the comfort constraints of the consumers are respected. Again, the constraints and interaction terms, such as the loss term L, must be quantified by the modeler ex-ante.

When this modeling approach is used to simulate a flexible storage type customer with electric heating system as demand side technology, the limits on the output

of the virtual generating unit (electric power demand) can easily be deducted from the nameplate capacity of all electric heating systems involved on the demand side. Ramping limits are not required in this case as the heat pumps can ramp up and down well within the time step of 1 hour. A similar reasoning applies to the limits of on- and off-times. Constraints are also required on the size of the 'storage' unit, which typically consist of minimum and maximum energy limits for the storage capacity combined with a loss term (or efficiency, L). The thermal losses, L, and the gains, G, in Eq. (4.2) capture the interaction of such a thermal system with its surroundings. These parameters, which can usually be easily quantified for some flexible loads such as electric vehicles, become rapidly more complex to estimate for thermal energy storage systems. Indeed, the thermal losses and gains are not only temperature and time dependent, but they are also dependent on user behavior (consumption of hot water, occupancy profiles), weather conditions (ambient air temperature, solar heat gains) and the building structure (wall thickness, ventilation rate [153]). The importance of solar and internal heat gains has been highlighted previously in Section 4.3.1 (Figure 4.3a), where it has been shown that they represent a considerable share of the building thermal demand. Neglecting these gains in the model would yield a significantly lower state of charge, which in turn may result in an overestimation of the electricity demand via a VGM. Thus, in reality, this may lead to a violation of the comfort constraints on the consumers side. In addition, the DRR, which by its definition can be interpreted as a measure for the loss term L, shows an erratic behavior with varying the RES and DR share, that is clearly difficult to be estimated ex-ante. Likewise, time-dependent limits on the state of charge of the storage system could be used to represent the thermal comfort requirements of the occupants. Similar to the thermal losses and gains, these limits are highly dependent on the user behavior and weather conditions. In conclusion, the representation of a demand side thermal energy storage system and its interaction with the supply side of the electricity generation system requires detailed knowledge of the temperatures and disturbances imposed on that storage system. In a VGM it is necessary to estimate these interactions ex-ante, which can affect the reliability of the results.

4.3.4 State-space models with a price profile-model on the supply side

A price profile is often considered as a possible way of representing the electricity wholesale market in a DR model focused on demand responsive consumers. Typically a fixed electricity price profile is assumed to represent the supply side, while a detailed physically based model is used for the demand side in order to determine the electricity demand profile that yields the minimum energy

cost for the customer. This approach however fails to identify the feedback or reaction of the supply side of the electricity generation system to a change in the demand side behavior. In fact, if one consumer shifts his electricity demand to a moment with lower electricity price, this will not affect the electricity price at that moment. If thousands of consumers shift their electricity demand to that moment, this can increase the electricity price at that moment, making load shifting less interesting.

Since in the reference case presented above, the flexible electricity demand has been assumed to be 25% of the total electricity demand, it is likely that changes in the demand profile of these electric heating systems have an impact on the electricity price. Neglecting this interaction between demand and supply side may have a severe effect on the validity of the obtained results, as shown below using the context of the methodological case study. Towards that end, the state-space demand side model and the unit commitment and economic dispatch supply side model are used separately, as illustrated in Figure 3.1. In a first iteration, the demand side model starts from a flat electricity price profile and determines the electricity demand resulting in minimal total energy cost for the owners. This corresponds to minimizing the energy use on the demand side. The supply side model starts from the fixed electricity demand profile, augmented with the demand profile of the electric heating systems determined by the demand side model in the previous iteration. This model determines the unit commitment and dispatch that minimizes the total operational cost for the system. The resulting price profile[2] is then passed on to the demand side model. Iteratively, the demand side model is used to calculate a new electricity demand in response to this new electricity price profile, which then is used as an input for the supply side model.

When this iterative process was performed, it soon diverged. The demand side model tends to overreact to differences in electricity price. This results in large peak demands, which can be higher than the generation capacity, when the price is low. A possible way of fixing this issue is by putting an extra constraint on the possible changes in the resulting electricity demand profile between iterations, e.g. by limiting the changes in the electricity demand in each hour to a certain percentage of the electricity demand profile in the previous iteration. Figure 4.6 shows the trajectory of the total operational cost of the electricity generation system in case of a maximum 10% deviation of the demand profile from the previous iteration. The operational costs shown in Figure 4.6 are the total operational costs obtained with the unit commitment model, considering

[2]Note that in this chapter, the electricity price for the demand side model is solely determined by the electricity generation system. Hence, the electricity price for the building owners is not augmented with a fixed tariff for electricity generation and distribution, as is typically the case in practice.

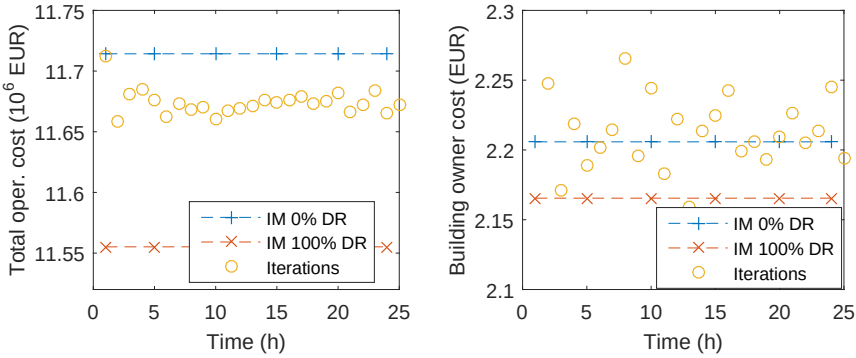

(a) Total operational cost

(b) Building owner energy cost

Figure 4.6: Evaluation of the total electricity production cost with the price profile demand model using the iterative procedure. The integrated model (IM) results for p^{DR} equal to 0% and 100% are indicated as reference (dashed lines).

the fixed demand and the demand profile from the electric heating systems as obtained from the demand side model. In the first iteration, the model yields the same result as if the electric heating systems would not adhere to any DR program. The following iterations show the reaction of the demand side model to a changing electricity price profile. The resulting decrease in operational costs is about one third of the total possible operational cost reduction due to DR as calculated with the IM[3].

However, 25 iterations result in a total calculation time in the same order of magnitude as the integrated model. Similarly, when looking at the costs for the building owners, an erratic oscillation of the solution is noted compared to the corresponding solution of the IM. The energy costs for the building owner are calculated as the demand profile of the electric heating systems times the electricity price profile used in the demand side optimization.

In conclusion, these results show that conclusions based on models in which the supply side is represented via a fixed price profile are biased if changes in demand affect those electricity price profiles. This interaction can be integrated in such a modeling approach to some extent. However, such an iterative approach may

[3]In this case, the IM reduces the total cost with about 1.8%, which is significantly higher than the 0.1% optimality gap imposed on the optimization. Note that these figures account only for operational costs and were obtained for this particular setting. E.g., investment costs are not taken into account. These numbers should not be interpreted as a comprehensive evaluation of the full possible benefits of DR.

not yield results of the same quality as an integrated model, but will require the same computational effort. Moreover, the same level of detail is needed in both models.

4.3.5 State-space models with a merit order model on the supply side

As an alternative to the iterative approach suggested in Section 4.3.4, a modeler focusing on demand side results could consider a merit order representation of the supply side of the electricity generation system, in combination with a physical model of the demand side. As explained below, this model allows to take into account the effect of a change in the demand profile on the electricity price profile directly, abolishing the need for iterative procedures. This MO model is computationally less intensive than a unit commitment model. Moreover, it requires far less detail on the supply side and is thus easier to set up.

This simplified model consists of a mere ranking of the different power plants in an ascending order of average operational production costs (Figure 4.5). These costs consist of fuel and carbon costs. The intersection of the demand and the merit order curve yields the electricity price in each hour. The objective function of this model is similar as in the IM, namely minimize the total operational costs. Furthermore, it couples the demand side model and the merit order model via the market clearing condition (Eq. (3.39)). As such, it is possible to consider the effect of the energy demand variation on the electricity price, even if in a simplified manner. This MO model however only considers the minimum and maximum output of each power plant and hence neglects ramping constraints, minimum on- and off-times and start-up costs, which are considered in a unit commitment model. As a consequence, power plants may be switched on/off in an unrealistic way in the merit order model. E.g., coal power plants are switched on and off within one hour, while in reality it takes multiple hours for such a power plant to start up. Results obtained with such a merit order model should thus always be interpreted with caution, e.g. via a re-evaluation of the resulting demand profile with a UC & ED model as discussed below. Figure 4.5 shows the ranking of the different power plants. Fuel costs and CO_2 costs are the same as those assumed for the unit commitment model in Section 4.2.

The costs from the MO model have been compared to those from the IM for 18 scenarios for the RES-based generation, namely three different RES profiles that cover 5%, 10%, 15%, 20%, 25%, 30% of the total electricity demand (energy basis) in the considered optimization period. Figure 4.7a shows the ratio of the total operational system costs as obtained with the MO model and the IM. Furthermore, this figure shows the ratio of the energy costs for the building

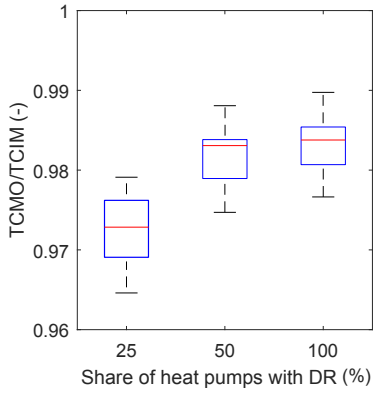

(a) Total operational system cost

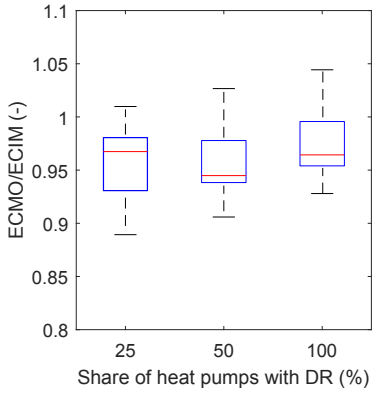

(b) Total cost for building owners

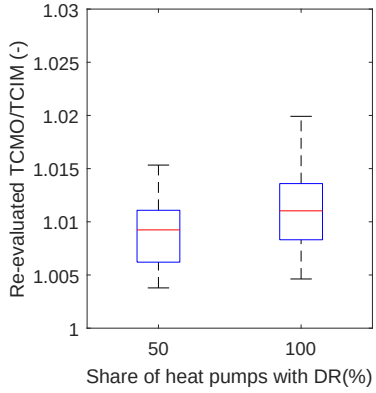

(c) Total operational system cost, re-evaluated with the UC & ED.

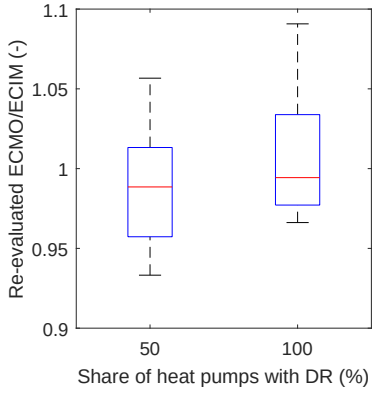

(d) Total cost for building owners, re-evaluated with the UC & ED.

Figure 4.7: Relative difference in total system costs (TC) and building owners energy costs (EC) between the merit order model (MO) and the integrated model (IM). The upper figures show the relative difference when considering the costs as obtained directly from the MO. The lower part of the figure contains the same results, but shows the costs after re-evaluation with the unit commitment model.

owners as obtained with the MO model compared to the IM. In the upper part of the figure, the costs of the MO model are directly compared to the results of the IM. In the bottom part of the figure, the demand profiles of the

electric heating systems, as obtained from the MO, are used as an input of the unit commitment model, in order to recalculate the costs, taking into account all operational constraints and costs of the power plants. With regard to the total operational cost, the merit order model yields a cost between 1 to 3.5% lower than in the case of the integrated model (Figure 4.7a). In this case, a modeler thus takes 96.5% to 99% of all operational costs into account when he employs a merit order model. Furthermore, the difference between both models decreases with a higher share of DR. DR has the effect of flattening the residual demand, which makes it less likely that the solution of the MO model violates any dynamic constraint of the power plants. In addition, start-up costs become relatively less important in the IM solution as less start-ups are required. Looking at Figure 4.7c, showing the re-evaluated operational cost for the system, one is able to judge the quality of the solution obtained from the MO model. This re-evaluated total operational cost is obtained by solving the UC & ED considering the electricity demand profile as obtained from the merit order-state space model. Total operational costs deviate as little as 0.4% to 2% from the solution obtained with the IM.

Fig 4.7b and 4.7d show the energy cost for building owners. The results from the MO model yield cost differences within a range of -12% to +3% compared to the IM solution. After re-evaluation this range changes to -7% to +10%. However, one should be careful in the interpretation of these results. Indeed, the objective of the optimization is to minimize total operational system cost, not the owners cost. The demand profile that yields the minimal operational system cost might not be unique. E.g., a change in the demand profile may lead to a significant difference in the cost for the building owner, but the effect of this change on the total operational cost might fall within the optimality gap of the optimization. From a system perspective, large variations may exist in the owners cost, while system costs remain unaffected.

To conclude, the merit order model successfully takes into account the interaction of electricity prices and the demand profile, especially if one is looking at DR from a system perspective. Results that are close to those of the integrated model can be obtained, especially after re-evaluation of the solution with the unit commitment model. Solving the MO model takes about 30 seconds, compared to 30 minutes for the IM. Re-evaluating the MO model with the UC & ED model additionally requires 30 seconds.

4.3.6 Model comparison

The analysis performed above allows us to state the following conclusions from using the different approaches for modeling demand response when storage-type

customers, such as electric heating systems coupled to any form of thermal storage, are involved. The integrated model, which employs a unit commitment and economic dispatch model for the supply side of the electricity generation system and a physical state space model to represent the demand side, is used as a benchmark. This model allows a modeler to correctly assess the effect of DR on the supply and demand side of an electricity generation system, but requires a significant computational effort and detailed information to set up the model. It can for example be employed to assess the quality of other modeling techniques.

If a modeler seeks to simplify the demand side model, price-elasticity and virtual generator models are often encountered in the literature due to their simplicity and low computational cost. However, in the setting of storage-type customers, in both cases it will be very difficult to estimate the models' parameters ex-ante. It is shown that e.g. price-elasticities and demand recovery ratios, as a measure for the losses in a system, fluctuate erratically with the share of DR and RES in the system. However, the assumptions on the set of model parameters will drastically affect the obtained results.

Likewise, if the modeler employs simpler models on the supply side, he should proceed cautiously. If one neglects the effect of a change in demand on the electricity price profile, results will only hold for a small group of consumers. Iterative price profile approaches will to some extent allow to take into account this feedback and are simple to implement, but results remain sub-optimal and become computationally intensive to solve.

In addition, not taking into account the limitations of the considered power plant portfolio might lead to demand profiles that cannot be met. Merit order models consist of a ranking of the power plants according to their operational costs. Although they do not take into account any operational constraints, nor all costs, they allow to approximate the solution of the integrated model in about 1/60th of the calculation time. However, one should take caution in interpreting the results, as the resulting dispatch might violate the constraints of the power plants and not all costs, such as start-up costs are taken into account.

4.4 Conclusion

This chapter illustrates how the integrated modeling approach allows to capture the full integrated effect of DR on the supply and demand side, as well as to quantify the benefits for the system. However, this comes at a significant computational cost. In order to reduce the computational effort, several

simplified approaches are investigated, such as price-elasticity-based models, virtual generator models, price-profile models and merit order models. In particular, the difficulty of representing storage type customers' behavior by means of price elasticity based models is demonstrated, together with the complexity of a proper estimation of all terms contained in a virtual generator model. Furthermore, fixed electricity price profile demand side models, that neglect the interaction between supply side and demand side, can be misleading for the determination of the flexible demand behavior. Merit order models, instead, provide good results in terms of operational cost estimates, even if the supply side is represented in a simplified way with respect to the integrated approach. Solving such a merit model takes about 30 seconds, compared to 30 minutes for the integrated model. A merit order model may thus be a good candidate for full year simulations.

The combination of the merit order model with the demand side model is employed in full year simulations in Chapter 5 and Chapter 6. These chapters explore the benefits of performing DR on buildings with heat pumps in terms of cost savings and CO_2 emission reductions.

Chapter 5

Case study I: Greenhouse gas abatement cost of heat pumps in a Belgian residential context

This chapter is based on a paper that was previously published as:
Patteeuw, D., Reynders, G., Bruninx, K., Protopapadaki, C., Delarue, E., D'haeseleer, W., Saelens, D., and Helsen, L. CO_2-abatement cost of residential heat pumps with active demand response: demand- and supply-side effects. Applied Energy 156 (2015), 490 – 501.

5.1 Introduction

In this chapter, the integrated model is employed in a first case study. The goal of this case study is to investigate the CO_2 emission saving potential of applying DR on heat pumps in Belgian residential buildings. Furthermore, as residential building characteristics can vary widely, it is hard to assess which building types should be given priority for installing a heat pump and applying DR. The benefits of installing a heat pump and contributing to DR programs are merged in a single indicator: the CO_2 abatement cost. This allows for a clear comparison between the different types of buildings and heating systems.

Heat pumps are often suggested as a key technology for decreasing the CO_2 emissions associated with space heating in the residential building sector [90]. According to a study made for the European Heat Pump Association [19], large scale introduction of heat pumps could reduce CO_2 emissions by 34% to 46% in the building sector of certain European countries by 2030. Bayer et al. [16] report a CO_2 emission saving in space heating for multiple European countries up to 80%, depending mainly on the heat pump efficiency, the replaced fuel type and the CO_2 intensity of the electricity generation system. In these studies, the CO_2 emissions associated with the electricity consumption of the heat pumps is assessed by considering an average carbon intensity of the electricity generation system. Such methodology can be questioned for multiple reasons. First, the heat pump electricity demand can be strongly correlated to high or low instantaneous CO_2 intensities of the electricity generation system, that can significantly deviate from the average CO_2 intensity. For instance, Reynders et al. [153] found that due to passive solar gains the space heating demand is mostly lower at times when PV panels are generating electricity; hence, a carbon intensity strongly affected by PV might not be a good measure for the CO_2 emissions related to space heating. Second, the electricity demand associated with a massive heat pump introduction could correlate with peak electricity demand, increasing the need for peak power capacity [111]. Finally, these published methods for accounting CO_2 emissions are unable to predict the emission reduction and peak shaving potential when heat pumps participate in demand response programs.

This chapter aims at a thorough assessment of the CO_2 emission savings potential of residential heat pumps with DR. The emission savings are determined from the integrated model developed in Chapter 3. According to Hewitt [84], buildings equipped with heat pumps can play a role in coping with the variability and limited predictability of renewable energy sources. Different studies illustrate how introducing heat pumps, possibly combined with DR, may be used to increase the penetration of RES and avoid curtailment losses [114, 142, 180] Hedegaard [81, 82] evaluated the added value of using heat pumps with DR in energy systems with 50% wind power penetration. However, in all of the above mentioned studies, which building types are better suited for installing heat pumps was not evaluated. Thereby, the main challenge lays in the wide variation of building types all with their own characteristics. The building parameters may affect many important indicators, such as the overall heat demand, the heat pump cost and heat pump efficiency as well as the load shifting potential and peak electric power demand. Hence, this chapter explicitly considers the variation in building parameters, as is not the case in Chapters 3, 4, 6 and 7.

In order to compare the suitability of different building types for installing heat pumps with DR, the CO_2 abatement cost is calculated, which is a measure

for the cost of reducing CO_2 emissions. Although CO_2 abatement costs are known to be sensitive to assumptions on economic parameters such as fuel prices [45] or discount rates [122], this quantity is employed in this chapter for relative comparison between building and heating system types. As such, the numerical results obtained from this chapter on CO_2 abatement costs can only be compared to other technologies if identical assumptions on technical and economic parameters are made. A few studies report a CO_2 abatement cost for installing a heat pump instead of another heating system, however with not fully adequate results due to simplifying modeling assumptions. Joelsson [89] reported an abatement cost of 100 EUR/ton CO_2 for a heat pump compared to a condensing gas boiler, -120 EUR/ton CO_2 compared to an oil fired boiler and -190 EUR/ton CO_2 compared to direct electric heating. These values are obtained by considering yearly average values for energy use, heat pump performance and efficiency of the electricity generation system. No attention is paid to the impact the heat pumps may have on the electricity generation. Kesicki [97] employed a long term energy planning model, UK MARKAL, which considers system wide interactions, and finds that heat pumps would become widely implemented in the UK if the CO_2 price exceeds 137 $£/ton$ CO_2. However, Kesicki reported that his study lacks the inclusion of more than two building types, heat pump peak demand, demand side management and occupants behavior. The current chapter goes beyond this work by thoroughly taking into account all important factors for determining the CO_2 abatement cost, specifically: the operational cost and CO_2 savings, the investment in heat pumps and the investment in extra peak electric power capacity needed to cover the additional peak electricity demand. All these factors can be accurately determined through the integrated modeling framework. The analysis in this chapter is carried out for an energy system inspired by the Belgian power system. A high RES future energy system is assumed with wind and PV providing respectively 30% and 10% of the electric energy on a yearly basis.

The chapter is structured as follows. First the modeling approach is discussed in Section 5.2. Section 5.3 shows the CO_2 abatement cost for the various building types, as well as the intermediate steps in determining this cost. The discussion section (Section 5.4) elaborates on some peculiar aspects of the results, in order to formulate the main conclusions in Section 5.5.

5.2 Methodology

Section 5.2.1 describes how the CO_2 abatement cost is determined. To quantify both costs and benefits which make up the CO_2 abatement cost, the parameters for the integrated model are presented in Section 5.2.2.

5.2.1 CO_2 abatement cost

In many Northern European countries, like Belgium, a commonly installed heating system is the condensing gas boiler (CGB) [141], which is assumed to be the baseline heating system in this chapter. Installing a heat pump (HP) instead of a CGB requires a higher investment cost, but may lower CO_2 emissions and operational costs. This can be expressed in a CO_2 abatement cost (AC^{CO_2}) which is the sum of the difference in annual operational costs of the system and the annuity, a_i^n, of the additional investment, divided by the annual CO_2 emission savings [1].

$$AC^{CO_2} = \frac{a_{0.035}^{20}(Inv^{hp} - Inv^{cgb} + Inv^{ocgt,IM}) - (OPEX^{cgb} - OPEX^{hp,IM})}{(CO_2^{cgb} - CO_2^{hp,IM})} \tag{5.1}$$

$$a_i^n = \frac{1-(1+i)^{-n}}{i} \tag{5.2}$$

In this expression, Inv^{hp} and Inv^{cgb} represent the investment cost of heat pump and condensing gas boiler, respectively. It is assumed that the investment in a heat pump is performed at the end of life of the previous heat production system. Hence, the difference in investment cost is considered. $Inv^{ocgt,IM}$ stands for the investment cost of extra peak electricity generation capacity in the form of open cycle gas turbines, determined from the integrated model (IM). $OPEX$ are operational costs as explained below while CO_2 stands for the CO_2 emissions. These annual operational costs are to be compared with the annuity of the investment cost, in which the number of years, n, is considered to be the life time of the heat pump. This life time is 20 years as also assumed by Blarke [22]. For the discount rate, i, two values are assumed, one choice leaning more towards a societal perspective, 3.5% [96], and one reflecting a more private viewpoint, 7%[5].

The cost of generating the additional electricity demand of the heat pumps, $OPEX^{hp,IM}$, is determined through the application of an integrated model approach presented in Section 5.2.2. This integrated model is a centralized

[1] During the life cycle of the heat pump, there are also greenhouse gas emissions associated with leakage of the refrigerant. As shown by Bettgenhäuser et al. [18], these greenhouse gas emissions can cancel out up to a quarter of the greenhouse gas emissions savings of installing a heat pump. There is a large debate on whether the use of these refrigerants should be phased out in favor of refrigerants with a lower greenhouse gas potential. In the interest of transparency, greenhouse gas emissions due to refrigerant leakage are not considered in this chapter. Hence, the reported CO_2 emission savings are only energy-related.

optimization towards minimal cost of generating the total electricity demand which includes the additional electricity demand of the heat pumps. In the baseline case, the operational costs stem from purchasing of natural gas for the CGB from the wholesale market, $OPEX^{cgb}$. The wholesale market price of natural gas is assumed to be constant at 25 EUR/MWh_{th}, based on the higher heating value of natural gas. For both electricity and natural gas, the costs such as costs for transmission, distribution, taxes and RES levies are ignored. The reported operational cost savings are hence system wide costs, as CO_2 abatement costs are more commonly reported from a societal perspective [97, 96, 4].

Assuming a CO_2 intensity of 205 $kg\ CO_2/MWh_{th}$ [75], based on the higher heating value for natural gas, both for CGB and gas fired power plants, and zero CO_2 intensity for PV and wind, the CO_2 abatement cost can be determined as the difference in emissions for the case of heating the building with a CGB, CO_2^{cgb}, and with a heat pump, $CO_2^{hp,IM}$. In the former case, the CGB burns natural gas directly but does not cause an increase in the electricity demand[2]. Hence, in the baseline case, the CO_2 emissions of the electricity generation system remain unaltered. In the latter case, the emissions due to the heat pump arises from a rise in electricity consumption. The CO_2 emissions associated with this increased consumption are determined by the integrated model.

The investment costs include both the investment in the heat pump, Inv^{hp}, the avoided investment in a condensing gas boiler, Inv^{cgb}, and the investment in extra electric peak power capacity, assumed to be open cycle gas turbines (OCGT), $Inv^{ocgt,IM}$. The investment in peak power units is assumed to be 750 EUR/kW [86]. This extra investment in peak capacity is determined by the integrated model, as it not only depends on the installed heat pump capacity but also on the simultaneity and stochastic aspects of both the electricity demand and RES based generation. Additionally, DR can further decrease the need for additional investment in peak capacity. The cost for DR infrastructure is not taken into account in this chapter.

The cost of a CGB is assumed to be $3,200$ EUR and independent of the size. The heat pump investment cost is based on Van der Veken et al. [172], although care should be taken with these data as the heat pump investment cost can vary significantly depending on the manufacturer and the installer. Depending on the nominal heating capacity, $\dot{Q}^{nom}$ in kW, of the heat pump, Van der Veken et al. [172] pose a cost for a ground coupled heat pump of $(1,000 \cdot \dot{Q}^{nom} + 10,000)$ EUR. The cost of a low temperature air coupled heat pump depends on whether it is connected to radiators $(675 \cdot \dot{Q}^{nom} + 7,150)$

[2]Both CGB and heat pump consume electricity for the controller and the circulation pump, but this is not considered as this will be about the same for both cases.

EUR or to floor heating $(410 \cdot \dot{Q}^{nom} + 7,650)$ EUR. For a high temperature air coupled heat pump, a cost of $(385 \cdot \dot{Q}^{nom} + 9,450)$ EUR is assumed, based on Heylen et al. [85].

5.2.2 Integrated model description

The aim of this chapter is to identify whether specific building types are better suited for installing heat pumps with DR, multiple building types (36 cases) and heating system types (3 cases) are considered. For every combination of building and heating system type, the CO_2 emission reduction, operational cost savings and increase in peak electricity demand are determined. In order to have a significant impact on the electricity generation side, it is assumed that for each case (combination of a building case and heating system case) the electricity demand is scaled up to 250,000 buildings [3]. According to the study made for the European heat pump association [19], this is the total number of heat pumps that is expected to be installed in Belgium by 2030.

As shown in Figure 5.1, the integrated model determines the operation of the buildings, heating systems and electricity generation simultaneously. Thermal energy storage is possible both in a passive manner in the building structure and in an active manner in the domestic hot water tank.

For each combination of building type and heating system, three cases are calculated: the case with heat pumps with or without DR and the baseline case with condensing gas boilers. When DR is applied, a centralized control is assumed in which the control of the heating systems interacts with the electricity generation system as presented in Section 3.7. Hence, arrow (2) in Figure 5.1 works bidirectionally. In the case of no DR, the consumers minimize their own electricity consumption regardless of the implications for the electricity generation side and arrow (2) works unidirectionally. The electricity generation system then minimizes the cost for supplying the resulting electricity demand profile. In the baseline case, where all buildings are equipped with a CGB, d_j^{hp} is zero and arrow (2) is not applicable.

The length of the time step is one hour and the prediction horizon is one week. The results reported in this chapter are for one year, obtained by solving the optimization problem for each week of the year. A receding horizon is

[3]The number of buildings is taken to be identical for all combinations of building types and heating system types, in order to make the relative comparison between these types independent of the number of buildings. Each case is calculated separately, meaning that the 250,000 buildings are always of one single building type with one single heating system type. Hence, the number of buildings for each case does not directly correspond to the distribution in the Belgian building stock as presented in [38].

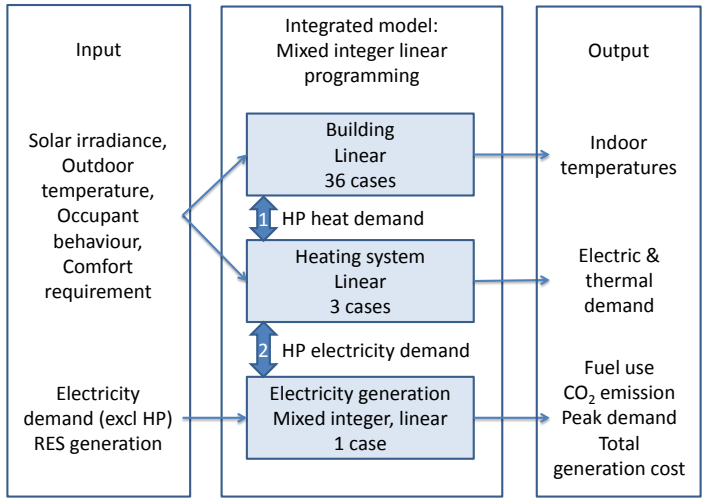

Figure 5.1: Schematic representation of the integrated model, which simultaneously dispatches electricity generation units and activates heat pumps in order to deliver the total electricity demand and maintain thermal comfort in the buildings, respectively.

employed, in which the states of the system at the end of a week are passed on to the next week. In this chapter, perfect prediction of disturbances in the system is assumed and hence the presented results serve as an upper bound of the practically attainable operational cost and CO_2 emission savings. The potential for peak shaving is determined through an a-priori optimization of the critical week with the highest residual electricity demand[4], in which the installed capacity of the power plants is minimized. This installed capacity is then applied as an upper bound for g_j^{pp} throughout the considered year.

The electricity system, as well as the building types, are based on a possible future Belgian setting with high RES penetration at the electricity generation side and increased insulation of the buildings. For the sake of consistency, all input profiles to the model, such as weather data, RES based electricity generation and electricity demand, are taken for the same year (2013) and for the same country (Belgium) as described in Section 2.4.3. The RES based electricity generation is scaled up in order to represent a high RES system.

[4]The residual electricity demand is the electricity demand from which the generation from renewable energy sources is subtracted. This is hence the demand which the traditional power plants need to deliver.

Electricity generation

Regarding the electricity generation side, profiles of fixed electricity demand and electricity generation from RES are taken from the Belgian transmission system operator Elia [54] for the year 2013. A high RES system is considered with 30% and 10% of the electric energy consumption covered by wind and PV respectively. This is largely in line with the European Commission's overall ambition of 45% RES in the power sector by 2030 [61]. This corresponds to an installed capacity of $8,274\ MW$ of wind onshore, $2,000\ MW$ wind offshore and $8,217\ MW$ of PV. The peak electric power demand, in the absence of heat pumps, amounts to $13,119\ MW$. With this assumed RES capacity and taking the meteorological conditions of 2013, the peak in residual electricity demand, without heat pumps, is found to be $12,392\ MW$. The latter peak demand is the most critical since it depicts the need for peak power plants, open cycle gas turbines in this chapter, which cause the high costs associated with covering peak demand. With these profiles the curtailment amounts to $0.55\ TWh$ when no heat pumps are installed.

The dispatchable power plants in the electricity generation system are assumed to consist solely of CCGTs and OCGTs with different efficiencies. 28 CCGTs are considered with a total installed capacity of $11,200\ MW$, with a nominal net efficiency between 60% and 48%. The rest of the electricity generation system comprises of OCGTs, for which the installed capacity depends on the a priori optimization of the critical week with the highest residual demand. These plants have a nominal net efficiency between 40% and 30%. For both power plant types, natural gas has a cost of 25 EUR/MWh_{th}. For RES based electricity generation, it is assumed that the marginal cost is zero. Curtailment costs are zero[5]. The electricity generation system is modeled via the merit order presented in Section 2.3.2, in order to allow yearly simulations. Taking into account the system efficiencies and gas consumption, the overall CO_2 emissions for electricity generation and the resulting average system efficiency (in this chapter defined as $\bar{\eta}^{egs}$, as used in Eq. (5.3)) can be calculated.

Buildings

In this chapter, only single family residential buildings are considered. The building descriptions for the dynamic models originate from a bottom-up building stock model based on the TABULA [38] building stock, as presented by

[5]In current European electricity markets, the price at the wholesale markets during curtailment is not zero but negative due to subsidies and must-run units. The current work does not take these two drivers of negative electricity prices into account and hence, the price during curtailment is zero.

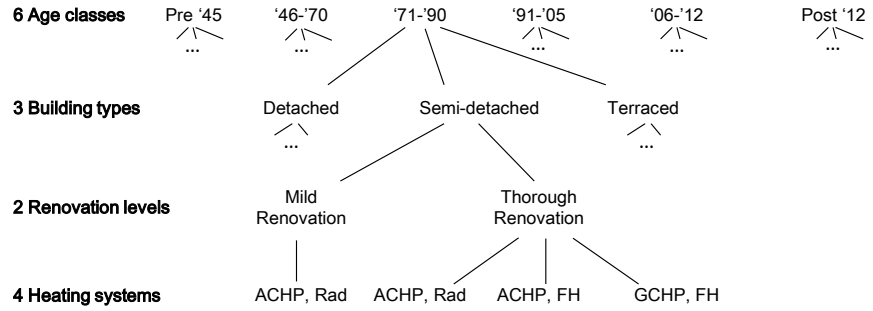

Figure 5.2: Overview of the different building types based on the Belgian residential building stock [147]. Given the 6 age classes, 3 building types and 2 renovation levels, there are in total 36 building cases.

Protopapadaki et al. [147], to which additions for new and renovated buildings are made. As illustrated in figure 5.2, a total of 36 different building types is considered, representing the Belgian residential building stock, which is divided in three typologies, six age classes and two renovation levels. The three different building typologies are typical for single family buildings (i.e., detached, semi-detached and terraced houses). Each of these typologies is subdivided in six age classes (i.e., before 1945, 1945-1970, 1971-1990, 1991-2005, 2006-2012, after 2012). The most recent class is represented by low energy houses with an average U-value of 0.3 W/m^2K and a ventilation rate of 0.4 ACH (air changes per hour), which are two necessary conditions for the nearly zero energy building standard, as set up by the Flemish government [175] and to the economic optimum for Belgium found by Verbeeck [176]. Only in the buildings after 2005 a ventilation system is installed for which two cases, with and without heat recovery, are considered according to the TABULA description. A thermal efficiency of 84% is assumed for the heat recovery unit. For each age class before 2005, two renovation scenarios are considered. First, a "mild" renovation scenario includes roof insulation, replacement of the windows and an improvement of the air tightness. In the second, "thorough", renovation scenario the outer walls and floor are additionally insulated [147]. The original buildings without renovation are not considered in this chapter since the supply water temperature required for these buildings is too high to be supplied by a heat pump. Additionally, all poorly insulated Belgian buildings are assumed to have undergone at least a mild renovation by 2030, in accordance with the proposed evolution of the Belgian building stock by Gendebien et al. [72]. The thermal behavior and heat demand of the dwellings are modeled using the two zone reduced order building model reflecting a 9 states lumped capacity model as shown in Figure 2.4. The assessment of the accuracy of this representation is described by Reynders et al.

[151].

In order to represent the user behavior regarding temperature set points and domestic hot water demand, 52 user stochastic behavior profiles were generated using the profiles Baetens2 as presented in Section 2.4.2 and developed by Baetens and Saelens [14]. In order to reduce calculation time, the user behavior is aggregated by averaging the predetermined, effective lower temperature bounds as explained in Section 3.6. The upper bound for the indoor temperature setpoint is $22\,°C$ and $20\,°C$ for the day zone and night zone respectively [140].

Heating systems

When considering the application of a heat pump, there are three relevant cases for the heating system: (1) an air coupled heat pump (ACHP) with radiators, (2) an ACHP combined with floor heating and (3) a ground coupled heat pump (GCHP) with floor heating[6]. Floor heating is only considered in the buildings built after 1990, for which the nominal heating power allows applying a low temperature heat emission systems, such as floor heating [10]. In each case, the heat pump also supplies the DHW demand, which is stored either in a 200 l or 300 l tank at $50\,°C$, depending on the maximum daily demand. For each renovation case with radiators, it was chosen to keep the original heat emission system for low temperature heating after renovation. For the "mildly" renovated building, depending on the age category, this leads to a nominal supply water temperature for zone heating that can be higher than $60\,°C$. This is too high to be supplied by a standard heat pump, in which case a double compression, high temperature air coupled heat pump is considered [85]. Furthermore, space heating is only considered during the heating season while DHW is supplied all year round.

The heat pump's efficiency is typically expressed by the COP which is the ratio of the instantaneous heating power delivered divided by the electric power of the heat pump. The seasonal performance factor (SPF) is defined as the ratio of the thermal energy delivered throughout the year to the yearly electric energy consumption of the heat pump. In this chapter, the COP is determined according to Bettgenhäuser et al. [19], which results in a SPF as shown in Table 5.1. The newer buildings (built after 2005) show very similar SPF values as the "thoroughly" renovated buildings and are not shown separately. Based on Verhelst et al. [179] and the results in Section 3.5, the COP is assumed to be constant during the course of each week, thus within one optimization horizon.

[6]The radiators in the "thoroughly" renovated buildings are assumed to have a nominal supply water temperature of $45\,°C$. GCHPs are generally not combined with this kind of radiators, as the relatively high supply water temperature of the radiators spoils the efficiency gain of the ground coupling.

Table 5.1: Range of heat pump seasonal performance factors (SPF) for the different building cases.

Renovation	Mild	Thorough	Thorough	Thorough
Heat pump source	Air	Air	Air	Ground
Heat emission	Radiator	Radiator	Floor	Floor
Min SPF	1.8	2.3	2.5	3.3
Max SPF	2.1	2.6	3.0	4.0

Hence, each week, the COP is predetermined based on the average supply and source temperature.

For the ground coupled heat pump, a borehole heat exchanger is assumed with average thermal properties for the ground as located in the north of Belgium, namely a thermal conductivity of 1.8 $\frac{W}{mK}$ and a volumetric heat capacity of 2.2 $\frac{MJ}{m^3K}$ [160]. The heat pump is sized to 80% of the nominal heat demand in accordance with the code of good practice in Belgium [127], with the peak heat demand delivered by a back-up electric heater. The model of the heating system comprises the set of linear equations presented in Section 3.4. The domestic hot water tank is assumed perfectly mixed and needs to be at a temperature higher than $50\,°C$ at times when DHW is demanded. It can be heated by the heat pump up to $60\,°C$, but also by the back-up electrical heater up to $90\,°C$. An exception to this is the high temperature heat pump, which can heat the DHW storage tank to $80\,°C$.

Illustration of the integrated model output

Figure 5.3 illustrates the output of the integrated model for the case of newly built detached dwellings with heat recovery on the ventilation, an ACHP and radiators. The left figure shows the sum of the demand of the heat pumps, d_j^{hp} and the fixed electricity demand, d_j^{fix}. When no DR is applied, the heating systems do not interact with the electricity generation system and thus present a specific demand profile without feedback. In this case the energy use is minimized, causing the mean temperature of the buildings (right figure) to stay as low as possible while maintaining thermal comfort. Note that when assuming no DR, optimal control is applied which results in an indoor temperature close to the minimum comfort temperature. When DR is applied, the building is preheated to higher temperatures in order to avoid electric demand at times of expensive electricity generation. Load shifting occurs during hours 26 to 31, avoiding demand when the fixed demand is already high and hence the least efficient power plants are running. From hour 56 to 67, the electricity demand

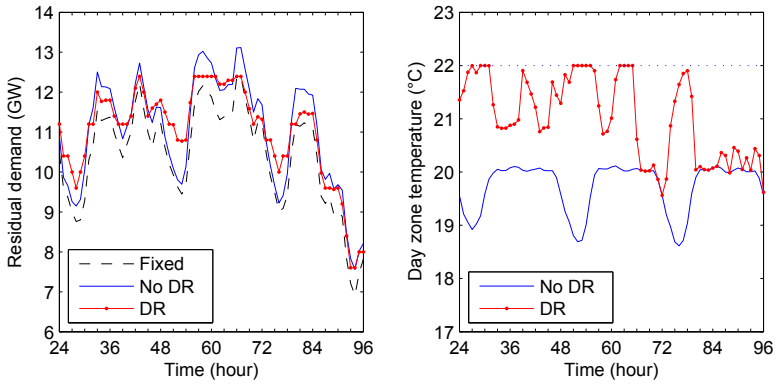

Figure 5.3: Electricity demand minus RES generation (left) and average day zone temperature (right) for three days of a typical week. The heat pumps cause an extra demand on top of the fixed electricity demand.

is also shifted in time in order to reduce heat pump demand at peak demand (peak shaving). Although DR has a direct impact on the indoor temperature, the temperature stays between the comfort bounds at all times and the rate of change of the indoor air temperature does not exceed $1\,°C$ per hour.

In practice, the temperature range that is available for DR is expected to vary significantly depending on occupant preference. Moreover, it should not be constant in time. Nevertheless, the comfort band of $2\,°C$ is assumed to be an acceptable range, taking into account the indoor temperature fluctuations observed for current state-of-the-art control strategies [104]. Traditional control systems apply a feedback control on the indoor air temperature with a typical spread of $1\,°C$ to $2\,°C$ [104] which will result in a similar average and similar fluctuations of the indoor air temperature.

5.3 Results

The first part of this section shows the CO_2 abatement cost for different building and heat pump cases, which allows a comparison between these cases. The sensitivity of this CO_2 abatement cost towards economical parameters is illustrated by the different discount rate cases. Next, the different factors determining this abatement cost are described in detail, namely the CO_2 emission (Section 5.3.2), the operational costs (Section 5.3.3) and finally the need for peak electrical capacity (Section 5.3.4).

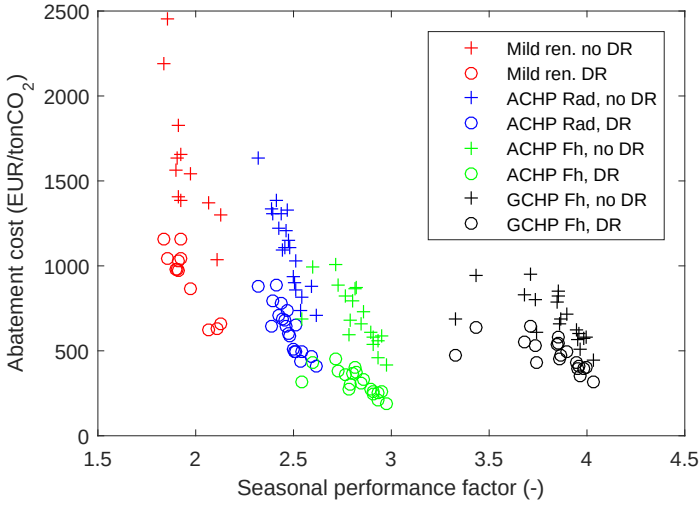

Figure 5.4: Overview of the CO_2 abatement cost as a function of the heat pump's seasonal performance factor (SPF) for a discount rate of 7%. The results are clustered depending on the presence of an air coupled heat pump (ACHP) or ground coupled heat pump (GCHP), the presence of radiators (Rad) or floor heating (Fh) and whether the buildings are mildly renovated (Mild ren.) or not.

5.3.1 CO_2 abatement cost

In Eq. (5.1), the CO_2 abatement cost includes operational cost savings, the additional investment in a heat pump and the extra investment in OCGT needed to cover the increase in peak electricity demand. In this abatement cost, the heat pump investment plays an important role. As shown in Figure 5.4, the CO_2 abatement cost depends strongly on the SPF. In Figure 5.4 there is a clear "clustering" of the results based on the four heat pump cases shown in Table 5.1. The "mildly" renovated buildings (SPF 1.8 to 2.1) are the least attractive buildings in which to install a heat pump, as these have the highest abatement costs. Applying DR for these buildings does bring the abatement cost closer to that of the "thoroughly" renovated buildings.

For these "thoroughly" renovated buildings, coupling the heat pump to the radiators leads to somewhat higher seasonal performance factors (SPF 2.3 to 2.6) and also to lower abatement costs. However, the lowest abatement costs are obtained with the air coupled heat pumps coupled with floor heating (SPF 2.5 to 3). For the best case, an abatement cost of 185 EUR/ton CO_2 is obtained.

Ground coupled heat pumps (SPF 3.3 to 4) lead to the highest CO_2 emission savings, as shown in the next section, but this is not enough to counteract the higher investment cost; hence the abatement cost is on average 100 EUR/ton CO_2 higher than for the air coupled heat pump with floor heating. Furthermore, it must be noted that all buildings have been at least "mildly" renovated and the original heat emission system was kept for low temperature heating after renovation. As such, the main differences in abatement cost are induced by the heat pump investment cost and the influence of the supply water temperature which is directly affecting the SPF of the heat pumps. These factors cause a large spread on the abatement cost as shown in Figure 5.4. What also follows from the strong clustering of the results based on the SPF, is that there are little differences between the considered building types. As soon as the buildings are well insulated, i.e. the "thoroughly" renovated buildings and buildings built after 2005, their CO_2 abatement cost depends mainly on the type and SPF of the heating system. In those cases, it is observed that the age class and building type are of less importance. In order not to overload the figures this is not illustrated. Throughout all cases, the application of DR is beneficial and lowers the abatement cost with 300 EUR/ton CO_2 on average.

The results in Figure 5.4 are determined using a discount rate of 7%, reflecting a more private perspective. In order to illustrate the sensitivity of this abatement cost to the discount rate, the results are shown for the more societally oriented discount rate of 3.5% in Figure 5.5. This lower discount rate lowers the weight of the investment cost in the determination of the CO_2 abatement cost (Eq.5.1). This causes the CO_2 abatement cost, on average, to reduce by 250 EUR/ton CO_2 and 150 EUR/ton CO_2 for the cases without and with DR, respectively. In the best case, the abatement cost becomes 110 EUR/ton CO_2. The relative differences and trends between the different building and heating system cases appear to be similar to Figure 5.4.

5.3.2 CO_2 emissions

Figure 5.6 shows the relative change in CO_2 emissions associated with replacing a condensing gas boiler with a heat pump. The relative CO_2 emission savings are highly dependent on the SPF of the heat pump, for which four groups can be distinguished based on Table 5.1. The first group consists of the mildly renovated buildings which are all equipped with a high temperature ACHP (SPF 1.8 to 2.1) for which the CO_2 emissions are lowered by 15% to 25%. For the second group, consisting of the thoroughly renovated buildings with an ACHP and radiators (SPF 2.3 to 2.6), the CO_2 emission reduction is higher: 25% to 35%. The third and fourth groups represent the buildings with floor heating combined with an ACHP (SPF 2.5 to 3) or a GCHP (SPF 3.3 to 4)

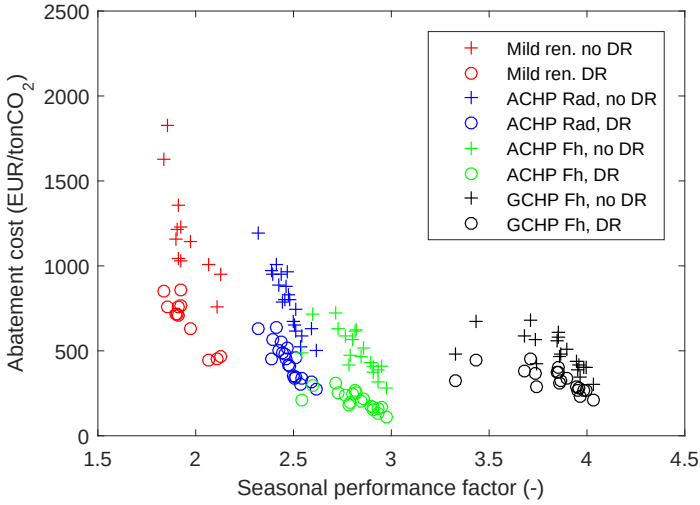

Figure 5.5: Overview of the CO_2 abatement cost as a function of the heat pump's seasonal performance factor (SPF) for a discount rate of 3.5%.

respectively. For these groups the decrease in CO_2 emission is 30% to 40% and 40% to 55%, respectively. Applying DR leads to an additional reduction in emission of approximately 15% on average. For the cases with floor heating, applying DR seems to cancel out the differences between the building types, leading to a general 45% or 60% emission reduction for an ACHP or GCHP, respectively. Note that these are all relative reductions in CO_2 emission. As buildings get better insulated and the annual heat demand lowers, the absolute CO_2 emission for the heat pump cases will converge.

One could also make a simplified estimation of the results in Figure 5.6. If one would assume that all electric demand of the heat pump is covered by an electricity generation system with a yearly average system efficiency, $\bar{\eta}^{egs}$, and the heat pump has a seasonal performance factor, SPF, the estimation of the relative CO_2 emission would be:

$$\frac{\sum^{year} CO_2(HP)}{\sum^{year} CO_2(CGB)} = \frac{\frac{CO_2^{gas} \cdot Q^{dem,year}}{\bar{\eta}^{egs} \cdot SPF}}{\frac{CO_2^{gas} \cdot Q^{dem,year}}{\eta^{cgb}}} = \frac{1/(\bar{\eta}^{egs} \cdot SPF)}{1/\eta^{cgb}} \tag{5.3}$$

with CO_2^{gas} the CO_2 intensity of burning natural gas and $Q^{dem,year}$ the yearly thermal energy demand of a building. This estimation is plotted in Figure 5.6 if $\bar{\eta}^{egs}$ would correspond to the minimal (48%) and maximal (60%) efficiency of a CCGT as well as the maximal efficiency of an OCGT (40%). As can be seen from

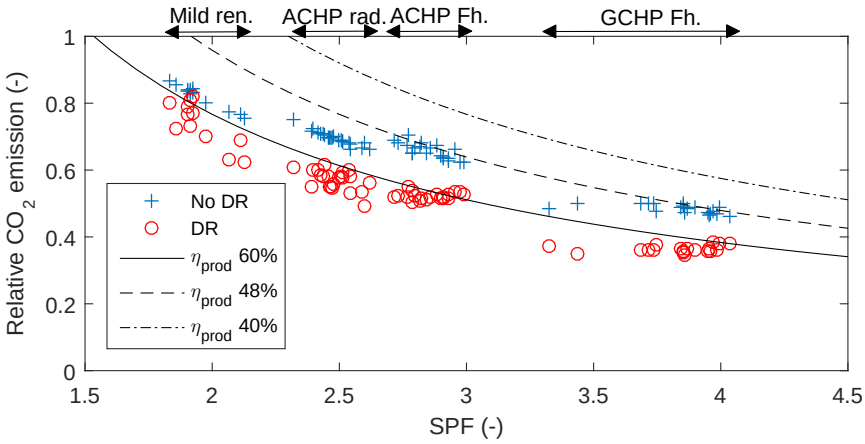

Figure 5.6: Relative CO_2 emission when replacing the reference condensing gas boiler with a heat pump which does not (no DR) or does participate in DR (DR), as a function of the seasonal performance factor (SPF) of the heat pump. Additionally, the simplified estimation based on three typical values of the yearly average electricity generation system efficiency $\bar{\eta}^{egs}$ (Eq. 5.3) is shown.

Table 5.2: Equivalent electricity generation system efficiency, $\bar{\eta}^{egs}$, which can also be interpreted as the inverse of the primary energy factor.

Case	Literature	no DR	DR
$\bar{\eta}^{egs}$	40%	52%	65%
PEF	2.5	1.9	1.5

Figure 5.6, this equation is good in estimating the relative CO_2 savings when no DR is applied. This is because, when no DR is applied, most of the electricity demand of the heat pumps is covered by gas fired power plants, as discussed in Section 5.3.3. If one assumes an η^{cgb} of 0.92, the fitted equivalent electricity generation system efficiency would be 52% with a coefficient of determination R^2 of 0.94. A similar fit can be found for the cases with DR, attaining an equivalent electricity generation system efficiency of 65% with a coefficient of determination R^2 of 0.95. This equivalent efficiency is higher than what the power plants can reach, as applying DR allows for a higher uptake of RES. Of course, the presented values will change if the boundary conditions of this study change.

The equivalent electricity generation system efficiency, $\bar{\eta}^{egs}$, can also be interpreted as the inverse of the primary energy factor (PEF) of electricity

(Table 5.2). For example for the boundary conditions of this chapter, a heat pump with DR has a PEF of 1.5 which means that for 1 kWh of electricity, on average 1.5 kWh of fuel is needed. In the literature, the PEF is typically around 2.5 [177] [161] [156] or varying between 2 and 3.5 [49]. The PEF is highly dependent on the mix of generation systems in the electricity generation system. In this chapter, the mix consists mainly of efficient CCGTs and RES, causing the PEF to be lower than the typical value in the literature. The integrated model is able to determine this PEF accurately and determine the change in PEF due to the application of DR.

5.3.3 Operational aspects

Regarding the operational cost savings, the trends of relative cost savings with respect to the heat pump SPF are identical to those of the CO_2 emission reduction. Indeed, as natural gas is the only fuel considered in the study and the cost of RES is considered to be zero, the only driver in this chapter that reduces CO_2 emissions and fuel cost is a reduction in natural gas demand. However, 250,000 heat pumps will have a significant impact on the electricity generation system, which is discussed in this section.

The increase in electricity demand due to the 250,000 heat pumps is covered either by a reduction in RES curtailment (left in Figure 5.7) or by an increase in generation by gas fired power plants (right in Figure 5.7). The reduction in RES curtailment is achieved by shifting heat pump electricity demand towards hours of curtailment. As such, the heat pumps use electricity which would have otherwise been curtailed. Figure 5.7 shows that the heat pump electricity demand is mainly covered by a higher generation from the gas fired power plants. When no DR is applied, a minor fraction of the heat pump demand is covered by RES. In this case, the CO_2 emission reduction of installing a heat pump instead of a condensing gas boiler is dominated by the difference in overall efficiency.

When DR is applied, CO_2 emissions do not only decrease due to a higher overall efficiency, but also due to load shifting. This load shifting improves the average efficiency of the power plants and, through a higher uptake of RES, decreases the generation by these power plants, as shown later in Figure 5.9. On average, DR causes these plants to produce 0.1 TWh less by increasing the use of RES by 0.2 TWh on average. In relative terms, the better insulated buildings will have a higher share (15% to 25%) of the heat pump electricity demand covered by RES compared to the less insulated buildings (5% to 15%).

Load shifting in heating systems typically leads to higher average temperatures (e.g. Figure 5.3) and hence higher thermal losses and higher energy use. Figure

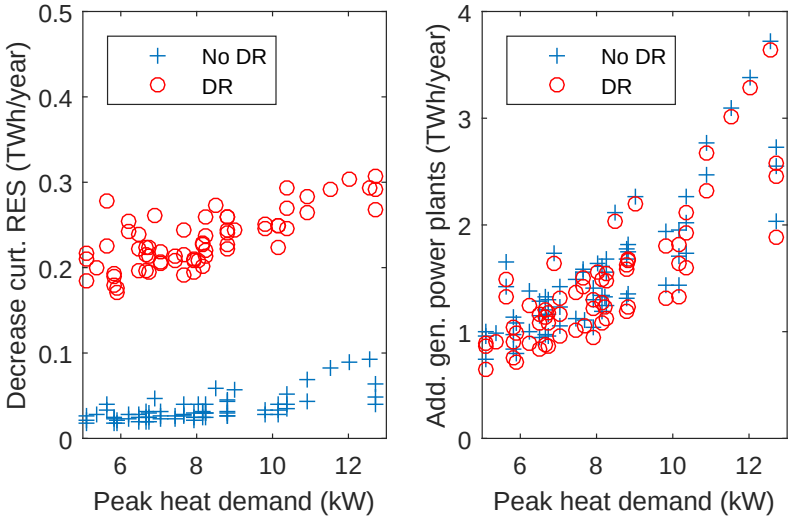

Figure 5.7: The electricity demand of the heat pumps is covered by reduction in RES curtailment (Left) and by additional generation from the gas fired power plants (Right). Mind the difference in y-axis. With no heat pumps, the curtailment amounts to 0.55 TWh while with heat pumps and no DR, the curtailment amounts to 0.52 TWh. Hence, performing DR approximately halves the curtailment in this case study.

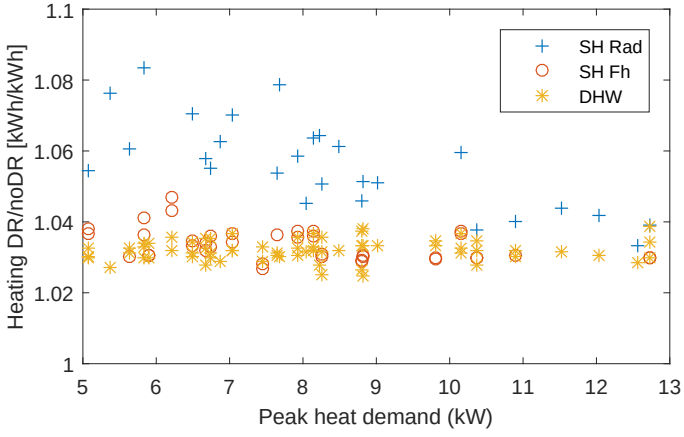

Figure 5.8: Rise in heat demand for space heating and domestic hot water demand when DR is applied.

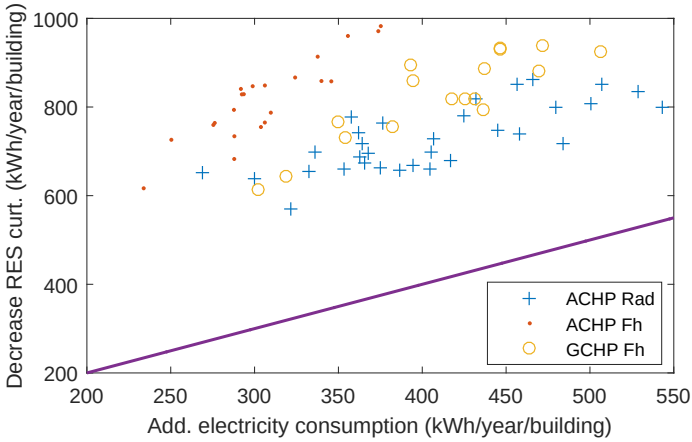

Figure 5.9: Decrease in curtailing RES per building with respect to extra electricity consumption per building when applying DR. The thick contour line depicts the situation in which, on a net basis, no net reduction is achieved.

5.8 shows this increase in energy use associated with load shifting. For all building cases, the domestic hot water tank is used almost identically: around 3% more thermal energy is added to this storage tank, causing the yearly average temperature of the storage tank for DHW to be $4\,°C$ higher. Regarding space heating with radiators (SH Rad), when DR is applied, a clear trend can be observed: as the peak heat demand decreases, relatively more heat is emitted to the building. On average, the energy use increases by 5.5% and the indoor air temperature by $0.5\,°C$. If the buildings are equipped with floor heating (SH Fh), the trend is less pronounced, leading to an average increase in energy use by 3.5% and an average increase in indoor air temperature by $0.2\,°C$.

One may perhaps argue that the extra energy use is wasted in higher thermal losses. To see whether this is the case, the decrease in RES curtailment per building is plotted against the increase in electricity use per building in Figure 5.9. For example, applying DR causes a building to consume 300 kWh_e of electricity more but reduces 800 kWh_e of RES curtailment, then on a net basis, the gas fired power plants produce 500 kWh_e less. From this figure it is clear that the decrease in curtailment is always higher than the increase in electricity consumption due to DR. Hence on a net basis, less electricity from gas fired power plants is used. For an ACHP with floor heating, this difference is the highest, reducing 325 kWh_e to 625 kWh_e electricity consumption from gas fired power plants per building. Note that, due to the high RES share assumption, the curtailment in the case with no DR is rather high to start with, namely

around 2000 kWh_e per building. Hence, the relative reduction in curtailment is between 30% and 45% and is similar to values found in the literature [81, 52].

5.3.4 Peak capacity

In the calculation of the CO_2 abatement cost, the investment in additional peak power plant capacity is taken into account (Eq. 5.1). At an investment cost of 750 EUR/kW_{el} (Section 5.2.1), this additional capacity can be an important term in the CO_2 abatement cost, which is typically not included in heat pump CO_2 abatement cost in the literature. The need for additional peak power plant capacity depends highly on the simultaneity of the heat pumps' demand and the other electricity demand, assumed to be fixed, at peak periods. Figure 5.10 shows how the heat pumps contribute to the electricity demand at peak periods, as also shown by Hawkes [79]. For the considered climate and demand profile, i.e. Belgium, the highest demand of the heat pumps will occur at cold and dark days which typically coincides with the peak electricity demand. As shown in Figure 5.10, when no DR is applied, the additional peak demand per building is strongly correlated with the nominal electric power demand of the heat pump. Regarding buildings with the same heat demand, a ground coupled heat pump would hence perform best in this case, as this system has the highest COP and therefore the lowest peak electricity demand.

Installing heat pumps with DR can cause the need for additional peak power plants to decline, as peak shaving can be applied. Below a certain capacity of the heat pump, the buildings are able to shift almost all demand away from the hour with the highest electricity consumption (Figure 5.10). The buildings with floor heating generally perform better than the same building with radiators. Figure 5.10 shows that peak shaving becomes less effective at higher design electricity demand. The reason for this is twofold. First, the buildings with a higher electricity demand at design conditions are also the less insulated buildings for which preheating is less efficient. Second, the load can only be shifted a limited number of hours. If a significant number of heat pumps perform this shift, the hours before the peak might become "saturated", e.g. in hour 56 in Figure 5.3. When this occurs, there is no other option than to increase the consumption in these hours, and therefore the installation of additional peak power is required. Note that in this chapter, for each case, the heat pump demand was scaled up to represent 250,000 buildings. Altering this number of buildings can alter this "saturation" and hence also alter the results shown in Figure 5.10.

Additionally to peak shaving, heat pumps with DR also demand less power when the peak power plants are running (Figure 5.11). Since these are typically

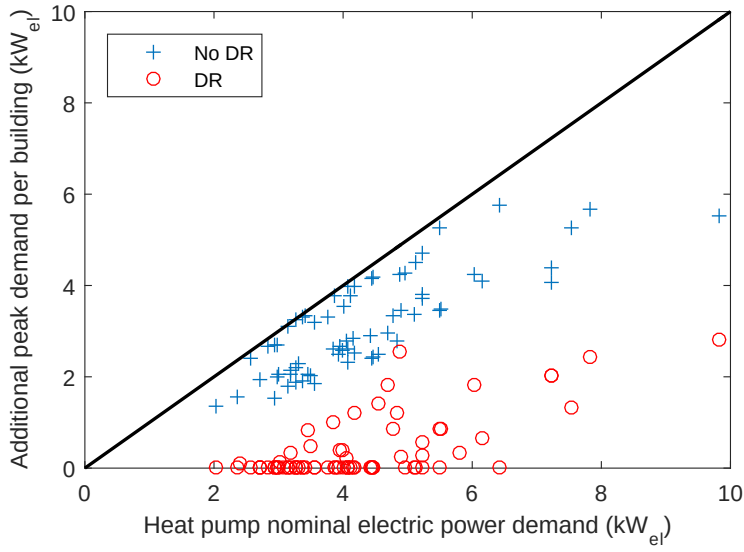

Figure 5.10: Performance of DR in peak shaving. The electric power that each building is contributing to the demand at peak time by installing a heat pump is shown with respect to the nominal electric power demand of the heat pump.

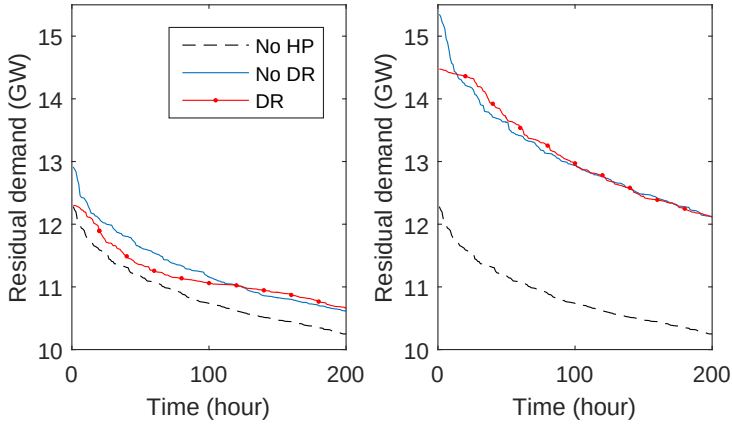

Figure 5.11: Part of the residual load duration curve for the cases of installing 250,000 ACHPs with radiators in the best (left) and worst (right) insulated detached buildings. DR decreases the need for extra peak power. For the best insulated buildings, the electricity generation covered by the peak power plants is also reduced.

less efficient OCGT, compared to CCGT, this also leads to lower CO_2 emissions for this case. This effect is predominantly observed for the better insulated buildings (left in Figure 5.11) where more load shifting is performed.

5.4 Discussion

The lower values of the CO_2 abatement cost found in this chapter are in the same order of magnitude as in the work of Joellson [89] and Kesicki [97]. However, those studies lack to highlight the large spread in abatement cost associated with the building renovation level, the type of heat pump installed and the application of DR. As shown in Figure 5.4, these factors cause the abatement cost to vary between 185 and $2,300$ EUR/ton CO_2. Furthermore, the abatement costs obtained here are not comparable to the other studies, as this chapter takes into account operational and investment costs at both demand and generation side.

What might also cause a large spread in the CO_2 abatement cost are the characteristics of the studied electricity generation system. Van den Bergh et al. [170] and Delarue et al. [45] illustrate that the abatement cost is highly dependent on RES deployment and RES cost as well as the fuel mix and fuel cost of conventional power plants in the electricity generation system. In order to limit the scope of this chapter, only natural gas was considered as a fuel.

Applying DR on heat pumps causes a reduction in peak electricity demand and RES curtailment. However, other technologies may be more cost effective in attaining these reductions. For example, Dupont et al. [52] studied the application of DR with battery electric vehicles and white good appliances. For a future scenario with 18% of electricity generation stemming from PV and wind and 8% of the cars being electric, this reduces RES curtailment with 41%. Hence, the potential for DR on heat pumps also lowers. Another possible source of DR competition stems from stationary batteries, which are a favourable option to combine with rooftop PV [163].

A number of factors influencing the CO_2 abatement cost could change by 2030. A limited sensitivity analysis towards these factors is shown in Table 5.3. A large scale introduction of heat pumps can increase the electricity demand up to the point that extra investments in the distribution and transmission grids is needed. It is hard to estimate the associated costs since these are very location dependent [67]. For an arbitrary value of 3000 EUR of grid enforcement per household based on [67], Table 5.3 shows that the CO_2 abatement cost rises. This rise is however limited for most cases and does not alter the difference among the demand side technologies. One can also argue whether the additional

Table 5.3: Sensitivity of the CO_2 abatement cost (in EUR/ton CO_2) towards grid infrastructure investment, heat pump investment cost and gas price. The results are only shown for the cases with DR for the detached buildings built between 1971 and 1990.

Renovation Heat pump source Heat emission	Mild Air Radiator	Thorough Air Radiator	Thorough Air Floor	Thorough Ground Floor
Reference ($i = 7\%$)	976	493	251	397
3000 EUR network investment [67]	1165	665	380	495
40% cheaper heat pumps [99]	555	193	52	152
25% higher natural gas price [171]	977	476	228	371

investment in grid infrastructure should be solely attributed to heat pumps, since a higher uptake of distributed PV needs similar investments [13]. On the other hand, the investment cost of heat pumps could be lower in 2030, due to the learning curve effect associated with higher production volumes [99]. If one assumes a similar cost reduction as in Switzerland [99], the CO_2 abatement cost significantly lowers as shown in Table 5.3. Thus, the heat pump investment cost represents a substantial part of the CO_2 abatement cost, and lowering this cost can make a heat pump a more attractive option in lowering CO_2 emissions. Finally, according to the World Energy Outlook [171] the price of natural gas could rise 25% compared to 2014 levels. The CO_2 abatement cost appears to be less sensitive to this price as Table 5.3 shows.

In this chapter, a large scale deployment of heat pumps is considered to cause an additional electricity demand on top of the fixed electricity demand, and the extent to which this additional demand can be covered by RES is quantified. Thus, this chapter employs the incremental emission factor as defined by Bettle et al. [20]. Bettle et al. advise applying this incremental emission factor for assessing a change in electricity demand and hence for the application in this chapter, the replacement of condensing gas boilers with heat pumps. According to Bettle et al., the incremental emission factor can lead to 50% higher CO_2 emissions than employing the average emission factor, in which the CO_2 emission of a particular electricity demand profile is assessed in each time step with the average CO_2 emission of the electricity generation in that time step.

This chapter does not include investment costs for building renovation, but assumes that the renovated buildings are already present. Of course, one could

Table 5.4: Yearly CO_2 emissions in ton for certain scenarios for the cases with a condensing gas boiler (no HP), heat pump without DR (no DR) and heat pump with DR (DR).

Renovation level	Mild			Thorough		
Ton CO_2/year	no HP	no DR	DR	no HP	no DR	DR
Detached pre 1945	12.9	10.9	10.4	3.8	2.6	2.2
Terraced 1971-1990	3.2	2.7	2.3	2.1	1.5	1.2

argue whether the investment in a heat pump is justifiable in a mildly renovated building, and whether this money should not better be spent on a more thorough renovation of the building envelope. Judging from the results, this appears to be very case dependent, as shown in Table 5.4. For example, for the worst building case (detached building pre 1945) renovating the building envelope is more effective in reducing CO_2 emissions. In case of a better insulated building (terraced building from 1971-1990), installing a heat pump and performing DR leads to almost the same emission reduction as renovating the building envelope. For these cases, installing a heat pump and performing DR is hence a viable alternative for newer and more compact buildings, where a thorough renovation of walls and floor might not be a feasible option.

For the ground coupled heat pumps, the CO_2 abatement cost is on average higher than for the air coupled heat pumps with floor heating (Figure 5.4). Ground coupled heat pumps are known to have high global efficiencies in applications where both heating and cooling are needed, such as office buildings, thanks to the high efficiency of direct cooling [178]. This benefit is not exploited in residential buildings in a climate similar to that of Belgium, leading to longer pay back periods.

It is important to note that from a consumer point of view, the increase in electricity consumption can demotivate the consumer of participating in DR. A consumer will only participate in DR schemes when facing a lower overall energy cost. This cost for the end consumer typically consists of energy related costs (the cost of electricity generation) and non-energy related costs (taxes, transmission and distribution tariffs), which are currently transferred as a proportional tariff (per kWh) to the end consumer. A time dependent price signal through the energy component of this tariff may be insufficient to motivate the end consumer to participate in an DR scheme: the decrease in energy related costs, via a time dependent tariff, may be fully offset by an increase in the non energy related costs. The latter increase can result from the increased energy use and hence, the time invariant non energy related component of the tariff.

5.5 Conclusion

This chapter makes an assessment of the suitability of heat pumps for reducing CO_2 emissions in the residential building sector. A large scale deployment of heat pumps with demand response, instead of the commonly installed condensing gas boilers, is investigated by taking into account the effects on the electricity generation system. To this aim, a detailed integrated model of buildings, heating systems and the electricity generation system is employed. This allows a thorough assessment of the CO_2 emissions, fuel usage and peak capacity investment. From the results, it appears that the reduction in CO_2 emission is dominated by the seasonal performance factor of the heat pump and the application of DR. This DR allows a higher uptake of RES based electricity generation that would have otherwise been curtailed. The heat pumps appear to contribute significantly to the peak electricity demand. The application of DR partially alleviates this problem, especially for the buildings with floor heating.

To allow comparison between combinations of heating systems and buildings, the above results are summarized in a CO_2 abatement cost. This CO_2 abatement cost is sensitive to assumptions on economical parameters, as illustrated by the difference in results due to a different discount rate. The numerical values on CO_2 abatement cost are hence only valid within the given assumptions on boundary conditions. Furthermore, the sensitivity on the assumptions of the electricity generation system characteristics was not considered in this chapter. Rather, the focus is on demand side, where it appeared that the CO_2 abatement cost is already strongly influenced by multiple factors at the building level. The result is a large spread on the CO_2 abatement cost as a function of the heating system and building characteristics. The first factor is the renovation level of the considered dwellings, which causes large differences in CO_2 abatement costs. Installing a heat pump in "mildly" renovated buildings causes a low relative reduction in CO_2 emissions and hence a high CO_2 abatement cost. Buildings which have undergone a "thorough" renovation, as well as new buildings, show a substantially lower CO_2 abatement cost and CO_2 emissions when installing a heat pump. The second factor is the heating system. For the new buildings and the "thoroughly" renovated buildings, an air coupled heat pump combined with floor heating is the most competitive heating system in terms of CO_2 abatement cost. The ground coupled heat pump leads to higher CO_2 emission savings, but results in a higher abatement cost due to the difference in investment cost and the absence of cooling demand in residential buildings in a Belgian climate. The third factor is the application of DR. This lowers the CO_2 abatement cost with on average 300 EUR/ton CO_2 because of a lower investment in peak power plant capacity, operational cost savings and lower CO_2 emissions. These savings are reached by load shifting which causes, on average, the heat demand for

domestic hot water to grow by 3% and the space heating demand by 5.5% for radiators and 3.5% for floor heating.

The proposed methodology can support policy makers in prioritizing investments in the building sector that reduce CO_2 emissions. It is shown that, within the boundary conditions assumed, particular buildings and heating system configurations are more cost effective than others in reducing CO_2 emissions by installing a heat pump. Additionally, the effects of a large scale deployment of heat pumps with DR on the electricity generation system are illustrated.

Chapter 6

Case study II: Impact of market penetration

This chapter is based on:
Arteconi, A., Patteeuw, D., Bruninx, K., Delarue, E., D'haeseleer, W., & Helsen, L. (2016). Active demand response with electric heating systems: impact of market penetration. Accepted for publication in Applied Energy.

6.1 Introduction

In the previous chapter, the value of DR was determined for different building and heating system types. In contrast to this, this chapter considers one building type and one heating system type. Rather, this chapter focuses on the effect of different penetration rates of DR programs among customers in order to point out positive and negative aspects of a variable introduction of such programs. The main effort is the attempt to quantify the economic benefits of DR programs both from a customer's and an overall system's perspective.

Mathieu et al. [116] modeled thermostatically controlled loads as a virtual energy storage and determined savings of 22 - 56 USD/year for heat pumps when these participate in ancillary service markets. Papaefthymiou et al. [131] considered a large set of buildings in the German market and showed cost savings of DR with heat pumps between 25 EUR and 40 EUR per year. Hedegaard and Munster [82] determined that the flexible operation of individual heat

pumps leads to a cost reduction of about 60 - 200 EUR per year per house in integrating wind power. This was mainly caused by savings on energy system investments. In contrast to these authors, this chapter analyses the operational cost savings while varying the participation rate in DR programs, rather than in a predetermined scenario. This allows evaluating to what extent deploying these residential DR resources is meaningful and how the gains per participating household[1] depend on this.

The analysis is conducted by employing the integrated model presented in Chapter 3. Section 6.2 provides the parameters of the integrated model for this chapter. In Section 6.3, the effect of a partial DR participation, see Eq.(6.1), is assessed in terms of difference in energy use and operational costs for the electricity generation system. Section 6.4 evaluates the difference in flexibility in the hot water storage tank and the thermal mass of the building, both separately and together. Moreover, different levels of RES integration in the generation mix are studied in Section 6.5, in order to highlight their effect on the operational performance of the system. Section 6.6 discusses the results further in order to end up with the conclusions in Section 6.7.

6.2 Methodology

In this chapter, the integrated model as presented in Section 3.7, is employed. The electricity generation system is modeled using the MO model as described in Section 2.3.2. The main focus of this chapter is on the DR participation parameter p^{dr} in Eq. 3.41, which is repeated here:

$$\forall j : d_j^{hp} = (1 - p^{\mathrm{dr}}) \cdot d_{\mathrm{j}}^{\mathrm{hp,fix}} + p^{\mathrm{dr}} \cdot d_{\mathrm{j}}^{\mathrm{hp,var}}. \tag{6.1}$$

The linear demand side model is employed to model the flexibility in the heat pump electricity demand $d_{\mathrm{j}}^{\mathrm{hp,var}}$. This model entails the buildings using electric heating systems, composed of heat pumps and auxiliary electric resistance heaters. These heating systems provide both space heating via floor heating and domestic hot water. Thermal energy storage, allowing shifting electricity demand in time, is provided both by the thermal mass of the building and the hot water storage tank. The same demand side model is used to predetermine the electricity demand of the heating systems not participating in a DR scheme ($d_j^{hp,fix}$) by minimizing the energy use to meet the required thermal comfort and neglecting any interaction with the supply side model. This electricity

[1] The presented gains are fully divided over the participating buildings. Note that in reality, this will not be the case as other parties, such as electricity generation companies and/or aggregators, will claim part of this profit. The intention of the presented earnings is to illustrate the maximum possible size of the gains.

demand is referred to in the following as the minimum energy scenario for heating systems ($p^{dr} = 0\%$).

In this chapter, the electricity supply and demand is inspired by the Belgian power system. The electricity generation system configuration is based on a hypothetical future energy mix, consisting solely of gas fired power plants and RES based electricity generation [57]. The installed capacity of gas fired power plants consists of $11,200\ MW$ CCGTs and $5,800\ MW$ OCGTs. The nominal net efficiency of the CCGT power plants varies between 60% and 48% while for the OCGT power plants, this varies between 40% and 30%. Both the traditional electricity demand profile and the electricity generation by RES (g_j^{RES}) are taken from the Belgian transmission grid operator [54] for the year 2013. Considering the traditional electricity demand profile, the peak electric power demand on the transmission grid amounts to $13,119\ MW$. When adding also the electric heating system to this traditional demand, the peak demand occurs at another moment in time, and amounts to $16,917\ MW$[2]. The gas price is assumed to be 25 EUR $/MWh$ [62]. RES based electricity generation is assumed to have zero marginal cost.

Regarding the demand side, the number of buildings (nb) is assumed to be about one million, which is the expected number of detached buildings for Belgium in 2030 [147]. In this study, the detached buildings are represented by an 'average' building as suggested in the TABULA [38] project, since Chapter 5 illustrated the similar DR potential for thoroughly insulated buildings. For this average building, the day zone and night zone have a surface area of 132 m^2 and 138 m^2 respectively. All these buildings are assumed to have undergone a renovation of windows, air tightness, walls, floor and roof resulting in low energy buildings with an average U-value of 0.3 W/m^2K and a ventilation rate of 0.4 ACH (air changes per hour), which are two necessary conditions for the nearly zero energy building standard, as set up by the Flemish government [175]. The dynamic building model is the linear state space model based on Reynders et al. [151], as shown in Figure 2.4. Table 6.1 provides an overview of the values for the thermal resistances and thermal capacities used in this building model.

Regarding the occupant behavior, the user behavior data from Baetens and Saelens [14] was used, as illustrated in the profiles Baetens2 in Section 2.4.2. The user behavior data was aggregated with the methodology presented in Section 3.6. The weather data is based on Uccle for the year 2013, as shown in Section 2.4.3. This weather data is taken for 2013 in order to have the correct simultaneity with the fixed electricity generation profile and the electricity generation by RES.

[2]This value refers to the case of minimum energy use by heat pumps ($d_j^{hp,fix}$)

Table 6.1: Resistance and capacitance values used in the RC network model of the building as illustrated in Figure 2.4.

Parameter	Day zone	Night zone
C_w (MJ/K)	20.3	8.8
C_f (MJ/K)	12.1	-
C_i (MJ/K)	2.43	1.47
C_{wi} (MJ/K)	26.2	4.09
C_{fi1} (MJ/K)	31	-
C_{fi2} (MJ/K)	-	31
R_{w1} (K/W)	0.003	0.002
R_{w2} (K/W)	0.031	0.043
R_{wi} (K/W)	0.001	0.009
R_{f1} (K/W)	0.02	-
R_{f2} (K/W)	0.047	-
R_{fi1} (K/W)	0.001	-
R_{fi2} (K/W)	0.002	-
R_{fi3} (K/W)	-	0.001
$vent$ (K/W)	0.006	0.009

The heating system consists of an air coupled heat pump which supplies heat to the floor heating system in the day and night zones, as well as to the storage tank for DHW. Space heating is only considered during the heating season while DHW is supplied all year round. The heat pump is sized to meet 80% of the peak heat demand, the rest of the peak demand is covered by a back up electric resistance heater. The COP of the heat pump is determined according to Bettgenhäuser et al. [19]. The nominal supply water temperature of the floor heating is $35\,^{\circ}C$. Based on this, the COP is predetermined and assumed to be constant throughout each optimisation period, based on Verhelst et al. [179] and the results of Section 3.5. Hence, during each optimization period of a week, the COP is predetermined based on the average supply and source temperature.

Cases In the reference case, it was assumed that RES based electricity generation is capable of covering 30% of the electricity demand and consists of 50% solar and 50% wind energy. The lower bounds for the indoor temperature set points are $20\,^{\circ}C$ and $18\,^{\circ}C$ for the day zone and night zone respectively, while, in the reference case, the upper bounds are $22\,^{\circ}C$ and $20\,^{\circ}C$ respectively [140]. The maximum allowed air temperature in the day zone is referred to as $T^{sh,max}$ in the rest of this chapter. The maximum allowed air temperature in the night zone is always assumed to be $2\,^{\circ}C$ less. The DHW storage tanks are

Table 6.2: Summary of the key parameters in the different cases studied in this chapter. The DR participation rate is expressed as a percentage of the total electricity demand of electric heating systems. The RES share is expressed as a share of the total electric demand.

Parameter Section	Reference 6.3	DR technology 6.4	RES share 6.5
DR participation rate [%]	5-25-50-100	5-25-50-100	5-25-50-100
RES share [%]	30	30	**0-30-50**
$T^{sh,max}$ [$^{\circ}C$]	22	**22-24**	22
$T^{tank,max}$ [$^{\circ}C$]	60	**60-90**	60
Tank size [–]	small	**small or big**	small

either 200 l or 300 l, depending on the maximum daily hot water demand at 50 $^{\circ}C$. The upper bound for the DHW storage tank is 60 $^{\circ}C$. This upper bound for the DHW storage tank is inspired by the maximum temperature at which the heat pump can still deliver heat. In this reference case, the share of flexible demand from electric heating systems (p^{dr}) is varied between 5% and 100%. The first column of Table 6.2 provides an overview of the key parameters of the reference case. The results for this reference case are shown in Section 6.3.

In a second case study, entitled 'DR technology' in Table 6.2, the difference in DR flexibility between space heating and domestic hot water provision is evaluated along with measures to increase the available flexibility: the upper boundaries are varied for the indoor air temperature, $T^{sh,max}$(up to 24 $^{\circ}C$), and the DHW storage tank, $T^{tank,max}$ (up to 90 $^{\circ}C$). The DHW storage tank can be heated up to a temperature higher than 60 $^{\circ}C$ by a back-up electric resistance heater. The effect of doubling of the DHW storage tank size is also investigated, so 400 l or 600 l tanks instead of 200 l or 300 l tanks. The results for this comparison are provided in Section 6.4.

In a third case study, entitled 'RES share' in Table 6.2, the impact of the RES share is evaluated by considering two extra cases, namely a 0% and 50% RES share in the end electric energy use. Moreover, the relative share of solar and wind energy, and its impact on the performance of DR programs, is studied. The results for this case study are provided in Section 6.5.

6.3 Results: reference case

In this section, the results for the reference case are illustrated both for operational cost savings (Section 6.3.1) and peak shaving (Section 6.3.2).

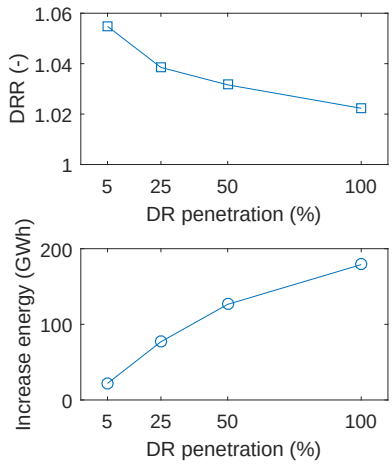

(a) The rate of DR participation influences the demand recovery ratio (squares, top figure) as well as the total increase in electricity demand (circles, bottom figure).

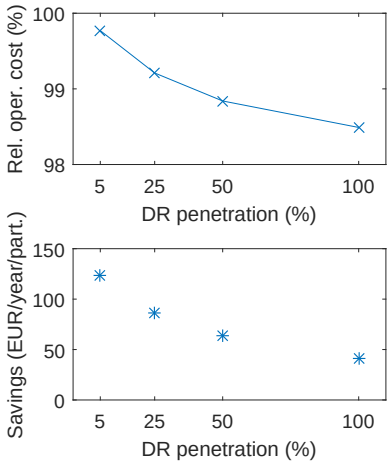

(b) Effect on the operational cost savings, both in relative total system cost (crosses, top figure) and per participant (asterisks, bottom figure).

Figure 6.1: Reference case: energy use and operational cost savings. The increase in energy use and difference in operational cost are determined with respect to the case of no DR participation (p^{dr} is 0%). These cost savings are for the electricity generation system as a whole.

6.3.1 Operational cost savings

One of the main purposes of this chapter is to illustrate the effect of a variable DR participation of customers using electric heating on the electricity generation system. This effect is presented both from the customers' and overall system's point of view. The controllable demand from the electric heating systems is assumed to participate to the DR program with a variable percentage, p^{dr}, namely 5%, 25%, 50% and 100% (see Table 6.2, 'Reference' case). When there is no full DR participation, a part of the consumers is not exposed to the hour to hour variations of the electricity generation cost. It is assumed that these consumers minimize their own electricity use. For the customers adhering to the DR program, the demand is shifted to hours of lower overall consumption, hence lower electricity costs, and so called 'valley filling' occurs. Load shifting however leads to higher temperatures in the building and DHW storage tank and hence to additional thermal losses and an increase in overall energy use. The absolute increase in electricity demand grows with p^{dr} (Figure 6.1a). This increase

varies between 20 GWh to 180 GWh annually at the country level, which is a small amount compared to the total electricity demand of about 88 TWh. The demand increases with increasing DR penetration rates in a sub-linear fashion. This sub-linear trend is due to a 'saturation' of the usefulness of flexibility in the power system. Additional DR based flexibility is not used as intensively, because the need for load shifting has already been fulfilled. During moments of load shifting, the burden of load shifting is however carried by more buildings when increasing the DR penetration rate, resulting in smaller deviations from the minimum energy use demand profile for each building individually. As a result, the increase in energy use rises sub-linearly with the DR penetration rate.

The ratio between the observed electric energy use by the flexible electric heating systems and the minimum electric energy use of those heating systems ($p^{dr} = 0\%$) is defined as the demand recovery ratio (DRR) [27, 41]. This ratio allows quantifying the increase in energy use due to load shifting of the demand side technology. It is always greater than or equal to one: in the case of 0% DR, the DRR is 1 as in this case there is no participation in the DR program and the buildings minimize their own electricity consumption ($p^{dr} = 0\%$). When the buildings participate in DR, the DRR exceeds one. Figure 6.1a illustrates the DRR for the buildings participating in the DR program. An important observation is that the DRR depends on the DR participation. When 5% of the buildings are participating, the relative increase in energy use per dwelling is the highest, because, as previously described, there are few customers involved in the load shifting process. The required deviations from the minimum energy use electricity demand profile are the highest, resulting in higher thermal losses. Additional DR consumers face lower opportunities for load shifting, because of the above mentioned saturation effect. Hence, when more buildings participate in DR, the thermal losses per building are lower, as can be seen in the DRR.

Another effect of the share of DR participation can be seen on the total operational cost of the electricity generation system. Figure 6.1b shows the trend of R_c, defined as the ratio between the total operational cost with DR and without DR participation. This operational cost includes only fuel costs and hence no investment costs, ramping costs, CO_2 emission costs nor start-up costs. The maximum cost reduction for the considered configuration of the system is about 1.5%[3]. This small percentage corresponds to an absolute cost saving of about 41.8 million EUR per year. In this case, the CO_2 emissions are at most reduced by 0.34 $Mton/year$. At current EU emission trading scheme price levels (i.e. 4-8 EUR/ton CO_2 [44]), the operational cost reduction stemming

[3]The optimality gap used in the mathematical optimisation of the model is 0.1%, an order of magnitude smaller than the operational cost reduction.

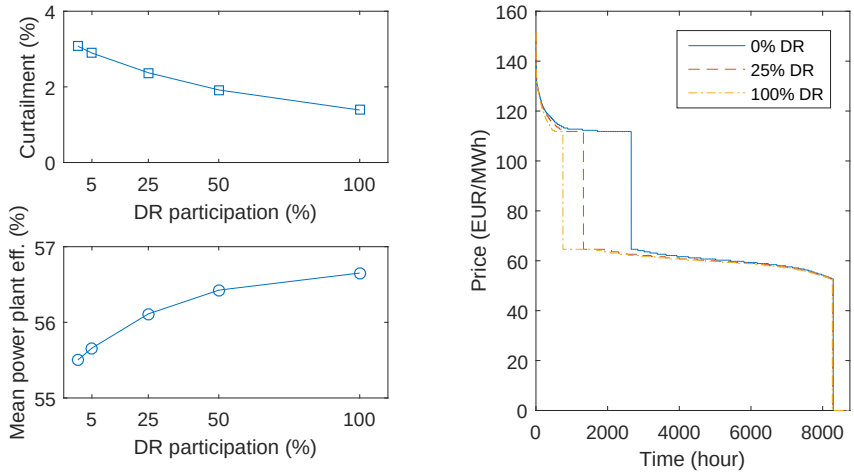

(a) Curtailment as a percentage of the available RES based generation (squares in top figure) and average gas fired electricity generation efficiency (circles in bottom figure)

(b) Price duration curves

Figure 6.2: Reference case: origin of operational cost savings.

from CO_2 emission lowering is thus an order of magnitude smaller than the operational cost reduction due to fuel cost savings.

The possible annual cost saving per customer is also shown in Figure 6.1b (circles, bottom figure). These results are made under the hypothesis that the operational savings can be entirely divided among the participants of the DR scheme. The yearly cost saving per building goes down in case of more participants, meaning again that a lower benefit per participant is attainable when more consumers are involved. Relative operational cost and cost savings per participant show a sub-linear trend in accordance with the behavior of the energy use previously illustrated in Figure 6.1a. This analysis gives an idea of the operational cost benefit that DR can bring not only to the system, but also to the customers: it ranges between 41 to 124 EUR per customer per year. These results, especially for high DR penetration rate, are similar to values reported by other authors [116, 131], that analyzed a large scale deployment of heat pump flexibility for space heating and cooling.

The decreases in operational cost and CO_2 emissions are due to a more efficient operation of the power plants and a reduction in curtailment of electricity generation by renewable energy sources. This is demonstrated in Figure 6.2a.

The average gas fired electricity generation efficiency[4] shows a slight increase (Figure 6.2a), while the curtailment is halved by increasing the DR participation from 5% to 100%. The sub-linear trend of these curves reflects the saturation effect.

Figure 6.2b, shows the electricity price duration curve. The electricity price is here determined as the marginal cost of the most expensive unit running in accordance with the MO model. Three different main plateaus can be detected: (i) for a small number of hours (about 400) the price is zero, when the RES based electricity generation fully satisfies the demand; (ii) an intermediate price level set by the CCGT power plants; (iii) the highest price corresponds to the OCGT power plants covering the peak demand. The duration of the peak electricity price decreases with an increasing penetration rate of DR, from about 3,000 hours to 1,000 hours. This is due to two effects, the first being the load shifting from peak hours to hours where the CCGTs can cover the load. The other is the increasing of demand above the minimal operating point of the CCGTs in order to avoid the use of the OCGTs with lower efficiencies. Note that already at a DR penetration rate of 25%, the high price hours only appear for $1375h$ in a year. This is already close to the final value of about $1000h$, illustrating the reduced incremental impact on the final price of increasing the DR participation above 25%. Additionally, the duration of the plateau where the price is zero, increases as the DR participation increases. The demand is shifted away from hours where the CCGTs set the price, towards hours with excess RES based electricity generation. This shift is very short in terms of duration: there are an additional $15h$ of zero electricity prices in the case of a 100% DR penetration rate compared to the case without DR.

Note that the cost evaluation above is not quantitatively exhaustive with respect to all the DR benefits such as reduced investment costs, start up costs and ramping costs. To evaluate the economic viability of a DR program, the operational cost savings (Figure 6.1b) should be compared with the investments for implementing the necessary DR technology in every dwelling and the deferred investment in peak production capacity of the electricity generation system (see the discussion below). The investments required to implement the necessary DR technology are however beyond the scope of this chapter and already treated by other authors [81].

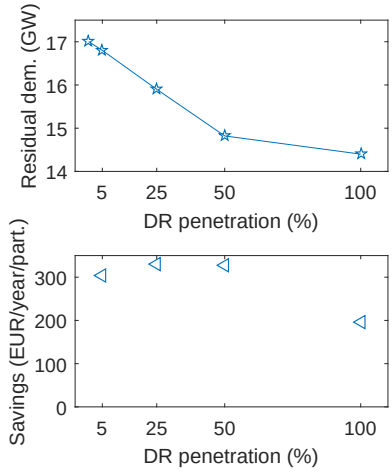

(a) The top figure shows the peak residual electricity demand (pentagrams), the bottom figure shows the corresponding investment cost saving per participant (triangles).

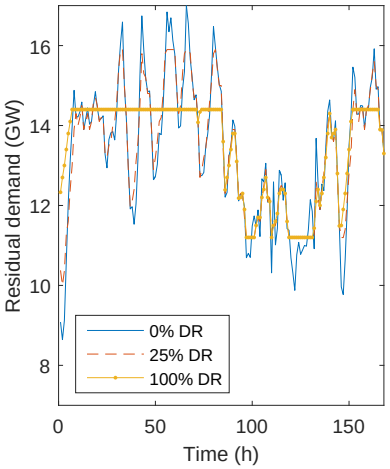

(b) Attaining of load shifting for the most critical week of the year

Figure 6.3: Reference case: peak shaving.

6.3.2 Peak shaving

Figure 6.3 illustrates the potential for peak shaving, which shows the peak residual electricity demand[5]. In order to quantify the potential for peak shaving, a new simulation was performed: the peak demand was minimized considering only the two most critical winter weeks with the highest peak residual electricity demand, namely the second and third week of January. In such simulation, an additional constraint, which limits the peak electricity demand, was included in the integrated model. This constraint was lowered until the potential for peak shaving via load shifting was exhausted, identifying the new peak demand. Figure 6.3a (solid line) shows how the residual peak demand goes down almost linearly with higher DR penetration, until 50% DR penetration is reached. From this point onward, a certain saturation of the peak shaving potential is observed.

[4]The average gas fired electricity generation efficiency is here defined as the total volume of electric energy produced by the gas fired power plants divided by the total amount of primary energy needed to produce that electricity.

[5]The residual demand is the electricity demand from which the electricity generation by RES is subtracted. The peak of this demand is the most critical, as this denotes the need for investment in, among others, power plants.

In fact, Figure 6.3b illustrates how, in the case of a 100% DR penetration, the heat pumps are not able to shift their demand earlier in time, as peak shaving is already occurring at that time. The power plants hence face a flat demand for three days.

The economic benefit of peak shaving (see Figure 6.3a) can be estimated by assuming an investment cost of $1,250$ EUR per kW installed peak production power plants [87]. Hence, a capacity decrease of $2,000$ MW corresponds to a deferred investment worth approximately $2,500$ million EUR . Assuming that the avoided investment costs are shared among the participants annually, with a plant life time of 25 years and a discount rate of 3.5% [138], the cost saving per participant fluctuates around 300 EUR per participant per year, until 50% DR penetration (Figure 6.3a, circles, bottom). This behavior depends on the almost linear relationship between number of buildings involved in the DR program and peak demand reduction for DR penetration rates between 5 and 50%. The above mentioned saturation, instead, limits the cost saving per participant at 100% DR penetration. Note that the exact value of these cost savings is highly dependent on the assumed investment cost, discount rate and plant life time. These factors will determine whether the economic benefits from peak shaving are higher than or similar to the operational cost savings (Figure 6.1b).

6.4 Results: influence of the DR technology

The results reported above take into account both the flexibility provided by the building thermal mass and the flexibility of the DHW tank, as the heat pump can supply heat to both. In this section, the two different types of thermal storage are analyzed separately in order to evaluate their own intrinsic potential. This is meaningful considering that installations are possible in which the heat pump is dedicated either to space heating or to domestic hot water production. Again both the customer's and the overall system's point of view are analyzed by means of the two parameters DRR and R_c. Figure 6.4 shows the demand recovery ratio for all the studied configurations of the demand side technologies ('DR technology' case in Table 6.2).

6.4.1 Flexibility in building thermal mass

For the scenarios with only flexibility in the building thermal mass, the electricity consumption for DHW is assumed to follow a fixed profile (corresponding to the minimal electricity consumption needed for providing DHW), and vice-versa. As already mentioned in Section 6.2, the flexibility in the building thermal mass

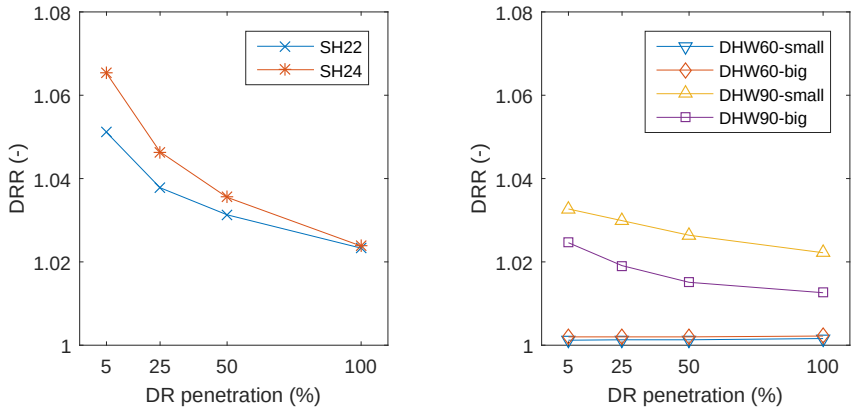

(a) Space heating: different upper temperature bounds. No flexibility in DHW.

(b) Domestic hot water: different sizes and upper temperature bounds. No flexibility in space heating.

Figure 6.4: DR Technology case. DRR by varying the DR penetration rate for the two DR technologies considered in different configurations.

stems from the difference between the lower and upper bound of the indoor temperature set point. The average lower bound for the building is about $20\,°C$, while two possible upper bounds are studied in this section, namely $22\,°C$ (SH22) and $24\,°C$ (SH24). The latter being already high for the inside winter comfort condition, it is assumed unnecessary to examine higher inside temperature set point bounds[6]. As expected, the DRR increases for a higher inside boundary temperature (Figure 6.4a), because employing more flexibility translates in a higher energy use. At 5% DR participation, the relative difference in electricity demand is the highest, corresponding to 20 GWh when $T^{sh,max}$ is $22\,°C$ and 26 GWh when $T^{sh,max}$ is $24\,°C$. Moreover, when the DR penetration rate increases, the two DRR curves tend to converge (Figure 6.4a), showing that it is unnecessary in these cases to rise the temperature above $22\,°C$ in order to grasp the associated operational benefits. Again, the value of the additional available flexibility of a higher temperature bound decreases as more buildings participate in DR.

On the other hand, the differences in operational costs (Figure 6.5a) for the two space heating temperature set point cases are negligible. The savings per

[6]Note also that the upper bound of $24\,°C$ can lead to unacceptable temperature swings of $4\,°C$ while the occupants are present. Hence, the results of this scenario should be handled with care, as thermal comfort in terms of temperature variation might not be attained.

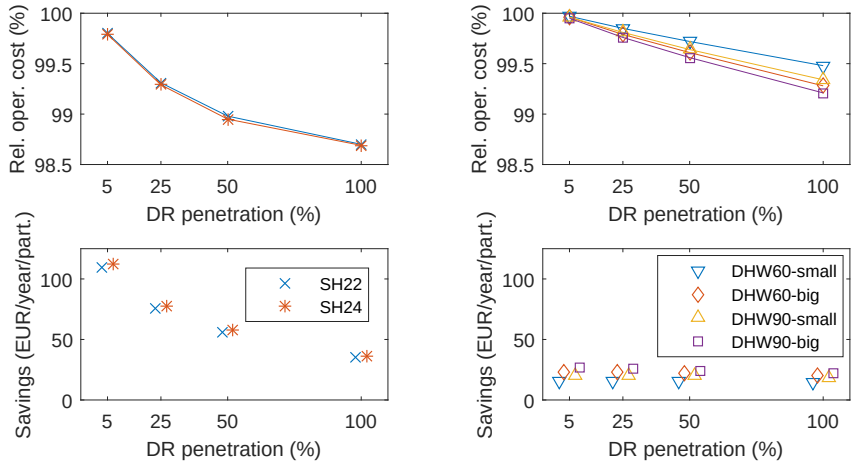

(a) Space heating

(b) Domestic hot water

Figure 6.5: DR Technology case. Influence on the relative operational cost and the cost savings per participant. The top figures show the relative operational cost while the bottom figure shows the cost savings per participant, both with the same legend.

DR participating building are similar (about 30 - 110 EUR per participant) to those examined in the previous section (Figure 6.1b). All these observations lead to the conclusion that it is not necessary to make a dramatic change in the upper bound for the inside temperature. Moreover a $2\,^{\circ}C$ dead band for the variation of the internal temperature is a standard operational range for space heating thermostats and it is demonstrated to be sufficient to comply with the flexibility requirements from the electricity generation system, as discussed above. Furthermore, this is also confirmed by the daily zone temperature during the year (averaged over the DR participating buildings): in the first case with $T^{sh,max}$ $=22\,^{\circ}C$, it is $20.4\,^{\circ}C$, while in the second case with $T^{sh,max}$ $=24\,^{\circ}C$ it is $20.5\,^{\circ}C$, meaning that the system rarely reaches the upper bound temperature and tends to be close to the lower bound (as it happens in case of no DR). This is especially the case for higher DR penetration rates, where less load shifting per participant is requested (Figure 6.6a).

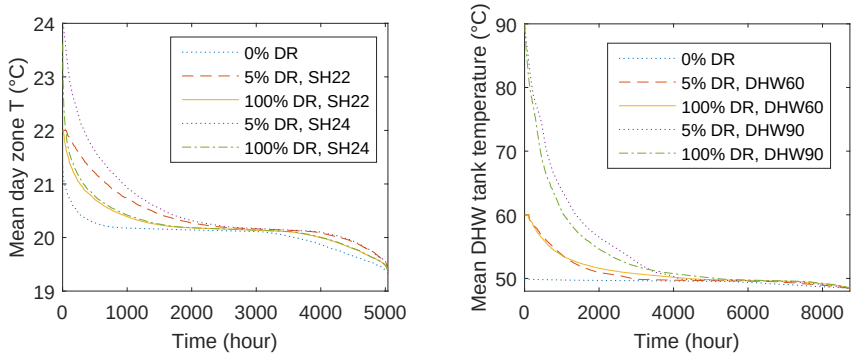

(a) Day zone temperature (heating season).

(b) DHW tank temperature.

Figure 6.6: DR Technology case: temperature duration curves. Given the demand side technology configuration, lower DR penetration rates show a longer duration of the temperatures close to the upper bound of the temperature dead band.

6.4.2 Flexibility in DHW tank

Similarly to the case with flexibility in the building thermal mass, the analysis was performed for the case in which thermal flexibility is only allowed in the DHW tank. The analyzed configurations consist of variations on the upper bound temperature of the stored hot water, which can be set at $60\,°C$ or $90\,°C$, and on the size of the tank: small size ($200\ l$ or $300\ l$) or big size ($400\ l$ or $600\ l$). Again more flexibility, i.e. bigger tank and higher boundary temperature, results generally in higher DRR (Figure 6.4b), while the difference in relative operational costs is limited (Figure 6.5b). As far as the energy use is concerned, when the upper bound temperature is set at $60\,°C$, the increase in energy use is below 0.5% regardless of the tank size. Conversely, when the upper bound temperature increases to $90\,°C$, the effect of the higher temperature bound is of greater influence than the doubling of the volume: the small tank needs to reach higher temperatures (and more losses) to store the same amount of energy.

The DHW tank temperature duration curve (Figure 6.6b) reveals that the temperature of the hot water tanks (averaged over the DR participating buildings) is about $51\,°C$ when the upper boundary is set to $60\,°C$ and $53\,°C$ when it is set to $90\,°C$. Hence, it is not necessary to choose extreme design configurations to benefit from the flexibility of this kind of demand side technology[7]. In contrast to the space heating flexibility, the relative operational

[7]The studied configurations are in line with the current design practices.

costs show a linear trend with respect to DR penetration (Figure 6.5b). This is due, as pointed out later on, to the lower electric demand by DHW that can not produce any saturation effect yet as in the case of the space heating. The highest savings are achieved for the configuration allowing more flexibility (highest upper bound temperature and big storage tank): it represents 0.8% of the total costs and corresponds to a saving of 22 million EUR per year. For the case with less flexibility (lower upper bound temperature and small storage), the maximum cost reduction drops to about 14 million EUR /year (Figure 6.5b).

From the point of view of the buildings participating in the DR program with DHW tank flexibility, the annual saving per dwelling is lower than the previous cases (Figure 6.1b and Figure 6.5). Also, the impact of the DR penetration rate is less evident. The operational cost savings amount to about 27 EUR per dwelling per year. Note however that in the case of flexibility in the DHW production, the shift in electricity consumption does not affect the perceived end energy service. Indeed, when providing flexibility via DR subjected space heating, residents may be aware of (small) deviations of the temperature from their preferred set point.

Domestic hot water will however always be available, when requested, at the same temperature year-round (while flexibility from space heating is available only during heating season[8]). Moreover, the total energy demand for space heating is about 6 times higher than the energy demand for providing DHW. At a 100% DR penetration rate, the maximum electric energy demand is 6.92 TWh/year for space heating versus 1.25 TWh/year for DHW. This puts the flexibility of the building thermal mass into perspective: its higher cost saving potential is in part related to the higher energy use. In terms of installed power, there is no difference in the two analyzed cases, because the considered heating system consists of a heat pump providing both space heating and DHW. The only difference is whether the control of the heat pump for supplying space heating and/or DHW undergoes DR or not.

On a further note, the reduction of the operational costs when the two demand side technologies work together (Figure 6.1b) is slightly below the sum of the reductions of the operational costs when they work separately (Figure 6.5). This demonstrates that there might not be a perfect superposition of the flexibility of different technologies. The more demand side technologies are participating in the DR program, the lower the additional benefit of additional flexibility.

[8]Note that throughout this work, space cooling is not considered, as it is assumed that this is achieved by passive measures in residential buildings in Belgium. If space cooling through the reversible heat pump would be allowed, this would of course open up the flexibility of the building outside the heating season.

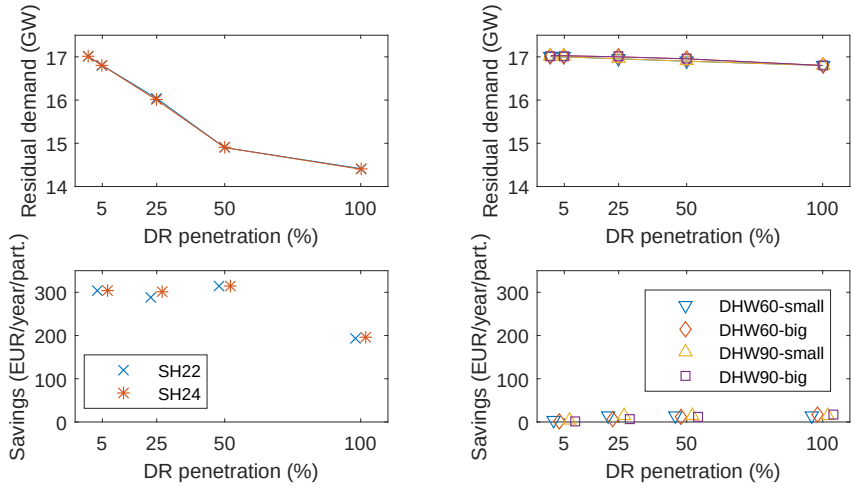

(a) Only flexibility in space heating.

(b) Only flexibility in domestic hot water.

Figure 6.7: DR Technology case. Peak residual power production trend and corresponding cost savings divided among participants. The top figures show the peak residual electricity demand while the bottom figures show the cost saving per participant.

6.4.3 DR technology and peak shaving

Finally, the difference between the flexibility provided by the building thermal mass versus the DHW tank with regard to peak shaving is shown in Figure 6.7. The flexibility in the building envelope allows a maximum peak shaving of about 2500 MW when the DR participation is 100% for space heating, while the DHW production system allows a reduction of the peak electricity demand that is an order of magnitude lower (about 200 MW). Moreover for DHW, this peak demand reduction does not change significantly with the DR penetration rate. This is due to the low DHW energy demand (much lower than the space heating electric demand, as previously mentioned), that does not cause any saturation effect yet. Also, this difference in peak shaving potential stems from the timing at which the heating of the building thermal mass and the DHW tank occurs. During cold months, high space heating demand coincides with the morning and evening peaks in the fixed electricity demand. Given the limited heat pump capacity, the loading of the DHW tanks is shifted towards the night, as the storage efficiency of these systems exceeds that of the building envelope. Hence, when peak shaving is needed, the potential of the DHW tank is low as

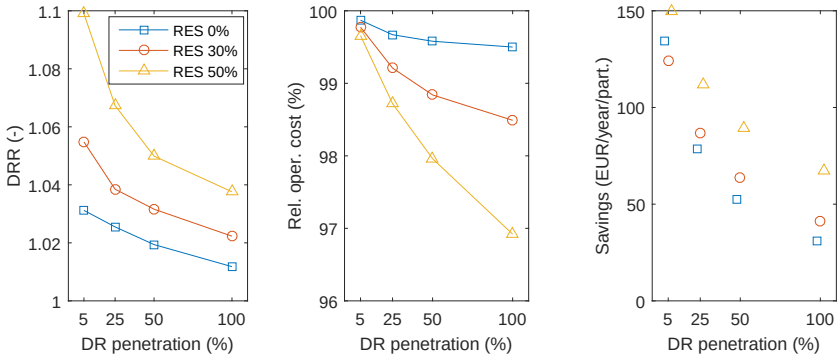

(a) DRR. (b) Relative operational cost. (c) Cost savings per participant.

Figure 6.8: RES share case. All figures share the same legend.

its demand was already shifted away from the typical peak electricity demand periods (morning and evening). Figure 6.7 also represents the behavior of the different configurations of the two demand side technologies with respect to the peak power demand. It is evident that the typology of technology has an impact, but not its setting: the load shifting potential does not vary significantly by changing the upper bound for the inside temperature or the upper bound for the DHW tank temperature and the tank volume. Finally, the savings per participant due to capital investment reduction (assessed as explained in section 6.3) are almost identical when the upper bounds or the tank sizes are higher. For the DHW tank, the costs savings are generally low (about 15 EUR per participant).

6.5 Results: influence of the RES share

As one of the main purposes of introducing DR programs lays in the possibility of a better match between electricity demand and variable electricity generation from RES, the sensitivity towards the RES mix share is studied in this section (Case 'RES share', Table 6.2). Figure 6.8 shows the DRR and the relative operational costs, R_c, when renewable energy sources cover 0%, 30% (reference case) or 50% of the total electricity demand. For a higher RES penetration in the generation mix, more load shifting is requested from the dwellings involved in the DR program (i.e. higher DRR, see Figure 6.8a). This is also accompanied

Table 6.3: RES share case. Curtailment of RES based electricity generation for a 30% RES penetration, provided fully by either wind or PV. The curtailment levels are split based on the time of year (heating season and rest of the year). In terms of DR penetration, two cases are shown (0% and 100%). DHW indicates the situation in which only the flexibility of the DHW tank is exploited (small tanks, $T^{tank,max}$ =60°C), SH corresponds to the case in which only the space heating system is DR adherent ($T^{sh,max}$ =22°C).

Curtailment (GWh)	30 % Wind, 0 % PV				0 % Wind, 30 % PV			
Heating season	Yes		No		Yes		No	
DR penetration (%)	0	100	0	100	0	100	0	100
Space heating	144	106	35	35	2932	1999	3018	3018
Domestic hot water	144	110	35	31	2932	2796	3018	2914

by higher annual operational benefits, reflected by the higher cost reduction, both in relative and absolute values (Figure 6.8b and 6.8c). For the cases with 100% DR penetration, the absolute value of cost savings for the system was estimated at 32 million EUR per year over a total production cost of about 4,000 million EUR per year for a RES share of 0%. For a RES share of 30% the cost saving is 42 million EUR per year over a total production cost of about 2,800 million EUR per year. Finally for a RES share of 50%, the cost saving is 68 million EUR per year over a total production cost of about 2,200 million EUR per year. Similar trends are observed for the cost savings per participant (Figure 6.8c). In case of 100% DR, the cost saving per participant for a RES share of 50% is twice the value for a RES share of 30%.

As more RES based generation is available, it is easily understood that a higher flexibility of demand side technologies is more relevant. For example, for the case with only building thermal mass flexibility and a 50% share of RES, the maximum system cost saving goes from 58 million EUR per year up to 62 million EUR per year by increasing the upper bound from 22 °C to 24 °C. This increase in cost savings is rather small but is in contrast to the previous section with a 30% share of RES, where there was almost no difference between the two cases.

Furthermore, the influence of the composition of the renewable mix between solar and wind power is evaluated in two extreme cases where RES based electricity generation is capable of providing 30% of the electricity demand. In the first case, only wind turbines are considered, delivering 30% of electric energy demand while PV does not produce anything. In the other case, the shares for wind and PV are reversed. For the case with flexibility only in building thermal mass and 100% DR, the wind dominated scenario produces

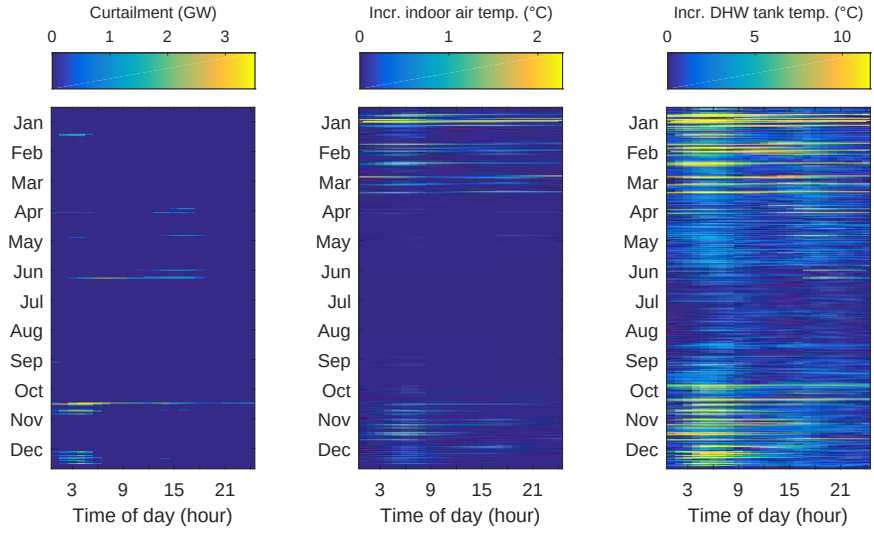

(a) Curtailment 0% DR. (b) Zone temperature. (c) DHW tank temperature.

Figure 6.9: Results from the year simulation in case the 30% RES share is fully provided by *wind turbines*. Figures 6.9b and 6.9c show the increase in temperature due to a 100% DR instead of a 0% DR participation.

an operational costs reduction up to 23 million EUR; per year. In the PV dominated scenario, an operational cost reduction of 85 million EUR per year is observed. Table 6.3 shows the reduction in RES curtailment by shifting only the space heating energy demand or only the domestic hot water energy demand. The DHW tank can reduce curtailment throughout the year, while for space heating, this is limited to the heating season. For domestic hot water flexibility the reduction in curtailment is lower compared to the space heating, but keep in mind that the DHW tank also represents a lower energy demand. These results further highlight that a massive PV deployment[9] gives higher incentives for DR than a massive wind deployment. This is due to the lower capacity factor of solar power: more capacity has to be installed to achieve the same RES share in the final energy demand. As a consequence, higher RES based electric power generation peaks are to be expected, which are more often curtailed, especially in absence of DR based flexibility.

[9]Note that the 30% RES share fully covered by PV is a rather extreme scenario. Within the assumption in this work of no export of electricity and no flexibility competitors, about 20% of the energy generated by PV panels gets curtailed.

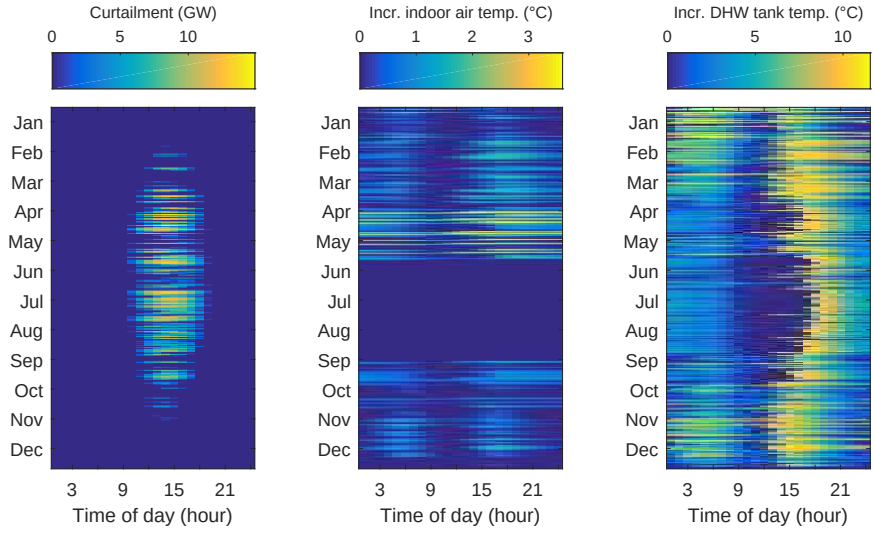

(a) Curtailment 0% DR. (b) Zone temperature. (c) DHW tank temperature.

Figure 6.10: Repetition of Figure 6.9 but in the case of a 30% RES share fully provided by *PV panels*.

The difference between both RES generation from wind turbines and PV panels is further illustrated by Figures 6.9 and 6.10. Figure 6.9 shows how the building thermal mass and DHW tank are employed as thermal energy storage, by increasing the temperature of both. One of the drivers to employ this TES is to make use of the curtailment present in the system. Note that the curtailment shown in Figure 6.9a is for the case of 0% DR and hence, where the heat pump demand is already added to the traditional demand. As shown by Hedegaard and Münster [82], this increase in electricity demand already lowers curtailment to some extent.

In the case of a 30% share of wind in electricity generation (Figure 6.9b), curtailment rarely occurs and occurs at random moments throughout the year. As can be seen in Figure 6.9b and 6.9c, this curtailment of wind is barely an incentive for preheating the building thermal mass or DHW tank. Preheating is triggered by other incentives, such as shifting electricity consumption to more efficient power plants. The DHW tank is preheated in the morning, mostly during the heating season, in order to avoid coincidence with the morning peak. Furthermore, both TES are preheated during a limited number of days in January, in order to lower the peak demand for the electricity generation

system on January 18th of the studied year.

In the case of a 30% share of PV panels in the yearly electricity generation, much clearer trends on a daily basis can be identified (Figure 6.10). As noted before, electricity generation from PV panels is far more curtailed due to a clear mismatch between supply and demand. This leads to spikes in curtailment of up to 14 GW. In the case of the same RES share of wind turbines, this curtailment reaches 3.5 GW only. The curtailment of PV is also far more predictable, occurring at a limited number of hours in the afternoon (Figure 6.10a). The TES potential of the thermal mass of the building is mainly activated in mid-season, which is represented by the months April to June for this particular year. The DHW tank is preheated actively throughout the year in this case (Figure 6.10c). The DHW tank is heated up to $60\,°C$ right at the end of the curtailment periods, typically beteen 15h and 19h, depending on the season. This timing makes the most of the curtailment. When the DHW tanks would be preheated at the beginning of the curtailment period, part of the stored energy would already be lost in the evening due to thermal losses of the DHW tank.

6.6 Discussion

The sum of operational costs savings and the avoided investment costs due to peak shaving ranges between about 400 EUR to about 200 EUR per DR adherent consumer. These total cost reductions are for a 5 % and 100 % participation rate, respectively. Hence, the value of participating in DR is halved for full DR participation. Hedegaard and Munster [82] obtained similar values when considering also investment costs in case of a large uptake of individual heat pumps systems. Mathieu et al. [116] attained lower values by participating in the ancillary service market and Papaefthymiou et al. [131] also realized lower cost savings.

The aspect of (operational) cost savings per building is of paramount importance in understanding the final customers' interest in DR participation. In fact, while it is evident that the electricity generation system benefits from a more flexible demand, it is less evident that the end consumer can sufficiently benefit to participate. The analysis performed in this study, even if based on some simplified assumptions, clearly shows that the customer could have a (sometimes limited) economic advantage, plus this advantage is reduced as more consumers adhere to the DR program. The consumer thus favors a lower penetration rate of the DR program, while in contrast, the system as a whole benefits most from a high DR participation rate. As a consequence, the DR incentive policy has to be carefully conceived by the stakeholders. From both points of view, the use

of the thermal flexibility of the building envelope introduces a larger margin for profit than the flexibility in the DHW tank. Moreover the operational cost savings per dwelling should be compared with the investments required to upgrade a.o. the heating system control with a communication platform for the exchange of information with the electricity generation system, already available on the market in some countries [81]. Note that at the demand side, the standard heating system installation, as conceived under current design practices, is sufficient to exploit the inherent flexibility of these thermostatically controlled loads just by varying the working temperature range.

6.7 Conclusion

This chapter analyses the role of the DR penetration on the performance of the integrated demand-supply electricity system. The demand side technologies considered are electric heating systems coupled with thermal energy storage. The analysis makes an attempt to evaluate the value of flexibility of thermal inertia in buildings and active TES in DHW tanks, in terms of energy use and operational costs. The main conclusions are the following.

First, higher DR penetration rates increase the reduction of operational costs, but on the other hand decreases the savings per participant since less load shifting per dwelling is necessary. A higher DR participation requires also smaller deviations from the minimum energy use electricity demand profile per dwelling to achieve the same load shifting, leading to lower thermal losses per dwelling. This also results in a reduction of the demand response ratio. Second, DR can be put into practice with the considered demand side technologies without changing the particular constraints or design configurations from current practice. The increase of the upper temperature bounds or a doubling of the DHW tank size show relatively little extra value. The flexibility due to the building thermal mass involves a higher energy demand than the DHW flexibility and is hence more attractive for DR purposes, even if its availability is only present during the heating season. Additionally, this demand contributes the most to the winter peak electricity demand and is thus also the most attractive for peak shaving. Third, the higher the generation based on renewable sources, the higher the benefits that can be attained by the DR application.

Finally, this chapter demonstrates the strict interaction between the demand and the supply side: the behavior of the flexible electric heating systems is not only dependent on the comfort constraints, but also on the boundary conditions under which they operate, such as the RES share in the system and the behavior of the other consumers. Thus, in order to assess the added value

and effects of DR, it is necessary to take both the demand and supply of the electricity generation into account, for example through integrated modeling approaches. Moreover, beyond the economic evaluation on its convenience, it is worth remembering that DR is interesting because it is a powerful tool to face the challenges of new energy supply systems, where renewables have a significant role in generation mix.

Chapter 7

Comparison of DR incentives in attaining integrated model performance

This chapter is based on a paper that was previously published as:
Patteeuw, D., Henze, G. P., and Helsen, L. Comparison of load shifting incentives for low-energy buildings with heat pumps to attain grid flexibility benefits. Applied Energy 167 (2016), 80–92.

7.1 Introduction

The case studies in Chapters 5 and 6 illustrate the potential of performing demand response with residential heat pumps by means of the integrated modeling approach presented in Chapter 3. However, this integrated modeling approach is not feasible for real life applications, as it is not practical to optimize the dispatch of a number of power plants simultaneously with the control of thousands to millions of heat pumps. The aim of this chapter is to investigate how the reductions in operational cost and CO_2 emissions as determined from the integrated model, can be attained in practice. Two typical approaches towards demand response, direct load control and time-of-use pricing, will be compared in their ability to realize the savings as determined from the integrated model.

Direct load control is typically assumed by authors studying the DR potential of heat pumps from an electricity system perspective, such as [15, 28, 81, 115, 181]. In this way, applying demand response to residential buildings with heat pumps allows numerous benefits, such as balancing short-term power fluctuations of wind turbines [28], providing reserves [115] or voltage stability [181], reducing wind energy curtailment by up to 20% [81], and reducing CO_2 emissions by up to 9% [15].

On the other hand, studies conducted from a building owner's perspective typically assume time-of-use pricing. A wholesale electricity price profile is considered and it is assumed that the actions taken under DR do not effect this price profile. For example, Kamgarpour et al. [92] found that for a set of 1000 residential buildings, savings of up to 14% can be reached with respect to a wholesale electricity price profile. Henze et al. [83] obtained savings up to 20% by employing the passive energy storage present in an office building with respect to an on-peak and off-peak electricity tariff. Kelly et al. [94] also investigated the use of thermal energy storage to shift electricity demand to off-peak periods, but reported significant increases in energy use. In addition, Kelly et al. observed a loss of load diversity causing a peak demand during off-peak tariff periods (rebound), which is up to 50% higher than normal. This loss of load diversity phenomenon for thermostatically controlled loads is explained well by Lu and Chassin [109]. More advanced and dynamic price profiles have been suggested in different studies, e.g. Oldewurtel et al. [124] suggest a price profile based on the spot price and on the level of the traditional electricity demand. A good overview of different price based incentives for consumers is provided by Dupont et al. [51].

Another difference in DR approaches is whether DR is performed manually by the building occupants or automatically. As shown by Wang et al. [183] and Dupont [50], automatic control achieves higher participation in demand response than manual control. The smart thermostat, an enabling technology to achieve automatic control for heating and cooling demand [1], has drastically increased its market share in recent years [78]. Apart from improving energy efficiency [108], some of these internet-connected smart thermostats already perform peak shaving while maintaining thermal comfort [117].

In this chapter, both models of the electricity generation system and the buildings equipped with heat pumps are used both separately and in the integrated model. Modeling both systems also allows studying different DR incentives. Both supply and demand systems are assumed to behave rationally and strive to minimize their observed cost. To this aim, all buildings considered feature a model predictive controller (MPC) developing optimal thermostat setpoint strategies. This could be achieved, for example, by a massive deployment of smart thermostats performing MPC. In this context, MPC is a control approach,

which optimizes the control of a building's heating system by harnessing a simplified physical model of the building's thermal characteristics and energy systems along with predictions on occupancy and weather conditions. As shown in experiments in tertiary buildings by Širokỳ et al. [159], MPC can reduce energy use up to 28% . Buildings with MPC can easily cope with dynamic price profiles, as shown by Oldewurtel et al. [124].

The main focus of the chapter is to compare two common approaches to attain the desired benefits through demand response with a practical implementation in mind: direct-load control and time-of-use pricing. These incentives are compared by determining to what extent the reductions in operational costs and CO_2 emissions, as reached by the integrated model, are reached. Hence, the results of the integrated model serve as a reference benchmark for this comparison.

This chapter will show that, even under the assumptions of perfect predictions, system perspective and absence of grid constraints, the performance of the studied demand response incentives already significantly deviates from the DR performance of the jointly optimized best-case scenario. Additionally, it is shown that this performance is very sensitive to the share of RES and the number of participating buildings.

The boundary conditions in this chapter are inspired by the Belgian context, with an electricity generation system dominated by nuclear power plants, gas-fired power plants, and RES. The buildings considered are all detached, heating-dominated low-energy buildings. As Chapter 5 shows, low-energy buildings are the best candidates for a widespread heat pump implementation in Belgium. Section 7.2 describes the different models and scenarios employed in this chapter. The results Section (Section 7.3) illustrates the output of the different models (Section 7.3.1) used to evaluate the DR potential (Section 7.3.2) and the performance of DR incentives (Section 7.3.3). The difference between the performance of these DR incentives is explained in Section 7.3.4 while results for mixtures of these incentives are shown in Section 7.3.5. Finally, a discussion is given in Section 7.4 in order to arrive at the conclusions in Section 7.5.

7.2 Methodology

This section consists of two parts. Section 7.2.1 elaborates on the different models used, and the case study for assessing the DR incentives. Section 7.2.2 illustrates the different scenarios considered for applying these incentives.

Table 7.1: Overview of the abbreviation and description of the models in this study.

Abbreviation	Description
Gen	Electricity generation system model
B20	Large building stock model, optimal control problem of 20 buildings.
B2	Aggregated building stock model based on B20.
Int20	Integrated model performing a co-optimization of B20 and Gen.
Int2	Integrated model performing a co-optimization of B2 and Gen.

7.2.1 Models and parameters

All models in this chapter are examined as deterministic optimal control problems as listed in Table 7.1. In the first model (Gen), the electricity generation system minimizes its total operational cost via a unit commitment and economic dispatch problem with profiles for electricity demand and electricity generation by RES. From a building owners' perspective (B20 and B2), the heat pumps in the buildings are controlled by MPC that minimizes individual electricity cost while maintaining thermal comfort. In the integrated models, the two optimal control problems are combined into one optimal control problem (Int20 or Int2) that jointly minimizes the total cost for generating electricity for both the traditional electricity demand and the total electricity demand, including the demand stemming from low-energy buildings with heat pumps whose temperature setpoints can be optimized. These models are MILP problems with an optimality gap of 0.1%. All presented results are from a full year simulation for which the electricity demand and weather conditions are based on Belgium in 2013 (see Section 2.4.3).

Electricity generation system The electricity generation system is modeled as a unit commitment and economic dispatch problem [169] as described in Section 2.3.1. The technical parameters and fuel costs for the power plants are taken from Bruninx et al. [26] and summarized in Table 7.2. These technical parameters and costs are inspired by the Belgian power system. However, in order to cope with the large production by RES, the technical parameters for the nuclear power plants are taken from more flexible nuclear power plants than currently present in Belgium. Hence, the generation system is inspired by,

Table 7.2: Parameters for the electricity generation system per fuel type [26, 54, 56, 157]

Type	Total cap. (MW)	Nr. of units (-)	Nominal cost ($\frac{EUR}{MWh_e}$)
Nuclear	5925	8	6
Coal	760	3	30
Gas	7018	47	60
Oil	215	13	83

but not completely representative for Belgium. Additionally, losses or capacity limits due to the electricity grid are neglected.

The profile for the traditional electricity demand consists of the Belgian electricity demand, from which the electricity generation by combined heat and power, run-off river, and pumped hydro are subtracted. The profiles for these demand and generation types are assumed to be constant and are taken from Elia [54] for Belgium for the year 2013. Electricity generation from PV, onshore wind and offshore wind are lumped together with a share based on the year 2013 in Belgium [54]: 3%, 2.2% and 2.7%, respectively. The generation profiles of these RES are also for Belgium in the year 2013 [54]. In order to study the sensitivity of the results towards the share of electricity generation from RES, the generation profile is scaled up in order to represent 15%, 20%, 30% and 40% of the yearly electricity demand, depending on the case. According to Devogelaer et al. [46], these are feasible shares for Belgium.

Furthermore, the sensitivity of the results to the number of buildings is also studied. This is varied in multiple steps between $50,000$ and $500,000$. Hence, on a yearly basis, the heat pumps of the buildings respectively add an electricity demand between 0.4 and 4 TWh to the traditional electricity demand of 85.6 TWh [56], i.e. at most roughly 5%.

Residences with heat pumps The residences with heat pumps are modeled using the linear optimal control problem formulated in Section 3.4. The building structure is the two zone reduced-order model by Reynders et al. [151], as shown in Figure 2.4. Furthermore, the building parameters are based on low energy detached buildings with an average U-value of 0.3 W/m^2K and a ventilation rate of 0.4 ACH, which are two conditions for the nearly zero energy building standard, as set up by the Flemish government [175] and to the economic optimum for Belgium found by Verbeeck [176].

In order to keep the problem size for the best case integrated model (Int20) manageable for the MILP solver, the number of buildings was chosen to be 20. Each of the 20 buildings has an identical building structure but different user behavior, based on Baetens and Saelens [14] as presented in Section 2.4.2. The user behavior profiles used in this chapter are described as Baetens2 in Section 2.4.2.

Each building is equipped with floor heating and a hot water storage tank for domestic hot water, which are both heated by an air coupled heat pump. The heat pump is sized to meet 80% of the peak heat demand while the remainder of the peak demand is covered by an auxiliary electric resistance heater. The COP of the heat pump is predetermined according to Bettgenhäuser et al. [19] and assumed constant throughout each optimization horizon of a week. Hence, during each week, the COP is predetermined based on the average supply and source temperature. Finally, weather data is based on measurements in Uccle for the year 2013, as discussed in Section 2.4.3.

Integrated model The integrated model as presented in Section 3.7 is also employed in this chapter. In the ideal case, this integrated model has available all details of buildings participating in demand response (Int20)[1]. In practice however, the number of participating buildings could go up to thousands, making an integrated optimization infeasibly large. Thus, an aggregation of this large building set is necessary. Assuming the presented average building to be representative for a wider set of buildings, an aggregation with respect to building parameters is not needed. However, an aggregation towards different occupant behavior is employed, as presented in Section 3.6, to determine an aggregated building stock for the integrated model (Int2). In this model, only two buildings remain, with the "average" building structure but with two different sizes of the DHW storage tank.

7.2.2 Incentive scenarios

Given the modeling framework discussed in Section 7.2.1, it is possible to study different incentive mechanisms for realizing the possible operational benefits of DR. Figure 7.1 gives an overview of the different incentive scenarios.

First, in the Reference scenario, no DR is performed. In this scenario, the controls of the heat pumps of the 20 buildings (B20) completely ignore the

[1] In some cases, the integrated optimization with 20 buildings (Int20) was not able to obtain a solution. For the other cases, the results were very close to the integrated model with the aggregated buildings (Int2), more precisely within the optimality gap of 0.1%. Hence, in the failed cases of Int20, the result from Int2 serves as result for Int20.

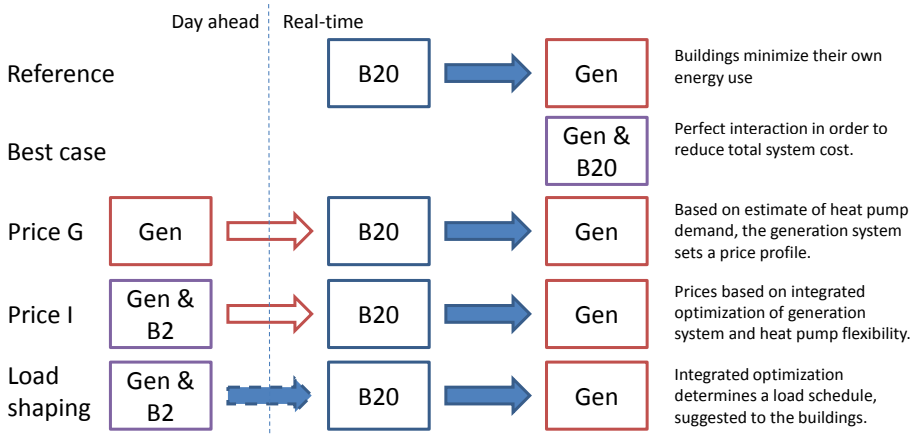

Figure 7.1: An overview of the studied scenarios. The red non-filled arrows denote the communication of a price profile. The blue filled arrows denote the communication of the electricity demand profile of the buildings equipped with a heat pump. In the load shaping scenario, the dashed blue arrow denotes the suggestion of an electricity demand profile. The color of the boxes denotes the model type. The red box denotes the electricity generation system model, the blue box the building stock model and the purple box the integrated model of both.

electricity generation system and focus on minimizing their own electricity use. Hence, in this scenario the buildings face a flat electricity price. This results in the following optimization criterion for the optimal control problem of the MPC:

$$\min \sum_j d_j^{hp}. \tag{7.1}$$

From this, the electricity generation system (Gen) needs to deliver this resulting heat pump electricity demand plus the traditional electricity demand.

In the Best Case scenario, the electricity generation system and all participating buildings simultaneously optimize their control by means of an integrated model (Int20). In this model, the building structure and domestic hot water tanks are occasionally preheated when this reduces the total cost for the electricity generation system. Simultaneously, the power plants are optimally dispatched in order to meet the resulting electricity demand. This Best Case scenario serves as upper bound of the operational cost savings attainable by applying DR.

A first time-of-use pricing scenario is the Price G scenario. In this scenario, the electricity generation system makes an estimate of the total electricity demand of the following day, including the electricity demand of the heat pumps, which minimize their own consumption. This estimate is assumed to be perfect in this chapter. However, the heat pump controllers receive the resulting price profile, $price_j^G$, and alter the electricity demand accordingly by applying the following optimization criterion:

$$\min \sum_j price_j^G \cdot d_j^{hp}. \tag{7.2}$$

In real-time, the electricity generation faces the traditional electricity demand plus the altered building electricity demand. This scenario hence represents a unilateral price communication from the electric power system to the buildings with heat pumps.

In contrast to this, the Price I scenario represents the situation where the electricity generation system makes an estimate of the flexibility of the buildings with heat pumps. In the estimate for the following day, the aggregated representation of the buildings with heat pumps (B2) is co-optimized with the dispatch of the electricity generation system. The resulting price profile from this integrated model, $price_j^I$, is then communicated to the controllers of the heat pumps, resulting in the following optimization criterion

$$\min \sum_j price_j^I \cdot d_j^{hp}. \tag{7.3}$$

Also in this scenario, the impact of the measure on the electricity generation system is determined. In this chapter, solely the electricity generation system determines the electricity price profiles. Hence, the electricity price for the building owners is not augmented with a fixed tariff for electricity generation and distribution, as is typically the case in practice. This causes the electricity price to be zero for the building owners at times of RES curtailment.

Finally, the Load Shaping scenario is identical to the Price I scenario except that, instead of communicating the resulting price profile, the resulting demand profile from the integrated model (d_j^{IM}) is communicated to the buildings. This demand profile, similarly to the work of Corbin and Henze [36, 37], acts as a centrally-suggested demand curve for the buildings with heat pumps. The resulting optimization criterion for the optimal control problem of the heat pump controllers is:

$$\min w_{ls} \cdot |d_j^{hp} - d_j^{IM}| + (1 - w_{ls}) \cdot \sum_j d_j^{hp} \tag{7.4}$$

in which d_j^{IM} represents the centrally-suggested demand profile from the integrated model. Hence, the heat pump controllers make a trade-off between the deviation with respect to the centrally-suggested demand profile ($|d_j^{hp} - d_j^{IM}|$) and minimizing electricity use ($\sum_j d_j^{hp}$) by means of the weighting factor w_{ls}, taken to be 0.5 in this chapter.

7.3 Results

This section consists of five parts. In the first part, Section 7.3.1, the output of the different models, presented in Table 7.1, is illustrated. In Section 7.3.2, the maximum attainable benefits of DR are investigated for the studied boundary conditions. The results for the different DR implementation scenarios are shown in Section 7.3.3 and the resulting metrics in Section 7.3.4. Finally, the different cost functions for the buildings, Eq. (7.1) to (7.4), are combined in Section 7.3.5.

7.3.1 Illustration of model output

Figure 7.2 shows the results for two days in the case where 30% of the yearly electricity demand is generated from RES and 250,000 buildings are equipped with heat pumps. The power plants need to generate the sum of the residual traditional electricity demand, Figure 7.2a, and the electricity demand of the heat pumps, Figure 7.2c. Note that, in some scenarios, both the heat pump and auxiliary heater are activated simultaneously, causing a high electricity demand of $10kW_e$ per building. Figure 7.2b shows how the day zone temperatures, averaged over the buildings, are manipulated to achieve these electricity demands. In the Reference scenario (blue lines in Figure 7.2), the indoor air temperatures are kept close to the lower comfort bounds, resulting in an electricity demand that doesn't strongly fluctuate. In this scenario, the buildings miss the opportunity of using the excess electricity generation by RES that gets curtailed in hours 4 to 5, hours 11 to 16 and hours 27 to 28. In the Best Case scenario (Int20, green lines in Figure 7.2) advantage of this abundant electricity generation by RES is taken by drastically increasing heat pump electricity demand (d_j^{hp}) in those hours. As a result, no electricity generation by RES is curtailed, as the buildings have perfect knowledge of the magnitude of the curtailment. This

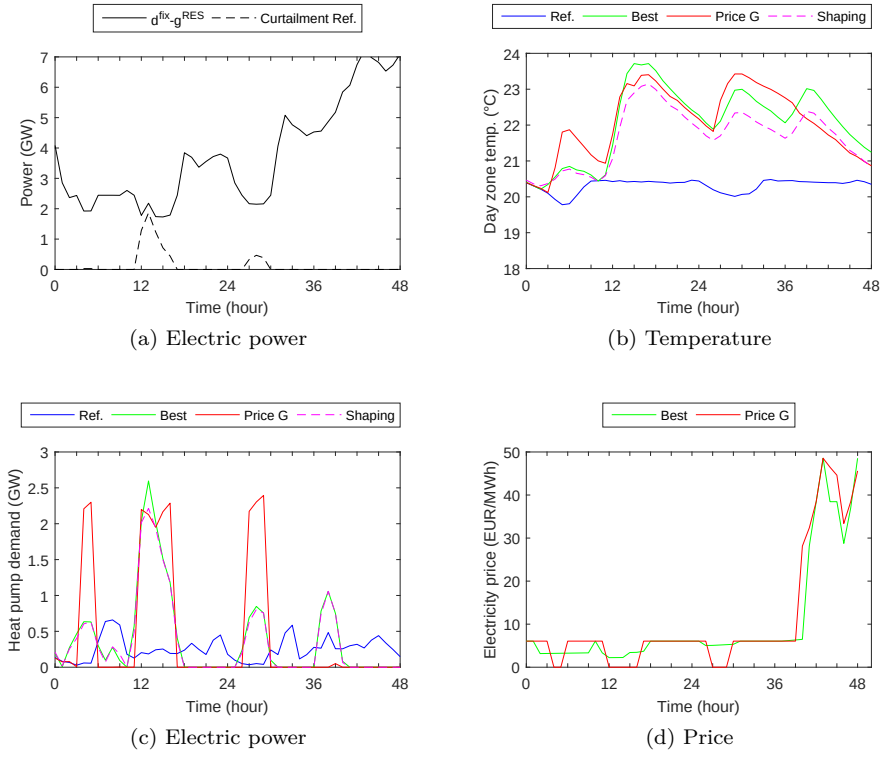

(a) Electric power (b) Temperature

(c) Electric power (d) Price

Figure 7.2: The power plants must deliver the sum of the traditional residual demand (Figure 7.2a) and the heat pumps demand (Figure 7.2c). The curtailment at hours 4 to 5, hours 11 to 16 and hours 27 to 28, in some cases communicated through a price profile (Figure 7.2d), forms an incentive to preheat the buildings (Figure 7.2b).

avoidance of curtailment causes the nuclear power plants to set the price (green line in Figure 7.2d) and, hence, no zero electricity price is observed.

This is not the case for the Price G scenario (red lines in Figure 7.2). In this scenario, the buildings face a zero electricity price at times of curtailment, see Figure 7.2d. This causes the so-called avalanche effect [39] to occur, meaning that the buildings drastically increase their electricity demand as they observe electricity to be completely for free at that time. However, this leads to an overshoot in demand, which will cause the electricity price to go up again in hours 4, 5, 11, 15, 16, 27 and 28. Clearly, this will increase the electricity

Table 7.3: The difference between the Reference and Best Case yields the upper limit for savings by applying DR. Both the relative savings and the savings per participant are shown for a different number of participating buildings.

RES share (%)	30				
No. of buildings (x1000)	50	100	250	375	500
Reference: cost (10^6 EUR)	671	686	731	772	815
Reference: CO_2 (10^6 ton)	4.69	4.82	5.24	5.59	5.95
Best case: cost (10^6 EUR)	663	671	698	725	756
Best case: CO_2 (10^6 ton)	4.62	4.69	4.98	5.25	5.53
Cost saving (%)	1.2	2.2	4.6	6.1	7.3
CO_2 reduction (%)	1.6	2.7	4.9	6.2	7.0
Cost saving (EUR/participant)	157	151	134	125	119
CO_2 reduction (ton/participant)	1.5	1.3	1.0	0.9	0.8

generation cost far more than expected. The Load Shaping scenario (pink dashed lines in Figure 7.2) does not cause this overshoot in demand, as it receives information on how much to increase electricity use in these time periods. As can be seen in Figure 7.2c, the electricity demand profile in the Load Shaping scenario is very close to that of the Best Case scenario.

7.3.2 Best case DR potential

In this section, the savings in operational cost and CO_2 emission of the Best Case scenario for DR are shown. This will serve as an upper bound to the possible savings of the different DR implementation scenarios in Section 7.3.3. Throughout this chapter, the results are given for a variation of two important parameters: the number of buildings equipped with heat pumps and the share of electricity generated by RES over a year. Tables 7.3 and 7.4 give an overview of the total yearly operational cost and CO_2 emissions. Note that the mentioned buildings switch from fossil fuel fired heat production to heat pumps. A higher number of buildings making this switch, causes a higher electricity demand and thus higher operational costs and CO_2 emissions for the electricity generation system[2].

Table 7.3 shows the decrease in operational costs and CO_2 emissions due to performing DR. The trend is however not linear, as can be seen in the savings

[2]When considering the entire system from a primary energy perspective, buildings and electricity generation system, the switch to heat pumps causes total operational costs and CO_2 emissions to lower, see Chapter 5. This chapter only discusses the effects for the electricity generation system.

Table 7.4: Table 7.3 is repeated for different RES shares.

RES share (%)	8	15	20	30	40
No. of buildings (x1000)			250		
Reference: cost (10^6 EUR)	1283	1056	925	731	603
Reference: CO_2 (10^6 ton)	10.98	8.73	7.32	5.24	3.98
Best case: cost (10^6 EUR)	1266	1033	897	698	568
Best case: CO_2 (10^6 ton)	10.95	8.64	7.17	4.98	3.70
Cost saving (%)	1.3	2.2	3.0	4.6	5.7
CO_2 reduction (%)	0.2	1.0	2.1	4.9	7.0
Cost saving (EUR/participant)	67	93	113	134	138
CO_2 reduction (ton/participant)	0.1	0.4	0.6	1.0	1.1

per participant as discussed in Chapter 6. A number of buildings higher than 500,000 is not studied as the peak in total demand approaches the maximum installed capacity of the assumed electricity generation system. A number of buildings lower than 50,000 is also not studied as for these small numbers, the operational cost savings approach the optimality gap of 0.1% used in this chapter.

Another important parameter is the share of electricity generated by RES over a year. As can be seen in Table 7.4, a higher share of RES causes the potential operational cost savings of DR to increase. For example, an increase in RES share from 8 to 40%, causes the potential operational cost savings to rise from 17 million EUR to 35 million EUR.

7.3.3 Comparison of incentives scenarios

The savings presented in Section 7.3.2 could be hard to realize in practice as the Best Case scenario is not feasible for a large set of buildings. Instead, a set of alternative scenarios for reaching these savings were introduced in Section 7.2.2. The performance of these different scenarios in striving towards the operational cost savings of the Best Case scenario is shown with respect to the RES share in Figure 7.3a for 250,000 buildings with heat pumps. In this figure, 100% represents the Best Case scenario, while 0% represents the Reference scenario. Most notable is the poor performance of the Price G scenario. Up to a RES share of 20%, this implementation causes the total operational cost to be even higher than the Reference scenario. This is because the buildings greedily overreact to price incentives and induce extra operational costs for the electricity generation system. Only when the RES share is high enough, does the Price G scenario start showing operational cost reductions with respect to

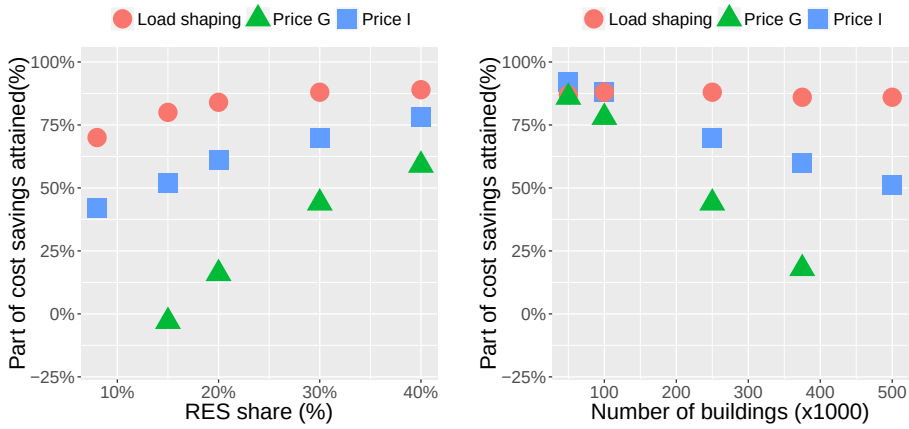

(a) For 250,000 buildings

(b) For a 30 % RES share

Figure 7.3: Scenario comparison for operational cost savings relative to the Best Case scenario of DR. In Figure 7.3a the share of RES is varied while 250,000 buildings are considered. In Figure 7.3b the number of participating buildings is varied while the RES share remains at 30%.

the Reference scenario. However, this increase in savings for a higher RES share is a general trend in all scenarios.

The price signal from the integrated model, scenario Price I, partly avoids the overreaction as it has information on both electricity generation system and buildings. In a sense, it represents the price signal after a long iteration of price and demand between electricity generation system and buildings. However, the Price I scenario is still outperformed by about 20% by the Load Shaping scenario, although the difference decreases for a higher RES share.

The difference between Price I and Load Shaping scenarios can be explained using Table 7.5. For a low RES share (8%), there is no curtailment in the electricity generation system and the operational cost savings by DR (Best Case) are dominated by improving the efficiency of the power plants (Fuel and CO_2 cost) and avoiding start-up and ramping costs. The efficiency of the power plants is improved by running these power plants closer to their full load capacity (see Part load in Table 7.5). These savings can be subtle to attain, as a slight increase in demand above the maximum generation capacity of the last power plant can trigger an extra power plant to be activated. Since in the Load Shaping scenario an exact indication of what the ideal electricity demand profile looks like is given, these subtleties are better retained. A price profile can give

Table 7.5: For two RES shares, the difference in curtailment of electricity generation by RES (Curt.), average part load of all operating power plants throughout the year (%), difference in fuel and CO_2 cost (Fuel+CO_2) and difference in costs related to starting up and ramping of power plants (Start-up + ramping).

RES share (%)	Scenario	Curt. (TWh)	Part load (%)	Fuel + CO_2 (cost in 10^6 EUR)	Start-up + ramping
8	Reference	0	95.7	1255	28
8	Best Case	0	97.9	1245	21
8	Price I	0	95.8	1252	23
8	Load Shaping	0	97.2	1249	21
40	Reference	2.32	88.3	567	36
40	Best Case	1.15	88.9	539	30
40	Price I	1.80	88.2	545	30
40	Load Shaping	1.63	88.7	542	30

an indication of when electricity demand should be increased or decreased, but not *how much* this increase or decrease should be.

On the other hand, for a high RES share (40%), the savings are dominated by reducing RES curtailment in order to decrease operational costs. Both Price I and Load Shaping scenarios are successful in decreasing RES curtailment. In the former, the buildings see a very low electricity price and act accordingly. In the latter, the buildings receive information on how much the demand should be increased when curtailment occurs. However, the Load Shaping scenario is better as it communicates *how much* the demand should be increased in order to exactly absorb all curtailment. This information is not present in a price profile.

The number of buildings having a heat pump installed, also has an impact on the performance of the incentive scenarios as shown in Figure 7.3b. In this figure, the share of RES in the yearly electricity generation is fixed to 30%. First of all, the Price G scenario performs very poorly as more people install a heat pump that participates in DR. In the case of 500,000 buildings, the demand overshoot in the coldest week is so high that the maximum cumulative capacity of the production park is exceeded. With respect to the Price I scenario, when a relatively low number of buildings is involved, this scenario performs the best. However, as more buildings are involved, these all respond to the same price profile, and cause demand overshoots. In this case, the buildings start influencing the price itself, and become price influencers instead of price takers.

Table 7.6: Metrics of the yearly residual load curve ($d_j^{trad} + nb \cdot d_j^{hp} - cur_j \cdot g_j^{res}$), similar to Corbin [35], for the case of a 30% RES share and 250,000 buildings with heat pumps. The metrics are provided for the Reference case (Ref.), Best case (Best), the Price G and Price I case and the Load Shaping (Load S.) case.

Name	Ref.	Best	Price G	Price I	Load S.
HP demand (TWh)	1.99	2.43	2.42	2.29	2.33
Peak (GW)	12.8	12.0	12.9	12.3	12.1
Mean ramping (MW/h)	556	424	589	509	444

In the case of 500,000 buildings with heat pumps, the performance is so abysmal that only about half of the potential savings are attained. In contrast to this, the Load Shaping scenario is far more robust to the number of buildings: No matter what this number of buildings is, the Load Shaping scenario reaches about 80% of the possible savings.

7.3.4 Comparison on metrics

Similar to the work of Corbin [35], Table 7.6 presents different metrics to evaluate the improvement of the different incentive scenarios with respect to the Reference scenario. In contrast to the work of Corbin, the full electricity generation system is modeled, which allows a direct interpretation of the residual demand curve. This is the total demand from which the electricity generation from RES is subtracted ($d_j^{trad} + nb \cdot d_j^{hp} - cur_j \cdot g_j^{res}$). In all DR scenarios, the electricity use of the heat pumps rises by between 13% to 20%. This is due to the high share of electricity generated by RES and nuclear power plants, which causes a lot of curtailment to occur in the Reference scenario. In the model, curtailment is deemed as for free and drastic increases in electricity use occur during these hours. This reduces electricity use after the time periods when curtailment occurred. Additionally, for the Best Case, an arbitrary choice between heat pump and auxiliary heater occurs at times of curtailment, since during these times electricity is observed as for free. The Load Shaping scenario, as shown in Eq. (7.4), partly minimizes own electricity use, and will mostly choose for the heat pump during times of curtailment. For the Price G scenario, the zero electricity price at curtailment causes a drastic increase in electricity use. The Price I scenario rarely observes this zero electricity price, as illustrated in Figure 7.2d, and hence increases electricity use far less.

The peak demand shows interesting differences between the different scenarios. During peak moments, expensive generation plants are running and the Best Case scenario will try to reduce electricity use during these hours as much as

Table 7.7: Hybrid incentive scenarios in which the optimization criteria are a mixture of minimizing energy use (Reference), minimizing cost with respect to a price profile from the generation (Price G) or the integrated model (Price I) and deviation towards a load profile (Load). The presented attained percentage of operational cost savings is for the case of a 30% RES share and 250,000 buildings with heat pump.

Name	% savings
Reference + Price G	45
Reference + Price I	43
Price I + Load	92
Reference + Price I + Load	94

possible. The Price I and Load Shaping scenarios are able to partially imitate this behavior. However, for the Price G scenario the situation becomes worse than the Reference scenario, as an overreaction to high prices in some hours causes an even higher peak in the hours before.

The mean ramping, calculated as the mean of the absolute value of the ramping from hour to hour, shows significant differences between the scenarios. The Best Case scenario is able to significantly decrease the hour to hour variations in residual demand. The Price I and Load Shaping scenario approximate this behavior while the Price G scenario again shows worse behavior than the Reference case. This is mainly due to the drastic ramping of the heat pump electricity demand right before and after hours of curtailment, as shown in Figure 7.2c.

7.3.5 Hybrid incentive scenarios

Multiple combinations of the above mentioned scenarios are possible by combining the optimization criteria from Eq. 7.1 to Eq. 7.4. The performance of a selection of these hybrid scenarios is summarized in Table 7.7.

Regarding the price-based scenarios, the addition of minimizing total energy use (Reference) could counteract the overshoot with respect to the price profile. For the Price G scenario, the addition of minimizing energy use in the optimization criterion (Reference + Price G) slightly improves the obtained savings from 32% to 45%. However, for the Price I scenario, adding the minimization of energy use in the optimization criterion (Reference + Price I) drastically decreases the attained savings from 72% to 43%. In this combined case, the price profile triggers the correct behavior far less.

In practice, the Load Shaping scenario may be difficult to implement as compensating the participating building owners is not straightforward. By combining this scenario with a fluctuating price profile, this compensation could be easier. The combination of the price from the integrated model with the load shaping (Price I + Load) reaches a slightly higher percentage of the operational cost savings (92%) than the load shaping scenario (85%). However, this cost function proved to be difficult to handle for the buildings, as in some days it drives the temperature close to its bounds in order to attain more drastic electricity demand profiles. These issues were not observed in the combination of the three scenarios (Reference + Price I + Load). This final hybrid scenario performs very well in terms of operational cost savings and realizes 94% of the maximal possible operational cost savings.

7.4 Discussion

Demand response applied to building portfolios with electrically driven heat pumps provides value for the electricity generation system, as it can contribute to lowering system operational costs and CO_2 emissions (Table 7.3). For a low number of buildings or a low RES share, these savings are about 1% and hence rather limited. As the number of buildings or RES share increases, the reductions in operational cost and CO_2 emissions go up to 7% in both cases. This is not a drastic change, but is nonetheless a significant contribution. For these cases, the cost savings are typically around 100 EUR per participant per year. Given the typical investment cost of enabling technologies such as the smart thermostat [78] or smart controllers [81] between 200 EUR and 350 EUR, the pay-back period is on the order of magnitude of a few years, for the boundary conditions employed in this chapter and assuming that all cost savings are directly allocated to the building owners. The order of magnitude of the annual reduction in CO_2 emissions is around 1 ton per participant but highly depends on the number of participating buildings and the RES share.

Regarding the magnitude of the operational cost savings of DR, Hedegaard and Münster [82] investigated the value of flexible operation of heat pumps in 716,000 buildings for an electricity generation system with a 60% share of wind generation and biomass fired combined heat and power plants. According to Hedegaard and Münster [82], this flexible operation results in an annual cost saving per participant of 30 EUR due to avoided operational costs and a 2% reduction in CO_2 emissions. When comparing these results with Table 7.3, the savings are on the same order of magnitude, but are not close. Given the similar climate, building and heat pump characteristics in both studies, the differences in savings are dominated by the composition of the electricity

generation system. This difference, along with the large spread of results in Table 7.3, illustrates that the reductions in operational cost and CO_2 emissions are highly case dependent.

Figure 7.2c illustrates the avalanche effect as discussed by Dallinger and Wietschel [39] for the Price G scenario: all heat pump controllers simultaneously observe a low electricity price and drastically increase demand in those moments. Kelly et al. [94] also observed this overconsumption due to low prices, along with a loss of load diversity. As shown by Ling and Chassin [109], this loss of load diversity can cause simultaneous oscillations in electricity demand of thermostatically controlled loads, causing problems for the electricity generation system following the low price period. As proposed by Dallinger and Wietschel [39], when all participants make individual price forecasts, the peak electricity demand is less concentrated and also the load diversity is better preserved.

The Load Shaping scenario suffers far less from the above mentioned effects. First, during the moments of curtailment, the buildings do not receive a low electricity price but information to increase demand and, equally important, up to which level to increase demand. In the hour 27 in Figure 7.2a for example, there is little curtailment of RES and the buildings know that only a limited increase of electricity demand is necessary. This is far more information than a price signal can hold. Second, the optimization criterion of the Load Shaping scenario, Eq. 7.4, shows that the centrally-suggested demand curve (d_j^{IM}) is merely a suggestion, not an obligation, towards increasing or decreasing electricity demand. Part of the optimization criterion is still the electricity use minimization of each individual building. This partly ensures the preservation of load diversity, as each building will make an individual trade-off. Nonetheless, preservation of load diversity could be improved even more by providing each building with a certain perturbation on the centrally-suggested demand curve [39].

The results for the different scenarios (Figure 7.3) show the potential benefit of applying the integrated optimization during the day ahead stage and distributing profiles from this source. The resulting price profile (Price I scenario) clearly outperforms the case where the price profile is unilaterally determined from the electricity generation system (Price G scenario). The Price I scenario can be regarded as the case where the electricity price is infinitely iterated between electricity generation system and the individual buildings. As Figure 7.3b shows, this price profile causes the system to attain a great amount of the theoretically possible savings, as long as the number of participating buildings remains small. In this sense the buildings are *price takers* up to this point, and will only have a minor effect on the price itself. As the number of participating buildings increases, this influence will no longer be negligible and the buildings become *price influencers*. In this sense, the approach of suggesting a load profile

instead of a price profile (the Load Shaping scenario) is generally better for a high number of participating buildings, over 100,000 in this chapter. The relative operational cost savings remain stable in this scenario, even for 500,000 participating buildings. On a total of 4.6 million households in Belgium [70], this is still a relatively small amount of participating buildings.

From the presented results, one should carefully consider whether time-of-use pricing is the correct way to achieve DR. In regions where a high share of the buildings employ electricity for either heating or cooling, a price profile can lead to unintended adverse effects. With the increasing share of smart thermostats [78], which are technically able to act upon such price profiles, these artifacts of greedy control actions could occur shortly afterwards. In these regions, a central determination of a load profile for all buildings to follow, appears to be a better option.

This chapter only investigates the effects of different DR incentives for low-energy buildings. Chapter 5 showed that buildings lacking proper insulation are not suitable candidates for heat pumps, at least not in a Belgian context. Hence, these buildings were not included in this chapter.

With respect to compensation for the building owner, either a yearly fee or a tempered price profile is possible. A yearly compensation can be based on the operational cost savings as presented in Table 7.3, although it can be a challenge to determine which party is responsible for paying this compensation. A tempered price profile can be used in a hybrid scenario, such as in the Reference + Price I + Load scenario, to automatically compensate the building owners.

For implementing the Load Shaping scenario in practice, the procedure can be followed as shown in Figure 7.1. A day ahead integrated optimization of the electricity generation system along with an aggregated representation of the building stock could be performed. The resulting load profile is communicated to the generation system operators to determine their dispatch. Furthermore, the centrally-suggested demand curve (d_j^{IM}) is communicated to the smart thermostats of all participating buildings, with a small perturbation applied in order to maintain load diversity. The electricity generation system thus runs business as usual, albeit in providing an altered electricity demand profile.

In the current European electricity markets, it is not straightforward which party should determine the load shaping signal, as there are conflicting interests involved. In the electricity generation system, multiple competitors could prefer a different load shape that maximizes their own profits. This could lead to a sub-optimal total cost for all electricity generators combined. Due to the monopoly of the transmission system operator (TSO) and his interest in low system wide

cost, this TSO could be the party that determines the load shaping profile. However, this might lead to the TSO stretching his allowed market power. Finally, as identified throughout this work, the application of DR increases the electricity consumption of the heat pumps. If this would significantly burden the local distribution grids, the distribution system operators should also be involved in shaping the load profile.

7.5 Conclusion

For the boundary conditions in this chapter, the Best Case scenario shows reductions in operational costs between 1.3% and 7.3%, depending on the number of participating buildings and the share of RES in the electricity generation. In addition, a reduction of CO_2 emissions is observed to be between 1.3% and 7.0%. These savings result from a better part-load operation of the power plants, a reduction in starting up and ramping of power plants and the reduction in curtailment of electricity generation from RES.

Multiple scenarios for a more practical DR application are studied, inspired by time-of-use pricing and direct-load control. The added value of the integrated formulation is shown, as it produces price profiles that clearly outperform price profiles coming from the electricity generation system optimization alone. However, as soon as a large amount of buildings, identified to be $100,000$ in this chapter, start participating in DR, the performance of price profiles drops significantly.

In general, and surely for a large amount of participants, it is shown that Load Shaping clearly outperforms the price-based incentives. Load Shaping gives clear information on the magnitude of RES curtailment and inefficient part-load operation of electricity generation plants. For this scheme, it does not matter how many buildings are participating, the performance remains in the same order of magnitude.

Finally, a practical implementation of this DR approach may be performed centrally, namely by performing the day-ahead optimization of the operation of the electricity generation system and an aggregated formulation of the building portfolio with heat pumps. The resulting load profile can then be communicated to the buildings as a suggestion on how to shape the heat pump electricity demand over time.

Chapter 8

Demand response: implications for residential heating system design

This chapter is based on:
Patteeuw, D., & Helsen, L. (2016). Combined design and control optimization of residential heating systems in a smart-grid context. Submitted to Energy and Buildings.

8.1 Introduction

The previous chapters studied the interaction between variable renewable energy sources and the building level by starting from a fixed heating system design. This chapter inverses the question of the impact of installing heat pumps on curtailment of RES: does a large-scale integration of RES has significant impact on the design of heating systems on a residential building level? In other words, will other residential heating systems or hybrid systems become more cost-efficient due to a large increase in electricity generation from RES? Examples could be the selection of a larger DHW tank or a storage tank coupled to floor heating in order to use more electricity during times of curtailment. Another option could be the installation of a heat pump with a supplementary gas-fired

boiler to avoid electricity demand during times of low electricity generation by RES.

To this aim, an investment model for residential heating systems is needed which takes the dynamics of the heating systems and building structure into account. Furthermore, the electricity generation by RES should be explicitly included in the decision process. In this chapter, *an optimization problem is proposed which simultaneously selects, sizes and operates the residential heating systems, in combination with an approximate modeling of the electricity generation system.* On a residential level, heating system investment costs typically have an important fixed cost component which is independent of the heating system size [172]. In order to take this into account in the sizing optimization, an integer decision variable is needed. Hence, the optimization problem for selecting, sizing and operating heating systems is modeled as a MILP problem.

The use of MILP for heating system optimization differs from the more widely used genetic algorithms. According to Attia et al. [9], these genetic algorithms combined with building simulation tools are the most common optimization methodologies applied in the field of building energy performance research. The main advantages of this method, according to Attia et al., are the suitability for multi-objective optimization such as in [30, 186], the ease of use and the robustness as it explores many points in the solution space simultaneously. The disadvantage lies in the large number of simulations needed and hence, the long calculation times.

Using the genetic algorithms, typically only controller setting parameters are included in design optimization [9, 34]. In contrast to this method, this chapter features a MILP optimization approach, where no building simulation tool is needed. The dynamics of the building envelope and heating system are explicitly modeled, in a simplified way within the optimization problem. This offers the advantage of faster simulation times, at the cost of lower accuracy. Another advantage is the aforementioned possibility of simultaneously optimizing design and control during each time step, which is necessary to accurately include the interaction with the electricity generation system [135]. This combined optimization approach has a long history in large scale energy system investment planning, using tools such as TIMES [107] and Balmorel [150], which are both based on linear programming.

The MILP approach has been applied before to multiple scales to study the effect of the integration of RES on investment decisions in the build environment. On a single building level, these studies were performed using MILP [8] or a combination of genetic algorithms and MILP [64]. On an urban scale, Allegrini et al. [3] provided a literature review focusing on multiple energy networks and

urban micro climate. The integration of RES on this scale was studied using a wide variety of approaches, from detailed multi-physics simulation models [13] to multi-objective operational approaches [66, 126]. In contrast to the literature, the current chapter studies the interaction of building energy demand with renewable energy on a national scale, which features a set of buildings in the order of magnitude of a million.

For this large scale, Hedegaard and Balyk [80] developed an investment model for buildings with heat pumps, which acts as an extension to the Balmorel model [150]. Investment in two technologies was considered, namely in a controller to activate the passive storage potential of the building structure and in a hot water storage tank for space heating. Given the combination with Balmorel, investment in these technologies is performed as a response to opportunities in the electric system. In this chapter, a more detailed representation of building structure and storage tanks is employed as well as a consideration of other technologies such as back-up fuel-fired heating, PV panels and solar thermal collectors.

Some of the heating system models presented in this chapter are similar to the framework of Ashouri et al. [8]. Ashouri et al. simultaneously optimized the selection, sizing and operation of both electrical and heating related system components in a single commercial building. These components are modeled as first-order linear differential equations. The main differences with the presented work and the work of Ashouri et al. lies in two points. First, different temperature levels are considered, which allows applying different efficiencies when a heating system is supplying heat to radiators, floor heating or a domestic hot water tank. This difference is crucial for heat pumps as these supply temperatures strongly influence system efficiency. A second difference lies in the explicit modeling of the electricity generation side. As shown in Chapter 5, a massive uptake of heat pumps can have a large impact on the electricity generation system and hence alter any price or CO_2 emission profile stemming from this electricity generation system.

A specific reason to combine these two additions, is the possibility to investigate the full energy storage potential of a thermal energy storage tank for space heating (TESsh), as illustrated in Table 8.1. For example, a residential heating system consisting of an ACHP and floor heating can be complemented with a 1000 l hot water storage tank. Suppose the floor heating has a supply temperature of 35 $°C$ and a return temperature of 30 $°C$, at an outdoor temperature of 5 $°C$. The air coupled heat pump could load the TESsh in a stratified manner to contain 6 kWh_{th} at a COP of 2.9. However, at a time of abundant electricity generation from RES which is being curtailed, it could be beneficial to load the tank even further. The ACHP could heat up the tank further to 45 $°C$ in order to contain 17 kWh_{th} at a COP of 2.4 and further to

Table 8.1: Energy content of a 1000 l hot water storage tank heated up by an air coupled heat pump or in the last row, by an electrical resistance heater (ERH). The numbers are for the case where the tank is coupled to floor heating and where the outdoor temperature is 5 $°C$.

Mean tank temperature $°C$	Heat pump COP (-)	Thermal energy stored (kWh)
30	3.3	0
35	2.9	6
45	2.4	17
60	1.9	35
90	(ERH) 1.0	70

60 $°C$ to contain 35 kWh_{th} at a COP of 1.9. After this, an electrical resistance heater (ERH) could heat up the TESsh even further to 90 $°C$ to contain 70 kWh_{th} at a COP of 1. Hence, *the different temperature levels are needed to model the TESsh in such a detailed manner while the explicit modeling of the electricity generation side provides the correct incentives to use this energy storage.*

The aim of this chapter is twofold. The first aim is to assess whether the addition of the different temperature levels and the explicit modeling of the electricity generation side is crucial in the selecting and sizing of heating systems in residential buildings. Given the large variety in electricity generation mixes, heating system investment costs and climates in different countries, it is hard to perform this assessment in a general way. Therefore, a general methodology is developed and this methodology is applied to the case study of Belgium. The value of the two modeling additions will be tested for nine different electricity generation scenarios. This will provide insight in the impact of variable RES in Belgium on the residential heating system design including optimal control, which is the second aim of this chapter.

This chapter is structured as follows. First, the MILP optimization problem for selecting, sizing and operating heating systems combined with the approximate modeling of the electricity generation system is presented in Section 8.2. This modeling framework is applied to a case study of Belgium, for which the parameters and assumptions are provided in Section 8.3. The results presented in Section 8.4 show two aspects, namely the added value of the modeling framework and the implications for the case study. This is discussed further in Section 8.5 and finally the results are summarized in Section 8.6.

8.2 Combined design and control optimization framework

This section provides a full description of the combined design and control optimization problem which is modeled as a MILP problem. The first part, Section 8.2.1, presents the optimization problem along with the objective function. The second part gives a description of the demand for space heating and domestic hot water (Section 8.2.3). Next, the equations for design and control of the heating system are explained in Section 8.2.4. Finally, a description of the models for electricity generation is provided in Section 8.2.5.

8.2.1 Optimization problem set-up

Figure 8.1 provides a schematic presentation of the combined design and control optimization. The heating system design and control are developed for multiple building types simultaneously. When the selected heating system is powered by electricity, the building and heating system will interact with the electricity generation system. In this optimization, the interaction is explicitly modeled by scaling up the buildings electricity demand. For example, in the case study (Section 8.3) four building types are considered. The electricity demand of these building types is scaled up to represent the demand of one million buildings. Hence, the multiple building types can simultaneously demand electricity and influence the electricity generation system. This couples the design and control optimization for the different building types.

Within each building type, multiple heat production systems can be selected, which can supply heat at 4 different temperature levels and hence with a different efficiency. This heat is used to satisfy the heat demands in the building, each at its respective temperature. The domestic hot water tank is typically heated to 60 $^{\circ}C$ in order to supply DHW. However, in case of abundant electricity generation by RES, the tank can be heated up further to 90 $^{\circ}C$. The space heating demand can either be supplied by radiators or by floor heating. The nominal supply and return water temperatures for the radiators are 45 and 35 $^{\circ}C$ respectively. For floor heating, these temperatures are 35 and 30 $^{\circ}C$ respectively. These temperatures vary in time on the average outdoor temperature. Both emission systems can be complemented with a dedicated storage tank TESsh. Finally, the building structure is represented by a thermal resistance and capacitance network, expressing its potential for passive energy storage.

In the presented optimization framework, four indices are used:

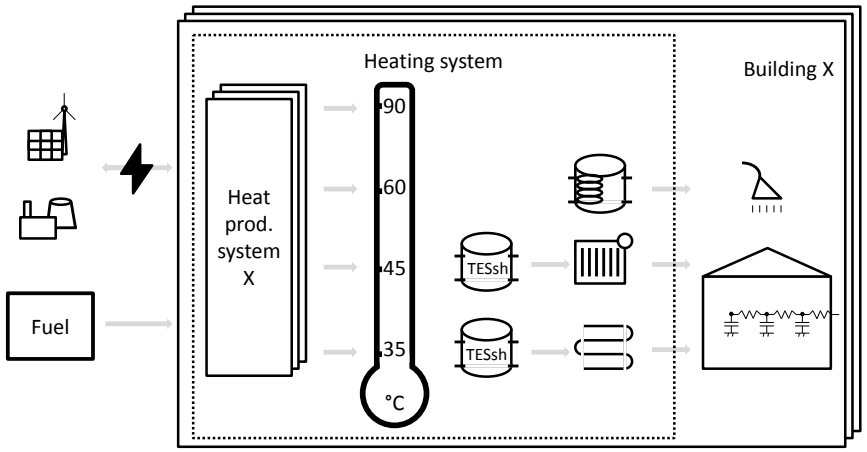

Figure 8.1: Schematic overview of the combined design and control optimization of heating systems in multiple building types. Given the impact on the electricity generation system, this optimization is performed for all building types simultaneously. In each building type, a different heat production, storage and emission system can be selected.

- Index j denotes a time step with duration Δt in seconds
- Index t denotes a time period (rescaling to a full year with weighing factor w_t)
- Index b denotes a building type
- Index l denotes a temperature level (at temperature $T_{l,t}^{level}$). For the two levels dedicated to space heating, this temperature depends on the average outdoor temperature of period t.

All variables in the equations, except temperatures, are positive.

8.2.2 Objective function

The optimization objective is to minimize the equivalent annual cost (EAC) of providing heating to all considered buildings:

$$min\ EAC = \sum_b nb_b \cdot \left(a^{hs} \cdot Inv_b^{hs} + \sum_j \sum_t w_t \cdot OPEX_{j,t,b}^{hs} + OPEX_{j,t,b}^{\text{tariff}} \right) + a^{pp} \cdot \Delta Inv^{pp} + \sum_j \sum_t w_t \cdot \Delta OPEX_{j,t}^{pp} \tag{8.1}$$

with w_t a scaling factor to rescale the operational costs for the considered periods to a year. The EAC stems partly from heating systems (HS) but also from power plants (PP) in case of electricity based heating. In each building type an investment Inv_b^{hs} is made in heating systems. The operational expenditures for providing heating, except those related to electricity generation, are lumped in the variable $OPEX_{j,t,b}^{hs}$. Furthermore, the electricity consumption at building level also faces an electricity tariff $OPEX_{j,t,b}^{\text{tariff}}$. Hence, the energy component of the electricity cost is explicitly modeled as described further, the non-energy component of the electricity cost is fixed to a tariff.

It is assumed that in the base case, the heating is supplied by a fuel-fired heating system. The building types' electricity demand is scaled up by the factor nb_b in order to represent a massive installation of electricity driven heating. This will cause extra investment in power plants ΔInv^{pp} and extra operational costs attributed to the electricity generation system $\Delta OPEX_{j,t}^{pp}$. Different annuities are considered for investment in heating systems, a^{hs}, and for investment in power plants, a^{pp}. The explanation of the heating system costs and the power plant costs is provided further in Section 8.2.4 and Section 8.2.5 respectively.

8.2.3 Heat demand

For each building type, the heat demand must always be met. Hence, there is no thermal discomfort allowed. The residential heating demand consists of space heating and domestic hot water production.

Given the potential of building structures to allow demand response [153, 81, 138], the demand for space heating is modeled through a dynamic building model rather than a fixed profile. This dynamic building model is a thermal resistance and capacitance network based on the two zone building model of

Reynders et al. [151] and described in Section 2.4.1. This network is translated to a discrete state-space model. The upper comfort bound is 24 °C for the day zone and 22 °C for the night zone, based on Peeters et al. [140]. The lower comfort bounds are based on Baetens and Saelens [14], which, in the day zone, is on average 20.2 °C when the occupants are present and on average 15.1 °C when the occupants are absent. For the night zone, the lower temperature bound is on average 12.8 °C.

In order to keep the problem size computationally feasible, only 4 building types are considered in the case study. The demand of these building types is scaled up with a factor nb_b (see Eq. 8.1), as if all buildings of this building type have an identical building structure. The user behavior for these building types is based on the correct user behavior data of Baetens and Saelens [14] as described in Section 2.4.2 and aggregated as described in Chapter 3.6.

The domestic hot water demand is modeled as a demand profile, based on Baetens and Saelens [14] (see Section 2.4.2). Similar to the aggregation of the building models, also the domestic hot water demand is averaged over multiple profiles. All buildings are assumed to have a storage tank for domestic hot water. This storage tank is modeled similar to Eq. 8.7-8.8. The temperature of the DHW storage tank must always be above 50 °C in order to maintain comfort.

8.2.4 Heating system

In this chapter, a wide range of heating system components is modeled. This section describes these components in detail. First, the general equations for investment in different components are provided. Second, the general equation that couples all heating system components is explained. Afterwards each component type for heat emission, heat storage and heat production is described.

General investment equations

For each component of the heating system, the selection and size of this component are optimization variables. In order not to repeat similar equations for each component, a general description of these investment equations is given

by Eq. (8.2)-(8.5).

$$\forall b : Inv_b^x = iz_b^x \cdot cost^{fix,x} + S_b^x \cdot cost^{var,x} \tag{8.2}$$

$$\forall b : iz_b^x \cdot S^{min,x} \leq S_b^x \leq iz_b^x \cdot S^{max,x} \tag{8.3}$$

$$\forall l, j, t, b : 0 \leq O_{l,j,t,b}^x \tag{8.4}$$

$$\forall l, j, t, b : \sum_l O_{l,j,t,b}^x \leq S_b^x \tag{8.5}$$

In a building with index b, the investment cost Inv_b^x in a specific component x consists typically of a fixed cost $cost^{fix,x}$ and a variable cost $cost^{var,x}$ proportional to the size S_b^x of that component. The operational characteristic $O_{l,j,t,b}^x$ of this component is limited by the size of that component (Eq. (8.5)). Note that the component can exchange heat at different temperature levels in the same time step, but the sum of these exchanges cannot exceed the maximum size (Eq. (8.5)).

The selection of whether this component is installed or not is expressed by the binary decision variable iz_b^x. When iz_b^x is zero, the component is not installed. This forces the size of the component to zero (Eq. (8.3)) which nullifies the operation of the component (Eq.(8.5)). When iz_b^x is one, the component is installed and its size can vary between a minimum $S^{min,x}$ and maximum size $S^{max,x}$.

General heating equation

In each time step and in each building type, each heat production system can provide heat $\dot{Q}_{l,j,t,b}^{prod}$ at a certain temperature level with index l. This heat is always taken up by one of the thermal energy storages $\dot{Q}_{l,j,t,b}^{toTes}$[1]

$$\forall l, j, t, b : \sum \dot{Q}_{l,j,t,b}^{prod} = \sum \dot{Q}_{l,j,t,b}^{toTes} \tag{8.6}$$

in which the summation works over all heat production and thermal energy storages. There are three TES involved, which are dedicated to their respective heat demand: DHW, radiators or floor heating. In case there is no thermal energy storage installed for a particular demand, $\dot{Q}_{l,j,t,b}^{toTes}$ is directly passed on to satisfy this demand, as shown later in Eq. 8.7.

[1] Given Eq. 8.6, there are no losses in the distribution pipes considered. However, this could be added in this framework.

Thermal energy storage

Regarding thermal energy storage, only sensible TES in the form of hot water storage tanks is considered. For other thermal storage technologies, such as phase change material tanks, absorption TES and adsorption TES, it is hard to obtain reliable cost data. Nevertheless, this framework can be easily extended to these technologies. Since the standby heat losses of a hot water storage tank depend on the application, each hot water storage tank is assumed to supply heat solely to its specific application ($\dot{Q}^{toDem}_{l,j,t,b}$). As such, there is a hot water storage tank dedicated to domestic hot water (TESdhw) and two storage tanks dedicated to space heating (TESsh): to the radiators (TESrad) and to the floor heating (TESfh). Each of the hot water storage tanks are modeled as follows:

$$\forall l,j,t,b : \frac{1}{\Delta t}\left(Q^{tes}_{l,j+1,t,b} - Q^{tes}_{l,j,t,b}\right) = \dot{Q}^{toTes}_{l,j,t,b} - \dot{Q}^{toDem}_{l,j,t,b} - f^{tes,prop} \cdot Q^{tes}_{l,j,t,b} - M^{tes}_{b} \cdot \dot{Q}^{standby}_{l,b} \tag{8.7}$$

$$\forall l,j,t,b : 0 \leq Q^{tes}_{l,j,t,b} \leq M^{tes}_{b} \cdot c_p \cdot \Delta T^{level}_{l} \tag{8.8}$$

in which $Q^{tes}_{l,j,t,b}$ is the amount of heat stored in the tank at a certain temperature level l. Part of the heat loss to the environment is proportional to the stored heat with the factor $f^{tes,prop}$. This factor depends on the size of the tank, which causes a multiplication of decision variables and thus makes the problem non-linear. Hence, it is chosen to predetermine this factor based on an expected tank size. The actual tank size is denoted by the variable M^{tes}_{b}. In the case of the TESrad and TESfh, the level connected to the emission system is assumed to work perfectly stratified. For this level there is also a standby heat loss to the environment proportional to the size of the tank $\dot{Q}^{standby}_{l,b}$ [173]. The maximum heat content of a level hence depends on whether the level is assumed to be perfectly stratified or mixed, determining the value of the allowed temperature spread ΔT^{level}_{l}. More detail on this modeling approach of the storage tank is provided in [11].

In the case where a storage tank is not installed, the heat to the tank equals the heat provided to the specific demand: $\dot{Q}^{toTes}_{l,j,t,b} = \dot{Q}^{toDem}_{l,j,t,b}$ and no thermal losses occur.

For example, as illustrated in Table 8.1, a hot water storage tank of 1000 l coupled to floor heating with a supply temperature of 35 $°C$ and return temperature of 30 $°C$ would be able to store 5.8 kWh in a stratified way at a supply temperature of 35 $°C$. To this aim, the temperature of the tank needs to stay above 30 $°C$ at all times. This results in the standby heat loss. If the tank

is heated above 30 $°C$ this leads to the proportional heat loss. Furthermore, the tank could be heated further to 45 $°C$, albeit with the heat pump working at a lower efficiency, allowing the tank to store an additional 11.6 kWh. The level at 45 $°C$ works perfectly mixed in this case, with only a heat loss proportional to the stored heat.

Heat emission

The two lowest temperature levels are dedicated to space heating, which can be supplied through two heat emission systems, namely floor heating and radiators. In this study, when an emission system is chosen, it is sized to meet the design heat demand. The circulation pump of the emission system demands an electric power $P_{l,j,t,b}^{pump,emi}$. In order to avoid an integer decision variable each time step, this electric power is assumed to be proportional to the designed power $P^{pump,emi,max}$ and the heat demand.

$$\forall l,j,t,b : P_{l,j,t,b}^{pump,emi} = P^{pump,emi,max} \cdot \frac{\dot{Q}_{l,j,t,b}^{emi,d} + \dot{Q}_{l,j,t,b}^{emi,n}}{\dot{Q}^{max,emi,d} + \dot{Q}^{max,emi,n}} \tag{8.9}$$

with $\dot{Q}_{l,j,t,b}^{emi,d}$ and $\dot{Q}_{l,j,t,b}^{emi,n}$ the heat supplied by the emission system to the day zone and night zone respectively.

The mean supply temperatures of these emission systems are determined for each period, based on the nominal heat demand and the mean outdoor temperature for that period, using a heating curve. Hence, during each period the heat production systems that supply space heating may have a different efficiency.

Traditional heat production

The considered traditional heat production systems consist of the following: condensing gas boilers, heating oil boilers, wood pellet boilers and electrical resistance heaters. The operational aspect of the condensing gas boilers is described by the following equation:

$$\forall l,j,t,b : \dot{Q}_{l,j,t,b}^{cgb} = \eta_{l,t}^{cbg} \cdot \dot{F}_{l,j,t,b}^{cgb}. \tag{8.10}$$

Hence, the heat delivered by the condensing gas boiler $\dot{Q}_{l,j,t,b}^{cgb}$ depends on the rate of fuel input to the boiler $\dot{F}_{l,j,t,b}^{cgb}$ and the efficiency $\eta_{l,t}^{cgb}$. This efficiency depends on the temperature level at which the boiler is supplying heat. For the two levels connected to space heating, this temperature depends on the ambient air temperature and thus varies in time. Hence, the efficiency of the CGB in supplying space heating varies each period.

The equations for the heating oil boiler, electrical resistance heater and wood pellet boiler are identical to Eq. 8.10, albeit with other parameters. In order to avoid an unrealistically high wood pellet consumption, an extra constraint is added which limits the annual wood pellet consumption to a total potential.

Combined heat and power

In this study, no micro combined heat and power plants (CHP) are considered at the building level. As shown by Pruitt et al. [148], the modeling of micro-CHP requires an integer decision variable in each time step, which would make the optimization problem infeasibly large to solve. Furthermore, as shown by Dorer and Weber [48], the primary energy saving of micro-CHP devices is typically far lower than for a heat pump. Given these factors combined with the high investment cost of a micro-CHP [155], this technology is not considered here.

Hence, in this chapter only macro CHP plants combined with district heating are considered. Three types are considered, which use natural gas, wood pellets or waste as a fuel. All 3 CHPs are modeled in a similar way:

$$\forall j,t,b : g^{chp}_{j,t,b} = \eta^{chp,el} \cdot \dot{F}^{chp}_{j,t,b} \tag{8.11}$$

$$\forall l,j,t,b : \dot{Q}^{chp}_{l,j,t,b} = \eta^{chp,th} \cdot \eta^{network} \cdot \dot{F}^{chp}_{l,j,t,b} \tag{8.12}$$

with $\dot{F}^{chp}_{l,j,t,b}$ the rate of fuel consumption of the CHP. The CHP generates electricity $g^{chp}_{j,t,b}$ at an efficiency of $\eta^{chp,el}$. The heat delivered by the CHP to the building $\dot{Q}^{chp}_{l,j,t,b}$ depends on the thermal efficiency of the CHP, $\eta^{chp,th}$, but also on the average efficiency of the district heating network $\eta^{network}$. This average efficiency of the district heating network is assumed to be constant. A macro CHP is only considered for a building type when the investment in a district heating network is made. Note that the electricity generation from the macro CHP is not considered in the tariff calculation in Eq. 8.26. Hence, the electricity generation from macro CHP observes the same market incentives as the CCGTs and OCGTs.

Solar thermal

In a residential context, solar thermal collectors are often installed for partially supplying domestic hot water [143]. According to Peuser et al. [143], the heat gain from a solar thermal collector $\dot{Q}^{stc}$ is typically modeled as follows:

$$\dot{Q}^{stc} = A^{stc} \cdot \left(\eta_0 \cdot \dot{q}^{sol} - k_1 \cdot (\bar{T}^{stc} - T^e) - k_2 \cdot (\bar{T}^{stc} - T^e)^2\right) \tag{8.13}$$

with A^{stc} the useful surface of the solar thermal collector (STC). The solar thermal collector is heated by $\dot{q}^{sol}$, the total solar irradiation per square meter in the inclination and azimuth of the solar thermal collector. Part of this heat is directly lost to the ambient air, which is at a lower temperature T^e, due to the high mean temperature of the water in the solar thermal collector $\bar{T}^{stc}$. The balance between heat gain and heat loss depends on the technical parameters η_0, k_1 and k_2. However, Eq. 8.13 is not practically useful for design and control optimization due to the quadratic term and the need for a binary variable to switch off the STC when there is insufficient solar irradiation. Another approach is taken, similar to Ashouri et al. [8], namely by assuming a fixed temperature of the water in the STC and defining the (useful) surface of the solar thermal collector $A^{stc}_{l,j,t,b}$ as the operational decision variable:

$$\forall l, j, t, b : \dot{Q}^{stc}_{l,j,t,b} = A^{stc}_{l,j,t,b} \cdot q^{stc}_{l,j,t} \tag{8.14}$$

$$\forall l, j, t : q^{stc}_{l,j,t} = \eta_0 \cdot \dot{q}^{sol}_{j,t} - k_1 \cdot (T^{level}_{l,t} - T^e_{j,t}) - k_2 \cdot (T^{level}_{l,t} - T^e_{j,t})^2. \tag{8.15}$$

This useful surface varies between zero and the installed size of the solar thermal collector and is multiplied by the heat gain per square meter $q^{stc}_{l,j,t}$ in order to know the heat gain to a certain temperature level. It is assumed that the STC can deliver to each considered temperature level at temperature $T^{level}_{l,t}$ and that this is also the mean temperature of the solar thermal collector.

Heat pump

In this study, two types of heat pumps are considered, namely ground coupled and air coupled heat pumps. Both heat pump types are coupled to a hydronic system. Since about 90 % of the Belgian residential buildings have a hydronic system [125], air-air heat pumps are not considered in this study. The heat supplied by the different heat pump types $\dot{Q}^{hp}_{l,j,t,b}$ is modeled as follows:

$$\forall l, j, t, b : \dot{Q}^{hp}_{l,j,t,b} = COP_{l,t} \cdot P^{hp}_{l,j,t,b} \tag{8.16}$$

$$\forall l \mid (T^{level}_{l,t} > T^{hp,max}) : P^{hp}_{l,j,t,b} = 0 \tag{8.17}$$

with $P^{hp}_{l,j,t,b}$ the heat pump electricity consumption in each time step. The heat pump is unable to supply heat above the temperature $T^{hp,max}$ which is $60\,°C$ in this study. In order to avoid non-linear constraints in the optimization problem, the heat pump's COP is approximated as constant in each period with index t. According to Verhelst et al. [179], this is the best linear approximation for the COP. Based on the average supply ($T^{level}_{l,t}$) and source ($\bar{T}^{source}_{l,t}$) temperature

for the period with index t, the COP is determined based on Bettgenhäuser et al. [19]:

$$\forall l,t : COP_{l,t} = a^{hp} \cdot \frac{T_{l,t}^{level}}{T_{l,t}^{level} - \bar{T}_{l,t}^{source} + b^{hp}} \tag{8.18}$$

for which the parameters a^{hp} and b^{hp} depend on the heat pump type and are also based on Bettgenhäuser et al. [19].

8.2.5 Electricity generation

The economic aspects of electricity generation strongly depend on the scale of the electricity generation units. Therefore, large-scale and local scale electricity generation are modeled separately.

Electricity generation system scale

As stated in the objective function (Eq. (8.1)), the additional cost for the electricity generation system caused by a widespread switch from fuel-fired to electricity-driven heating is explicitly modeled. This study does not consider import and export of electricity and neglects grid constraints. Hence, the following equation holds:

$$\begin{aligned} \forall j,t : d_{j,t}^{trad} + \sum_b nb_b \cdot d_{j,t,b}^{build} = & g_{j,t}^{ccgt} + g_{j,t}^{ocgt} + g^{nuc} + curt_{j,t} \cdot g_{j,t}^{res} \\ & + \sum_b nb_b \cdot \left(g_{j,t,b}^{chp} + g_{j,t,b}^{rPV,g} \right) \end{aligned} \tag{8.19}$$

with $d_{j,t}^{trad}$ the traditional electricity demand before a widespread switch from fuel-fired to electricity-driven heating. When a switch towards electricity based heating is performed, this electricity demand $d_{j,t}^{build}$ becomes an important fraction of the total demand. This additional demand is met by electricity generation from multiple sources. The first source is gas-fired power plants, namely combined cycle gas turbines $g_{j,t}^{ccgt}$ and open cycle gas turbines $g_{j,t}^{ocgt}$. The second source is nuclear g^{nuc}, which is assumed not to modulate and run at full capacity in each time period. Electricity generation from renewable energy sources $g_{j,t}^{res}$ is the third source, for which curtailment is modeled through a factor $curt_{j,t}$ between zero and one. Finally, there is electricity generation from the buildings' level when combined heat and power is installed $g_{j,t,b}^{chp}$ or when

residential PV panels supply electricity directly to the grid $g_{j,t,b}^{rPV,g}$. Electricity generation from RES is assumed to have zero marginal cost.

The equations for the operational cost for the combined cycle and open cycle gas turbines are similar. The equations are given for the combined cycle gas turbines:

$$\forall j,t : OPEX_{j,t}^{ccgt} = \frac{fc^{gas}}{\eta^{ccgt}} \cdot g_{j,t}^{ccgt} + dc_{j,t}^{ccgt} \tag{8.20}$$

$$\forall j,t : dc_{j,t}^{ccgt} \geq (suc^{ccgt} + rac^{ccgt}) \cdot (g_{j,t}^{ccgt} - g_{j-1,t}^{ccgt}) \tag{8.21}$$

$$\forall j,t : dc_{j,t}^{ccgt} \geq rac^{ccgt} \cdot (g_{j-1,t}^{ccgt} - g_{j,t}^{ccgt}) \tag{8.22}$$

with fc^{gas} the fuel cost of natural gas including costs due to the CO_2 price and $dc_{j,t}^{ccgt}$ the dynamic cost of operating the power plant. Hence, Eq. (8.21)-(8.22) represent a linear approximation of the electricity generation system, neglecting part-load efficiencies of the power plants and linearly modeling start-up costs. The power plants have a constant efficiency η^{ccgt}. The start-up cost suc^{ccgt} is expressed per MW and assumed proportional to the upward increase in power generation. Costs associated with ramping rac^{ccgt} are proportional to both upward and downward ramping. This simplified approach was taken as it was observed in Chapter 4 that when a large number of buildings with heat pumps participate in demand response, merit order modeling of the power plants leads to an error of only up to 2 % compared to a full unit commitment model. Furthermore, it was observed in Chapter 6 that the presence of a large number of buildings with heat pumps participating in demand response also brings the efficiency of the power plants closer to its maximum value.

As a large set of buildings make a switch to electricity-driven heating, an investment in additional generation capacity could be needed. Again, only the equations for the CCGT are given:

$$\Delta Inv^{pp} = Inv^{ccgt} \cdot \Delta g^{ccgt,max} \tag{8.23}$$

$$\forall j,t : g_{j,t}^{ccgt} \leq g^{ccgt,inst} + \Delta g^{ccgt,max} \tag{8.24}$$

$$\tag{8.25}$$

with Inv^{ccgt} the investment cost for CCGT per MW for the generation capacity $\Delta g^{ccgt,max}$ that comes on top of the already installed capacity $g^{ccgt,inst}$.

Local electricity generation scale

Since all costs in this chapter are calculated at building level, the costs for electricity transmission, distribution, taxes and levies should be included. Otherwise electricity would be unrealistically cheap compared to other energy sources at the building level:

$$\forall j,t,b : OPEX^{\text{tariff}}_{j,t,b} = \text{tariff}^{dem} \cdot d^{build}_{j,t,b} - \text{tariff}^{gen} \cdot g^{rPV,g}_{j,t,b}. \tag{8.26}$$

As the energy component of the electricity cost is already explicitly modeled by Eq. 8.21-8.22, the tariff tariff^{dem} is the domestic electricity price minus the energy component. Electricity can be generated at the building level by means of PV panels and supplied to the grid, for which a certain tariff tariff^{gen} is received. In case of net metering policy, the two tariffs equal each other. Throughout this chapter, a net metering policy is assumed. The sensitivity towards this policy is investigated in Section 8.4.5. The residential PV panels can either supply electricity for use in the building $g^{rPV,b}_{j,t,b}$ or supply electricity to the grid $g^{rPV,g}_{j,t,b}$:

$$\forall j,t,b : g^{rPV,b}_{j,t,b} + g^{rPV,g}_{j,t,b} \leq cf^{PV}_{j,t} \cdot g^{rPV,inst}_{b}. \tag{8.27}$$

The sum of these electricity generation terms cannot exceed the actual electricity generation from the PV panels, which is the product of the capacity factor in each time step $cf^{PV}_{j,t}$ and the installed capacity $g^{rPV,inst}_{b}$. In Belgium, the yearly electricity generation by PV panels is not compensated for when the yearly generation exceeds the yearly electricity demand [55]. Hence, the following constraint is added:

$$\forall b : \sum_{j}\sum_{t} w_t \cdot \left(g^{rPV,b}_{j,t,b} + g^{rPV,g}_{j,t,b}\right) \leq \sum_{j}\sum_{t} w_t \cdot \left(d^{build}_{j,t,b} + g^{rPV,b}_{j,t,b}\right). \tag{8.28}$$

In this study, the building electricity demand *consists solely of the electricity demand for heating purposes*. Hence, the electricity demand for lighting and appliances is not modeled explicitly, but is assumed to be included in the traditional electricity demand $d^{trad}_{j,t}$. The electric heating demand $d^{build}_{j,t}$ is hence determined as follows:

$$\forall j,t,b : d^{build}_{j,t,b} = \sum_{l}\left(P^{pumps}_{l,j,t,b} + P^{hp}_{l,j,t,b} + P^{erh}_{l,j,t,b}\right) - g^{rPV,b}_{j,t,b} \tag{8.29}$$

and consists of the electricity consumption of circulation pumps $P^{pumps}_{l,j,t,b}$, heat pumps $P^{hp}_{l,j,t,b}$ and electrical resistance heating $P^{erh}_{l,j,t,b}$ from which the momentary self-consumed local generation by PV is subtracted.

Table 8.2: The four building types considered in this study. Detached is abbreviated as Det.

Index b	1	2	3	4
Building typology	Det.	Semi-det.	Terraced	Det.
Location	Urban	Urban	Urban	Rural
Peak heat demand (kW)	6.5	4.8	4.5	6.5
Yearly heat demand (MWh)	12	9	7	12
Day/night zone area (m^2)	132/138	98/136	60/140	132/138
South oriented roof size (m^2)	90	70	40	90
Number of buildings	350.000	250.000	250.000	150.000
Natural gas allowed	yes	yes	yes	no
District heating allowed	no	no	yes	no

8.3 Case study

The optimization problem formulated in Section 8.2 is applied to a case study. The aim is to investigate whether the addition of the different temperature levels and the explicit modeling of the electricity generation system add value to the design of heating systems in residential buildings. This investigation is performed by using the combined design and control optimization framework to determine which heating systems should be selected in thoroughly insulated buildings in Belgium, for nine electricity generation mix scenarios. This section provides the assumptions on cost and performance data of all considered systems. These costs vary substantially in practice. Hence, the results with respect to cost should be considered with care.

8.3.1 General

The annuity for all heating systems is based on a lifetime of 20 years [22] while the power plants annuity is based on a lifetime of 25 years [157]. For both, the same discount rate is taken, namely 7 % which reflects the point of view of a private investor [5]. The gas fired power plants face a natural gas price of 25 EUR/MWh [60] in which the cost for CO_2 emission is included. Furthermore, the buildings face an electricity tariff of 150 EUR/MWh_{el} [58].

8.3.2 Buildings

In this study, only thoroughly renovated buildings are considered. As shown in Chapter 5, these buildings are appropriate candidates for heat pumps and hence show potential interaction with the electricity generation system. Four typologies are considered for which the demand is scaled up to represent a larger set of buildings, based on Gendebien et al. [72] and Protopapadaki et al. [147] (Table 8.2).

According to the economic optimum for Belgium [176], these buildings have an average U-value of 0.3 W/m^2K and a ventilation rate of 0.4 ACH, which are two conditions for the nearly zero energy building standard, as set up by the Flemish government [175]. The resulting peak heat demand and yearly heat demand are listed in Table 8.2. The user behavior is based on the data from Baetens and Saelens [14] as described as Baetens2 in Section 2.4.2 and aggregated as described in Section 3.6. This results in a diversity factor of 75 %, which means the peak heat demand per building in Table 8.2 is possibly underestimated. However, in this study the control is optimized which, as shown by Verhelst [178], enables a smaller design. Typically, even with a smaller sized heating system, the control is able to determine a correct start-up time for heating, as is already implemented in smart thermostats [78].

8.3.3 Heating system

Table 8.3 gives an overview of the technical and economical parameters of the heating systems considered in this study. Combustion of wood pellets and waste is assumed to have a zero net CO_2 emission. Waste is assumed to come at zero cost, but constructing the CHP for this fuel type is expensive, see Table 8.3. The total wood pellet potential is taken to be 3 TWh, halfway between Belgians own production and demand, based on Goh et al. [74]. The potential of waste for energy conversion is assumed to be 1 TWh based on Govaerts et al. [77]. The condensing gas boiler uses natural gas at the residential level and hence faces a different natural gas price (75 EUR/MWh) than the large scale CHP and power plants (25 EUR/MWh) [62].

8.3.4 Electricity system

The only conventional power plants considered, except CHP, in this study are open cycle gas turbines, combined cycle gas turbines and nuclear power plants. The prices for gas fired electricity generation units are based on [157] and given in Table 8.4. The natural gas price for these power plants is 25 EUR/MWh

Table 8.3: Overview of economical and technical parameters employed in the case study. Efficiencies are based on the higher heating value and given between brackets for the 4 temperature levels: (η at 90 $^{\circ}C$; η at 60 $^{\circ}C$; η at 45 $^{\circ}C$; η at 35 $^{\circ}C$). Costs are given per building and are mainly based on [172]. Technical data is based on [31, 24, 19] and technical specifications from various heating system producing companies. All fuel prices are given with respect to the primary energy content.

Component	$cost^{fix}$ EUR	$cost^{var}$ EUR	Technical parameters
Elec. resistance heater	-	100 $/kW_{el}$	$\eta = 1$
Condensing gas boiler	3000	-	η = (0.84; 0.86; 0.92; 0.95) Fuel 75 EUR/MWh
Heating oil boiler	5500	-	η = (0.95; 0.95; 0.98; 0.98) Fuel 85 EUR/MWh
Wood pellet boiler	9000	-	$\eta = 0.9$; Fuel 55 EUR/MWh
District heating	5000		$\eta^{network} = 0.95$
Gas CHP	-	900 $/kW_{el}$	$\eta^{el} = 0.41$; $\eta^{th} = 0.40$ Fuel 25 EUR/MWh
Wood pellets CHP	-	2300 $/kW_{el}$	$\eta^{el} = 0.22$; $\eta^{th} = 0.75$ Fuel 55 EUR/MWh
Waste CHP	-	6200 $/kW_{el}$	$\eta^{el} = 0.18$; $\eta^{th} = 0.61$ Fuel 0 EUR/MWh
PV panels	-	1.6 $/W_{peak}$	150 W_{peak}/m^2
Solar thermal collector	3150	410 $/m^2$	$\eta_0 = 0.84$; $k_1 = 3.66$; $k_2 = 0.017$
DHW tank	150	1.5 $/liter$	$f^{tes,prop} = 5 \cdot 10^{-7}$ 50 $l \leq$ size $\leq$ 300 l
TESsh	1000	0.5 $/liter$	$f^{tes,prop} = 2 \cdot 10^{-7}$ 500 $l \leq$ size $\leq$ 5000 l
Air coupled HP	4650	1000 $/kW_{th}$	$a^{hp} = 0.38$ $b^{hp} = 10$
Ground coupled HP	7000	4500 $/kW_{th}$	$a^{hp} = 0.5$ $b^{hp} = 10$
Radiators	950	500 $/kW_{th}$	$P^{ppump} = 30$ W $T^{sup}_{nom} = 45\,^{\circ}C$; $T^{ret}_{nom} = 35\,^{\circ}C$
Floor heating	3000	100 $/kW_{th}$	$P^{ppump} = 40$ W $T^{sup}_{nom} = 35\,^{\circ}C$; $T^{ret}_{nom} = 30\,^{\circ}C$

[62]. The annuity for these plants is calculated based on a period of 25 years. The nuclear power plants have an operational cost of 20 EUR/MWh_{el} [157]. These nuclear power plants operate at full capacity in the scenarios where these are considered and hence no ramping costs or start-up costs are applicable.

Table 8.4: Electricity generation costs, based on [157].

Power plant type	Investment EUR/MW	Efficiency %	Start-up cost EUR/MW	Ramping cost EUR/MW
CCGT	876	62	60	0.25
OCGT	498	40	10	0.66

The electricity generation from RES is assumed to have a marginal cost of 0 EUR/MWh_{el}. The installed capacity of nuclear power and RES depends on the scenario and the accompanying investment cost is not taken into account in this study so they are considered as existing units. Finally, the capacity limits and losses associated with electrical grids are not considered in this study.

8.3.5 Disturbance profiles

The modeled system faces four dynamic disturbances: the traditional electricity demand $d_{j,t}^{trad}$, the electricity generation from RES $g_{j,t}^{res}$, the ambient air temperature $T_{j,t}^{e}$ and the solar heat gains $\dot{Q}_{j,t}^{sol}$. These disturbances are taken for Belgium for the period of the years 2013 to 2016, since national RES profiles are only fully available from 2013 onwards [54]. Both the electricity generation from RES and the traditional electricity demand are based on data from the Belgian transmission system operator [54]. Weather data is based on measurements in Brussels. Three types of centralized RES generation are considered in this study: PV-panels, onshore wind turbines and offshore wind turbines.

In an ideal case, the optimization horizon would be the full period of 3 years, but this would lead to infeasible calculation times. Instead, representative periods are determined based on the methodology of Poncelet et al. [145]. In order to take into account the lower traditional electricity demand during weekends, the length of the representative periods is chosen to be one week. After applying the methodology of Poncelet et al., six representative periods were chosen, depending on the scenario. In scaling up the variables of these periods to a year, weighting factors are determined in order to have a similar load duration curve for the residual electricity demand (electricity demand minus electricity generated by RES) and the heat demand of the buildings (Figure 8.2). The periods were also chosen in order to assure that a cyclic boundary condition can be imposed.

One weakness of choosing the representative weeks this way, is that the correlation between the heat demand and the residual electricity demand can change. For example, two extreme weeks could be chosen: a week with high

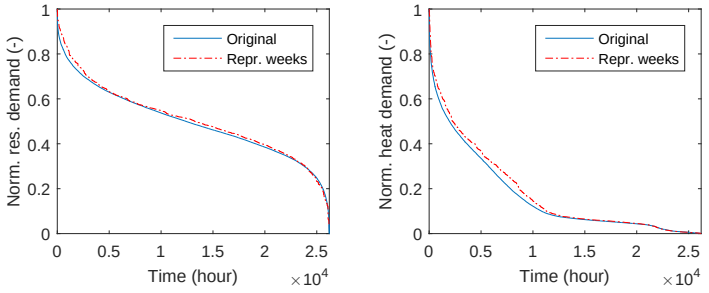

(a) Residual electricity demand (b) Heat demand detached building

Figure 8.2: Illustration of the normalized (norm.) load duration curves in the case of the original profiles for the period 2013 to 2016 (Original) and the rescaled load duration curve in the case of the six representative weeks (Repr. weeks).

curtailment but low heat demand and a week with low curtailment and high heat demand. This could lead to an underestimation of how much the heat demand can be shifted to times of curtailment. Regarding the peak demands, this mismatch is avoided. In the profiles for Belgium in 2013 to 2016, the coldest week and the week with the highest electricity demand coincide, namely in the second week of 2013. Hence, while applying the methodology of Poncelet et al., a constraint is set that this coldest week is always one of the six chosen representative weeks.

8.3.6 Scenarios

The scenarios are based on the mix in the electricity generation system. In this chapter, this mix is assumed to consist solely of gas-fired and/or nuclear power plants and generation from wind turbines and PV panels. The different scenarios can be chosen based on Figure 8.3, which is determined from profiles for electricity demand and RES generation from the TSO of Belgium [54] from January 2013 to January 2016. Hence, it is assumed that wind energy generation stems for two thirds from offshore wind turbines and for one third from onshore wind turbines. The maximum allowable capacities for onshore wind, offshore wind and PV are 9 GW, 8 GW and 50 GW respectively, based on Devogelaer et al. [46].

The black squares in Figure 8.3 denote the currently installed capacities of wind and PV in Belgium, while the black triangles show the chosen scenarios. An

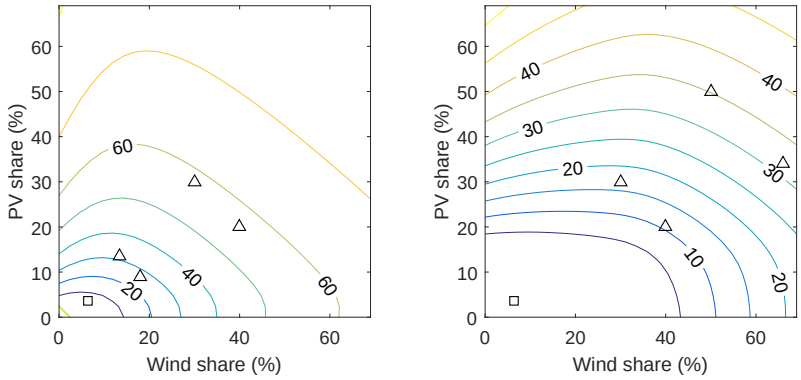

(a) Curtailment ($\%_{RES}$) in case of 66 % nuclear

(b) Curtailment ($\%_{RES}$) in case of 0 % nuclear

Figure 8.3: Situating the different scenarios for the shares of electricity generation by wind, PV and nuclear. Figures 8.3a and 8.3b show the percentage of curtailment with respect to the total electricity generation from wind and PV. The black squares denote the current share of wind and PV in Belgium at the end of 2015. The black triangles denote the other scenarios in the cases with or without nuclear capacity installed.

overview of these scenarios is given in Table 8.5. In the first five scenarios, the currently installed capacity of nuclear power plants is still available. Assuming that the nuclear power plants run at their full capacity of 5925 MW all year through, these deliver about 66 % of the electricity generation. As can be seen in Figure 8.3a, the presence of these nuclear power plants causes much curtailment already at low shares of RES. Hence, with nuclear power plants present, only scenarios are chosen up to a 60 % RES share. In the last four scenarios, no nuclear power plants are present. In these cases, curtailment only starts occurring at high RES shares and the scenarios are chosen accordingly. Regarding the division of the RES generation between wind turbines and PV panels, two options were chosen. In one option, wind turbines provide two times as much energy as PV panels, as is currently the case. In the other option, wind turbines and PV panels provide an equal amount of energy throughout the year.

Table 8.5: Scenarios with respect to the electricity generation system. The shares are calculated as the yearly electricity generation by a source divided by the yearly demand, without taking curtailment into account.

Scenario Name	#	Nuclear %	Wind %	PV %
N66W06P03	1	66	6,5	3,7
N66W18P09	2	66	18	9
N66W13P13	3	66	13,5	13,5
N66W40P20	4	66	40	20
N66W30P30	5	66	30	30
N00W40P20	6	0	40	20
N00W30P30	7	0	30	30
N00W66P34	8	0	66	34
N00W50P50	9	0	50	50

8.4 Results

In this section, the results are shown step by step. In Section 8.4.1 an example illustrates the typical model output. Next, the results are set up step by step. In a first step, the heating system design is fixed and hence the components are selected and sized according to common practice. Hence, only the control is optimized in Section 8.4.2. In a next step, only the selection of the heating system is fixed in Section 8.4.3 and hence the sizing and control of the components can be optimized. In a third step, Section 8.4.4 shows the results of the full combined design and control optimization with integer variables where the selection, sizing and control of the heating systems can be optimized. Finally, section 8.4.5 investigates the sensitivity of the results to some of the assumptions.

8.4.1 Example result of integrated design and control

Figure 8.4 illustrates part of the output in the scenario of the current electricity generation mix (N66W06P03) where all buildings are equipped with an air coupled heat pump and a back-up electrical resistance heater. Figure 8.4 shows the output of these models for the coldest week. In this period, the heat pumps are almost continuously running at their maximum capacity (Figure 8.4b) which causes the average day zone air temperature in these buildings to remain above 20 $°C$ all the time (Figure 8.4c). This is due to the incorporation of the investment decisions in the optimization. At building level, this minimizes the installed capacity of the heat pumps. The buildings and DHW tanks

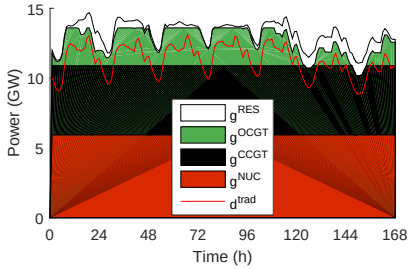

(a) Electricity generation system

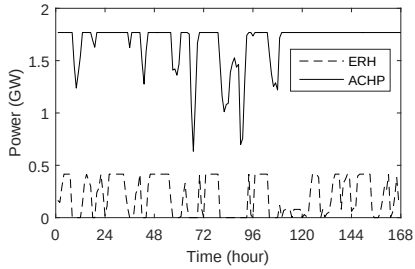

(b) Buildings electricity generation/demand

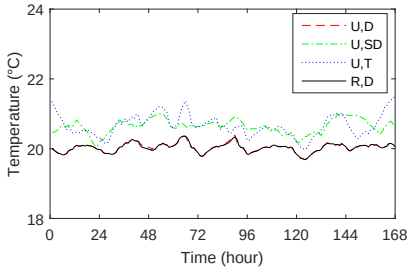

(c) Average day zone temperature

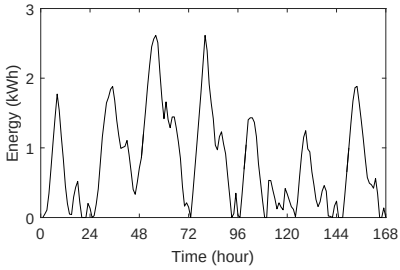

(d) Average DHW tank energy content

Figure 8.4: Illustration of the model output for the coldest week in the scenario of the current electricity generation mix (N66W06P03), in the case where all buildings are equipped with an air coupled heat pump (ACHP) and a back-up electrical resistance heater (ERH). The total electricity demand of these heat pumps (Figure 8.4b) affects the electricity generation by renewable energy sources and gas fired power plants (Figure 8.4a). In order to attain a good interaction, the day zone temperature (Figure 8.4c) and energy content of the domestic hot water tank (Figure 8.4d) are manipulated. For clarity reasons, only the day zone temperature (Figure 8.4c) is shown for the 4 building types, in which U and R stand for urban and rural. D, SD and T stand for detached, semi-detached and terraced.

are preheated to a minor extent in hours 65 to 80, in order to partly avoid electricity demand during hours 80 to 92. This leads to a lower investment in peak electricity generation capacity. The remainder of the heating demand is covered by the electrical resistance heater (Figure 8.4b), which is solely used for heating the domestic hot water tank. Note also how the temperature in the detached buildings (Figure 8.4c) remains closer to the lower boundary than in the other building types. This can either mean that the investment cost is more

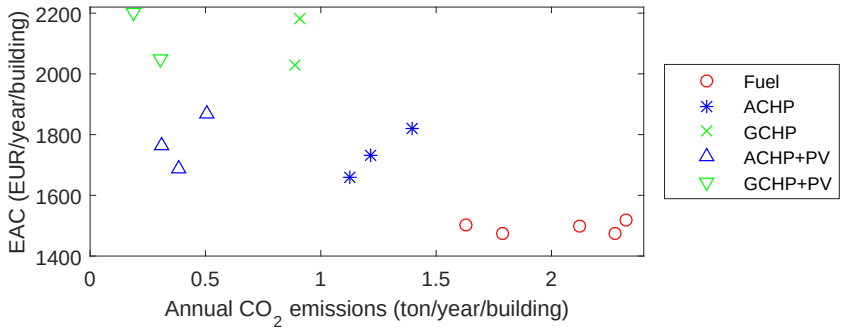

Figure 8.5: Overview of the equivalent annual cost (EAC) and CO_2 emission of different heating system cases for scenario N66W06P03, averaged over all buildings, with a fixed design.

critical for this building type or that the potential for load shifting is smaller.

8.4.2 Results with fixed design (selection and sizing)

In a first step, the optimization is performed for a fixed design: when a heating system is chosen, it is sized to meet the peak heat demand. Also, when a PV system is considered, it is sized to meet the annual electricity consumption of the household. Hence, only the control of the components can be optimized. The results are shown in Figure 8.5.

The cases with combinations of condensing gas boiler, heating oil boiler, wood pellet boiler or gas-fired CHP are named "Fuel" in this figure. These systems clearly lead to the lowest EAC, but also to the highest annual CO_2 emissions. For these heat production systems, the lowest average CO_2 emission, 1.5 ton per building per year, is attained when the detached and semi-detached urban buildings have a condensing gas boiler, the terraced urban building is coupled to a macro CHP running on natural gas and waste while the rural buildings have a wood pellet boiler. This shows a clear influence of the building type on the most appropriate heating system.

In all cases where a heat pump is installed, the CO_2 emission is lower. The cases with an air coupled heat pump show a somewhat higher CO_2 emission and lower equivalent annual cost than the cases with a ground coupled heat pump. These results include the option where the urban, terraced buildings are coupled to a CHP through a district heating network and all other building types are equipped with a heat pump. This combination leads to the lowest

Table 8.6: Results of optimized sizing and control for different heating system selections in the scenario N66W06P03: the main heat production system size (Main), the size of the electrical resistance heater (ERH) and the thermal energy storage tank for space heating (TESsh). Also the need for extra OCGT capacity per building is given (OCGT) along with the reduction in yearly curtailment (curt.).

Heating system selections Values per building	Main kW_{th}	ERH kW_{th}	TESsh $liter$	STC m^2	OCGT W_{el}	Curt. kWh
CGB, HOB; Fh	30	0	0	0	0	-0.001
CGB, HOB and STC; Fh	30	0	0	1	0	-0.006
ACHP; Rad	4.14	0.50	0	0	972	-0.160
ACHP; Fh	4.42	0.42	0	0	642	-0.159
ACHP + TESsh; Fh	4.27	0.55	500	0	550	-0.159
GCHP; Fh	3.03	2.41	0	0	365	-0.135
GCHP + TESsh; Fh	2.88	2.45	500	0	321	-0.131

EAC of all cases shown with an ACHP. The highest EAC of the options with an ACHP is the one where this heat pump is coupled to a radiator.

Complementing the heat pumps with PV panels drastically lowers the annual CO_2 emissions with 0.6 to 0.9 ton per building per year, at a surplus EAC of only 30 EUR per building per year. The lowest CO_2 emission of 0.19 ton per building per year is attained when all buildings are equipped with a ground coupled heat pump and PV panels, at the highest annual cost of 2202 EUR per building per year.

8.4.3 Results with fixed selection

A second step before getting to the results of the combined design and control optimization, is to perform the optimization multiple times with fixed integer decision variables. This means that in each calculation, the selection of heat production, storage and emission system is fixed. However, the sizing and control of these components are optimized. The absence of integer decision variables turns the optimization problem into an LP problem, which drastically decreases the calculation time from the order of days to two minutes.

Table 8.6 presents the results for some cases in the scenario of the current electricity generation mix (N66W06P03). For the case where a condensing gas boiler (CGB) is installed in the urban buildings and a heating oil boiler (HOB) in the rural buildings, the results are of little interest: both heat production

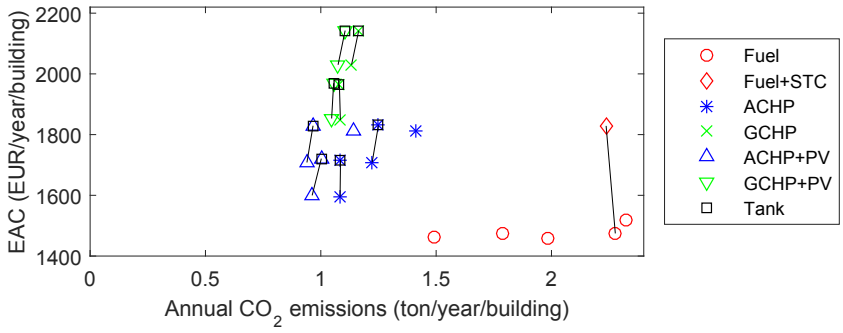

Figure 8.6: Overview of the equivalent annual cost (EAC) and CO_2 emissions of different heating system cases for scenario N66W06P03, averaged over all buildings, with fixed system selection but optimized size and control. The black squares denote the cases where a thermal energy storage tank is added to the heating system (TESsh). The results of these cases are connected to the results of the respective case without TESsh.

systems are typically over-sized. Since these heat production systems only use electricity for the circulation pumps, the influence on the electricity generation system is negligible.

For the ACHP and GCHP, part of the investment cost is proportional to the heat pump size. For both heat pump types, this causes part of the peak heat demand to be covered by a back-up electrical resistance heater. Note that the sum of both thermal capacities is lower than the expected heating power as provided in Table 8.2, meaning that combined design and control optimization is able to lower the investment cost in the heat pump, by optimizing the system control.

For the GCHP, the proportional component of the investment cost is that high, that the size of the back-up resistance heater almost equals the size of the GCHP. However, this does not lead to a drastic increase in peak electricity demand, as can be seen in the capacity of OCGT installed per building (Table 8.6). Similar as in Figure 8.4, the building structure is preheated at night, but to a larger extent. As was also found in Chapter 5, the highest increase in peak electricity generation capacity occurs when the buildings are equipped with the combination of an air coupled heat pump and radiators.

Figure 8.6 gives an overview of the equivalent annual cost and CO_2 emission for some selected heating systems for the scenario with the current electricity generation mix: N66W06P03. For the cases with heat pumps, the differences

Table 8.7: Equivalent annual cost and CO_2 emission per building for different heating system selections and different scenarios.

Scenario	N66W06P03		N66W40P20		N00W66P34	
Heating system selections	EAC	CO_2	EAC	CO_2	EAC	CO_2
Values per building per year	EUR	Ton	EUR	Ton	EUR	Ton
CGB, HOB; Fh	1520	2,32	1466	2.16	1423	2.05
CGB, HOB and STC; Fh	1829	2.24	1772	2.06	1735	1.97
ACHP; Rad	1812	1.41	1651	0.39	1596	0.55
ACHP; Fh	1709	1.22	1571	0.30	1520	0.41
ACHP + TESsh; Fh	1830	1.25	1692	0.30	1637	0.41
GCHP; Fh	2030	1.13	1905	0.38	1874	0.62
GCHP + TESsh; Fh	2143	1.16	2022	0.37	1985	0.60

with Figure 8.5 are clear: generally a lower EAC is attained, but at the cost of a higher annual CO_2 emission. For the cases with a GCHP, the EAC lowers with about 200 EUR per building per year but increases the CO_2 emissions with about 0.25 ton per building per year. This is due to the installation of the large electrical resistance heater (Table 8.6). Also the PV system is drastically downsized, reducing the EAC but increasing the annual CO_2 emissions. The difference in results illustrates a handicap of the combined design and control optimization framework: it is single objective optimization towards EAC.

Regarding the solar thermal collector and the storage tank for space heating, a general trend is visible in Table 8.6 and Figure 8.6, which is also confirmed for other scenarios. This trend is that both systems are sized as small as allowed by the constraints. This means that for these components, even when these are obliged to be installed, the marginal cost of the proportional part of the investment cost is still higher than the marginal gains by sizing these components larger.

One square meter of a solar thermal collector (Table 8.6) only reduces the CO_2 emission by 0.1 ton per building per year, at an increased cost of about 300 EUR per building per year. For a similar increase in EAC, an ACHP reduces the CO_2 emission with 1 to 1.5 ton per building per year (Figure 8.7).

Regarding the thermal energy storage tank for space heating, Figure 8.6 and Table 8.7 illustrate that in most cases this technology causes the CO_2 emission to *rise*. This means that the flexibility offered by the TESsh does not pose significant added value with respect to the flexibility already provided by the building structure and the tank for domestic hot water. Hence, the main effect of the TESsh is an increase in heat demand, due to its standby losses.

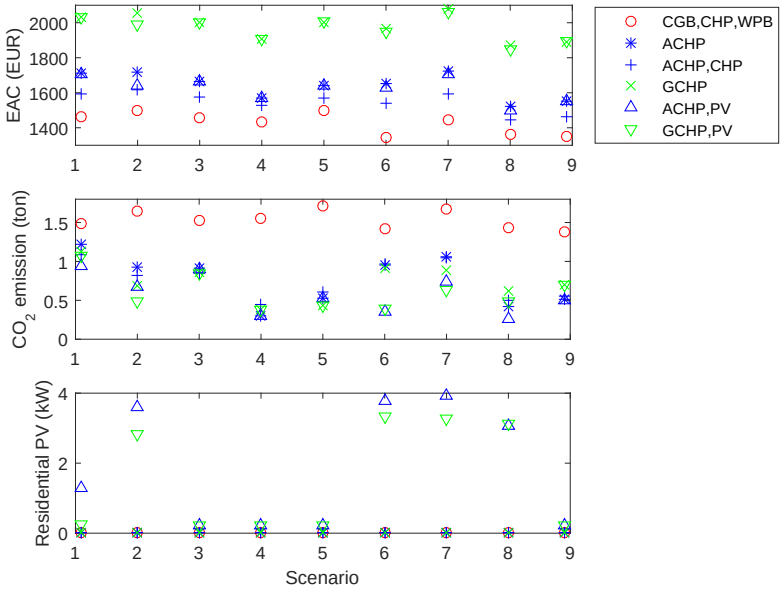

Figure 8.7: Equivalent annual cost (top) and CO_2 emission (middle) per building per year for a selected number of cases over all scenarios (the scenarios corresponding to the numbers on the x-axis can be found in Table 8.5). The average installed PV capacity per building is shown in the bottom figure.

The results for the heating system selections which are close to pareto optimality in Figure 8.6 are shown in Figure 8.7 for all electricity generation mix scenarios. The scenarios corresponding to the numbers on the x-axis can be found in Table 8.5. Both figures show the same trends in the results. First, the fuel based options (CGB,CHP,WPB) show the lowest EAC of these cases, but also the highest CO_2 emission. The variation in CO_2 emission between the different scenarios stems from the macro CHP.

Regarding the options with a heat pump, the EAC for the air coupled heat pump is between 300 and 400 EUR lower than that of the ground coupled heat pump cost in all scenarios (Figure 8.7). The option in which all buildings are equipped with an air coupled heat pump except the terraced buildings, which are coupled to a macro CHP, leads to the lowest EAC. Regarding the CO_2 emission, the difference between the different heat pump cases is rather small. For cases with a ground coupled heat pump, this is partly because of the large size of the electrical resistance heater (Table 8.6), to limit the investment cost.

Finally, in the cases where the heat pump is complemented with rooftop PV panels, the CO_2 emission drops and the equivalent annual cost slightly decreases (Figure 8.7). However, the installed capacity greatly varies throughout the scenarios. In the cases where already a large fraction of the electricity generated by PV is curtailed, i.e. scenarios 3 to 5 and scenario 9, there is practically no investment performed in additional residential PV. In the other cases, the PV is sized to such an extent that the constraint in Eq. 8.28 becomes active: the annual electricity demand from the heating systems is met.

One exception in this is scenario 1 (N66W06P03), where one would expect the residential PV to be also sized to meet the annual electricity demand, which is not the case. The reason for this deviation is the choice of representative weeks. When the cases in scenario 1 were recalculated with the representative weeks of scenario 2, the residential PV was sized to meet the annual electricity demand. This shows a weakness in the approach of using representative weeks, as this can influence the result.

8.4.4 MILP results

In this section, the results are shown for the full combined design and control optimization, with inclusion of all integer decision variables, as described in Section 8.2. This leads to a very large optimization problem, consisting of 42 integer decision variables and 2 million continuous decision variables. This MILP problem is solved using CPLEX 12.6 using all 20 threads on a Xeon E5-2680v2 processor. The optimization problem proves to be very hard to solve, as it takes typically 3 days to find a solution.

The MILP returns one single solution. As the first row in Table 8.8 shows, the MILP is still far from optimal after 3 days of calculating. In order to get a solution and to make a comparison with the results from the fixed heating system design or selection, the MILP is calculated again but with a limit on the CO_2 emission. In this way, it is possible to determine the technology selection which lead to a certain CO_2 emission reduction at the lowest cost. In Figure 8.8, the results are visualized together of all three approaches: the MILP, the fixed designs and the fixed selections. This figure shows that the MILP results do not deviate a lot from the results with fixed design or selection. This is because these approaches lead to almost the same technology selection (Table 8.8): in all results, there is only one main heating system installed.

In the MILP results with different constraints on the CO_2 emissions in Table 8.8, the terraced buildings are always coupled to the macro CHP, which runs on natural gas and waste. The installed capacity of the waste CHP is low throughout all solutions due to the high investment cost and the limited waste

Table 8.8: Results of the MILP for the current electricity generation mix (scenario N66W06P03), reaching an optimum after 3 days of calculation. For each technology, the size is added between brackets in kW_{th}, except for CHP and PV in kW_{el}. Both the CO_2 limit and EAC are shown per building per year.

CO_2 limit ton	Selected technology Urban Detached	Urban Semi-det.	Urban Terraced	Rural Detached	EAC EUR
None	Too far from convergence				3447
1.5	CGB (30)	CGB (30)	CHP:	ACHP (5,2)	1486
	PV (0.2)	PV (0.2)	gas (2.5)	PV (5)	
	ERH (0.1)	ERH (0.1)	waste (0.2)	ERH (0.2)	
1	ACHP (5.2)	ACHP (3.9)	CHP:	GCHP (3.1)	1645
	PV (0.4)	PV (0.3)	gas (2.6)	PV (2)	
	ERH (0.3)	ERH (0.3)	waste (0.1)	ERH (3.3)	
0.9	ACHP (5.3)	ACHP (3.9)	CHP:	ACHP (5.3)	1595
	PV (1.1)	PV (0.8)	gas (2.7)	PV (1.2)	
	ERH (0.3)	ERH (0.3)	waste (0.1)	ERH (0.3)	
0.75	ACHP (5.3)	ACHP (3.9)	CHP:	ACHP (5.3)	1596
	PV (1.7)	PV (1.3)	gas (2.5)	PV (2.3)	
	ERH (0.3)	ERH (0.3)	waste (0.1)	ERH (0.3)	
0.50	ACHP (5.3)	ACHP (3.9)	CHP:	GCHP (3.2)	1652
	PV (4.0)	PV (2.0)	gas (2.5)	PV (2.8)	
	ERH (0.3)	ERH (0.3)	waste (0.1)	ERH (3.3)	
0.25	ACHP (5.2)	ACHP (3.9)	CHP:	GCHP (3.2)	1668
	PV (5.5)	PV (3.9)	gas (2.5)	PV (4.6)	
	ERH (0.4)	ERH (0.4)	waste (0.1)	ERH (3.1)	

potential. In the rural buildings, typically an ACHP or GCHP is installed. For the urban detached and semi-detached buildings, this is also the case when a low limit on the CO_2 emission is imposed. Otherwise, a condensing gas boiler is installed in these buildings. In the case of a GCHP in the rural buildings, these are complemented with a large electrical resistance heater, similar to the result in Table 8.6.

Furthermore, all buildings except the terraced buildings are equipped with a typically small electrical resistance heater and an occasionally small PV system. For the electrical resistance heater, no fixed cost or minimum size was imposed (Table 8.3) and hence this technology is attractive for covering the last peak in meeting the heating demand. The net metering scheme then stimulates the investment in PV to meet the electricity consumption of the electrical resistance heater on a yearly basis. In the cases with a more stringent CO_2 limit, the PV

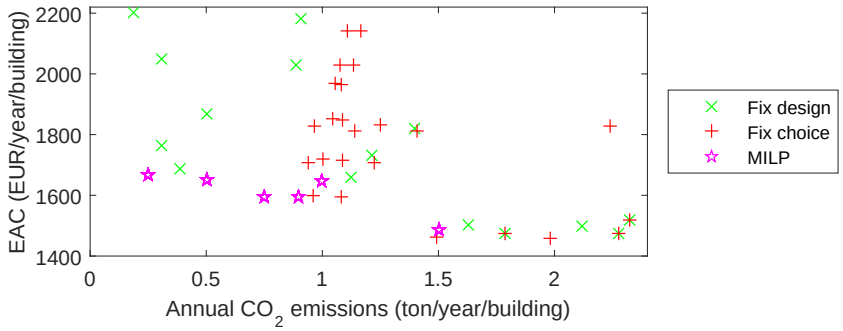

Figure 8.8: Situating the MILP results with respect to the results of the optimizations with fixed design (Figure 8.5) and with fixed selection of heating systems (Figure 8.6) for the current electricity generation mix (scenario N66W06P03).

system is sized larger.

Note that in all results, no other components were added to the heating system. In none of the results were there any solar thermal collectors installed. Also, in none of the buildings where a heat pump is selected, are these heat pumps accompanied by a TESsh or by another heat production system to meet the peak heat demand. Hence, it appears that in all buildings, a rather straightforward selection of heating system is made, namely one main heat production system without much auxiliary systems, except for an electrical resistance heater and PV. This is partly due to the large fixed part of the investment cost, in this model, in heating production systems in a residential context, which forms an important threshold to install a second heat production system. In practice however, the cost of installing two systems might be lower than the sum of installing both separately due to a reduced margin per component taken by the installer.

Since the MILP usually ends up choosing one heat production system per building, it shows little added value with respect to the approach of optimizing multiple cases with fixed design (Section 8.4.2) or selection (Section 8.4.3). The MILP takes around 3 days to calculate for one single solution, while a case with fixed design or selection only takes 2 minutes. Hence, calculating the latter results for the cases in Figures 8.5 and 8.8 took less than an hour, while calculating the MILP results took multiple days.

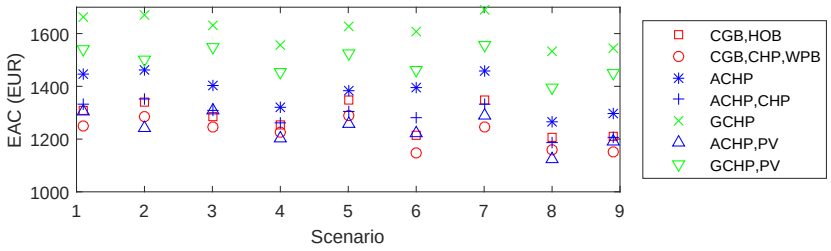

Figure 8.9: Equivalent annual cost per building for a discount rate of 3.5 %, for all scenarios.

8.4.5 Sensitivity analysis

The results in this chapter are based on a large set of parameters, as listed in Section 8.3. A full sensitivity analysis with respect to these parameters is outside the scope of this chapter. Rather, this part illustrates the sensitivity of the results towards a selected set of parameters and assumptions. The sensitivity towards the net metering scheme and the discount rate is shown. Later, the results for the TESsh for these sensitivity analyses are shown. Finally, the sensitivity towards the method of calculating the CO_2 emission is discussed. Given the long simulation times of the MILP model, the sensitivity analyses are performed with fixed heating system selection as in Section 8.4.3.

Net metering

To test the sensitivity towards the net metering policy, supplying electricity to the grid by the residential PV panels is made less attractive by reducing tariff^{gen} to only half of tariff^{dem}. With this policy, the residential PV panels were sized very small: the maximum installed capacity over all scenarios is 320 W. This also holds for the cases with TESsh. Hence, the presence of this energy storage is not able to make an investment in PV more attractive in this case. Overall, the attractiveness of residential PV strongly depends on the net metering policy as well as the already installed PV capacity in the central electricity generation system (Figure 8.7).

Discount rate

In practice, the investment cost of heating systems can vary widely. A full sensitivity towards the investment cost is beyond the scope of this work. However,

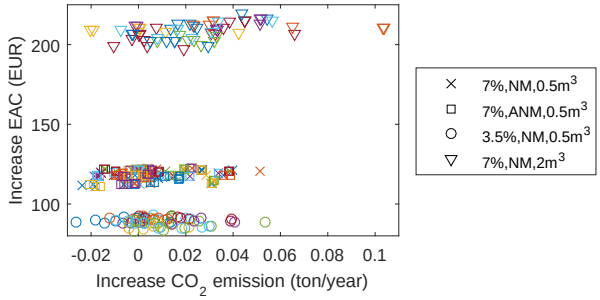

Figure 8.10: Increase in equivalent annual cost and CO_2 emission per building per year over all results with fixed integer decision variables, due to the installation of a TESsh. The results are shown for a discount rate of either 7 % and 3.5 %, for either a normal net metering scheme (NM) or attenuated net metering scheme (ANM) and for a minimum tank size of either 0.5 m^3 or 2 m^3.

in order to get a grasp of what the sensitivity towards the investment cost can be, the impact of a different discount rate is illustrated. Figure 8.9 shows the results when the discount rate is changed from 7 % to a discount rate which reflects more a societal point of view, namely 3.5 % [96]. A lower discount rate favours technologies which show a high initial investment cost but low operational costs.

Figure 8.9 shows the equivalent annual cost in the different scenarios, for the discount rate of 3.5 %. This is to be compared with the results in Figure 8.7 with a discount rate of 7 %. A first logical observation is that the EAC for all heating systems lowers. However, the change in relative difference between the heating systems is interesting: the combination of ACHP and residential PV becomes cheaper than the typical fuel fired options in a number of scenarios. In the other scenarios, the difference in EAC also lowers. Throughout the scenarios, the lower discount rate also causes the heat pumps' size to rise, as well as the residential PV systems to be sized to meet the annual electricity demand in all scenarios.

Thermal energy storage tank for space heating

Throughout this section, the thermal energy storage tank for space heating shows poor performance. All results with respect to this TESsh are summarized in Figure 8.10. This figure shows the increase in equivalent annual cost and CO_2 emission due to the installation of a TESsh, for the optimization results

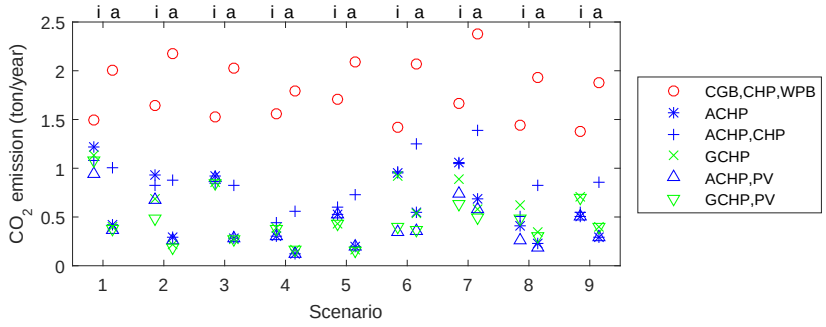

Figure 8.11: Comparison of CO_2 emissions using the incremental (i) and average (a) CO_2 emission in each hour, for all scenarios.

with fixed selection where a heat pump is installed. A first general observation, not shown in the figure, is that the TESsh size always equals the lower bound on this size. Furthermore, installing a TESsh always increases the equivalent annual cost. This cost increase mainly depends on the investment cost of the TESsh, as can be seen in the clear clustering around a tank size in Figure 8.10. Finally, the difference in CO_2 emission is highly system and scenario dependent. The CO_2 emissions per building per year drop in some of the heating system cases, mostly in the scenarios with high curtailment. Note however, that this CO_2 emission saving does not exceed 0.03 ton per building per year and is highly case dependent.

CO_2 emission calculation method

Throughout this chapter, the CO_2 emission of the electricity consumption and/or generation by the heating systems is determined by using the incremental emission factor as defined by Bettle et al.[20]. In this methodology, the electricity consumption is delivered by the marginal unit. In this chapter, the marginal units are typically the gas-fired power plants, except during the periods when electricity generation by RES overshoots the demand. In the latter situation, RES functions as the marginal unit. However, as pointed out by Bettle et al.[20], another approach is to use the average emission factor. In this approach, the CO_2 emission in each time step of the electricity consumption of the heating systems is determined as the average CO_2 emission of all electricity generation units active at that time step. In case of electricity generation by the heating system, this replaces the average CO_2 emission at that time step.

The results of employing both emission factors are compared in Figure 8.11,

which repeats the incremental emission factor results shown in Figure 8.7. Independent of the scenario, the same trends occur. First, by employing the average emission factor, the CO_2 emission of the CHP is drastically higher than employing the incremental emission factor. In the case of the incremental emission factor, the electricity generation by the CHP is typically replacing generation from a gas-fired power plant, next to which it is more efficient. In the case of the average emission factor, electricity generated by the CHP replaces a mix of nuclear, RES and gas-fired generation, compared to which it emits more CO_2.

A similar trend occurs for the residential PV panels. For example in scenario N00W40P20 (scenario number 6), the residential PV systems substantially lower the CO_2 emission by 0.6 ton per building when the incremental emission factor is employed. Using the average emission factor however, the residential PV panels only lower the CO_2 emission by 0.2 ton per building.

Finally, for the heat pump options, employing the average emission factor leads to substantially lower CO_2 emissions: below 0.5 ton per building, except in Scenario N00W40P20 (scenario number 6) and N00W30P30 (scenario number 7). As in all scenarios large shares of nuclear and RES are assumed (Table 8.5), this leads to a low average CO_2 emission for electricity consumption. Employing the average emission factor also drastically lowers the difference between the CO_2 emission of the air coupled and the ground coupled heat pump to below 0.15 ton per building.

Electricity versus natural gas tariff

As shown by Heylen et al. [85], the ratio between the electricity price and natural gas price is a key indicator for the economic feasibility of a heat pump. This ratio determines the operational cost savings of a heat pump over its lifetime with respect to a natural gas boiler, which should compensate for the higher investment cost of a heat pump. In order to illustrate the importance of this ratio, the electricity tariff is varied while the natural gas tariff (at 50 EUR/MWh) and natural gas wholesale market price (at 50 EUR/MWh) remains fixed. Instead of the value of 150 EUR/MWh_{el} used throughout this chapter, the electricity tariff is now varied between 100 EUR/MWh_{el} and 200 EUR/MWh_{el}, inspired by the tariffs in France and Germany respectively [85].

Figure 8.12 illustrates the sensitivity of the equivalent annual cost towards the electricity tariff. This electricity tariff is a dominant factor in the EAC of the heat pump options, regardless of the scenarios. When a low electricity tariff of 100 EUR/MWh_{el} holds, the air coupled heat pumps options become very competitive with the fuel fired option in terms of EAC. However, the EAC

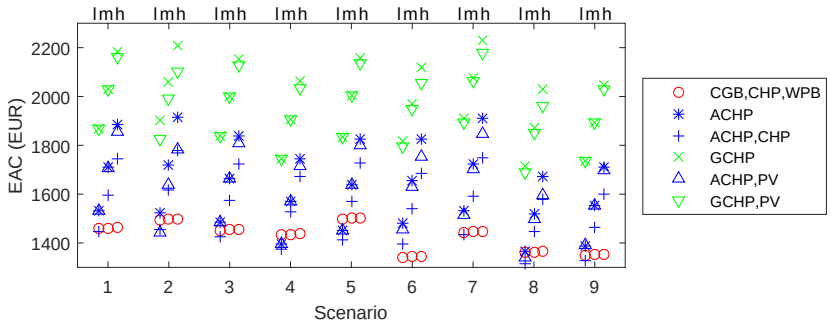

Figure 8.12: Sensitivity of the equivalent annual cost per building towards the ratio in electricity and natural gas price. This is illustrated by varying the electricity tariff between 100 EUR/MWh_{el} (low (l)), 150 EUR/MWh_{el} (medium (m)) and 200 EUR/MWh_{el} (high (h)). 150 EUR/MWh_{el} is the electricity tariff assumed throughout the chapter.

of the ground coupled heat pump options remains 400 EUR higher. In the other extreme case of an electricity tariff of 200 EUR/MWh_{el}, the EAC of all heat pump options is at least 250 EUR higher than the fuel fired option. This illustrates the strong sensitivity of the heat pump's economic attractiveness to this electricity tariff.

8.5 Discussion

This section discusses the observations with respect to the added value of the addition of the temperature levels and the electricity generation park in the optimization framework. Furthermore, the use of a MILP approach towards the combined design and control optimization is discussed along with some strong and weak points of this approach. Finally, the impact of including the electricity generation system in the residential heating system design is discussed.

As stated in the introduction, the main motivation towards including the different temperature levels is to have an accurate representation of the energy storage potential of the TESsh. However, Figure 8.10 shows that this TESsh has little added value in the case study: the equivalent annual cost typically rises with around 100 EUR per building and the reduction in CO_2 emissions is highly case dependent and smaller than 0.03 ton per building per year. Of course, these numerical results highly depend on the parameters of the current case study, but already give a strong indication that the TESsh and the accompanying modeling

of the temperature levels, are superfluous in the studied residential framework. The inclusion of the temperature levels does allow for an elegant modeling of the interaction and cascading of different heating system components, but has the downside of increasing the problem size proportionally with the number of temperature levels.

The addition of the electricity generation park influences the heating system design, as shown for example for the different scenarios in Figure 8.7. Especially the design of the residential PV system, heat pump and macro CHP sees an impact. The electricity generation system forms an extra incentive in the operation of the heat pump and macro CHP during the coldest week. As also seen in Chapter 5, this stimulates the heat pumps to greatly preheat the buildings during the night. As during the coldest periods, the indoor air temperature is almost constant, the heat pump size can be smaller. This is because a smaller start up is needed after the period of the temperature set-back at night, which plays a role in sizing of the heat pump. Regarding the equivalent annual cost per building, Figure 8.7 shows that the relative order between the different heating system options stays rather unaltered throughout the different electricity generation mix scenarios.

Explicitly modeling the interaction with the electricity generation park also allows to determine the incremental CO_2 emission accurately. However, interpreting the CO_2 emission results should be done carefully, as Figure 8.11 illustrates the difference of up to 1 ton per building per year between the incremental and average CO_2 emission calculation methods. Bettle et al.[20] discussed that the incremental emission factor should be used to assess the short term impact of a change in electricity demand. Given that the electricity generation system has more time to adapt to the change in electricity demand, in terms of investment in new power plants and RES generation, the average emission factor should be used. Bettle et al. suggest to employ a weighted average of both resulting CO_2 emissions to assess the impact of the electricity demand. The weighing factor between the two is off course open for discussion. The main aim of Figure 8.11 is to illustrate the high sensitivity of the CO_2 emissions on the (arbitrary) choice between incremental and average emission factors.

Using the MILP approach, it is possible to combine all heating system design decisions in one single optimization problem. However, solving the MILP takes more than 3 days and returns only one single solution. From the MILP results in the current case study it also appears that only one main heating system is selected per building type. Hence, the MILP shows little added value with respect to the approach of multiple calculations with fixed heating system design or selection (Figure 8.8). The latter approach only takes 2 minutes per calculation, which allows for a quick computation of the solution space. In this

way, it is possible to quickly situate the different technologies with respect to each other. This provides much more knowledge and insight in the different heating system options. This approach is similar to the large scale energy system investment models TIMES [107] and Balmorel [150], which both employ LP problem and avoid the use of integer decision variables.

Note that the presented MILP combined design and control optimization determined the heating system selection for four different building types simultaneously. This means that the number of integer decision variables is four times higher than when a single building would be considered. Also, it appears that the fixed cost component in a residential context is a large barrier for implementing two main heat production systems as well as for implementing a TESsh and STC. In the work of Ashouri et al. [8], the MILP approach was also used, but from the perspective of a single office building. That setting appears to be better suited for a full MILP approach.

Given the short calculation time of two minutes when the integer decision variables are fixed, this model is suited for a combination with a genetic algorithm. The genetic algorithm can make the selection between the heating system options, while the presented model with fixed integer decision variables optimizes the system size and control. The latter model would work as a subroutine which provides the lowest achievable cost given a certain system selection. This approach is close to the one applied by Evins [64], who applied a genetic optimization for heating system selection and building design parameters around a MILP for control of the heating system. Similar to Ashouri et al. [8], Evins' framework was applied to a single office building. The approach of Evins could prove to be too calculation intensive for the scale in this chapter, but nonetheless can provide valuable insight in the combination of a genetic optimization for system selection and a subroutine providing the optimized control.

As shown in Figure 8.13, the percentage of RES that gets curtailed, varies widely throughout the scenarios. Installing heat pumps instead of the fuel fired options reduces the curtailment with 1.5 to 7 % as compared to the total electricity generation by RES. This translates to a 9 to 33 % reduction in terms relative to the total curtailment. Employing this last metric, Hedegaard et al.[81] reported reductions in curtailment of 8 % to 19 %, Meibom et al. [118] found 13 % to 20 % while in Chapter 5 a reduction of 50 % in curtailment was reported. This illustrates the wide diversity of the impact of heat pumps on curtailment and the sensitivity towards the boundary conditions. Furthermore, this also shows that installing heat pumps with smart controllers cannot fully limit the curtailment of RES to zero, as was also found by Waite and Modi [180]. Hence, in energy systems with high RES, smart heat pumps should be complemented with extra energy storage technologies.

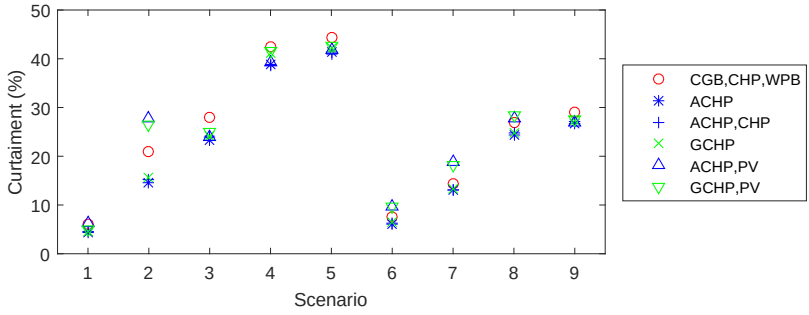

Figure 8.13: Curtailment of RES as a percentage of the total electricity generation of RES. Comparison for the same scenarios as presented in Figure 8.7.

Regarding the case study for Belgium, some general trends could be found throughout the results. First, the CHP with district heating appears cost competitive for the assumed costs but the CO_2 emission savings strongly depend on whether the CO_2 emission is determined according to the incremental or average approach. Second, the cases with heat pumps lead to the lowest CO_2 emissions independent of the CO_2 emission calculation method. From the heating system options, the air coupled heat pump coupled to floor heating is the most cost competitive, as was also found in Chapter 5. As shown in Figure 8.12, this cost competitiveness strongly depends on the tariff structure for natural gas and electricity in residential buildings. When heat pumps are combined with PV panels and given a low discount rate of 3.5 %, this option was even cheaper than the classical gas condensing boiler in some scenarios (Figure 8.9). Finally, the solar thermal collector and TESsh appear to be expensive technologies leading to only a small reduction in CO_2 emission. For the TESsh, the CO_2 emissions even rose in a large part of the studied cases and scenarios. Hedegaard et al. [81] also observed the little added value of the TESsh, as the flexibility in the building structure and domestic hot water tank already provide most of the flexibility benefits.

Note that the numerical results should be handled with care. First of all, real heat production systems are sold in discrete sizes, for which the linear variable cost in Eq. 8.2 is an approximation. A home owner will hence probably not install the small auxiliary systems as depicted in the MILP results in Table 8.8. Also, the investment cost for heating system components vary widely. Furthermore, the share of nuclear power generation and RES varies greatly throughout the different scenarios. This will affect the fixed tariff $tariff^{dem}$ for electricity consumption at the household level. Hence, the equivalent annual

costs in the different scenarios should be handled with care.

Regarding residential PV, the investment decisions are particularly sensitive to the investment cost and to the local policy. The investment cost of PV panels is still expected to decrease substantially in the future [29] and hence the results involving residential PV should be handled with caution. Regarding policy, a net metering scheme ameliorates the decision for the combination of PV and heat pump, making it competitive with a condensing gas boiler. Of course, this scheme presents a challenge for the transmission and distribution grid operators to recover their costs, also given the increased load on their networks[2]. Given an attenuated net metering scheme, the PV system appears to be sized much smaller. The potential for self consumption of heating systems is hence rather limited, as discussed already by Reynders et al. [153].

8.6 Conclusion

This chapter presents a combined design and control optimization framework to investigate the design of different residential heating system options under varying electricity generation mixes. Towards this aim, two concepts were added to the optimization framework, as compared to combined design and control optimization in the literature. The first, the inclusion of temperature levels for exchange of heat, allows for an elegant modeling of the heat exchange between different components and the inclusion of temperature dependent efficiencies, but increases the problem size and hence the calculation time. Also, the main reason to add these temperature levels was to accurately model the potential of the thermal energy storage for space heating, which proved to be an unattractive technology in the studied residential context.

The second concept is the addition of the electricity generation park to the optimization problem. This provides valuable insight in the impact of different heating system selections and influences the heating system design. Throughout the different scenarios, the relative differences between the different heating system selections remained almost the same regarding equivalent annual cost, but widely varied regarding CO_2 emission.

The combined design and control optimization was implemented as a MILP. However, this approach showed unreasonable long calculation times and ended up with rather straightforward heating system selections. This is partly due to the high fixed part of the investment cost in the residential context. Calculating a variety of heating system designs and or selections proved to be a far better

[2]This also forms a challenge for a wide scale integration of heat pumps.

approach than solving the full MILP: it gives a wide overview of the solution space with a calculation time of only two minutes per case.

Regarding the results of the case study, the combination of air coupled heat pump, floor heating and PV panels showed substantial CO_2 emission reductions of up to 2 ton per building per year for an increase in equivalent annual cost below 350 EUR per building, as compared to typical fuel fired heating systems. The CHP coupled to district heating is cost competitive, but the CO_2 emission reduction highly depends on the calculation method. Finally, the solar thermal collector and thermal energy storage for space heating appeared to be very expensive technologies for the limited, and for the latter technology highly uncertain, reduction in CO_2 emissions.

Chapter 9

Conclusion

This section summarizes the conclusions of the work (Section 9.1) along with general commentary on these conclusions (Section 9.2) and provides recommendations for future research (Section 9.3)

9.1 Main conclusions

The main conclusions of this work are summarized as a response to the four research questions posed in the introduction (Section 1.2):

- How should the interaction between residential heat pumps and the electricity generation system be modeled?
- What are the maximum attainable benefits from applying DR to residential heat pumps?
- How could DR with residential heat pumps be realized in practice?
- Will the residential heating system be designed differently in order to benefit from the DR potential?

How should the interaction between residential heat pumps and the electricity generation system be modeled? Chapters 2 and 3 illustrate the bottom up modeling of a large set of residential buildings with heat pumps in an optimal control problem. This bottom up model involves a physical

representation of the thermal dynamics of a building structure, the weather conditions, the occupants' demand for thermal comfort and a physical model of the heating system consisting of a heat pump, heat emissions system and a domestic hot water tank. Chapter 3 presents and verifies a linear representation for the heating system along with an aggregation methodology towards the user behavior. In this way, the entire bottom up model is an optimal control problem with a linear set of equations with a limited number of states, which is applied to identical building parameters in this thesis. Extending the framework to multiple building parameters can be easily implemented but would rapidly increase the calculation time. The difference in DR performance due to different building parameters is discussed in Chapter 5.

This linear optimal control problem of residential buildings with heat pumps is suitable to be combined with a unit commitment and economic dispatch model of the electricity generation system (Chapters 2 and 3). The resulting "integrated model" explicitly integrates the electricity demand and flexibility therein of residential buildings with heat pumps, together with the incentives from the electricity generation system.

Chapter 4 shows that this integrated modeling approach is the correct way of investigating the aforementioned interaction in comparison to typical approaches in the literature. From a supply side perspective, the buildings with heat pumps are typically represented by a price elasticity or by a virtual generator model. Both approaches fail to represent the flexibility of the buildings with heat pumps well since significant erratic variations are found on the most important parameters for these models: the own-elasticity, the cross-elasticity and the demand response ratio. From a demand side perspective, the electricity generation system is typically simplified to an electricity price profile. However, the heat pump controllers overreact to this price profile thereby causing additional demand peaks that increase the cost for the electricity generation system. Even iterating with a price profile is unable to reach the cost savings of the integrated modeling approach. Finally, chapter 4 also investigates the demand side perspective of representing the electricity generation system by a merit order instead of the full unit commitment and economic dispatch model. This simplification of the electricity generation system, when combined with a significant electricity demand from residential buildings with heat pumps, appears to be promising: calculation times decrease more than a factor 10 for a change in total system cost below 3.5 %.

Answer to the research question: In order to correctly model the interaction, both the electricity generation system and the buildings with heat pumps should be modeled simultaneously. To this aim, a fully linear representation of the buildings with heat pumps is possible.

What are the maximum attainable benefits from applying DR to residential heat pumps? The integrated model is applied to two case studies in a Belgian context, exploring the potential benefits of employing DR on heat pumps in residential buildings. In Chapter 5, an electricity generation system with 40 % RES is studied along with multiple heating system configurations and building types. Applying DR is shown to lower the CO_2 emissions relative to the use of a condensing gas boiler with on average 15 % by increasing the electricity demand at times of curtailment. Around half of this increase in electricity demand is directly 'wasted' in higher heat losses of the building structure and domestic hot water tank. The other half replaces electricity demand for the gas fired power plants. Furthermore, the contribution of the heat pumps to the peak in electricity demand is significantly reduced under DR. On average, the application of DR lowers the CO_2 abatement cost with 300 EUR/ton CO_2. Nonetheless, even with DR the heat pump is still an expensive CO_2 abatement technology in Belgium, showing an abatement cost between 100 and 2500 EUR per ton CO_2. Especially the mildly renovated buildings show abominable results. For the thoroughly renovated and new buildings, the difference between the results is mainly dominated by the seasonal performance factor of the heat pump and not by the building characteristics. The air coupled heat pump with floor heating shows the lowest CO_2 abatement cost of all heating system types considered.

Focusing on the thoroughly renovated buildings with air coupled heat pump and floor heating, chapter 6 studies the sensitivity of the market value with respect to market penetration, comfort temperature bounds and RES penetration. Regarding market penetration, it is shown that, the more participants join the DR program, the more the cost savings for the electricity generation system as a whole but the smaller the cost savings per participant. The same trend is identified when allowing a higher upper bound for the indoor temperature or installing a larger DHW tank: there is less need for this flexibility when there are more participants. Finally, the yearly cost savings per participant are up to 150 EUR attributed to operational cost savings and up to 300 EUR assigned to reducing peak electricity demand. However, the exact cost savings are shown to be highly sensitive to market penetration of the DR program and RES share.

For a different set of electricity generation mix scenarios, chapter 7 identifies the same order of magnitude for the cost savings, along with reductions of yearly CO_2 emissions between 0.1 and 1.4 ton per participating building.

Answer to the research question: DR lowers the CO_2 *abatement cost with on average 300 EUR/ton* CO_2*. Per participating household per year, demand response can lower* CO_2 *emissions with up to 1.4 ton and save up to 150 EUR in operational cost savings and 300 EUR in peak demand reduction. These savings per household decrease as more participants join in. Note however that*

these numbers are shown to be very sensitive to the assumptions on both the electricity generation system and the residential heat pumps.

How could DR with residential heat pumps be realized in practice? Chapters 5 to 7 show that performing DR lowers costs for the electricity generation system, but increases the yearly electricity demand of the heat pump by up to 20 %. This poses a challenge when setting up a compensation scheme for the building user. This building user should get a compensation for joining DR that at least outweighs the costs associated with a higher electricity consumption.

The presented integrated model is impractical for real life control, as it would involve the operation of thousands of buildings to be co-optimized with the electricity generation system. Hence, it can serve as an upper bound of the maximum attainable benefits thanks to DR. Chapter 7 investigates three incentives that can be employed to realize these electricity generation cost savings identified by the integrated model. The first incentive, the day ahead price, shows abominable performance: residential buildings with heat pumps overreact on the price signal and in some cases even increase the system costs. The second incentive, the price profile from the integrated model, performs better as it already anticipates the buildings reaction. However, this price profile suffers from low performance as more buildings participate in DR, for which the threshold is identified as 100,000 buildings for the studied boundary conditions. The third incentive called load shaping, based on the electricity consumption profile from the integrated model, proves to be the most robust incentive. Even when a large number of buildings participate in DR, load shaping is still able to attain 80 % of the cost savings predicted by the integrated model.

Answer to the research question: It is shown that the response of residential heat pumps to DR incentives should be anticipated by using an integrated model. A centrally determined load profile outperforms a price profile, but poses challenges in compensating the building user.

Will the residential heating system be designed differently in order to benefit from the DR potential? Chapter 6 identifies the decreasing market incentive per participating building as more participants step in on DR. Chapter 8 elaborates on this and investigates whether the incentives of the electricity generation system are a driver to alter the heating system design on a residential building level. To this aim, the integrated model is complemented with a heating system design model. From the case study, it appears that the storage tank for space heating is an unattractive technology, increasing the total cost for a negligible and uncertain reduction in CO_2 emission. The integration with the

electricity generation system shows little alteration of the residential heating system design, except for a small impact on heat pump sizing. From the considered heating system components, the condensing gas boiler is still the most cost efficient but shows a higher CO_2 emission. The combination of air coupled heat pump with floor heating and rooftop PV is a close competitor with respect to cost but leads to CO_2 emission savings of up to 2 ton per building per year. Finally, CHP with district heating performs well in cost, but the CO_2 emission savings highly depend on the way these savings are calculated.

Answer to the research question: When optimizing towards minimal cost, the residential heating system design is only influenced to a limited extent by the DR possibilities with respect to the electricity generation system.

9.2 Critical reflections

The numerical results presented throughout this work should be handled with care as these should be interpreted within the assumptions taken in the corresponding chapters. Some of these assumptions can severely alter the numerical results.

First, curtailment of RES is considered to come at zero cost, zero CO_2 emission and is solely available for the heat pumps to use. This assumption is one of the main drivers towards the cost and CO_2 emission savings presented in this work. However, a number of alternatives can also avoid this RES curtailment such as export through the transmission grid, batteries, electric vehicles, white good appliances or demand response in the commercial building sector or in industry. This competition could take away the incentives for the heat pumps regarding curtailment.

Second, the limited capacity and energy losses of the electricity transmission and distribution grids are not taken into account in this work. These grid limitations can pose serious thresholds for the presented cost and CO_2 emission savings throughout this work. One limitation is that the coordinated response of heat pumps to increase electricity consumption during moments of RES curtailment, could not be met in practice due to the limited transmission and/or distribution grid capacity. In order to allow the suggested coordinated response of the heat pumps, substantial investment in grid infrastructure could be needed which in turn could hamper the development of DR.

Third, all simulations in this work are deterministic. In other words, no prediction errors are taken into account. These uncertainties can lower the presented savings as certain subtleties, such as avoiding the part-load operation

of a power plant or exactly avoiding the curtailment of RES, may not be attained in practice.

Finally, the bottom-up representation of the residential building stock with heat pumps is still a simplified representation of the real life situation. The number of buildings are scaled up starting from an identical building structure. Furthermore, the presented verification was only performed over a time span of two days for a specific combination of building and heating system parameters.

Hence, the strength of this work does not lie in the numerical values presented but in the methodological contributions and identifications of trends. The main methodological work concerns the aggregation of user behavior, linear representation of residential heating systems, integrated modeling with the electricity generation system and combined heating system design and control optimization. These methodologies are thoroughly explained and demonstrated throughout this work, along with an in-depth evaluation of their practical use.

Furthermore, within the above mentioned assumptions, some clear messages could be distilled from the case studies concerning the order of magnitude of cost and CO_2 emission savings by performing DR with residential heat pumps. These order of magnitudes can be interpreted as upper bounds to what can be possible in practice. Also the identified trends on the impact of RES share, building participation, building parameters and heating system configurations provide valuable insights in the possible value of DR for residential heat pumps.

9.3 Recommendations for future research

The recommendations for future research are split up in two parts. First, several ways of improving the impact assessment of DR with residential heat pumps are discussed. The second part discusses the pathway towards a practical implementation.

Improving the impact assessment of DR with residential heat pumps This work is built on a number of simplifications which are commented upon in the previous section. A way of improving the presented work is to explicitly model the disregarded aspects into the integrated model.

This model can be expanded by taking the electricity transmission and hence import and export into account. This requires the modeling of building stocks in different regions and hence needs an extensive data base, since different countries possess numerous differences in building habits, climate and electricity

generation mixes. Hence, the potential for applying DR on heat pumps, or air conditioning in hotter climates, can vary widely and should be studied case by case. The presence of electricity transmission can lower the incentives for DR.

Also the limitations of the distribution grid can be included, as a limit to the coordinated demand peak of heat pumps participating in DR. In this sense, a trade off can appear between investing in distribution grid infrastructure and operational cost savings for the electricity generation system.

Likewise, competing technologies for providing flexibility can be included in the integrated model. This does require the operational aspects of these technologies to allow integration in a MILP optimization.

Furthermore, this thesis focuses on tackling the variability of RES, while another major challenge is the hard predictability of RES. DR for buildings with heat pumps can be employed to counterbalance prediction errors of RES. This requires techniques from robust optimization and stochastic MPC.

The bottom up representation of the building stock with heat pumps is also open for improvement. A manageable representation of the variety in building properties and heating system configurations is still to be developed. Furthermore, the impact of DR on the COP of the heat pump should be represented more accurately in the integrated model. A convex approach employing a piecewise linear function can be appropriate in this context. Also the dynamic inputs to the bottom up model, being the weather and occupancy behavior, are prone to prediction errors. These prediction errors show correlations with the prediction errors on RES, which can complicate the assessment. Finally, other building types such as commercial buildings and apartment blocks could be promising candidates for DR.

Pathway to practical implementation As shown in chapter 7, the integrated model can be employed to determine a day-ahead scheduling of the electricity demand by a large set of heat pumps. There are still obstacles towards a real life implementation of this load shaping scheme. First, some of the aforementioned methodological obstacles should be removed: the variety in building and heat pump characteristics should be properly and efficiently represented. Also, the robustness towards prediction errors of RES and climate should be improved. The second step is to adapt heating system controllers to be able to follow the centrally determined incentive. Third, a demonstration project should be set up to show whether the whole set of buildings with heat pumps behave as expected. Finally, a monetary compensation scheme should be developed to reward the participants.

Bibliography

[1] Albadi, M. H., and El-Saadany, E. A summary of demand response in electricity markets. *Electric power systems research 78*, 11 (2008), 1989–1996.

[2] Ali, M., Jokisalo, J., Siren, K., and Lehtonen, M. Combining the demand response of direct electric space heating and partial thermal storage using LP optimization. *Electric Power Systems Research 106* (2014), 160–167.

[3] Allegrini, J., Orehounig, K., Mavromatidis, G., Ruesch, F., Dorer, V., and Evins, R. A review of modelling approaches and tools for the simulation of district-scale energy systems. *Renewable and Sustainable Energy Reviews 52* (2015), 1391–1404.

[4] Anandarajah, G., and Gambhir, A. India's CO_2 emission pathways to 2050: What role can renewables play? *Applied Energy 131* (2014), 79–86.

[5] Arrow, K., Cropper, M., Gollier, C., Groom, B., Heal, G., Newell, R., Nordhaus, W., Pindyck, R., Pizer, W., Portney, P., et al. Determining benefits and costs for future generations. *Science 341*, 6144 (2013), 349–350.

[6] Arteconi, A., Hewitt, N., and Polonara, F. State of the art of thermal storage for demand-side management. *Applied Energy 93* (2012), 371–389.

[7] Arteconi, A., Patteeuw, D., Bruninx, K., Delarue, E., D'haeseleer, W., and Helsen, L. Active demand response with electric heating systems: impact of market penetration. *Applied Energy 177* (2016), 636–648.

[8] Ashouri, A., Fux, S. S., Benz, M. J., and Guzzella, L. Optimal design and operation of building services using mixed-integer linear programming techniques. *Energy 59* (2013), 365–376.

[9] Attia, S., Hamdy, M., O'Brien, W., and Carlucci, S. Assessing gaps and needs for integrating building performance optimization tools in net zero energy buildings design. *Energy and Buildings 60* (2013), 110–124.

[10] Babiak, J., Olesen, B. W., and Petras, D. *Low temperature heating and high temperature cooling.* REHVA, 2009.

[11] Baeten, B., Rogiers, F., Patteeuw, D., and Helsen, L. Comparison of optimal control formulations for stratified sensible thermal energy storage in space heating applications. In *The 13th International Conference on Energy Storage.* (Beijing, China, May 2015).

[12] Baetens, R., De Coninck, R., Jorissen, F., Picard, D., Helsen, L., and Saelens, D. OpenIDEAS-an open framework for integrated district energy. In *Proceedings of Building Simulation 2015* (2015).

[13] Baetens, R., De Coninck, R., Van Roy, J., Verbruggen, B., Driesen, J., Helsen, L., and Saelens, D. Assessing electrical bottlenecks at feeder level for residential net zero-energy buildings by integrated system simulation. *Applied Energy 96* (2012), 74–83.

[14] Baetens, R., and Saelens, D. Modelling uncertainty in district energy simulations by stochastic residential occupant behaviour. *Journal of Building Performance Simulation* (2015), 1–17.

[15] Barton, J., Huang, S., Infield, D., Leach, M., Ogunkunle, D., Torriti, J., and Thomson, M. The evolution of electricity demand and the role for demand side participation, in buildings and transport. *Energy Policy 52* (Jan. 2013), 85–102.

[16] Bayer, P., Saner, D., Bolay, S., Rybach, L., and Blum, P. Greenhouse gas emission savings of ground source heat pump systems in europe: A review. *Renewable and Sustainable Energy Reviews 16*, 2 (2012), 1256–1267.

[17] Bernard, J. T., Bolduc, D., and Belanger, D. Quebec residential electricity demand: a microeconometric approach. *Canadian Journal of Economics 29*, 1 (Feb. 1996), 92–113.

[18] Bettgenhäuser, K., Offermann, M., Boermans, T., Bosquet, M., Grözinger, J., von Manteuffel, B., and Surmeli, N. Heat pump implementation scenarios until 2030. Tech. rep., Ecofys, 2013.

[19] Bettgenhäuser, K., Offermann, M., Boermans, T., Bosquet, M., Grözinger, J., von Manteuffel, B., and Surmeli, N. Heat pump implementation scenarios until 2030, appendix. Tech. rep., Ecofys, 2013.

[20] Bettle, R., Pout, C., and Hitchin, E. Interactions between electricity-saving measures and carbon emissions from power generation in England and Wales. *Energy Policy 34*, 18 (2006), 3434–3446.

[21] Birol, F. World energy outlook 2015. Tech. rep., International energy agency, 2015.

[22] Blarke, M. B. Towards an intermittency-friendly energy system: Comparing electric boilers and heat pumps in distributed cogeneration. *Applied Energy 91*, 1 (2012), 349–365.

[23] Bompard, E., and Carpaneto, E. The role of load demand elasticity in congestion management and pricing. *Power Engineering Society Summer Meeting, 2000, IEEE 4* (2000), 2229–2234.

[24] Börjesson, M., and Ahlgren, E. O. Biomass gasification in cost-optimized district heating systems-a regional modelling analysis. *Energy Policy 38*, 1 (2010), 168–180.

[25] Bruninx, K. *Improved modeling of unit commitment decisions under uncertainty*. PhD thesis, KU Leuven, 2016.

[26] Bruninx, K., Delarue, E., and D'haeseleer, W. The cost of wind power forecast errors in the belgian power system. In *2nd BAEE Research Workshop,(Leuven, Belgium)* (2013), pp. 1–20.

[27] Bruninx, K., Patteeuw, D., Delarue, E., Helsen, L., and D'haeseleer, W. Short-term demand response of flexible electric heating systems: the need for integrated simulations. In *European Energy Market (EEM), 2013 10th International Conference on the* (2013), IEEE, pp. 1–10.

[28] Callaway, D. S. Tapping the energy storage potential in electric loads to deliver load following and regulation, with application to wind energy. *Energy Conversion and Management 50*, 5 (May 2009), 1389–1400.

[29] Candelise, C., Winskel, M., and Gross, R. J. The dynamics of solar PV costs and prices as a challenge for technology forecasting. *Renewable and Sustainable Energy Reviews 26* (2013), 96–107.

[30] Carlucci, S., Cattarin, G., Causano, F., and Pagliano, L. Multi-objective optimization of a nearly zero-energy building based on thermal

and visual discomfort minimization using a non-dominated sorting genetic algorithm (NSGA-II). *Energy and Buildings 104* (2015), 378–394.

[31] Che, D., Liu, Y., and Gao, C. Evaluation of retrofitting a conventional natural gas fired boiler into a condensing boiler. *Energy Conversion and Management 45*, 20 (2004), 3251–3266.

[32] Clement, K., Haesen, E., and Driesen, J. Coordinated charging of multiple plug-in hybrid electric vehicles in residential distribution grids. In *Power Systems Conference and Exposition, 2009. PSCE'09. IEEE/PES* (2009), IEEE, pp. 1–7.

[33] Clement-Nyns, K., Haesen, E., and Driesen, J. The impact of charging plug-in hybrid electric vehicles on a residential distribution grid. *IEEE Transactions on Power Systems 25*, 1 (2010), 371–380.

[34] Congradac, V., and Kulic, F. HVAC system optimization with CO_2 concentration control using genetic algorithms. *Energy and Buildings 41*, 5 (2009), 571–577.

[35] Corbin, C. D. *Assessing Impact of Large-Scale Distributed Residential HVAC Control Optimization on Electricity Grid Operation and Renewable Energy Integration.* PhD thesis, University of Colorado, CO, U.S.A., 2014.

[36] Corbin, C. D., and Henze, G. P. Residential HVAC as a supply following resource part I: Simulation framework and model development. *Submitted to Journal of Building Performance Simulation* (2016).

[37] Corbin, C. D., and Henze, G. P. Residential HVAC as a supply following resource part II: Simulation studies and results. *Submitted to Journal of Building Performance Simulation* (2016).

[38] Cyx, W., Renders, N., Van Holm, M., and Verbeke, S. IEE TABULA typology approach for building stock energy assessment. Tech. rep., VITO, Vlaamse instelling voor technologisch onderzoek, 2011.

[39] Dallinger, D., and Wietschel, M. Grid integration of intermittent renewable energy sources using price-responsive plug-in electric vehicles. *Renewable and Sustainable Energy Reviews 16*, 5 (2012), 3370–3382.

[40] De Coninck, R., Baetens, R., Saelens, D., Woyte, A., and Helsen, L. Rule-based demand-side management of domestic hot water production with heat pumps in zero energy neighbourhoods. *Journal of Building Performance Simulation 7*, 4 (July 2014), 271–288.

[41] De Jonghe, C. *Short-term demand response in electricity generation planning and scheduling.* PhD thesis, KU Leuven, 2011.

[42] De Jonghe, C., Hobbs, B. F., and Belmans, R. Optimal Generation Mix With Short-Term Demand Response and Wind Penetration. *IEEE Transactions on Power Systems 27*, 2 (May 2012), 830–839.

[43] Delarue, E. *Modeling electricity generation systems generation optimization and simulation models.* PhD thesis, KU Leuven, 2009.

[44] Delarue, E., and den Bergh, K. V. Carbon mitigation in the electric power sector under cap-and-trade and renewables policies. *Energy Policy 92* (2016), 34 – 44.

[45] Delarue, E., Ellerman, A. D., and D'haeseleer, W. Robust MACCs? The topography of abatement by fuel switching in the European power sector. *Energy 35*, 3 (2010), 1465–1475.

[46] Devogelaer, D., Duerinck, J., Gusbin, D., Marenne, Y., Nijs, W., Orsini, M., and Pairon, M. Towards 100% renewable energy in Belgium by 2050. *VITO, Mol (2013, April)* (2012).

[47] Dietrich, K., Latorre, J. M., Olmos, L., and Ramos, A. Demand response in an isolated system with high wind integration. *IEEE Transactions on Power Systems 27*, 1 (Feb. 2012), 20–29.

[48] Dorer, V., and Weber, A. Energy and CO_2 emissions performance assessment of residential micro-cogeneration systems with dynamic whole-building simulation programs. *Energy Conversion and Management 50*, 3 (2009), 648–657.

[49] Dorer, V., Weber, R., and Weber, A. Performance assessment of fuel cell micro-cogeneration systems for residential buildings. *Energy and Buildings 37*, 11 (2005), 1132–1146.

[50] Dupont, B. *Residential Demand Response Based on Dynamic Electricity Pricing: Theory and Practice.* PhD thesis, KU Leuven, Belgium, 2015.

[51] Dupont, B., De Jonghe, C., Olmos, L., and Belmans, R. Demand response with locational dynamic pricing to support the integration of renewables. *Energy Policy 67* (2014), 344–354.

[52] Dupont, B., Dietrich, K., De Jonghe, C., Ramos, A., and Belmans, R. Impact of residential demand response on power system operation: A Belgian case study. *Applied Energy 122* (2014), 1–10.

[53] Dussault, J.-M., Sourbron, M., and Gosselin, L. Reduced energy consumption and enhanced comfort with smart windows: comparison between quasi-optimal, predictive and rule-based control strategies. *Energy and Buildings 127* (2016), 680–691.

[54] ELIA. Grid data, 2013.

[55] ENERGY REGULATOR OF THE ENERGY MARKET, F. Compensation for overproduction electricity? (in Dutch: Vergoeding overtollige elektriciteit?). Tech. rep., VREG, 2016.

[56] ENTSO-E. Internal document, 2013.

[57] ENTSO-E. Ten-Year Network Development Plan 2014 – Maps and Data, 2015. Tech. rep., 2015.

[58] EURELECTRIC. Analysis of european power price increase drivers. Tech. rep., Eurelectric, 2014.

[59] EUROPEAN COMMISSION. A roadmap for moving to a competitive low carbon economy in 2050, 2011.

[60] EUROPEAN COMMISSION. Commission staff working document: Energy prices and costs report. Tech. rep., European Commission, 2014.

[61] EUROPEAN COMMISSION. A policy framework for climate and energy in the period from 2020 to 2030. Tech. rep., European Commission, 2014.

[62] EUROPEAN COMMISSION. Quarterly report on European gas markets. Tech. rep., European Commission, 2014.

[63] EUROPEAN PARLIAMENT. Directive 2010/31/EU of the European parliament and of the council of 19 May 2010 on the energy performance of buildings, 2010.

[64] EVINS, R. Multi-level optimization of building design, energy system sizing and operation. *Energy 90* (2015), 1775–1789.

[65] FARHANGI, H. The path of the smart grid. *Power and energy magazine, IEEE 8*, 1 (2010), 18–28.

[66] FAZLOLLAHI, S., BECKER, G., ASHOURI, A., AND MARÉCHAL, F. Multi-objective, multi-period optimization of district energy systems: IV–A case study. *Energy 84* (2015), 365–381.

[67] FERNANDEZ, L. P., ROMÁN, T. G. S., COSSENT, R., DOMINGO, C. M., AND FRIAS, P. Assessment of the impact of plug-in electric vehicles on distribution networks. *Power Systems, IEEE Transactions on 26*, 1 (2011), 206–213.

[68] FERRIS, M. C., JAIN, R., AND DIRKSE, S. GDXMRW : Interfacing GAMS and MATLAB, 2011.

[69] Filippini, M. Short- and long-run time-of-use price elasticities in Swiss residential electricity demand. *Energy Policy 39*, 10 (Oct. 2011), 5811–5817.

[70] FPS Economy Belgium. Structure of the population according to households: per year, region and number of children. Online: `http://statbel.fgov.be/nl/statistieken/cijfers/bevolking/structuur/huishoudens/`.

[71] Gellings, C. The concept of demand-side management for electric utilities. *Proceedings of the IEEE 73*, 10 (1985), 1468–1470.

[72] Gendebien, S., Georges, E., Bertagnolio, S., and Lemort, V. Methodology to characterize a residential building stock using a bottom-up approach: a case study applied to Belgium. *International Journal of Sustainable Energy Planning and Management 4* (2015), 71–88.

[73] Goddard, G., Klose, J., and Backhaus, S. Model development and identification for fast demand response in commercial hvac systems. *IEEE Transactions on Smart Grid 5*, 4 (2014), 2084–2092.

[74] Goh, C. S., Junginger, M., Cocchi, M., Marchal, D., Thrän, D., Hennig, C., Heinimö, J., Nikolaisen, L., Schouwenberg, P.-P., Bradley, D., et al. Wood pellet market and trade: a global perspective. *Biofuels, Bioproducts and Biorefining 7*, 1 (2013), 24–42.

[75] Gómez, D., Watterson, J., Americano, B., Ha, C., Marland, G., Matsika, E., Namayanga, L., Osman-Elasha, B., Kalenga Saka, J., and Treanton, K. Guidelines for national greenhouse gas inventories. Tech. rep., IPCC, 2006.

[76] Good, N., Navarro-espinosa, A., Mancarella, P., and Karangelos, E. Participation of electric heat pump resources in electricity markets under uncertainty. In *10th International Conference on the European Energy Market (EEM)* (2013).

[77] Govaerts, L., Pelkmans, L., Dooms, G., Hamelinck, C., Geurds, M., De Vlieger, I., Schrooten, L., Ooms, K., and Timmermans, V. Potentieelstudie biobrandstoffen in vlaanderen. *Studie uitgevoerd in opdracht van ANRE en ALT* (2006).

[78] Grand View Research. Smart thermostat market analysis by technology (Wi-Fi, ZigBee) and segment forecasts to 2022. Tech. rep., Sept. 2015.

[79] Hawkes, A. Long-run marginal CO_2 emissions factors in national electricity systems. *Applied Energy 125* (2014), 197–205.

[80] Hedegaard, K., and Balyk, O. Energy system investment model incorporating heat pumps with thermal storage in buildings and buffer tanks. *Energy 63* (2013), 356–365.

[81] Hedegaard, K., Mathiesen, B. V., Lund, H., and Heiselberg, P. Wind power integration using individual heat pumps - analysis of different heat storage options. *Energy 47*, 1 (Nov. 2012), 284–293.

[82] Hedegaard, K., and Münster, M. Influence of individual heat pumps on wind power integration–energy system investments and operation. *Energy Conversion and Management 75* (2013), 673–684.

[83] Henze, G. P., Felsmann, C., and Knabe, G. Evaluation of optimal control for active and passive building thermal storage. *International Journal of Thermal Sciences 43*, 2 (Feb. 2004), 173–183.

[84] Hewitt, N. J. Heat pumps and energy storage–The challenges of implementation. *Applied Energy 89*, 1 (2012), 37–44.

[85] Heylen, E., Jordens, R., Patteeuw, D., and Helsen, L. The potential of air-water heat pumps in a Belgian residential retrofit context in relation to future electricity prices. In *9th International Conference on System Simulation in Buildings* (Liège, Belgium, Dec. 2014), pp. 694–712.

[86] International Energy Agency, and OECD Nuclear Energy Agency. *Projected Costs of Generating Electricity, 2010 Edition.* Projected Costs of Generating Electricity. 2010.

[87] International Energy Agency, and OECD Nuclear Energy Agency. *Projected Costs of Generating Electricity.* Projected Costs of Generating Electricity. 2015.

[88] Jiang, T., Cao, Y., Yu, L., and Wang, Z. Load shaping strategy based on energy storage and dynamic pricing in smart grid. *Smart Grid, IEEE Transactions on 5*, 6 (2014), 2868–2876.

[89] Joelsson, A. *Primary energy efficiency and* CO_2 *mitigation in residential buildings.* PhD thesis, Mid Sweden University, 2008.

[90] Johnston, D., Lowe, R., and Bell, M. An exploration of the technical feasibility of achieving CO_2 emission reductions in excess of 60% within the UK housing stock by the year 2050. *Energy Policy 33*, 13 (2005), 1643–1659.

[91] Judkoff, R., and Neymark, J. International energy agency building energy simulation test (BESTEST) and diagnostic method. Tech. rep., National Renewable Energy Lab., Golden, CO (US), 1995.

[92] Kamgarpour, M., Ellen, C., Esmaeil, S., Soudjani, Z., Gerwinn, S., Mathieu, J. L., Nils, M., Abate, A., Callaway, D. S., and Fr, M. Modeling Options for Demand Side Participation of Thermostatically Controlled Loads. In *IREP Symposium-Bulk Power System Dynamics and Control -IX (IREP)* (August 25-30, 2013, Rethymnon, Greece, 2013), pp. 1–15.

[93] Karangelos, E., and Bouffard, F. Towards Full Integration of Demand-Side Resources in Joint Forward Energy/Reserve Electricity Markets. *IEEE Transactions on Power Systems 27*, 1 (Feb. 2012), 280–289.

[94] Kelly, N. J., Tuohy, P. G., and Hawkes, A. D. Performance assessment of tariff-based air source heat pump load shifting in a UK detached dwelling featuring phase change-enhanced buffering. *Applied Thermal Engineering* (2013).

[95] Kersting, W. H. *Distribution system modeling and analysis*. CRC press, 2012.

[96] Kesicki, F. Marginal abatement cost curves for policy making - expert-based vs. model - derived curves. In *IAEE International Conference* (Rio de Janeiro, Brazil, June 2010).

[97] Kesicki, F. Costs and potentials of reducing CO_2 emissions in the UK domestic stock from a systems perspective. *Energy and Buildings 51* (2012), 203–211.

[98] Kirschen, D. S., and Strbac, G. Factoring the elasticity of demand in electricity prices. *IEEE Transactions on Power Systems 15*, 2 (May 2000), 612–617.

[99] Kiss, B., Neij, L., and Jakob, M. Heat pumps: A comparative assessment of innovation and diffusion policies in sweden and switzerland, 2012.

[100] Koch, T., Achterberg, T., Andersen, E., Bastert, O., Berthold, T., Bixby, R. E., Danna, E., Gamrath, G., Gleixner, A. M., Heinz, S., Lodi, A., Mittelmann, H., Ralphs, T., Salvagnin, D., Steffy, D., and Wolter, K. Miplib 2010. *Mathematical Programming Computation 3*, 2 (2011), 103–163.

[101] Kondoh, J., Lu, N., Member, S., and Hammerstrom, D. J. An evaluation of the water heater load potential for providing regulation service. In *Power and Energy Society General Meeting* (2011).

[102] Kosek, A. M., Costanzo, G. T., Bindner, H. W., and Gehrke, O. An overview of demand side management control schemes for buildings in smart grids. In *Smart Energy Grid Engineering (SEGE), 2013 IEEE International Conference on* (2013), IEEE, pp. 1–9.

[103] Kyte, B. Roadmap for a low-carbon power sector by 2050. Tech. rep., EEI, ESAA, EURELECTRIC, CEA, FEPC and EPRI, 2009.

[104] Liao, Z., Swainson, M., and Dexter, A. L. On the control of heating systems in the UK. *Building and Environment 40* (2005), 343–351.

[105] Lin, Y., Barooah, P., Meyn, S., and Middelkoop, T. Experimental evaluation of frequency regulation from commercial building HVAC systems. *IEEE Transactions on Smart Grid 6*, 2 (2015), 776–783.

[106] Long, H., Xu, R., and He, J. Incorporating the Variability of Wind Power with Electric Heat Pumps. *Energies 4*, 10 (Oct. 2011), 1748–1762.

[107] Loulou, R., and Labriet, M. ETSAP-TIAM: the TIMES integrated assessment model Part I: Model structure. *Computational Management Science 5*, 1-2 (2008), 7–40.

[108] Lu, J., Sookoor, T., Srinivasan, V., Gao, G., Holben, B., Stankovic, J., Field, E., and Whitehouse, K. The smart thermostat: using occupancy sensors to save energy in homes. In *Proceedings of the 8th ACM Conference on Embedded Networked Sensor Systems* (2010), ACM, pp. 211–224.

[109] Lu, N., and Chassin, D. P. A state-queueing model of thermostatically controlled appliances. *Power Systems, IEEE Transactions on 19*, 3 (2004), 1666–1673.

[110] Lu, N., and Vanouni, M. Passive energy storage using distributed electric loads with thermal storage. *Journal of Modern Power Systems and Clean Energy* (Nov. 2013).

[111] Luickx, P., Peeters, L., Helsen, L., and D'haeseleer, W. Influence of massive heat-pump introduction on the electricity-generation mix and the GHG effect, Belgian case study. *International Journal of Energy Research 32*, 1 (2008), 57–67.

[112] Malhame, R. Electric load model synthesis by diffusion approximation of a high-order hybrid-state stochastic system. *IEEE Transactions on Automatic Control 30*, 9 (Sept. 1985), 854–860.

[113] Marwan, M., Ledwich, G., and Ghosh, A. Demand-side response model to avoid spike of electricity price. *Journal of Process Control 24*, 6 (2014), 782 – 789.

[114] Mathiesen, B. V., Lund, H., Connolly, D., Wenzel, H., Østergaard, P., Möller, B., Nielsen, S., Ridjan, I., Karnøe, P., Sperling, K., et al. Smart Energy Systems for coherent 100% renewable energy and transport solutions. *Applied Energy 145* (2015), 139–154.

[115] Mathieu, J., Dyson, M., Callaway, D., and Rosenfeld, A. Using residential electric loads for fast demand response: The potential resource and revenues, the costs, and policy recommendations. In *Proceedings of the ACEEE Summer Study on Buildings* (Pacific Grove, CA, 2012), pp. 189–203.

[116] Mathieu, J. L., Dyson, M. E., and Callaway, D. S. Resource and revenue potential of california residential load participation in ancillary services. *Energy Policy 80* (2015), 76 – 87.

[117] Matsuoka, Y. Our first rush hour rewards results. Online: https://nest.com/blog/2013/07/18/our-first-rush-hour-rewards-results/, July 2013.

[118] Meibom, P., Kiviluoma, J., Barth, R., Brand, H., Weber, C., and Larsen, H. V. Value of electric heat boilers and heat pumps for wind power integration. *Wind Energy 10*, 4 (July 2007), 321–337.

[119] Meteotest. Meteonorm version 6.1 edition 2009. Tech. rep., Meteotest, 2009.

[120] Missaoui, R., Joumaa, H., Ploix, S., and Bacha, S. Managing energy smart homes according to energy prices: Analysis of a building energy management system. *Energy and Buildings 71* (2014), 155–167.

[121] Muratori, M., Roberts, M. C., Sioshansi, R., Marano, V., and Rizzoni, G. A highly resolved modeling technique to simulate residential power demand. *Applied Energy 107* (July 2013), 465–473.

[122] Nordhaus, W. D. To slow or not to slow: the economics of the greenhouse effect. *The economic journal* (1991), 920–937.

[123] Oldewurtel, F., Parisio, A., Jones, C. N., Gyalistras, D., Gwerder, M., Stauch, V., Lehmann, B., and Morari, M. Use of model predictive control and weather forecasts for energy efficient building climate control. *Energy and Buildings 45* (2012), 15–27.

[124] Oldewurtel, F., Ulbig, A., Parisio, A., Andersson, G., and Morari, M. Reducing peak electricity demand in building climate control using real-time pricing and model predictive control. In *Decision and Control (CDC), 49th IEEE Conference on*, pp. 1927–1932.

[125] Olivier, L., Paul, N., and Christophe, R. Central heating, which brands are most succesful? (in Dutch: Centrale verwarming, welke merken slaan het meest aan?). Tech. rep., Test-aankoop, 2010.

[126] Orehounig, K., Evins, R., and Dorer, V. Integration of decentralized energy systems in neighbourhoods using the energy hub approach. *Applied Energy 154* (2015), 277–289.

[127] Organisatie duurzame energie. *Code van goede praktijk voor de toepassing van warmtepompsystemen in de woningbouw*, 2004.

[128] Pachauri, R., Allen, M., Barros, V., Broome, J., Cramer, W., Christ, R., Church, J., Clarke, L., Dahe, Q., Dasgupta, P., et al. IPCC, 2014: Climate change 2014: Synthesis report. contribution of working groups i. *II and III to the Fifth Assessment Report of the Intergovernmental Panel on Climate Change, edited by R. Pachauri and L. Meyer (IPCC, Geneva, Switzerland)* (2014).

[129] Palensky, P., and Dietrich, D. Demand side management: Demand response, intelligent energy systems, and smart loads. *Industrial Informatics, IEEE Transactions on 7*, 3 (2011), 381–388.

[130] Papadaskalopoulos, D., Strbac, G., Mancarella, P., Aunedi, M., and Stanojevic, V. Decentralized participation of flexible demand in electricity markets—part II: Application with electric vehicles and heat pump systems. *IEEE Transactions on Power Systems 28*, 4 (2013), 3667–3674.

[131] Papaefthymiou, G., Hasche, B., and Nabe, C. Potential of heat pumps for demand side management and wind power integration in the german electricity market. *Sustainable Energy, IEEE Transactions on 3*, 4 (Oct 2012), 636–642.

[132] Parkinson, S., Wang, D., Crawford, C., and Djilali, N. Comfort-Constrained Distributed Heat Pump Management. *Energy Procedia 12* (Jan. 2011), 849–855.

[133] Parkinson, S., Wang, D., Crawford, C., and Djilali, N. Wind integration in self-regulating electric load distributions. *Energy Systems 3*, 4 (jul 2012), 341–377.

[134] Parkinson, S., Wang, D., and Djilali, N. Toward energy systems: The convergence of wind power, demand response, and the electricity grid. *Innovative Smart Grid Technologies - Asia (ISGT Asia), 2012 IEEE* (May 2012), 1–8.

[135] Patteeuw, D., Bruninx, K., Arteconi, A., Delarue, E., D'haeseleer, W., and Helsen, L. Integrated modeling of active demand response with electric heating systems coupled to thermal energy storage systems. *Applied Energy 151* (2015), 306–319.

[136] Patteeuw, D., Bruninx, K., Delarue, E., Helsen, L., and D'haeseleer, W. Short-term demand response of flexible electric heating systems : an integrated model. KU Leuven Energy Institute Working Paper WP2014-28, 2014.

[137] Patteeuw, D., Henze, G. P., and Helsen, L. Comparison of load shifting incentives for low-energy buildings with heat pumps to attain grid flexibility benefits. *Applied Energy 167* (2016), 80–92.

[138] Patteeuw, D., Reynders, G., Bruninx, K., Protopapadaki, C., Delarue, E., D'haeseleer, W., Saelens, D., and Helsen, L. CO_2 -abatement cost of residential heat pumps with active demand response: demand- and supply-side effects. *Applied Energy 156* (2015), 490 – 501.

[139] Pedersen, T. S., Andersen, P., Nielsen, K. M., Stæ rmose, H. L., and Pedersen, P. D. Using heat pump energy storages in the power grid. In *IEEE International Conference on Control Applications (CCA)* (Sept. 2011), pp. 1106–1111.

[140] Peeters, L., Dear, R. d., Hensen, J., and D'haeseleer, W. Thermal comfort in residential buildings: comfort values and scales for building energy simulation. *Applied Energy 86*, 5 (2009), 772–780.

[141] Peeters, L., Van der Veken, J., Hens, H., Helsen, L., and D'haeseleer, W. Control of heating systems in residential buildings: Current practice. *Energy and Buildings 40*, 8 (Jan. 2008), 1446–1455.

[142] Pensini, A., Rasmussen, C. N., and Kempton, W. Economic analysis of using excess renewable electricity to displace heating fuels. *Applied Energy 131* (2014), 530–543.

[143] Peuser, F., Remmers, K.-H., and Schnauss, M. *Solar thermal systems, succesful planning and construction.* Beuth Verlag GmbH, Berlin, Germany, 2010.

[144] Picard, D., Sourbron, M., Jorissen, F., Vana, Z., Cigler, J., Ferkl, L., and Helsen, L. Comparison of model predictive control performance using grey-box and white-box controller models of a multi-zone office building. In *International High Performance Buildings Conference.* (West Lafayette, US, July 2016).

[145] Poncelet, K., Höschle, H., Delarue, E., and D'haeseleer, W. Selecting representative days for investment planning models. *Submitted to IEEE Transactions on Power Systems* (2016).

[146] Protopapadaki, C., Baetens, R., and Saelens, D. Exploring the impact of heat pump-based dwelling design on the low-voltage distribution grid. In *Proceedings of BS2015: 14th Conference of International Building Performance Simulation Association* (Hyderabad, India, Dec. 2015), pp. 2530–2537.

[147] Protopapadaki, C., Reynders, G., and Saelens, D. Bottom-up modelling of the Belgian residential building stock: impact of building stock descriptions. In *International Conference on System Simulation in Buildings Edition 9* (Liège, Belgium, Dec. 2014), pp. 652–672.

[148] Pruitt, K. A., Braun, R. J., and Newman, A. M. Evaluating shortfalls in mixed-integer programming approaches for the optimal design and dispatch of distributed generation systems. *Applied Energy 102* (2013), 386–398.

[149] Qureshi, W. A., Nair, N.-K. C., and Farid, M. M. Impact of energy storage in buildings on electricity demand side management. *Energy Conversion and Management 52*, 5 (2011), 2110 – 2120.

[150] Ravn, H., Munksgaard, J., Ramskov, J., Grohnheit, P., and Larsen, H. Balmorel: A model for analyses of the electricity and CHP markets in the baltic sea region. Appendices. Tech. rep., Elkraft System, Ballerup (Denmark), 2001.

[151] Reynders, G., Diriken, J., and Saelens, D. Bottom-up modelling of the Belgian residential building stock: influence of model complexity. In *International Conference on System Simulation in Buildings Edition 9* (Liège, Belgium, Dec. 2014), pp. 574–592.

[152] Reynders, G., Diriken, J., and Saelens, D. Quality of grey-box models and identified parameters as function of the accuracy of input and observation signals. *Energy and Buildings 82* (2014), 263–274.

[153] Reynders, G., Nuytten, T., and Saelens, D. Potential of structural thermal mass for demand-side management in dwellings. *Building and Environment 64* (2013), 187–199.

[154] Richardson, I., Thomson, M., and Infield, D. A high-resolution domestic building occupancy model for energy demand simulations. *Energy and Buildings 40*, 8 (2008), 1560–1566.

[155] Riveros, J. V. Z. *Facilitating the integration of renewable energy through combined-heat-and-power flexibility.* PhD thesis, KU Leuven, Belgium, 2015.

[156] Schicktanz, M., Wapler, J., and Henning, H.-M. Primary energy and economic analysis of combined heating, cooling and power systems. *Energy 36*, 1 (2011), 575–585.

[157] Schröder, A., Kunz, F., Meiss, J., Mendelevitch, R., and Von Hirschhausen, C. Current and prospective costs of electricity generation until 2050. *DIW Data Documentation 68* (2013).

[158] Sioshansi, R., and Short, W. Evaluating the impacts of real-time pricing on the usage of wind generation. *IEEE Transactions on Power Systems* (May 2009), 1–14.

[159] Širokỳ, J., Oldewurtel, F., Cigler, J., and Prívara, S. Experimental analysis of model predictive control for an energy efficient building heating system. *Applied Energy 88*, 9 (2011), 3079–3087.

[160] Smart Geotherm. Geothermische screeningstool, 2013.

[161] Smeds, J., and Wall, M. Enhanced energy conservation in houses through high performance design. *Energy and Buildings 39*, 3 (2007), 273–278.

[162] Spitler, J. D. Editorial: Building performance simulation: The now and the not yet. *HVAC&R Research 12*, S1 (2006), 711–713.

[163] Stadler, M., Kloess, M., Groissböck, M., Cardoso, G., Sharma, R., Bozchalui, M. C., and Marnay, C. Electric storage in California's commercial buildings. *Applied Energy 104* (2013), 711–722.

[164] Strbac, G. Demand side management: Benefits and challenges. *Energy policy 36*, 12 (2008), 4419–4426.

[165] Su, C. L. *Optimal Demand-Side Participation in Day-Ahead Electricity Markets.* PhD thesis, University of Manchester, 2007.

[166] Tan, Y., and Kirschen, D. Co-optimization of Energy and Reserve in Electricity Markets with Demand-side Participation in Reserve Services. *2006 IEEE PES Power Systems Conference and Exposition* (Oct. 2006), 1182–1189.

[167] Tröster, E., Kuwahata, R., and Ackermann, T. European grid study 2030/2050. *Brussels/Langen, Study Commissioned by Greenpeace International* (2011).

[168] United Nations FCCC. Conference of the parties twenty-first session. Paris, 30 November to 11 December 2015, 2015.

[169] Van den Bergh, K., Bruninx, K., Delarue, E., and D'haeseleer, W. LYSUM: a mixed-integer linear formulation of the unit commitment problem. KU Leuven Energy Institute Working papers EN2014-07 (2014) Online: `http://www.mech.kuleuven.be/en/tme/research/energy_environment/Pdf/wpen2014-07.pdf`.

[170] Van den Bergh, K., and Delarue, E. Quantifying CO_2 abatement costs in the power sector. *Energy Policy 80* (2015), 88 – 97.

[171] van der Hoeven, M. World energy outlook 2014. Tech. rep., IEA, 2014.

[172] Van der Veken, J., Creylman, J., and Lenaerts, T. Studie naar kostenoptimale niveaus van de minimumeisen inzake energieprestaties van nieuwe residentiële gebouwen. Tech. rep., Knowledge center Energy, Thomas More Kempen / KU Leuven, 2013.

[173] Vandewalle, J., and D'haeseleer, W. The impact of small scale cogeneration on the gas demand at distribution level. *Energy Conversion and Management 78* (2014), 137–150.

[174] Vanthournout, K., D'hulst, R., Geysen, D., and Jacobs, G. A smart domestic hot water buffer. *Smart Grid, IEEE Transactions on 3*, 4 (2012), 2121–2127.

[175] VEA. What is a nearly zero energy building (in Dutch: Wat is een BEN-woning?). Tech. rep., Vlaams Energieagentschap (Flemisch energy agency), 2015.

[176] Verbeeck, G. *Optimisation of extremely low energy residential buildings.* phd-thesis, K.U.Leuven, Belgium, 2007.

[177] Verbeeck, G., and Hens, H. Energy savings in retrofitted dwellings: economically viable? *Energy and buildings 37*, 7 (2005), 747–754.

[178] Verhelst, C. *Model predictive control of ground coupled heat pump systems for office buildings.* PhD thesis, Katholieke Universiteit Leuven, Belgium, 2012.

[179] Verhelst, C., Logist, F., Van Impe, J., and Helsen, L. Study of the optimal control problem formulation for modulating air-to-water heat pumps connected to a residential floor heating system. *Energy and Buildings 45* (2012), 43–53.

[180] Waite, M., and Modi, V. Potential for increased wind-generated electricity utilization using heat pumps in urban areas. *Applied Energy 135* (2014), 634–642.

[181] Wang, D., Parkinson, S., Miao, W., Jia, H., Crawford, C., and Djilali, N. Online voltage security assessment considering comfort-constrained demand response control of distributed heat pump systems. *Applied Energy 96* (Jan. 2012), 104–114.

[182] Wang, D., Parkinson, S., Miao, W., Jia, H., Crawford, C., and Djilali, N. Hierarchical market integration of responsive loads as spinning reserve. *Applied Energy 104* (Apr. 2013), 229–238.

[183] Wang, J., Biviji, M., Wang, W. M., et al. Lessons learned from smart grid enabled pricing programs. In *Power and Energy Conference at Illinois (PECI)* (2011), IEEE, pp. 1–7.

[184] Warren, P. A review of demand-side management policy in the UK. *Renewable and Sustainable Energy Reviews 29* (2014), 941–951.

[185] Williams, T., Wang, D., Crawford, C., and Djilali, N. Integrating renewable energy using a smart distribution system: Potential of self-regulating demand response. *Renewable Energy 52* (Apr. 2013), 46–56.

[186] Yu, W., Li, B., Jia, H., Zhang, M., and Wang, D. Application of multi-objective genetic algorithm to optimize energy efficiency and thermal comfort in building design. *Energy and Buildings 88* (2015), 135–143.

Curriculum

Dieter Patteeuw
Born on 11 October 1988 in Kortrijk
Personal email address die.trudo@gmail.com

Experience

2011 - 2016: PhD-student at KU Leuven - GOA project

Education

2009-2011: Master in Mechanical Engineering, KU Leuven
2006-2009: Bachelor in Engineering, KU Leuven
2000-2006: Science-Mathematics, Spes Nostra Heule

International exchange

September 2011: Summer course on energy efficiency, Sofia Bulgaria
August 2010: Summer course on sustainable development, Uppsala Sweden

Miscellaneous

Creator of the website Healthy, Economical and Environmentally conscious (in Dutch: Gezond, Spaarzaam en Milieubewust): www.GSenM.be

Member working group KU Leuven “Energy and Buildings” as part of “KU Leuven climate neutral” initiative

List of publications

Articles in internationally reviewed academic journals

Patteeuw, D., Henze, G. P., & Helsen, L. (2016). Comparison of load shifting incentives for low-energy buildings with heat pumps to attain grid flexibility benefits. Applied Energy, 167, 80–92.

Patteeuw, D., Reynders, G., Bruninx, K., Protopapadaki, C., Delarue, E., D'haeseleer, W., Saelens, D. & Helsen, L. (2015). CO_2-abatement cost of residential heat pumps with active demand response: demand- and supply-side effects. Applied Energy, 156, 490–501.

Patteeuw, D., Bruninx, K., Arteconi, A., Delarue, E., D'haeseleer, W., & Helsen, L. (2015). Integrated modeling of active demand response with electric heating systems coupled to thermal energy storage systems. Applied Energy, 151, 306–319.

Arteconi, A., Patteeuw, D., Bruninx, K., Delarue, E., D'haeseleer, W., & Helsen, L. (2016). Active demand response with electric heating systems: impact of market penetration. Applied Energy, 177, 636–648.

Atam, E., Patteeuw, D., Antonov, S. P., & Helsen, L. (2016). Optimal control approaches for analysis of energy use minimization of hybrid ground-coupled heat pump systems. IEEE Transactions on Control Systems Technology, 24 (2), 525–540.

Articles submitted to internationally reviewed academic journals

Patteeuw, D., & Helsen, L. (2016). Combined design and control optimization of residential heating systems in a smart-grid context. Submitted revised version to Energy and Buildings.

Lawrence, T. M., Boudreau, M., Helsen, L., Henze, G. P., Mohammadpour, J., Noonan, D., Patteeuw, D., Pless, S. & Watson, R. (2016). Ten questions concerning integrating smart buildings into the smart grid. Submitted to Building and Environment.

Papers at international scientific conferences

Baeten, B., Rogiers, F., Patteeuw, D., & Helsen, L. (2015). Comparison of optimal control formulations for stratified sensible thermal energy storage in space heating applications. 13th International Conference on Energy Storage: IEA-ECES Greenstock, Beijing, 19-21 May 2015.

Patteeuw, D., & Helsen, L. (2014). Residential buildings with heat pumps, a verified bottom-up model for demand side management studies. 9th International Conference on System Simulation in Buildings: SSB 2014, Liège, 10–12 December 2014.

Heylen, E., Jordens, R., Patteeuw, D., & Helsen, L. (2014). The potential of air-water heat pumps in a Belgian residential retrofit context in relation to future electricity prices. 9th International Conference on System Simulation in Buildings: SSB 2014, Liège, 10–12 December 2014.

Patteeuw, D., Verhelst, C., & Helsen, L. (2013). The Potential of Floor Heating in Residences as a Passive Energy Storage in a Smart Grid Context. 11th REHVA world congress – Energy efficient, smart and healthy buildings: CLIMA 2013, Prague, 16-19 June 2013.

Bruninx, K., Patteeuw, D., Delarue, E., Helsen, L., & D'haeseleer, W. (2013). Short-term demand response of flexible electric heating systems: the need for integrated simulations. 10th International Conference on the European Energy Market: EEM 2013, Stockholm, 28–30 May 2013.

Technical reports

Dams, Y., Al Koussa, J., Patteeuw, D., Meynaerts, E., Wetzels, W., Van Bael, J. (2015). Vision EnergyVille - smart heat pumps (in Dutch: Visie EnergyVille – slimme warmtepompen). By order of the Flemish Energy Agency.

Articles in other journals

Patteeuw, D., & Helsen, L. (2015). Interactie van warmtepompen met elektriciteitsproductie. TVVL Magazine, 44 (7), 46-50.

FACULTY OF ENGINEERING SCIENCE
DEPARTMENT OF MECHANICAL ENGINEERING
APPLIED MECHANICS AND ENERGY CONVERSION
Celestijnenlaan 300A box 2420
B-3001 Leuven
dieter.patteeuw@kuleuven.be
https://www.mech.kuleuven.be/en/tme